

Some pages of this thesis may have been removed for copyright restrictions.

If you have discovered material in AURA which is unlawful e.g. breaches copyright, (either yours or that of a third party) or any other law, including but not limited to those relating to patent, trademark, confidentiality, data protection, obscenity, defamation, libel, then please read our [Takedown Policy](#) and [contact the service](#) immediately

DEVELOPMENT OF VISUAL EVOKED RESPONSES TO TRITAN, RED-
GREEN AND LUMINANCE STIMULI IN HUMAN INFANTS

CATHERINE MAY SUTTLE

Doctor of Philosophy

THE UNIVERSITY OF ASTON IN BIRMINGHAM

February 1997

This copy of this thesis has been supplied on condition that anyone who consults it is understood to recognise that its copyright rests with its author and that no quotation from the thesis and no information derived from it may be published without proper acknowledgement.

The University of Aston in Birmingham

Development of Visual Evoked Responses to Tritan, Red-Green and
Luminance Stimuli in Human Infants

Catherine May Suttle

PhD

1997

The principal aim of this work was to investigate the development of the S-cone colour-opponent pathway in human infants aged 4 weeks to 6 months. This was achieved by recording transient visual evoked responses to pattern-onset stimuli along a tritanopic confusion axis (tritan stimuli) at and around the adult isoluminant match. For comparison, visual evoked responses to red-green and luminance-modulated stimuli were recorded from the same infants at the same ages. Evoked responses were also recorded from colour-normal adults for comparison with those of the infants.

The transient VEP allowed observation of response morphology as luminance differences were introduced to the chromatic stimuli. In this way, an estimate of isoluminance was possible in infants. Estimated isoluminant points for a group of six infants aged 6 to 10 weeks closely approximated the adult isoluminant match. This finding has implications for the use of photometric isoluminance in infant work, and suggests that photopic spectral sensitivity is similar in infants and adults.

Abnormalities of the visual evoked responses to tritan, red-green and luminance-modulated stimuli in an infant with cystic fibrosis are reported. The results suggest abnormal function of the retino-striate visual pathway in this infant, and it is argued that these may be secondary to his illness, although data from more infants with cystic fibrosis are needed to clarify this further.

A group of nine healthy infants demonstrated evoked responses to tritan stimuli by 4 to 10 weeks and to red-green stimuli by 6 to 11 weeks post-term age. Responses to luminance-modulated stimuli were present in all nine infants at the earliest age tested, namely 4 weeks post-term. The slightly earlier age of onset of evoked responses to tritan stimuli than for red-green may be explained by the relatively lower cone contrast afforded by red-green stimuli. Latency of the evoked response to both types of chromatic stimuli and to luminance-modulated stimuli decreased with age at a similar rate, suggesting that the visual pathways transmitting luminance and chromatic information mature at similar rates in young infants.

Key words: development, vision, chromatic, infant, tritan.

This thesis is dedicated to my parents,
George and Peggy Suttle
and to my husband, Russell.

ACKNOWLEDGEMENTS

The environment in which I have carried out the work reported in this thesis has been made very pleasant by a unique group of people. I would like to thank Ola Willis, Fiona Fylan, Gareth Barnes, Ian Holliday, Krish Singh, Paul Furlong, Vivica Tipper, Andrea Edson and Lesley Jones for creating such a happy and supportive atmosphere in which to work.

In particular, I thank Vivica Tipper, for teaching me the practical aspects of visual electrophysiology during my first year, and Ian Holliday for help with my first few computer programmes.

I am very grateful to the infants and their parents, the adult subjects and to the staff of Newtown Health Centre and Aston University Nursery for their co-operation, without which this study would not have been possible. I thank Dr. Christine Spray of the Birmingham Children's Hospital Liver Unit for collaboration on part of the work reported in Chapter 8.

I am indebted to Dr. Steve Anderson, my associate supervisor for two years, for friendly advice and very helpful discussion.

Finally, I thank my supervisor, Professor Graham Harding, for unintrusive guidance and support throughout the past three years.

LIST OF CONTENTS

	Page No.
Title page	1
Summary	2
Dedication	3
Acknowledgements	4
List of Contents	5
List of Figures and Tables	9
Chapter 1: Chromaticity and the Neural Processing of Chromatic Signals	17
1.1 The Colour Signal	17
1.2 Colour-Matching Functions	17
1.3 Derivation of Chromaticity Diagrams	18
1.4 The CIE Colorimetric System	21
1.5 Isochromatic Zones	24
1.6 Cone Excitation Space	26
1.7 Luminance and Brightness of Chromatic Stimuli	28
1.8 Perceptual Attributes of Chromatic Stimuli	30
1.9 Chromatic Contrast	33
1.10 Cone Signals: The Principle of Univariance	35
1.11 Retinal Ganglion Cells	35
1.12 Magnocellular and Parvocellular Pathways	38
1.13 Multiplexing: The Double Duty Hypothesis	40
1.14 Cortical Processing of Chromatic Information	43
1.15 Prestriate Area V4	45
1.16 Summary	46
Chapter 2: Anatomical Development of the Visual System	48
2.1 The Central Nervous System	48
2.2 The Cerebral Cortex	51
2.3 Development of the Eye	54
2.4 Optic Media	54
2.5 Retinal Development	57
2.6 Foveal Development	59
2.7 Macular Pigment	63

2.8	Neural Plasticity	64
2.9	Myelination	66
2.10	Cranial Development	66
Chapter 3: Spatial and Chromatic Vision in Infants		69
3.1	Measurement Techniques	69
3.2	Infant Visual Psychophysics	69
3.3	Infant Visual Electrophysiology	71
3.4	Visual Acuity	73
3.5	Contrast Sensitivity	75
3.6	Infant Accommodation	76
3.7	Photopic Spectral Sensitivity	78
3.8	Scotopic Spectral Sensitivity	80
3.9	The Perception of Long and Middle Wavelength Stimuli in Infants	80
3.10	The Perception of Short Wavelength Stimuli in Infants	84
3.11	Restrictions on Spatial and Chromatic Infant Vision	86
3.12	Rod Contributions to Colour Vision in Infants	91
3.13	Colour Vision in the Peripheral Visual Field	93
3.14	The Genetic Basis of Defective Colour Vision	93
3.15	Colour Vision Screening in Infants and Children	97
3.16	Summary	98
Chapter 4: Rationale and Aims of the Present Study		100
4.1	The Processing of Chromatic Information by the Infant Visual System	100
4.2	Investigative Techniques	102
4.3	Specification of Infant Age	103
4.4	Aims and Methods of the Present Study	103
Chapter 5: General Methods		106
5.1	Computer-Generated Stimuli	106
5.2	Chromatic Luminance Ratios	110
5.3	Chromatic Contrast Stimuli	114
5.4	Isoluminance	117
5.5	Determination of Isoluminant Stimuli	117
5.6	Choice of Colour Axes and White Point	119
5.7	Chromatic Aberration	120

5.8	Pattern-Onset Stimuli	121
5.9	Determination of EEG Noise Levels	121
5.10	VEP Recording Procedure	122
5.11	Subjects	124
Chapter 6: The Adult Chromatic Visual Evoked Response		126
6.1	Introduction	126
6.2	Methods	128
6.3	Responses to Pattern-Onset Chromatic Stimuli	131
6.4	Evoked Responses to Pattern-Offset Stimuli	131
6.5	The Response to Non-Isoluminant Chromatic Stimuli	142
6.6	Chromatic Contrast	144
6.7	Intrusion of Rod Responses	151
Chapter 7: The Infant Visual Evoked Response at Isoluminance		157
7.1	Introduction	157
7.2	Methods	158
7.3	Results	159
7.4	Discussion: Luminance Artifacts	177
7.5	Discussion: Infant Isoluminance	178
Chapter 8: The Visual Evoked Response to Chromatic and Luminance Stimuli in Infants with Vitamin and Fatty Acid Deficiency		182
8.1	Introduction	182
8.2	Methods	184
8.3	ERG Recording	185
8.4	VEP Recording	186
8.5	Schedule	186
8.6	Results: Cystic Fibrosis	187
8.7	Results: Infants with Liver Disease	205
8.8	Discussion: Cystic Fibrosis	211
8.9	Discussion: Infants with Liver Disease	213
Chapter 9: A Longitudinal Study of the Visual Evoked Response to Chromatic Stimuli in Human Infants		215
9.1	Introduction	215
9.2	Subjects and Schedule	216

9.3	Stimuli and Recording Parameters	217
9.4	Responses to Luminance Stimuli	218
9.5	Responses to Chromatic Stimuli	222
9.6	Responses to Lower Contrast Chromatic Stimuli	237
9.7	Evidence for the Photopic Nature of Responses to Chromatic Stimuli	240
9.8	Evoked Responses at 3 to 6 Months of Age	242
9.9	Discrimination of Luminance and Chromatic Stimuli	248
9.10	Development of Luminance and Chromatic Pathways	252
9.11	Diminution of Responses at 3 Months Post-Term	254
9.12	Intrusion of Rod Responses	255
9.13	Colour Axes	255
9.14	Summary	256
	Chapter 10: General Discussion	257
10.1	The Infant Visual Evoked Response around Isoluminance	257
10.2	The Maturation of Evoked Responses to Chromatic and Luminance-modulated Stimulation	257
10.3	The Diminution of Evoked Responses at 3 Months of Age	259
10.4	Scotopic vs Photopic Mechanisms	260
10.5	Abnormal Evoked Responses	261
10.6	Conclusions	262
	List of References	263
	Appendix 1: Calculation of Cone Contrast	289
	Appendix 2: Blue-Yellow Stimuli	292
	Appendix 3: The Chromatic Visual Evoked Response in a Colour-Defective Adult	294

LIST OF FIGURES AND TABLES

		Page No.
Figure 1.1	Tristimulus values represented on a colour matching function	19
Figure 1.2	The r,g chromaticity diagram and corresponding colour matching functions	22
Figure 1.3	The CIE x,y chromaticity diagram and corresponding colour matching functions	23
Figure 1.4	Isochromatic zones for dichromats	25
Figure 1.5	An isoluminant plane in MBDKL colour space	27
Figure 1.6	The Munsell system representing hue, chroma and value	32
Figure 1.7	The mean absorbance spectra of each cone photopigment and of rhodopsin	34
Figure 1.8	Organisation of colour-opponent centre-surround retinal ganglion cells	37
Figure 1.9	Two alternative hypotheses for neural processing of chromatic signals	42
Figure 1.10	The processing of chromatic signals in the visual system	47
Figure 2.1	Glial cells of a developing cerebral hemisphere	50
Figure 2.2	Sections through the eye of a human embryo	55
Figure 2.3	Stages of development of human foveal cones	60
Figure 2.4	The developing human skull	68
Figure 3.1	Sweep VEP acuities over the first year of life	74
Figure 3.2	Neonate and adult foveal cone dimensions	90
Figure 3.3	The pattern of sex-linked inheritance of the gene for defective colour vision	96
Figure 5.1	CIE chromaticity co-ordinates of the red screen phosphor with respect to time	107
Figure 5.2	CIE chromaticity co-ordinates of the green screen phosphor with respect to time	108
Figure 5.3	CIE chromaticity co-ordinates of the blue screen phosphor with respect to time	109

Figure 5.4	The isoluminant tritan stimulus	111
Figure 5.5	The isoluminant red-green stimulus	112
Figure 5.6	The luminance-modulated stimulus	113
Table 5.1	L-, M- and S-cone contrast values of the tritan and red-green stimuli at each colour ratio	115
Figure 5.7	Tritan and red-green stimuli colour axes in CIE space	116
Figure 5.8	CIE co-ordinates of a red-green stimulus at a range of chromatic contrasts	118
Figure 5.9	An infant in situ watching the tritan stimulus	123
Figure 6.1	Individual isoluminant points for three colour-normal adults	130
Figure 6.2	Visual evoked responses to tritan stimuli (Adult AE)	132
Figure 6.3	Visual evoked responses to red-green stimuli (Adult AE)	133
Figure 6.4	Visual evoked responses to tritan stimuli (Adult VT)	134
Figure 6.5	Visual evoked responses to red-green stimuli (Adult VT)	135
Figure 6.6	A scatterplot showing latency of the response to tritan stimuli with respect to colour ratio (Adult FF)	136
Figure 6.7	A scatterplot showing latency of the response to red-green stimuli with respect to colour ratio (Adult FF)	137
Figure 6.8	Latencies of the evoked response to isoluminant chromatic stimuli are shown for each of the five adult subjects	138
Figure 6.9	The response to stimulus offset (Adult FF)	139
Figure 6.10	A scatterplot showing amplitude of the response to stimulus offset with respect to tritan colour ratio (Adult AE)	140
Figure 6.11	A scatterplot showing amplitude of the response to stimulus offset with respect to red-green colour ratio	141

	(Adult AE)	
Figure 6.12	Visual evoked responses to chromatic stimuli at a range of chromatic contrasts (Adult VT)	143
Figure 6.13	Response amplitude is plotted against log tritan chromatic contrast, to estimate contrast threshold (Adult AE)	145
Figure 6.14	Response amplitude is plotted against log red-green chromatic contrast, to estimate contrast threshold (Adult AE)	146
Figure 6.15	Response amplitude is plotted against log tritan chromatic contrast, to estimate contrast threshold (Adult VT)	147
Figure 6.16	Response amplitude is plotted against log red-green chromatic contrast, to estimate contrast threshold (Adult VT)	148
Figure 6.17	Response amplitude is plotted against log tritan chromatic contrast, to estimate contrast threshold (Adult FF)	149
Figure 6.18	Response amplitude is plotted against log red-green chromatic contrast, to estimate contrast threshold (Adult VT)	150
Figure 6.19	Responses to chromatic stimuli at 30 cd/m ² and at 40 cd/m ² (Adult VT)	153
Figure 6.20	Visual evoked response latency is shown with respect to mean luminance for isoluminant tritan and red-green stimuli (Adult VT)	154
Figure 6.21	Visual evoked response amplitude is shown with respect to mean luminance for isoluminant tritan and red-green stimuli (Adult VT)	155
Figure 7.1	Visual evoked responses to tritan stimuli (Infant DH; 6 weeks pta)	160
Figure 7.2	Visual evoked responses to red-green stimuli (Infant DH; 6 weeks pta)	161
Figure 7.3	Visual evoked responses to tritan stimuli (Infant MB; 9 weeks pta)	162

Figure 7.4	Visual evoked responses to red-green stimuli (Infant MB; 9 weeks pta)	163
Figure 7.5	Mean amplitude of the early positive response component (P_{130}) with respect to tritan colour ratio (Infant PR)	164
Figure 7.6	Mean amplitude of the early positive response component (P_{130}) with respect to red-green colour ratio (Infant PR)	165
Figure 7.7	Mean amplitude of the early positive response component (P_{130}) with respect to tritan colour ratio (Infant MB)	166
Figure 7.8	Mean amplitude of the early positive response component (P_{130}) with respect to red-green colour ratio (Infant MB)	167
Figure 7.9	Mean amplitude of the early positive response component (P_{130}) with respect to tritan colour ratio (Infant AE)	168
Figure 7.10	Mean amplitude of the early positive response component (P_{130}) with respect to red-green colour ratio (Infant AE)	169
Figure 7.11	Mean amplitude of the early positive response component (P_{130}) with respect to tritan colour ratio (Infant DC)	170
Figure 7.12	Mean amplitude of the early positive response component (P_{130}) with respect to red-green colour ratio (Infant DC)	171
Figure 7.13	Mean amplitude of the early positive response component (P_{130}) with respect to tritan colour ratio (Infant DH)	172
Figure 7.14	Mean amplitude of the early positive response component (P_{130}) with respect to red-green colour ratio (Infant DH)	173
Figure 7.15	Mean amplitude of the early positive response component (P_{130}) with respect to tritan colour ratio	174

	(Infant JC2)	
Figure 7.16	Mean amplitude of the early positive response component (P_{130}) with respect to red-green colour ratio (Infant JC2)	175
Figure 7.17	Estimated tritan and red-green isoluminant points are shown for each of a group of six infants	176
Figure 8.1	Visual evoked responses to tritan stimuli at 8 weeks pta (Infant RH)	189
Figure 8.2	Visual evoked responses to red-green stimuli at 8 weeks pta (Infant RH)	190
Figure 8.3	Visual evoked responses to tritan stimuli at 7 weeks pta (Infant AE)	191
Figure 8.4	Visual evoked responses to red-green stimuli at 6 weeks pta (Infant AE)	192
Figure 8.5	A scatterplot of luminance response latency with respect to age for healthy infants and for infant RH	193
Figure 8.6	Visual evoked responses to luminance stimuli at 25 weeks pta (Infants RH and AM)	194
Figure 8.7	Photopic ERGs at 12 weeks pta (Infant RH and control)	196
Figure 8.8	30 Hz flicker ERGs at 12 weeks pta (Infant RH and control)	197
Figure 8.9	Scotopic ERGs at 12 weeks pta (Infant RH and control)	198
Figure 8.10	Scotopic, photopic and 30 Hz ERGs (Infant RH; 19 weeks pta)	199
Figure 8.11	A scatterplot of photopic ERG b-wave latency with respect to age for healthy infants and for infant RH	201
Figure 8.12	A scatterplot of 30 Hz flicker ERG b-wave latency with respect to age for healthy infants and for infant RH	202
Figure 8.13	A scatterplot of scotopic ERG b-wave latency with respect to age for healthy infants and for infant RH	203
Figure 8.14	Scotopic ERG (Infant RH; 25 weeks pta)	204
Figure 8.15	Latency of the evoked response to flash stimulation	206

	is plotted with respect to age for healthy infants and for those with liver disease	
Figure 8.16	Latency of the evoked response to achromatic pattern-reversal stimulation is plotted with respect to age for healthy infants and for those with liver disease	207
Figure 8.17	A scatterplot of photopic ERG b-wave latency with respect to age for healthy infants and for those with liver disease	208
Figure 8.18	A scatterplot of 30 Hz flicker ERG b-wave latency with respect to age for healthy infants and for those with liver disease	209
Figure 8.19	A scatterplot of scotopic ERG b-wave latency with respect to age for healthy infants and for those with liver disease	210
Figure 9.1	The response to luminance-modulated stimulation at 5 weeks pta (Infant MB)	219
Figure 9.2	Latency of the evoked response to luminance stimulation is shown with respect to age for a group of 5 infants	220
Figure 9.3	Amplitude of the evoked response to luminance stimulation is shown with respect to age for a group of 5 infants	221
Figure 9.4	Visual evoked responses to tritan stimuli at 5 weeks pta (Infant MB)	223
Figure 9.5	Visual evoked responses to red-green stimuli at 5 weeks pta (Infant MB)	224
Figure 9.6	Visual evoked responses to tritan stimuli at 6 weeks pta (Infant PR)	225
Figure 9.7	Visual evoked responses to red-green stimuli at 6 weeks pta (Infant PR)	226
Figure 9.8	Standard deviation values for EEG noise levels, and for responses to tritan and red-green stimuli are shown with respect to colour ratio (Infant DH)	227
Figure 9.9	Standard deviation values for EEG noise levels, and	228

	for responses to tritan and red-green stimuli are shown with respect to colour ratio (Infant MB)	
Figure 9.10	Standard deviation values for EEG noise levels, and for responses to tritan and red-green stimuli are shown with respect to colour ratio (Infant PR)	229
Figure 9.11	The age of onset of visual evoked responses to tritan and red-green stimuli are shown for each of a group of 9 infants	231
Figure 9.12	Latency of the evoked response to tritan stimuli is shown with respect to age for a group of 5 infants	232
Figure 9.13	Amplitude of the evoked response to tritan stimuli is shown with respect to age for a group of 5 infants	233
Figure 9.14	Latency of the evoked response to red-green stimuli is shown with respect to age for a group of 5 infants	235
Figure 9.15	Amplitude of the evoked response to red-green stimuli is shown with respect to age for a group of 5 infants	236
Figure 9.16	Visual evoked responses to tritan stimuli at a range of chromatic contrasts (Infant PR; 8 weeks pta)	238
Figure 9.17	Visual evoked responses to red-green and tritan stimuli at maximum chromatic contrast, and to the tritan stimulus at 18% contrast (Infant PR; 8 weeks pta)	239
Figure 9.18	Visual evoked responses to the tritan stimulus at 20 cd/m ² and 40 cd/m ² (Infant OG; 8 weeks pta)	241
Figure 9.19	Latency of the evoked response to luminance stimulation is shown with respect to age for two infants tested from 1 to 6 months of age	243
Figure 9.20	Amplitude of the evoked response to luminance stimulation is shown with respect to age for two infants tested from 1 to 6 months of age	244
Figure 9.21	Visual evoked responses to chromatic and luminance stimuli at 3 months of age (Infant MB)	245
Figure 9.22	Visual evoked responses to chromatic and	246

	luminance stimuli at 3 months of age (Infant KB)	
Table 9.1	This table indicates whether evoked potentials to each type of stimuli were present in infants tested up to and over 3 months of age	247
Figure A2:1	A photometrically isoluminant blue-yellow stimulus	293
Figure A3:1	The result of the Farnsworth-Munsell 100-Hue test carried out under room lighting (Adult FF)	295
Figure A3:2	The result of the Farnsworth-Munsell 100-Hue test carried out under illuminant C (Adult FF)	296
Figure A3:3	The result of the Farnsworth-Munsell 100-Hue test carried out under illuminant C on colour-defective adult IP	297
Figure A3:4	Visual evoked responses to red-green stimuli recorded from adult IP	298

CHAPTER 1

CHROMATICITY AND THE NEURAL PROCESSING OF CHROMATIC INFORMATION

Chromaticity - the Specification of Colour

1.1 The Colour Signal

The colour appearance of an object depends upon the spectral composition of the incident light, the surface reflectance function (SRF) of the object and the state of the chromatic adaptation of the observer. The incident light and the SRF together constitute the colour signal. That is, the spectral composition of light emitted from the object.

The SRF may be described as the reflectance of light of wavelengths across the spectrum, from a surface, or object. If a greater proportion of a certain wavelength band is reflected, the surface colour signal will be dominated by light of this wavelength. If the illuminant is spectrally flat, the colour signal of the object will be determined solely by the SRF. Most illuminants, however, are not spectrally flat, being dominated by certain parts of the spectrum. In this case, the colour signal is an additive combination of the SRF and the illuminant (Lennie and D'Zmura, 1988).

1.2 Colour Matching Functions

For the normal, trichromatic, observer any one light may be matched by a combination of three lights in the short-, medium- and long-wavelength range of the visible spectrum, respectively. These primary lights are, by definition, unique, so that it is not possible to match any one of the lights by a combination of the other two. The light to be matched (A) is of a known wavelength and luminosity. Its wavelength determines which of the three cone types (long-, medium- and short-wavelength-sensitive) are more or less likely to be excited by it, and its luminosity determines the quantum catch made by each type. The three lights provided to make a match (R=long, G=medium and B=short wavelength) are of fixed wavelength, but can each be altered in luminosity, so that the quantum catch of each cone type may be made the same for light A as for light R+G+B. This type of

match illustrates the phenomenon of *silent substitution* (Estevez and Spekreijse, 1982) in which the quantum catch of the three cone types is the same for both patches of light, so they appear indistinguishable (Wyszecki and Stiles, 1982).

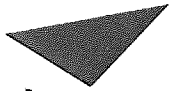
In some cases, a trichromatic match may be non-additive, so that one or possibly two of the three primary lights must be added to light A in order for a match to be made. Thus, one light has been subtracted from the trichromatic match, rather than added. Fig. 1.1 shows that colour matching functions may be represented graphically, so that a line drawn on the graph at a particular wavelength will indicate the relative amounts (positive and negative) of each primary required to make a match with light of this wavelength. The amount of each of the three primaries is known as a *tristimulus value*, so that three tristimulus values may be used to describe a particular light.

1.3 Derivation of Chromaticity Diagrams

Chromaticity diagrams are used to describe colours in terms of their chromaticity without regard for their luminance. The determination of colour matching functions is essential to the chromaticity diagram, as tristimulus values are used to find the chromaticity co-ordinates to describe a particular colour.

Representations of colour by tristimulus values and chromaticity co-ordinates offer objective descriptions of colours, as opposed to the more subjective descriptions of hue, saturation and brightness (see page 31). This is important in the accurate specification of colours. Four laws are assumed to be obeyed in colour matching:

- (i). Symmetry law - if A matches B, then B matches A.
- (ii). Transitivity law - if A matches B and B matches C, then A matches C.
- (iii). Proportionality law - if A matches B then x A matches x B.
- (iv). Additivity law (Abney's Law) - if A matches B, C matches D, and $A+C$ matches $B+D$, then also $A+D$ matches $B+C$.



Aston University

Content has been removed for copyright reasons

Figure 1.1

Tristimulus values for three lights to make a match with a fourth light, are represented on a colour matching function by drawing a vertical line from the wavelength of light to be matched. The points of intersection of this line with each of the three functions gives the tristimulus value for each (from Wyszecki and Stiles, 1982).

Observational conditions are also assumed, such that the two patches of light observed (A and R+G+B) must stimulate similar areas of retina, in terms of rod and cone population. Incorrect viewing conditions could allow one patch to stimulate a cone-dominated area and the other a rod-dominated area, for example by viewing slightly to the side of one patch. In addition, the observer's state of light and chromatic adaptation should be taken into account.

From the colour match, tristimulus values of R, G, and B are determined for a light A, such that $A=R+G+B$. Alternatively, if one of the primaries (such as R) has been added to A to make a match, $A+R=G+B$, or $A=G+B-R$. This relationship may be expressed diagrammatically as a three-dimensional arrangement of vectors, the lengths of which represent the R, G and B tristimulus values. The direction and length of the vector for A may be determined by addition of the primary vectors, R, G and B. Within this tristimulus space, a two-dimensional plane may be described, in which each of the three primary vectors is equal to 1.0. This is known as the unit plane, and the point at which the vector A intersects this plane specifies its chromaticity, but bears no relation to its intensity, which is represented by the length of the vector.

By converting tristimulus values found from colour matching to chromaticity co-ordinates, a two-dimensional representation, the r,g,b chromaticity diagram, may be described. Here, lines perpendicular to the three sides of an equilateral triangle are the r, g and b axes, each extending from 0 to 1.0. The point of intersection of these axes represents the light A, and the extents along each axis prior to intersection represents the contributions of each of R,G and B.

From the tristimulus values, R, G and B, chromaticity co-ordinates of A are found as follows:

$$r=R/R+G+B$$

$$g=G/R+G+B$$

$$b=B/R+G+B$$

In deriving chromaticity diagrams, colour matching functions are determined for a range of monochromatic lights of various wavelengths at known wavelength intervals across the visible spectrum. If these lights have unit radiant power (are all at the same intensity) then the stimulus comprising the full spectrum of wavelengths is known as the equal energy stimulus. In order to place the equal energy stimulus (E) at the centre of the chromaticity diagram, lights chosen to make a trichromatic match have radiant power of 72.1(R), 1.4(G) and 1.0(B), In this case, $r+g+b=1.0$, and so only two of the co-ordinates need to be specified, as is the case in the two-dimensional representation of r and g co-ordinates (Figure 1.2).

1.4 The CIE Colorimetric System

The aim of colorimetry is to obtain an objective measure for all real colours, derived from the colour matching functions of normal trichromatic observers. This objective is the domain of the Commission Internationale de l'Éclairage (the CIE). This body lays down specifications for standard observers and viewing conditions.

In the r, g, b system, negative values arising from subtraction of one of the primaries from the match are included, which causes complications in calculation and specification of colours. For this reason, the CIE adopted the x,y,z system, using imaginary primary stimuli as primaries. Imaginary stimuli are those which are specified by a set of tristimulus values, in the same way as real stimuli, but which cannot be realised as colours. In the CIE xyz system, imaginary stimuli lie outside of the area bounded by the spectral locus and purple line, and real colours lie within this area (see figure 1.3).

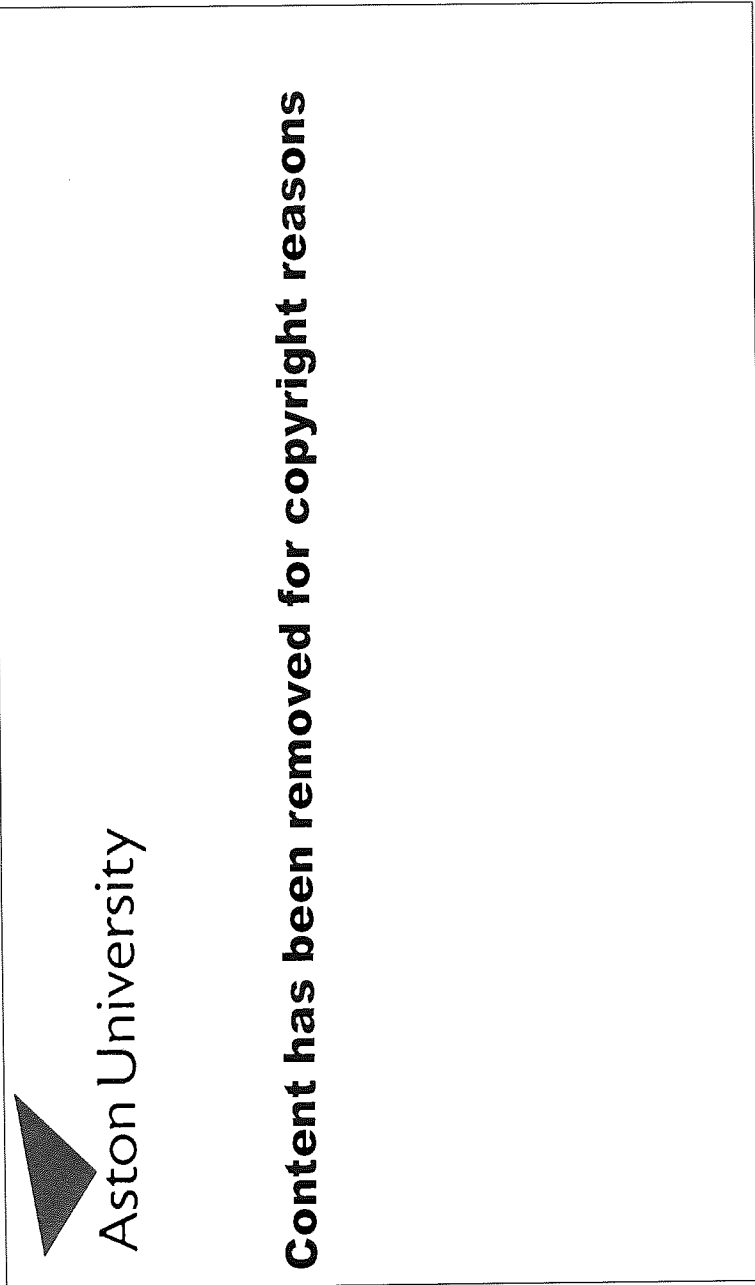


Figure 1.2
The r, g chromaticity diagram and corresponding colour matching functions (from Wyszecki and Stiles, 1982).

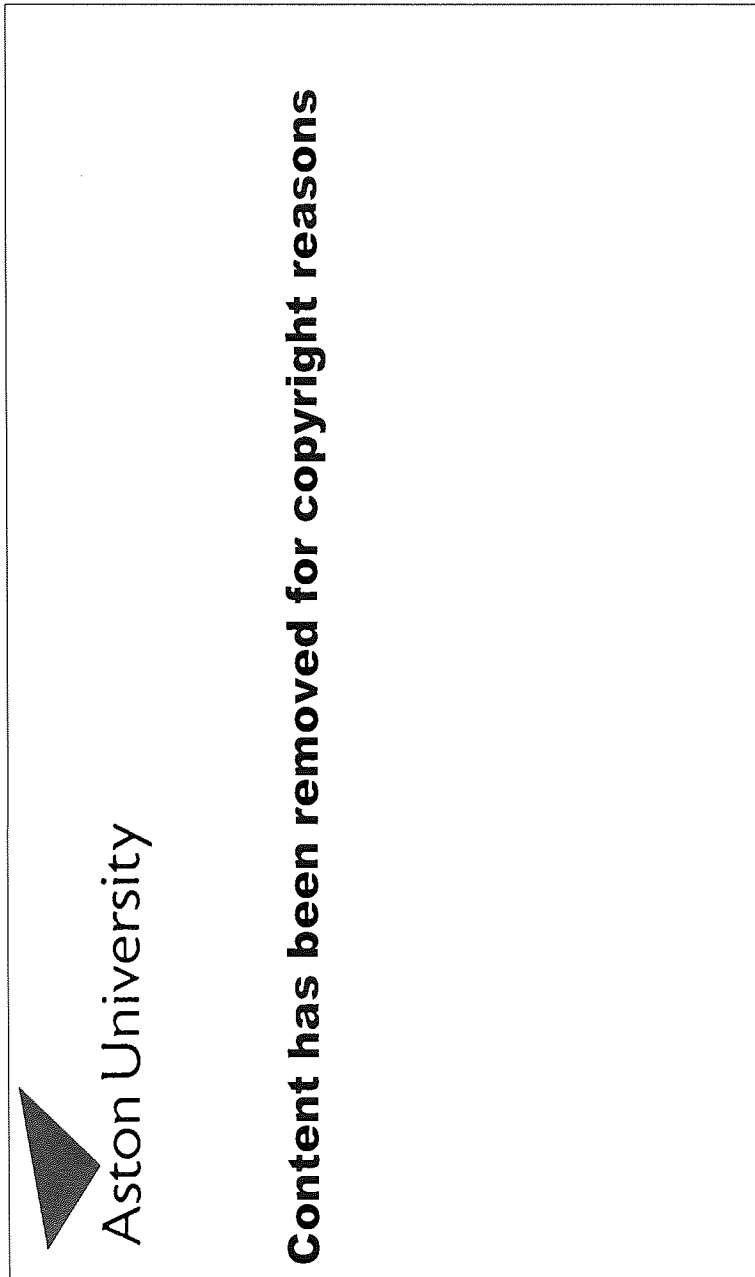


Figure 1.3
The CIE x,y chromaticity diagram and corresponding colour matching functions (from Wyszecki and Stiles, 1982).

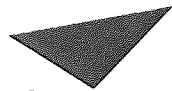
Here, colours on the spectral locus and the purple line are most saturated, and colours become less saturated towards the white point (E). The chromaticity co-ordinates r,g,b may be converted to x,y,z values using calculations specified by the CIE (Wyszecki and Stiles, 1982).

The first CIE standard observer recommendations were made in 1931, defined by the observers' colour matching functions for a wavelength range of 380 to 780 nm, in 5 nm intervals. These functions were extended by the CIE in 1971 to cover a range from 360 to 830 nm, at 1 nm intervals. Both of these sets of data were determined from actual observers, using a field size of 2 deg angular subtense to eliminate the contributions of rods to the perceived colour. In 1964, the CIE introduced a table of colour matching functions viewed centrally with an angular subtense of 10 deg. With these viewing conditions, retinal areas populated by rod receptors are stimulated, and the stimulus must therefore be of sufficiently high intensity to discount the scotopic mechanism.

1.5 Isochromatic Zones

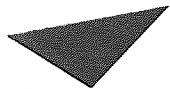
While trichromats require three primaries for colour matching, dichromats require only two, as the absent cone type requires no input from the corresponding primary colour. As dichromats have only two functioning cone types, colours which stimulate these in constant proportions are confused by the observer, as they appear to match. A trichromat would be able to distinguish such colours provided that the third cone type is stimulated by each to a different degree.

The CIE diagram represents these colours on isochromatic zones, within which chromaticity co-ordinates specify colours which dichromats would be unable to distinguish from other colours within that zone. Isochromatic zones are described for protanopes, deuteranopes and tritanopes (Fig. 1.4). Anomalous trichromats of each type would have isochromatic zones of the same orientation but shorter, indicating that only desaturated colours would be confused.



Aston University

Content has been removed for copyright reasons



Aston University

Content has been removed for copyright reasons

Figure 1.4

Isochromatic zones for deuteranopes (a), protanopes (b), and tritanopes (c) (from Birch, 1993).

1.6 Cone Excitation Space

Cone excitation may be represented in colour space, using axes along which silent substitution pairs exist. Thus, colours along these axes may be interchanged without any change in excitation of specific chromatic mechanisms. Macleod and Boynton (1979) suggested a cone excitation space with orthogonal axes, the ordinate representing S-cone excitation, and the abscissa representing both L- and M-cone excitation. Along this latter axis, the excitation of L- and M-cones is constant, being entirely due to L-cones at one end and entirely due to M-cones at the other. Colours along the axis are isoluminant at all points, and relative excitation of L- and M-cones varies, with total excitation of the two cone types always summing to the same value.

Colours along the ordinate are, again, isoluminant, and have a variable effect on S-cone excitation, increasing from zero, at which L- and M-cones only are excited, to 1.0 at which point only S-cones are excited. The effect on L- and M-cones is the same across this axis, just as the effect on S-cone excitation is the same across the abscissa (Kulikowski and Walsh, 1991).

The Macleod and Boynton axes of cone excitation were developed into a three-dimensional space by Derrington, Krauskopf and Lennie (1984) which became known as the MBDKL colour space (figure 1.5). Here, movement along a vertical axis represents changes in luminance only, and no change in chromaticity. Movement within a horizontal plane represents isoluminant changes. This is the isoluminant plane which consists of two cardinal axes, one of which represents constant S-cone modulation, in which the level of S-cone excitation does not change. The second major axis is one of constant L-M cone modulation, so that only S-cones are excited in this case, and is also known as a tritanopic confusion axis because an observer lacking short-wavelength-sensitive cones would fail to discriminate stimuli along such an axis.

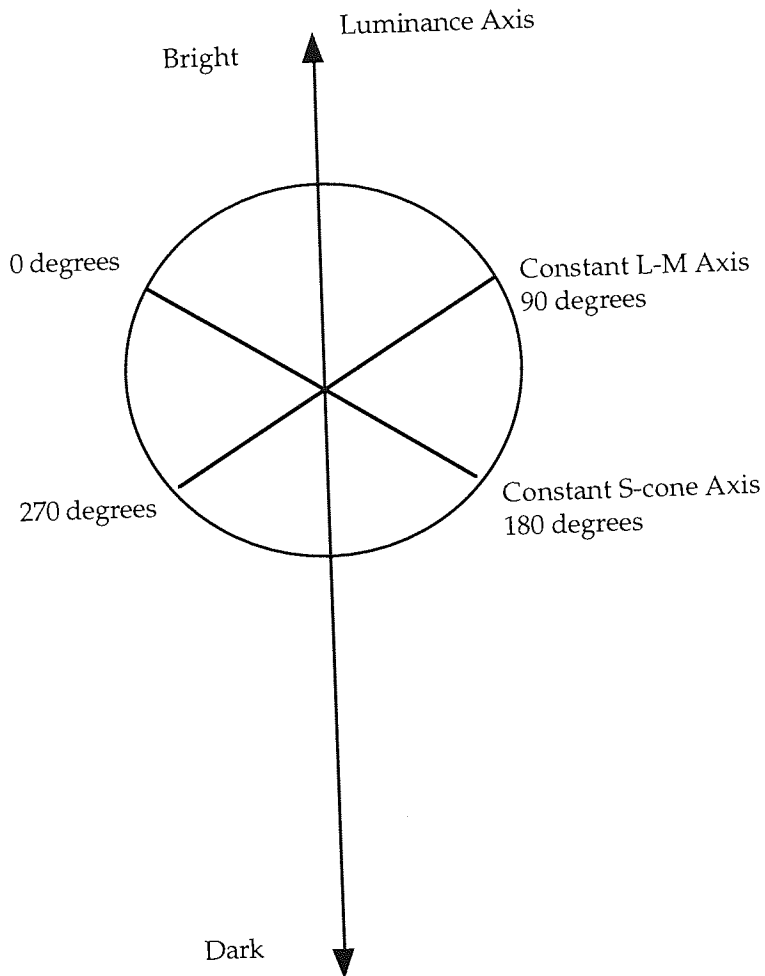


Figure 1.5
 This diagram shows one isoluminant plane in MBDKL colour space. The three-dimensional space consists of a luminance-only axis, running through the centre of a sphere. Within the sphere, any real colour of a known chromaticity may be located in terms of its depth within the sphere (luminance) and its distance from the achromatic axis towards the periphery (chromaticity). Within the isoluminant plane, two colour axes are shown. The constant S axis is one along which all colours have the same effect on short-wavelength-sensitive cones (S). Thus, pairs of colours along this axis stimulate L and M cones and have no net effect on S cones. Along the constant L-M axis, colours have an equal effect on L and M cones, and so only S cones are modulated.

Colours may be represented at any point within this space, according to whether the colours are isoluminant (occurring within a horizontal plane only), isochromatic (in a vertical plane, differing only in luminance) or they differ in luminance and chromaticity, in which case they would occur at different horizontal and vertical planes to each other. Luminance levels may be specified in terms of elevation from the isoluminant (horizontal) plane, and may be from -90.0 to 90.0 deg, 0.0 degrees representing isoluminance, -90.0 or 90.0 representing luminance only, and intermediate values representing modulations of chromaticity and luminance in the same stimulus. The cardinal cone excitation axes within the isoluminant plane are specified in terms of their azimuth, which is 0.0 to 180.0 deg for the constant S axis and 90.0 to 270.0 deg for the constant L,M axis.

The centre of the colour sphere (its origin) is the white point, and as on the CIE chromaticity diagram the distance from here to the colour position indicates the degree of saturation of the colour, being less saturated towards the white point. If two colours are diametrically opposite in colour space, lying on a vector passing through the origin, distance from the origin represents chromatic contrast of the two stimuli.

1.7 Luminance and Brightness of Chromatic Stimuli

Experiments using chromatic stimuli usually require them to be equal in luminance and brightness, thus allowing the observer no non-colour cues with which to discriminate them. Luminance is defined by the CIE, in terms of the $V\lambda$ function. Heterochromatic stimuli may be rendered isoluminant by a number of different methods. *Physical photometry*, measured using a photometer, is derived from the mean of spectral sensitivities of a group of colour-normal adult observers, and may differ from that of other individuals, due to normal variations in ocular media density and proportions of long-, medium- and short-wavelength-sensitive cones at the fovea. A measurement of isoluminance by physical photometry does not necessarily, therefore, ensure that heterochromatic stimuli are isoluminant for each individual observer.

Visual photometry is the determination of isoluminance by observation,

and may be achieved by a number of methods which yield significantly different results. These differences arise because some methods produce additive stimuli, which obey Abney's Law (see page 18), while others do not. A test of additivity provides a means of determining whether the additive (luminance) channel or the colour-opponent channels, or both, are involved in the perception of stimuli. One such experiment (Kaiser, 1991) involves the adjustment of the amount of red light (R) in a heterochromatic stimulus comprising red and green elements, for example, until a point of minimum flicker is reached. This is now repeated with the second of the two colours, such as green (G). At this point, the intensity of the red element is increased (r), and the observer changes the green light intensity (g) until minimum flicker is reached once again. The additivity index may be calculated as follows:

$$(r/R) + (g/G)$$

If this index equals 1.0, the stimulus is said to be additive.

The method of heterochromatic flicker photometry (HFP) involves the observation of heterochromatic stimuli flickering at around 20Hz, and the adjustment of their relative luminance until the perceived flicker is minimised (Pokorny et al, 1989; Capilla and Aguilar, 1993). This method has been found to be additive while appropriate flicker rates are used, with additivity failures occurring below 10Hz (Kaiser, 1991). The minimally distinct border (MDB) technique requires an observer to adjust the relative luminances of two precisely juxtaposed heterochromatic stimuli, until the border between them appears least distinct. This method has also been shown to be additive (Boynton and Kaiser, 1968). Thirdly, the minimum motion technique involves the presentation of a heterochromatic grating stimulus, alternating with a monochromatic grating with dark and light phases. As the two alternate, luminance differences between the two colours of the heterochromatic stimulus cause the grating to appear to be moving laterally. At isoluminance, this motion is minimised. This method is thought to be additive, as it appears to have the same physiological basis as the minimum flicker method (Anstis and Cavanagh, 1983). Finally, the heterochromatic brightness matching method involves simply the observation of heterochromatic stimuli and adjustment of their

relative luminance until the two appear equally bright. This method differs from the others in that it generally produces additivity failures (Kaiser, 1991).

Physiologically, the significance of additivity is that additive stimuli have been found to produce minimal activity of phasic ganglion cells of the magnocellular channel, while non-additive stimuli produce a mixed magnocellular and parvocellular response, demonstrated by single-cell recordings in the macaque (Kaiser, 1991). In experiments of colour perception on the basis of chromatic differences only, it is preferable to define isoluminance by an additive method, so that the luminance channel is relatively inactive, and the colour-opponent channels are stimulated.

Heterochromatic stimuli of equal luminance are also equally bright when additivity is demonstrated *and* brightness judgments are used as a criterion. As mentioned above, such additivity is generally not found, as stimuli matched in brightness show additivity failures. The exception to this is when complementary stimuli are used, in which case heterochromatic stimuli may be rendered equal in both luminance and brightness (Boynton and Kaiser, 1968).

1.8 Perceptual Attributes of Colour

The CIE system gives us a means of specifying colours numerically, but is not instantly descriptive. The precise and objective colorimetry of the CIE system is essential, but many situations require descriptions of colours in terms of their perceptual attributes.

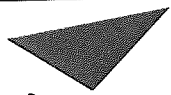
Colours viewed in a multicoloured scene, all illuminated in the same way, are perceived correctly by the visual system. This is due to *colour constancy*, which allows the constant appearance of colours viewed within a scene, regardless of the spectral properties of their illuminant. The visual system compares colours within the scene, and in this way discounts the spectral properties of the illuminant, so that each colour is perceived correctly.

Colours viewed in isolation are known as *aperture colours*, their appearance

being unaffected by surrounding colours (Lennie and D'Zmura, 1988). Colours viewed in aperture mode may be described in terms of hue, saturation and brightness. Hue is a description of chromaticity, and may be compared with the dominant wavelength of the CIE chromaticity diagram. Saturation describes the purity of the colour, desaturated colours being paler than those of higher purity. For example, a pink is a desaturated red. This may be compared to position on the CIE diagram, chromaticities closer to the spectral locus or purple line being purer (more saturated) than those nearer to the white point. Brightness simply describes luminosity. As all points on the CIE chromaticity diagram are within the same luminance plane, this attribute is ignored by the CIE diagram.

One example of such a model of colour is the Munsell Book of Colour (1905). This contains over 1200 samples of matt and glossy colours arranged in equal perceptual steps. Notations given for each colour are such that they can be converted to the CIE x,y,z system. Colours in the Munsell system are described in terms of hue, chroma (saturation) and value (brightness) (Figure 1.6).

There are five principal hues: Blue, Green, Yellow, Red and Purple, and five intermediate hues, which are mixtures of adjacent principles hues, such as Blue-Green and Red-Purple. These ten hues are arranged around a hue circle in order of perceptual difference. Chroma is represented along lines joining the hue circle to the centre of the model, with colours of maximum purity being on the hue circle. Value is modulated along a vertical axis through the centre of the hue circle, on which a value of zero is black and 10 is white. Intermediate numbers represent greys. In this way, a colour of any luminosity, saturation and chromaticity may be represented as a point on this three-dimensional model.



Aston University

Content has been removed for copyright reasons

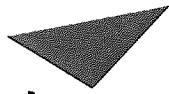
Figure 1.6

The Munsell system representing hue, chroma and value (from Birch, 1993).

1.9 Chromatic Contrast

A heterochromatic stimulus is composed of two or more chromatic stimuli, such as gratings in spatial antiphase. Each grating may be described in terms of its luminance contrast, which is the Michelson contrast between its light and dark phases. Physical chromatic contrast is the spectroradiometrically measured difference between the two colours. At maximum luminance contrast, physical contrast is also at a maximum, and may be described as two colours at the opposite ends of an axis connecting them in CIE colour space. As luminance contrast is reduced, the dark phase of each monochromatic grating is no longer at minimum luminance, so some of each colour is added to the other. This reduces the difference between the two colours, bringing them closer together in CIE space, and the heterochromatic grating now has a lower chromatic contrast. At zero chromatic contrast, there is no difference between the colours, and the stimulus has a uniform colour (no pattern) which is a mixture of the two component colours.

The chromatic elements of a heterochromatic stimulus may have an unequal effect on each cone type, even at isoluminance, so that each cone mechanism may be more excited by one grating than by the other. This difference in cone excitation is known as *cone contrast*, and is due to the difference between spectral sensitivity functions for each of the three cone mechanisms, as shown by figure 1.7 (Bowmaker and Dartnall, 1980). Cone contrast is a more physiologically meaningful measure than physical contrast because it indicates the effect the stimulus is having on elements of the colour-opponent pathways. Cone contrast may be calculated for L, M and S cones, given a knowledge of the chromaticity co-ordinates of each of the chromatic gratings (see Appendix 1), and cone fundamentals. Cone fundamentals are values of excitation, or quantal catch, of each cone type, and are derived from cone sensitivities at a range of wavelengths across the visible spectrum (Vos and Walraven, 1970). These have been derived psychophysically (Smith and Pokorny, 1975) and show good agreement with microspectrophotometric measurements of cone photopigments (Bowmaker and Dartnall, 1980).



Aston University

Content has been removed for copyright reasons

Figure 1.7

The mean absorbance spectra of each of the three cone photopigments and of rhodopsin, the rod photopigment. The SWS cone pigment peaks at 420 nm, the MWS at 534 nm and the LWS at 564 nm, while rhodopsin peaks at 498 nm (from Bowmaker and Dartnall, 1980).

The Processing of Chromatic Information in the Visual System

1.10 Cone Signals: The Principle of Univariance

The three cone types are sensitive to different but overlapping regions of the visible spectrum (see figure 1.7). They are generally classified as having peak sensitivity to long, medium or short wavelength light. As a result of their spectral overlap, any one light may excite more than one mechanism, but to different degrees, as one mechanism will be more sensitive than the others to this wavelength.

Cones respond simply to the number of photons captured, and a change in quantum catch could signify either a change in intensity or in wavelength. The cone mechanism has no means of distinguishing between these two. This one-dimensional response characteristic of cones is known as the *principle of univariance*, the significance of which is the inability of cones to distinguish between lights of different wavelengths.

1.11 Retinal Ganglion Cells

Around six million cones, heavily concentrated at the fovea, and 110 million rods converge on 1.5 million ganglion cells, the axons of which comprise the optic nerve. Retinal ganglion cells have centre-surround organisation, which affords sensitivity to edges and contrast, at the expense of spatially uniform stimuli. In addition, the ratio of ganglion cells to cones is much higher at the fovea than elsewhere in the retina. These two characteristics of ganglion cell organisation allow the efficient transmission of information along the relatively few neurones of the optic nerve.

Several distinct groups of retinal ganglion cells have been identified in cats and primates. In the macaque, Gouras (1968, 1991) has identified two ganglion cell types termed Phasic and Tonic, in view of their respectively transient and sustained response characteristics (see also Ueno, 1992). Phasic cells were of centre-surround organisation, with both L (long-wavelength-sensitive cone) and M (medium-wavelength-sensitive cone) input to the centre and surround. Here, the cell types have antagonistic input, but the antagonism is consistent in both regions so that in effect the unit is spatially

but not colour-opponent. These cells were found to be far fewer in number than tonic cells, and were relatively more concentrated in the periphery. Tonic cells were of single cone opponency, with one cone type providing input to the centre, and the surround supplied by a different cone type. The two cone types showed antagonistic responses, one being excitatory and the other inhibitory. This organisation allows for both spatial and chromatic opponency (Michael, 1978) as illustrated by figure 1.8. Retinal ganglion cells with the anatomical and response characteristics of Tonic cells have more recently been identified as midget or P-cells (Lennie and D'Zmura, 1988).

Leventhal et al (1981) labelled retinal ganglion cells of Old World monkeys using HRP (horseradish peroxidase) injections into the LGN, superior colliculus and pretectum. They were able to identify four groups on the basis of morphology and dendritic field size. Two of these groups, labelled A and B, were shown by the HRP stain to project to the magnocellular and parvocellular layers of the LGN, respectively. Group A cells were characterised by large cell bodies and medium dendritic fields, and Group B by their small cell bodies and small receptive (dendritic) fields. Both groups showed an increase in cell body size and dendritic field size with eccentricity from the fovea. These two cell types, also known as $P\alpha$ (phasic) and $P\beta$ (tonic) respectively are thought to comprise approximately 10% and 80% of retinal ganglion cells respectively (Lennie and D'Zmura, 1988).

Other ganglion cells which have been identified in the primate fovea are bistratified and parasol cells. Parasol ganglion cells project to the magnocellular laminae and are not concerned with chromatic processing. Bistratified ganglion cells do project to parvocellular laminae of the LGN and may be distinguished from P-cells (midget cells) by their much larger receptive fields (Rodieck, 1991).



Figure 1.8
 Organisation of colour-opponent retinal ganglion cell receptive fields with various combinations of cone input to centre and surround.

Post-receptoral pathways transmitting signals from cones may also receive some input from rods. Retinal ganglion cells at the fovea receive single-cone input, while those of the more peripheral retina may be driven by both rods and cones (D'Zmura and Lennie, 1986). Thus, rod signals are transmitted via ganglion cells projecting to the magnocellular and the parvocellular layers of the LGN. Parvocellular units receiving input from the fovea, however, are exclusively driven by cones.

Gouras and Zrenner (1979), using psychophysical techniques in the rhesus monkey, found that chromatically-opponent ganglion cells showed reduced sensitivity to colour contrast when stimulus flicker rate was increased. This was explained by the fact that the surround response is delayed with respect to that of the centre. This difference increases with flicker rate, so that eventually the two are completely out of phase, and responses which were antagonistic at lower frequencies become synergistic. They concluded that the organisation of chromatically-opponent retinal ganglion cells enhances chromatic contrast at low temporal frequencies and luminance contrast at high temporal frequencies.

Derrington et al (1984), using electrophysiological techniques, found no difference in chromatic sensitivity of both Red-Green (L-M) and Blue-Yellow (S-cone) colour-opponent cells of the parvocellular LGN from 3.5 to 15 Hz. This suggested that the reduction in sensitivity found psychophysically (Gouras and Zrenner, 1979) arises in the cortex.

1.12 Magnocellular and Parvocellular Pathways

The LGN, situated in the thalamus, is composed of six distinct laminae. The four dorsal layers, numbered 3 to 6, are parvocellular and the ventral two are magnocellular. Cells of the magnocellular (M-cells) and parvocellular (P-cells) laminae differ anatomically and functionally. P-cells have small dendritic fields and small axons, relative to M-cells. The larger axons of the M-cells allow faster conduction along these fibres. Functionally, most P-cells show strong chromatic opponency, while most M-cells do not.

The selective damage of LGN M and P cells by ibotenic acid injection has

been used to assess the functional properties of M and P cells in the macaque (Merigan, 1991). When P-cells were damaged, they found that achromatic contrast sensitivity was reduced at low temporal frequencies. Following M-cell damage, however, no sensitivity loss was observed until a higher temporal frequency (20Hz) was reached. This suggests that M-cells transmit high temporal frequency information while P-cells are sensitive to low temporal frequencies. They also investigated the effects of M and P lesions on spatial resolution, and found that M-cell lesions had no effect on visual acuity while P-cell lesions caused a four-fold reduction. These results are consistent with the greater retinal sampling density of P-type (colour-opponent) ganglion cells. In addition, chromatic contrast sensitivity is abolished following a complete lesion of parvocellular laminae, while a magnocellular lesion has no effect on chromatic sensitivity, indicating that P-cells only are sensitive to chromatic contrast.

Schiller et al (1990) used similar methods to observe functional properties of LGN M and P cells in rhesus monkeys. They investigated the effects of lesions on stereopsis, and found that following a parvocellular lesion, stereopsis is reduced for stimuli comprising fine detail. For coarser stimuli, stereopsis was only affected after magnocellular lesions.

Schiller et al suggest that the M (broad-band) and P (colour-opponent) pathways represent two distinct systems, whose functions overlap to allow the perception of a wide range of stimuli in the spatial and temporal domain. Stereopsis and temporal resolution by M and P cells serve to illustrate this relationship. Psychophysical work on humans and rhesus monkeys, and single-cell recordings in monkeys, have demonstrated that magnocellular and parvocellular systems are not mutually exclusive (Logothetis et al, 1989). When isoluminant red-green stimuli are viewed, the activity of neurons in both systems is reduced, but not abolished. In addition, the perception of texture, motion and depth of patterns is reduced at isoluminance. Texture perception is thought to be a function of the parvocellular system, while motion and depth perception are determined by the magnocellular system. It appears, therefore, that both pathways are affected to some degree, at isoluminance. Further evidence against the

exclusive function of magnocellular and parvocellular systems was provided by Ferrera et al (1992, 1994). By selectively inactivating the magnocellular or parvocellular layers of the LGN, they found that responses from pre-striate area V4 were reduced in both cases, suggesting a mixed input to this area from both systems.

Colour-opponent ganglion cells project to the striate cortex via the LGN, while some broad-band ganglion cells, with transient response characteristics, project to the superior colliculus (Schiller and Malpeli, 1977). Input to the superior colliculus is also supplied from the striate cortex. The selective inactivation of magnocellular and parvocellular neurones in rhesus monkeys has demonstrated that this projections consists of broad-band cells only, with no input from colour-opponent cells (Schiller et al, 1979). Thus, all input to the superior colliculus is from the magnocellular system, with no parvocellular contribution.

Schiller and Malpeli (1978) found that S-on centre cells (those activated by input from short-wavelength-sensitive cones) are found mainly in layers 3 and 4 of the LGN, where M- and L-off centre cells dominate. S-off centre cells (inhibited by SWS cone input) are few in number (Dow, 1991) and tend to have antagonistic input from M-cones only (Lee et al, 1987). This is in contrast to the (L+M)-S input to Blue/Yellow (S-cone) opponent units originally suggested by Hering in 1878 (see Lennie and D'Zmura, 1988).

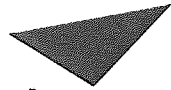
1.13 Multiplexing - The Double Duty Hypothesis

Chromatic information in primates passes from the retina to the visual cortex via the parvocellular cells of the LGN (Schiller, 1991). It is generally agreed that the retinal ganglion cells which project chromatic information to the parvocellular laminae are the spatially and chromatically opponent P-cells, or midget ganglion cells, which make up around 80% of the foveal population of ganglion cells (Lennie and D'Zmura, 1988). As described earlier, these are centre-surround cells with single cone opponency, so the centre and surround are supplied by cones of different wavelength sensitivities. The result of this arrangement is that P-cells are excited by light of one wavelength and inhibited by another, resulting in sensitivity to

chromatic contrast. Another consequence of their centre-surround organisation is that they also show sensitivity to luminance contrast (Wiesel and Hubel, 1966; DeValois and Pease, 1971; Gouras and Kruger, 1979) and so may be said to perform a “double duty”, in coding for both chromatic and luminance contrast. The double-duty nature of P-cells is also referred to as *multiplexing* (Mullen and Kingdom, 1991) and the process of separating luminance and chromatic information is termed *demultiplexing* (Kingdom and Mullen, 1995).

Three types of parvocellular units have been identified in the LGN (Wiesel and Hubel, 1966). Type I shows both spectral and spatial opponency, Type II shows spectral opponency but is spatially co-extensive, and Type III shows spatial opponency only. Lennie and D’Zmura (1988) state that there is no sharp distinction between Type I and Type II, the difference being a matter of degree. The characteristics of Type I cells are the same as those of P-cells, so these two are equivalent. Rodieck (1991) argues that there is a strong distinction between Type I, or P-cells, and Type II cells, citing in particular a significant difference in receptive field size.

Lennie and D’Zmura (1988) described the double-duty hypothesis of multiplexing and demultiplexing on the basis that P-cells only are responsible for projecting chromatic and luminance information to the parvocellular laminae of the LGN. Rodieck has proposed an alternative hypothesis for the coding of separate achromatic and chromatic information in the visual system, which he terms the two-channel hypothesis (Rodieck, 1991). The hypothesis suggests that achromatic information is transmitted via P-cells, or Type I cells, making use of their centre-surround organisation (see figure 1.9). Chromatic signals are transmitted in this model via bistratified ganglion cells and Type II parvocellular cells. As Type II cells are spatially co-extensive, this pathway is less efficient in terms of spatial detail. In this way, the two-channel model segregates luminance and chromatic signals at retinal level.



Aston University

Content has been removed for copyright reasons

Figure 1.9
Two alternative hypotheses for neural processing of chromatic signals (from Rodieck, 1991). The double-duty hypothesis proposed by Lennie and D'Zmura (1988) assumes that only midget cells provide input to the LGN. The two-channel hypothesis suggested by Rodieck (1991) also takes into account bistratified retinal ganglion cells and Type II cells of the LGN. In this model, chromatic signals are processed independently from luminance signals.

Opposition to this theory rests on the fact that, in the main, small numbers of Type II cells have been found in the primate LGN, ranging from 1.6 % to 39 % (DeMonasterio and Gouras, 1975; Reid and Shapley, 1992). In addition, it is unclear how luminance and chromatic information might be separated in P-cells so that the chromatic element may be discarded (Lennie and D'Zmura, 1988).

1.14 Cortical Processing of Chromatic Information

The striate cortex and area V2 of the prestriate cortex may be distinguished in terms of their metabolic architecture (Livingstone and Hubel, 1983; Hubel and Livingstone, 1985; Shipp and Zeki, 1985). Observation of this has been achieved in primates by cytochrome oxidase staining, revealing in V2 a pattern of alternating light and dark stripes, the latter being alternately thick and thin (Livingstone and Hubel, 1983). Thus, a section through V2 parallel to the cortical surface would show a thick dark stripe, light stripe, thin dark stripe, light stripe, and so on.

A similar distinction of cell groups within V1 (striate cortex) has also been observed. Cytochrome oxidase staining shows darkly stained columns of cells extending from the cortical surface towards white matter. If a section of V1 is taken parallel to the cortical surface, these columns appear in cross-section as darkly-staining "blobs" separated by lighter areas known as "interblobs". Cells within V1 blobs are not orientation-selective, but show chromatic opponency, many being of the double-opponent type. Conversely, interblob cells show no chromatic opponency, but are orientation selective (Livingstone and Hubel, 1983).

Vautin and Dow (1985) found four classes of chromatic cell in V1, with spectral sensitivities corresponding to red, green, yellow and blue. "Red" and "blue" type cells were found in non-orientation-selective blob cells, while "yellow" and "green" units were found in the orientation-selective interblob regions. Their findings were consistent with "yellow" cells receiving excitatory input from M-cones only, rather than L+M, and S+ cells receiving inhibitory input from M-cones only (Dow, 1991).

Cells responding to luminance information are well represented in the macaque striate cortex, while those which respond maximally to chromatic stimuli modulated along standard colour axes of MBDKL colour space (see page 26) are less numerous in striate cortex than required to explain psychophysical results (Lennie et al, 1990). This suggests that cells with characteristics of S-cone and L-M cone colour axes may be found in higher cortical areas.

Using cytochrome oxidase staining, Livingstone and Hubel (1983) found that cells within blobs project to the thin stripes of V2, while interblob cells project to the lighter interstripe regions. They were uncertain as to the origin of cells within thick stripes of V2. They also carried out electrophysiological tests of the cells of thin V2 stripes in macaque and squirrel monkeys, in order to determine their functional characteristics. They found that these cells showed no orientation-selectivity, while around two-thirds of them showed colour-opponency, in the macaque (less in the squirrel monkey). In addition, they found that cells of thick stripes and of interstripe regions were orientation-selective, and were not colour-coded. These results are consistent with their earlier findings on the origins of these distinct groups of cells.

Cells in the thin V2 stripes project to prestriate area V4, while those of the thick stripes project to the middle temporal area (MT), otherwise known as V5 (Shipp and Zeki, 1985). V4 is known to be specialised primarily for colour vision (Desimone et al, 1985; Zeki, 1980). Cells of area V5 are directionally-selective, and are instrumental in the perception of motion (Zeki, 1973; Zeki, 1983). These projections to V4 and V5 from distinct regions of V1 and V2 has led to the conclusion that cortical pathways for the perception of motion and colour are segregated (Shipp and Zeki, 1985).

Parallel pathways for the analysis of luminance and chromatic information are not entirely independent, however. Schiller et al (1991) found in monkeys that the detection of isoluminant chromatic stimuli is compromised but remains, in the absence of functional colour-opponent channels. Likewise, the perception of luminance flicker and motion

remains in a weakened form following the ablation of achromatic channel cells.

1.15 Prestriate Area V4

The prestriate area V4, which runs from the anterior bank of the lunate sulcus to the prelunate gyrus, comprises a large proportion of chromatically selective cells (Zeki, 1973; Desimone et al, 1985). Desimone et al (1985) studied the characteristics of V4 cells, in a single-cell electrophysiological study. They found that the cells' receptive fields are up to six times larger in area than those of V1 cells, their antagonistic surrounds being as large as 30 deg. in diameter, which they suggested might be an important factor in colour constancy. In agreement with other workers (Kruger and Gouras, 1980; Zeki, 1983) they found that, far from being specialised only for colour, these cells also showed sensitivity to the dimensions and direction of motion of a bar, comparable in degree to the sensitivity of V1 cells to these stimulus characteristics. This was in contrast to Zeki's earlier findings (1973) that V4 cells show little or no response to achromatic stimuli. By selectively inactivating either parvocellular or magnocellular cell types of the LGN in macaque, Ferrera et al (1992) found mixed geniculate input to V4, while input to V5 has been found using the same methods to be magnocellular only (Maunsell et al, 1991). Zeki suggests (1983) that disagreement between studies on the characteristics of V4 may be due to actual variations in cell populations.

The vast majority of V4 cells are spectrally selective (Zeki, 1980; Desimone et al, 1985), showing a peak response at a preferred wavelength. Cells with particular wavelength preferences appear to be grouped together (Zeki, 1973; Zeki, 1980). Thus, the arrangement of V4 cells with respect to each other appears to be ordered functionally, and not at random.

Zeki (1980) compared the responses of V4 cells in monkey to the perception of the human observer, using a Mondrian display. The responses of V4 cells were found to be consistent with the human observer's perception of the stimulus, and unrelated to the proportions of long, medium and short wavelength light in the illuminant.

Further investigations into colour constancy have been carried out in primates with V4 lesions (Carden et al, 1992; Walsh et al, 1993). Such primates demonstrate poor colour constancy but have unimpaired hue discrimination, suggesting that V4 is an important visual area for colour constancy, but is not crucial for identifying aperture colours.

Thus, area V4 may not be essential in the perception and discrimination of colour. Kulikowski and Walsh (1993) measured visual evoked responses in a monkey after the surgical removal of area V4. They found normal chromatic VEPs recorded over the striate cortex, which taken in conjunction with work on earlier stages in the visual pathway (Kulikowski, 1991), suggests that basic colour categorisation occurs no earlier than area V1 and no later than V2. This conclusion is supported by behavioural experiments in monkeys with V4 lesions (Walsh et al, 1992).

1.16 Summary

Distinct groups of cells which are either colour-opponent (responsive to chromatic stimuli) or broad-band are found along the visual pathway, from retinal ganglion cells to the prestriate cortex (see figure 1.10). Colour-opponent cells are not exclusively responsive to colour, but also to spatial and temporal properties of the stimulus. The two cell types have different but overlapping spatio-temporal response characteristics, allowing the perception of a wide range of stimuli in the spatial, temporal and chromatic domains.

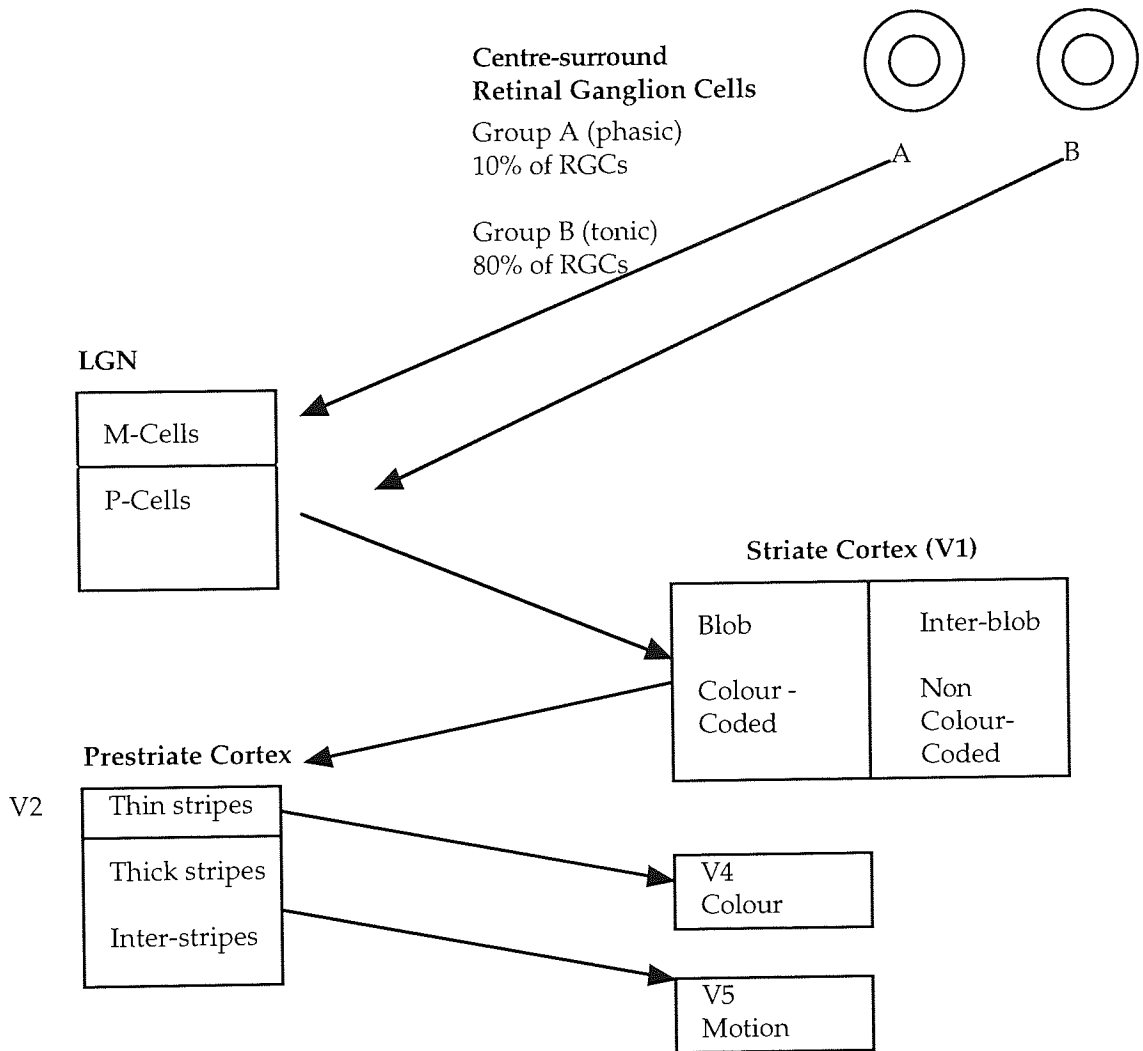


Figure 1.10
A simplified diagram to illustrate the processing of chromatic signals in the visual system.

CHAPTER 2

ANATOMICAL DEVELOPMENT OF THE VISUAL SYSTEM

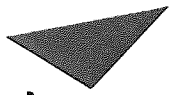
2.1 The Central Nervous System

In the developing human embryo, nerve tissue is derived from a plate of ectoderm adjacent to mesoderm. Mesodermal cells migrate towards the ectoderm, where the combined tissue results in the formation of nerve tissue, a process known as neural induction. The order in which mesodermal cells migrate determines which part of the nervous system the resulting cells will eventually serve. Those migrating first become forebrain cells, cells which migrate later become those of the mid and hindbrain and those migrating last become spinal cord cells. The plate of ectoderm combined with mesoderm in this way is known as the neural plate. Constituent cells migrate towards the centre line of the plate and proliferation of different populations of these cells allows formation of the neural groove. This deepens and closes at the junction with the neural plate, to form a fluid-filled cylinder known as the neural tube, which becomes separated from the plate and closes at both ends.

The cells of the neural tube wall proliferate particularly at the rostral end, allowing three bulges from which the forebrain (prosencephalon), midbrain (mesencephalon) and hindbrain (rhombencephalon) derive. Caudally, tissue of the neural tube goes on to form the spinal cord. The forebrain becomes subdivided into the telencephalon, with primitive cerebral hemispheres, and the diencephalon. At about 4 weeks gestational age, two protuberances, formed by cell proliferation, appear on either side of the diencephalon, and invaginate to form the optic vesicles. The connection between forebrain and vesicle thins to form the optic stalk, while the optic vesicle invaginates further and becomes lined by pigment epithelial and retinal cells. Two more vesicles develop on the forebrain, to form the telencephalon. The cells of the wall of each proliferate and differentiate into specific regions of neural tissue. Cell proliferation in the dorsal wall of the midbrain allows two pairs of protrusions, which form the superior and inferior colliculi.

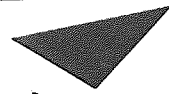
The mature human brain comprises approximately 100 billion neurones. It has been estimated that to reach this number by birth, 250,000 cell divisions must occur per minute in the embryonic human brain (Cowan, 1979). A population of neural cells will proliferate for a determined period of time at the end of which they will begin to migrate towards their final destination. Embryonic neural tissue, a wall of developing neural cells arranged around a vesicle, is segregated into a number of zones according to cell behaviour. In the forebrain, cells in the ventricular zone, adjacent to the ventricle migrate towards the marginal zone, which at an early stage is the most superficial layer of developing cells, and accumulate between the ventricular and marginal zones, forming the cortical plate. Fibres between the cortical plate and ventricular zone form the subventricular zone. Cells of the ventricular zone, which stop proliferating and begin migrating earliest, are destined to lie deepest in the tissue, while those beginning their migration at a later stage in development migrate further from their origin and lie more superficially.

The means by which migrating neurones navigate the often tortuous path to their destination has been widely investigated but is not fully understood. It is thought that glial cells offer physical guidance, as illustrated by figure 2.1, while cues are also offered by environmental structural and chemical changes and gradients (Cowan, 1979). Cells will migrate and grow only in an appropriate substrate and migration is most efficient in an adhesive medium, which facilitates amoeboid movement. In the embryonic tectum, a different pattern of cell generation and migration to that in the forebrain is found. Here, a more complex arrangement exists whereby cells migrating earliest lie deepest, those migrating later lie most superficially while cells which migrate last lie in a zone between these two.



Aston University

Content has been removed for copyright reasons



Aston University

Content has been removed for copyright reasons

Figure 2.1

Glial cells extending from the ventricular to marginal zones of a developing cerebral hemisphere are shown, guiding migrating neurones. Neurones are seen progressing from the inner surface, adjacent to the ventricle, towards the outer surface. The relationship between neurone and glial cell is also depicted (right). (From Cowan, 1979).

Growth of a dendrite or an axon is effected by the growth cone at its tip. Cell membrane tissue passed to the tip from the cell body is added at the tip. Growth in a particular direction is not thought to be mediated by the cell nucleus, and is probably influenced by the cell environment. This is demonstrated by developing retinal ganglion cells, the axons of which emerge at any part of the cell, then once axon formation is begun growth progresses towards the optic disc. Axons of neurones of the same type and destination tend to grow along the same route and in close proximity, as is apparent in the optic nerve. This is known as fasciculation and is thought to be due to the presence of recognisable molecules on the cell membrane surface.

2.2 The Cerebral Cortex

The human cerebral cortex increases in thickness from 800 μm at 113 days gestation to 2000 μm at birth, then reduces to 1700 μm by 12 weeks postnatal. Cortical layers 6, 5 and deep cells of layer 4 are present in the cortex by 75 days gestation. At this stage, many layer 4 cells are in the migration process and the cells of layer 2 are not yet generated. Layer 6 axons are myelinated at birth, while those of layer 2 are less mature, lacking myelin until about 12 weeks postnatal (Arey, 1974). In the macaque, cortical synapses demonstrate a similar innermost first, outermost last developmental trend, appearing first in layer 6 and latest in layer 2, at 140 days gestation (Zielinski and Hendrickson, 1992).

At an early stage in development, dendrites are covered in many hair-like processes, which are thought to be sensors for the detection of axons with which connections may be made. Later, these processes are replaced by shorter spines, which synapse with others spines, and the dendrites themselves grow longer and more uniform in diameter along their length. The number of dendritic spines rises to a peak in monkey brain at five to eight weeks postnatal, then decreases to adult levels over the next seven months. In humans, the number of synapses rises to a peak at 8 months postnatal and falls to adult levels by up to 10 years of age (Cowan, 1979).

In the monkey, and shortly after eye opening in the cat, most neurones of

the striate cortex respond regardless of which eye is stimulated, whereas in layer 4 of the adult striate cortex a number of monocular cells exist, which are responsive to input to one eye only. Investigation of this phenomenon has led to the conclusion that connections between axons originating from each eye and layer 4 of the striate cortex are made at random initially and are changed postnatally, when visual input is received (Shatz, 1992).

It is thought that in the visual pathway cells which fire together become synaptically connected, so that the timing of action potentials is crucial in the establishment and maintenance of synaptic connections (Shatz, 1992). The synapse is strengthened whenever the pre- and post-synaptic neurones generate action potentials simultaneously. In the prenatal and early postnatal striate cortex, each post-synaptic neurone is supplied by a number of neurones from the lateral geniculate nucleus (LGN). When signals arrive from one eye, an action potential will be generated in the post-synaptic neurone as a result of signals from pre-synaptic neurones from that eye reaching the synapse. If pre- and post-synaptic activity coincides, the signal will be strengthened, but if post-synaptic activity occurs without stimulation from a pre-synaptic neurone, the connection is weakened. In this way, connections from one eye are strengthened while those from the other are weakened, so that a number of striate cortex cells have input from one eye only. A further group of striate cortex cells represent both eyes, and develop in the same way as the result of input to the cell being approximately equal for both eyes, so that the two are represented equally. Synapses which strengthen and weaken in this way are known as Hebb synapses, and connection between pre- and post-synaptic neurones is thought to be effected by the transfer of a chemical messenger from the post- to pre-synaptic cell whenever activity of the two coincides. This competitive strengthening of synaptic connections will clearly be possible from birth once vision is taking place. In addition, bursts of activity of groups of neighbouring retinal ganglion cells have been demonstrated in the foetal mammalian eye, suggesting that such competition may begin prenatally (Shatz, 1992).

Regions of the visual cortex populated by cells of the magnocellular

processing stream have been found to reach maturity earlier than those of the parvocellular stream. Layer 4B of the striate cortex receives input mainly from the magnocellular channel, while layers 2 and 3 receive mixed magnocellular and parvocellular input. Burkhalter et al (1993) found that horizontal connections between parts of the human cortex representing different parts of the visual field exist in layer 4B by four months postnatal, while such connections are not present in layers 2 and 3 at this age, being evident by 2 years of age.

Cytochrome oxidase (CO) staining is used as an indicator of degree of metabolic activity, as cells which are highly active contain large numbers of mitochondria, which are rich in the enzyme. In this way, CO-staining blobs and interblob regions of the striate cortex and CO-staining thick and thin stripes of area V2 have distinguished processing streams of the visual system in adults (see Chapter 1). At birth, blobs are not clear in humans, although they are distinct in monkeys at this stage. They are discernible in human infants at 24 days postnatal, and are well organised and adultlike by 4 months postnatal. In the human neonate, layer 4C α of the striate cortex, which receives mainly magnocellular input, has been found to stain more densely for CO than layer 4C β , which receives input mainly from the parvocellular channel. By four months postnatal and in the adult, the opposite is true, with 4C β staining more densely than 4C α . This suggests that the magnocellular system is more active than the parvocellular system in the immature striate cortex, and that this situation reverses with maturity (Wong-Riley et al, 1993).

Intercolumnar connections are those connecting cells which represent information about the same part of the visual field. In the human brain, connections of this type are present by 24 weeks gestational age, while horizontal connections are not present until four months to 2 years, suggesting that individual aspects of the visual scene are perceived earlier than the visual scene as a whole (Burkhalter et al, 1993).

In the developing human brain, formation of the lateral geniculate nucleus begins around the 10th week of gestation. Cellular laminae begin to form

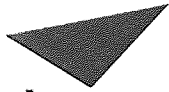
around the 22nd week of gestation and are complete by the 25th week. In the rhesus monkey, distinct laminae form as input from the two eyes becomes separated, and a similar arrangement is thought to exist in humans. The LGN of the human newborn infant resembles that of the adult in terms of lamination and optic disc representation, but differs in that magnocellular and parvocellular cell bodies are smaller than in the adult. Cells in the parvocellular layers (3 to 6) reach adult dimensions by about six months postnatal while those of the magnocellular layers (1 and 2) are adultlike by 12 months postnatal (Hickey and Peduzzi, 1987).

2.3 Development of the Eye

The eye of the newborn human infant is immature and continues to develop for several years (see figure 2.2). The diameter of the newborn eye is 16 to 19 mm, while that of the adult is about 25 mm. The human eye increases in volume only two-fold from birth to adulthood, most of which takes place within the first two years of life. The human body as a whole increases in size and weight approximately 20-fold from birth to adult. This relatively small increase in eye size is consistent with other parts of the nervous system which increase 3 to 4 times in size and weight from birth to adulthood (Arey, 1974).

2.4 Optic Media

The crystalline lens develops from surface ectoderm known as the lens plate, a single layer of undifferentiated cuboidal cells on the optic vesicle surface of the four-week old human embryo. The cells become columnar and undergo rapid division. A slight depression close to the centre of the lens plate is known as the lens pit, or fovea lentis. The columnar cells become covered with a single layer of superficial squamous cells. The lens pit deepens, and closes around the lens vesicle at five to six weeks gestational age, after which event the cells begin to differentiate further.



Aston University

Content has been removed for copyright reasons



Aston University

Content has been removed for copyright reasons

Figure 2.2

A section through the eye of a human embryo at 5 weeks gestation is shown (top). The optic vesicle separates the thick layer of neural retina and the thinner layer of pigmented epithelial cells. Early lens fibres and the lens vesicle are also shown. At about 3 months gestational age, there is considerably less separation of the neural and pigmented retinal layer and early lens fibres have completed their journey across the lens vesicle. (From Williams et al, 1989).

From six weeks gestation, cells of the posterior wall of the lens vesicle increase in length, extending towards the anterior surface, to form primitive lens fibres. In this way, the lens vesicle is obliterated by 7 weeks gestation. The centralmost fibres lose their nuclei, while those at the lens equator retain nuclei and divide to produce more lens fibres from 2 months gestation onwards. The crystalline lens is round in shape before the addition of equatorial fibres, which cause the lens to become oval by 3 months gestation.

Lens fibres contain chromophores, the absorption spectrum of which show a sharp increase at wavelengths below 450 nm (Norren and Vos, 1974). As lens fibres are added throughout life, the accumulation of pigment causes an increase in ocular media density with age, resulting in reduced transmission of short wavelength light by the older eye. Ocular media densities have been found to increase significantly with age (Coren and Girgus, 1972; Werner, 1982; Hansen and Fulton, 1989), although some work suggests that variations with age are not significant (Powers et al, 1981). The discrepancies found in such studies may be due to the large range of normal adult media densities (Wyszecki and Stiles, 1982). Most light absorption by the optic media is due to the crystalline lens, that due to the cornea, vitreous and retina being negligible (Wyszecki and Stiles, 1982). The ocular density of the cornea, aqueous humour and vitreous humour show no change in transmittance of any visible wavelength with age, over the range 4 weeks to 75 years (Boettner and Wolter, 1962).

Surface ectoderm, from which crystalline lens cells differentiate, and the neural ectoderm are separated by a layer of mesoderm cells. The retinal and lental surfaces are both involved in the production and deposition of protoplasm into the mesoderm, which consequently increases in depth. By 6 weeks gestational age, this region is invaded by vascular mesoderm, the hyaloid vessel, and at this stage is known as the primary vitreous.

Progression into the secondary vitreous stage is marked by formation of the hyaline capsule of the crystalline lens, which precludes further involvement of lens tissue in the production of protoplasm. At 6 to 7

weeks, the hyaloid vessel gives off a system of branches, and Muller cells of the retina are thought to produce further protoplasm. At about 10 weeks, smaller vessels begin to atrophy, forming an avascular secondary vitreous. The hyaloid vessel continues to grow in length with the eye, being attached to both the optic disc and the posterior lens surface. At 3 to 4 months gestational age, the hyaloid vessel degenerates and postnatally hangs perpendicularly from the posterior lens surface.

The cornea is derived from mesodermal cells, which at two months gestational age form epithelial, stromal and endothelial layers. The epithelium at this stage comprises two layers of cells, the outermost being squamous and the inner layer cuboidal, while the endothelium is a single layer of cuboidal cells. The cornea and sclera have the same radius of curvature and are continuous, until at 4 months gestation the corneo-scleral junction is formed and the corneal radius of curvature becomes reduced. By seven months gestation the cornea is histologically similar to that of the adult, comprising five distinct layers. At birth, the human cornea has similar dimensions to that of the adult in terms of radius of curvature and thickness at the vertex and at the margin. They differ only in that the diameter of the neonate cornea is 2 mm smaller horizontally and 1 mm smaller vertically than in the adult (Duke-Elder, 1961).

2.5 Retinal Development

The wall of the optic vesicle is composed of neural ectoderm, which is continuous with the neural ectoderm of the forebrain. Differentiation of this tissue results in formation of the retina, pigment epithelium, iris muscle tissue and the neuroglia and nerve fibres of the optic nerve. Formation of the optic vesicle includes a cleft inferiorly, which offers continuity between the inner neural tissue of the vesicle and the optic stalk. This pattern of development of the human eye allows an open path to the developing cortex for retinal ganglion cell axons growing from the eye along the optic stalk, and forming the optic nerve (Mann, 1964).

Differentiation of neuroepithelial cells of the optic vesicle results in separation into two zones by 5 weeks gestational age, the deeper of which

contains cell nuclei and the more superficial zone being free of nuclei. The nucleated layer of actively differentiating cells forms the neural retina and is 0.1 mm thick, while the outer layer from which pigment epithelium is derived is 0.3 mm at this stage. A small gap between the two layers is all that remains of the optic vesicle cavity. This gap persists to a certain extent in the adult retina, where the connection between outer photoreceptor segments and pigment epithelial cells is loose, and the two may become separated relatively easily. The neural retina is itself composed of two distinct layers of cells, the inner and outer neuroblastic layers, formed by proliferation of the immature neural retinal cells and their migration towards the inner optic vesicle surface.

The time course of cell differentiation is such that innermost retinal elements including ganglion cells are the first to appear and photoreceptors are the last. The inner and outer neuroblastic layers become separated by non-nucleated tissue known as the transient layer of Chievitz. This is a thin, fibrous acellular zone which first appears on the foveal slope at about 25 weeks gestation in humans and reduces in thickness until it is no longer evident at 45 months post natal (Abramov et al, 1982; Hendrickson and Youdelis, 1984). An innermost layer of non-nucleated tissue lies anterior to the inner neuroblastic layer and is known as the marginal layer. By 7 months gestation the inner neuroblastic layer has differentiated into ganglion cells, amacrine cells and Muller fibres, the outer neuroblastic layer has differentiated to form bipolar and horizontal cells and rod and cone cell bodies, and the marginal layer forms the retinal nerve fibre layer.

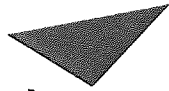
In the macular region of the human eye, the density of pigment epithelial cells increases steadily as a result of centripetal shifting, reaching a plateau at 6 months postnatal age. Peripherally, pigment epithelium reduces in density during the first two postnatal years, and enlargement of individual cells allows coverage of the expanding retinal surface area which increases from 300 mm² at 26 weeks gestation to 907 mm² at 6 years of age (Robb, 1985). In the monkey retina, pigment epithelial and cone cells show different patterns of migration and are thought to develop independently of one another (Robinson and Hendrickson, 1995).

2.6 Foveal Development

The cones of the foveola are the first photoreceptors to stop dividing and to start differentiating, at about the 14th week of gestation in humans (Hendrickson, 1992) and the last to reach maturity, the final stages of development occurring well into adulthood (Youdelis and Hendrickson, 1986). Early reports of retinal development stated that the persistence of the transient layer of Chievitz was the main sign of foveal immaturity (Mann, 1964). It is now clear that the fovea is immature for much longer, and that degree of maturity is marked by photoreceptor characteristics.

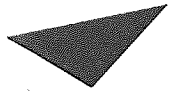
The anatomy of the human fovea has been analysed qualitatively and quantitatively from 22 weeks gestation to 72 years of age (Hendrickson and Youdelis, 1984; Youdelis and Hendrickson, 1986; Diaz-Araya and Provis, 1992; Hendrickson, 1992). Figure 2.3 illustrates stages of development of the foveal cone from 22 weeks gestation to 45 months postnatal age. At 22 weeks gestational age, the internal limiting membrane is present anterior to the ganglion cell layer, horizontal, bipolar and Muller cells are developing in the inner nuclear layer, and there is no evidence of the transient layer of Chievitz. The outer plexiform layer is well defined, although thin, and contacts may be seen between these processes and the cone bases. The outer nuclear layer is a single layer of columnar epithelium, each of which is an undifferentiated cone cell, and cone density at the central fovea is 18×10^3 per mm^2 .

The foveal depression found in the central rod-free area of the mature retina is absent at 22 weeks gestational age, the foveal area is circular or elliptical, approximately 1.5 mm in diameter. At this stage, the region contains only cones, although at the earlier age of 13 weeks rods have also been identified in the central foveal region.



Aston University

Content has been removed for copyright reasons



Aston University

Content has been removed for copyright reasons

Figure 2.3
Diagram illustrating stages of development of human foveal cones. From left to right, cone ages are: 22 weeks gestation, 34 to 36 weeks gestation, term, 15 months postnatal and 45 months postnatal. The fibre of Henle (FH), inner (IS) and outer (OS) segments become longer and thinner throughout this period. (From Hendrickson and Youdelis, 1984).

The number of rods at the human foveola is constant at 13, 15, 18 and 24 weeks gestation, while the number of cones increases so that the region becomes heavily populated by cone cells. At 15 to 18 weeks, there is a marked accumulation of rods parafoveally, and the density of rods 2 mm away from the fovea increases with age (Diaz-Araya and Provis, 1992).

At 24 to 26 weeks gestation, a slight foveal depression forms, due to thinning of the ganglion cell layer and the inner nuclear layer. The inner and outer nuclear layers are thicker; the former is mainly composed of Muller cells and the latter contains vertical processes entering from the inner nuclear layer to meet the cone pedicles. The transient layer of Chievitz appears on the nasal foveal slope. The photoreceptor layer remains a single layer of cones, but pedicles are formed on their proximal bases and inner and outer segments begin to appear. By 28 to 29 weeks gestation, the foveal pit is deeper and the inner nuclear layer thinner at the fovea. The layer of Chievitz now appears on both foveal slopes, although it is more prominent nasally.

By 34 to 36 weeks gestation, the foveal pit is prominent, due to the diminution of the ganglion cell and the inner nuclear layers. A single layer of cones exists in the foveal pit, with a double layer on the foveal slope, where the cones are much more elongated than more central cones, with well defined inner and outer segments and pedicles. The pigment epithelial cells have fine apical processes which interdigitate with cone outer segments.

At five days postnatal, the foveal depression is more prominent, and has a diameter of 675 μm . Ganglion cells are reduced to a single layer and the inner nuclear layer is less than 3 cells thick in this region. At this stage, the foveal cones are thinner and more elongated (inner segment width of 6 μm , length of 9 μm ; outer segment width 1.2 μm , length 3.1 μm) the pedicles are larger and are invaginated with synaptic contacts. Cone density at the foveola is increased to 36×10^3 . Again, cones on the foveal slope are at a more advanced stage in development, with longer and thinner inner and outer segments than cones at the centre.

At 13 to 15 months postnatal, the ganglion cell layer and the inner nuclear layer fuse at the foveal slope, being one cell thick at the central fovea. The cones are 3 to 4 cells deep on the foveal slope and 2 to 3 deep at the centre. At 45 months of age, the transient layer of Chievitz is no longer evident, the foveola is 330 μm in diameter, the central foveal cones have inner segments reduced in width to 2 μm and increased in length to 26 μm and outer segments with an unchanged width of 1.2 μm and an increase in length to 50 μm . Cone density at this age is 108×10^3 , and increases to 208×10^3 at 37 years of age.

Visual acuity is ultimately limited by the efficiency of foveal cones, and the findings summarised above indicate that spatial vision in humans is limited by anatomy of the fovea until well into the second year of life. Limitations imposed on the infant visual system by foveal cone immaturity and density were considered by Banks and Bennett (1988). Front-end properties including optics, cone density and cone dimensions of the neonate visual system were programmed into an ideal observer from which visual acuity, contrast sensitivity and chromatic discrimination could be computed. By comparing the efficiency of the neonate ideal observer to that of the mature visual system, Banks and Bennett were able to determine that front-end and post-receptoral properties of the infant visual system impose limitations on spatial and chromatic vision.

The width of the neonatal foveal cone inner segment is significantly greater than that of the adult, one consequence of which is that neonate cones are more widely spaced, allowing less efficient sampling of the retinal image. In addition, the neonate inner segment is of uniform width, while in the adult the inner segment is tapered, so that the mature foveal cone demonstrates more efficient light-catching properties (see figure 3.3). The length of the cone outer segment in the neonate fovea is significantly less than that of the adult, so that fewer isomerizations are produced per unit number of photons by the foveal cone than by the adult. As a result of this factor in addition to cone spacing and shape, the neonate central fovea effectively absorbs 350 times less light than the adult central fovea (Banks and Bennett,

1988).

2.7 Macular Pigment

Macular pigment is present in the embryonic eye by at least 17 weeks gestational age, although the macular reflex seen on ophthalmoscopic examination of the fundus is imperceptible at this stage (Bone et al, 1988). With wide inter-individual variations, the absorption spectrum of human macular pigment peaks at about 460 nm, with negligible absorption at wavelengths greater than 560 nm (Pease et al, 1987). In the macaque monkey, macular pigment is found in cone axons and to a lesser extent in the inner plexiform layer and is most heavily concentrated in the rod-free foveola (Snodderley et al, 1984a,b), where it is thought to serve two main functions. Firstly, spectrally selective intra ocular filters may serve to reduce chromatic aberration by reducing the transmission of short wavelength light. A quantitative analysis of this function has demonstrated that the density and spectral characteristics of macular pigment are appropriate to prevent the perception of chromatic blur in light such as daylight, containing short wavelengths (Reading and Weale, 1974). In addition, macular pigment is thought to protect the retina against photochemical damage caused by prolonged exposure to short wavelength light (Ham et al, 1978).

Macular pigment comprises two carotenoids, zeaxanthin and lutein. The presence and density of macular pigment has been measured using psychophysical means (Werner et al, 1987). Wide inter-individual variations were found, but there was no significant age-related variation over the range 10 to 90 years. Similar measurements have also been made using the more objective method of high performance liquid chromatography (HPCL) to determine the presence and density of macular pigment in prenatal eyes and postnatally at an age range of one day to 95 years (Bone et al, 1988). This work also found no significant variation in density with age over the range 3 to 95 years. The mean ratio of lutein to zeaxanthin was also constant over this age span, at 0.77. In the 0 to 2 year age range, however, this ratio was 1.44, and prenatal eyes (17 to 22 weeks gestational age) showed a mean ratio of 2.51. A five-fold increase in mass of

total macular pigment was found between 3 and 6 months postnatally, although this dropped back again at 9 months. In prenatal eyes the mean macular pigment mass was 3 ng (individual values not given), while within the first postnatal year it was 10.2 +/- 9.65 ng and from one year onward mass had increased to 38.3 +/- 15.35 ng. The difference between values during and after the first postnatal year are statistically significant ($p=0.012$).

2.8 Neural Plasticity

Development of neuronal circuitry of the mature visual pathway occurs pre and postnatally. Prenatal development is independent of external influences. Postnatally, the establishment and maintenance of neural connections depends largely on visual experience. Following observations that the removal of congenital cataracts in childhood results in no improvement in visual acuity, Wiesel and Hubel (1963) began a series of experiments to investigate the effects on the visual system of monocular visual deprivation in early postnatal life.

The visual system which is allowed to develop with good and equal quality visual input to each eye has an equal number of cortical cells devoted to each eye, with a greater number responsive to input from both eyes (Wiesel, 1982). If one eye is deprived of normal visual input at an early age, an abnormally large number of cortical cells becomes devoted to the other eye, with few cells responsive to the deprived eye and to binocular visual input.

The effects of different types of visual deprivation demonstrate that it is the deprivation of form rather than light which causes this cortical change. In addition, visual deprivation has a profound effect on the visual system at an early age, but little or no effect at a later age. The period during which deprivation has a significant effect on the visual system is known as the sensitive period (Hubel, 1995).

In monkey, during the first four to six postnatal weeks input to layer 4C becomes segregated, so that monocular injection of radioactive amino acid reveals striations which represent axon terminals on groups of cortical cells responsive to each eye. Input from each eye is represented in alternate

stripes, or groups of cells. Interruption of normal visual input from one eye during the sensitive period does not disrupt the pattern of alternating stripes, but results in the stripes of cells representing the deprived eye being diminished. That is, the deprived eye has less cortical representation than normal, and the unaffected eye has greater representation (Hubel, 1995).

The cells of the lateral geniculate nucleus are physically but not physiologically affected by visual deprivation (Wiesel and Hubel, 1963). The geniculate cells corresponding to the deprived eye respond normally, but are diminished in size. This is a reflection of the fact that the affected eye is less well represented in the cortex, so geniculate cells corresponding to that eye have less axon terminals to support. The consequence of this is that, although the LGN cells responds normally, they are physically diminished.

Following a period of visual deprivation, improvements in visual function may be effected by normalising visual input to the previously deprived eye. This is a manifestation of the plasticity of cortical connections, which is demonstrated to a high degree at an early age and reduces with age until cortical connections are firmly established and little or no plasticity is demonstrated in adulthood. In humans, cortical plasticity is used clinically to partially or fully correct the condition of amblyopia, a condition in which monocular or binocular visual acuity is lower than normal (Snellen 6/9 or worse) in the absence of ocular pathology, reflecting the cortical under-representation of a deprived eye. Amblyopia may be caused by cataract or ptosis (deprivation amblyopia), astigmatism (meridional amblyopia), strabismus, anisometropia or ametropia.

In cats, cortical plasticity has been demonstrated by imposing monocular visual deprivation during the first few months of life, then restoring normal visual input to that eye while depriving the second eye (Mitchell, 1990). Initially, the deprived eye showed reduced visual acuity, while that of the fellow eye was normal. After reversal of the monocular occlusion, normal visual acuity was recovered in the first eye, and acuity degenerated in the second eye. An optimal period of reverse occlusion was found to be 70% of daily visual experience. This allowed the vision of each eye to

develop normally following initial monocular deprivation.

Clinical experience with humans generally suggests that plasticity of the visual system exists until 10 to 12 years of age (Stidwill, 1990), although some workers have demonstrated visual acuity improvements in the amblyopic eyes of patients aged 60 to 80 years (Mallett, 1988). In the somatosensory system, the region of cortex devoted to a limb adopts input from neighbouring parts of the body after the limb is amputated. Work such as this demonstrates plasticity of cortical connections, which may continue to some extent well into adulthood (Hubel, 1995).

2.9 Myelination

Myelin is a fatty substance consisting mainly of phospholipids, lipo-protein, free cholesterol and lipids containing carbohydrate, which surrounds nerve fibre axons to form a sheath to insulate the cell and maximise impulse transmission speed. In the peripheral nervous system, myelin is produced by Schwann cells, but in the central nervous system myelin sheaths are formed when oligodendrocytes wrap around nerve axons. Myelination in the brain usually proceeds from the cell body to its destination. The optic nerve is the exception to this, with myelination occurring first at the cortex and progressing towards the lamina cribrosa.

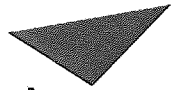
Myelin is not evident in the human visual pathway until 23 to 32 weeks of gestational age (Bembridge, 1956; Magoon and Robb, 1981), when it appears on the optic tract and the cortical portion of these axons. Myelination reaches the lamina cribrosa by term and the myelin sheath increases in density dramatically during the first postnatal year and more gradually during the second year (Magoon and Robb, 1981).

2.10 Cranial Development

A brief discussion of development of the skull is relevant here, as resistance caused by the skull and scalp tissue affects the visual evoked response, and may be expected to change with development in early life. Cranial bones develop from mesenchymal cells surrounding the cranial vesicles of the embryo. At about one month gestational age, the mesenchyme thickens

and condenses, forming localised masses of specialised tissue. The first of these masses to be formed is the occipital plate, from which the occipital bone develops (Ford, 1956).

Ossification of cranial bone tissue is incomplete at birth, and many bones at this stage are composed of several elements linked by layers of fibrous tissue or cartilage (Pritchard et al, 1956). The occipital bone at birth comprises squamous, lateral and basilar parts which are not fused. Regions of the cranium where bones are not fused at their junction are known as fontanelles (Soames, 1995). Six fontanelles are present at birth, the largest of which is the anterior fontanelle, which has a diameter of about 25 mm at this stage, at the junction of the sagittal, coronal and frontal bone sutures (see figure 2.4). The posterior fontanelle is at the junction of the sagittal and lambdoid sutures, and is triangular in shape. The sphenoid and mastoid fontanelles are the smallest, and occur at the junctions of each of these bones with the parietal bones. The sphenoid, mastoid and posterior fontanelles close within two to three months of birth. The larger anterior fontanelle closes towards the middle of the second year of life.



Aston University

Content has been removed for copyright reasons



Aston University

Content has been removed for copyright reasons

Figure 2.4

The superior aspect of the full-term human neonate skull illustrates fontanelles and incomplete sutures (top). Most of the increase in size of the human skull from birth to adulthood occurs in the viscerocranium, as seen here. The neonate and adult cranial vaults are similar in height (a-b). (From Soames, 1995).

CHAPTER 3

SPATIAL AND CHROMATIC VISION IN INFANTS

The Development of Spatial Vision

3.1 Measurement Techniques

By necessity, infant vision is assessed using objective methods, including both electrophysiological and behavioural techniques. Visual psychophysics attempts to determine measures of absolute threshold (the weakest or smallest detectable stimulus) and difference threshold (the smallest detectable change in stimulus). Threshold measures give an indication of visual limits and provide information about the characteristics of underlying sensory mechanisms. In adults this is achieved by voluntary responses from the observer, such as 'yes' or 'no' answers, or pressing a button.

3.2 Infant Visual Psychophysics

Visual psychophysical techniques applicable to infants include the method of constant stimuli and the adaptive staircase method (Banks and Dannemiller, 1987). The method of constant stimuli involves presentation to the infant of a number of visual stimuli estimated to span detection threshold. Percent correct scores at each stimulus level are recorded, which usually extend from 50% (chance performance; not seen) to 100% (stimulus always seen). Threshold is determined by plotting performance as a psychometric function, which is usually steepest at 70 to 75% correct. For this reason, threshold is arbitrarily assumed to be around this point and values of between 70 and 75% are generally taken to indicate threshold.

The adaptive staircase method involves the presentation of stimuli which depend upon the observer's response to the preceding stimulus. This method allows a relatively small number of trials to be carried out, because stimuli converge on the threshold point. This is particularly desirable in infant work, to minimise the loss of attention brought about by a large number of trials. However, the majority of trials in the adaptive staircase are close to threshold, which itself may result in loss of attention. In

addition, the experimenter may more accurately identify unreliable data sets using the method of constant stimuli, when infants become inattentive to those stimuli which should be easily detected.

The two psychophysical methods most commonly used with infants are preferential looking (Fantz, 1965) and forced-choice preferential looking (Teller, 1979). Both involve the presentation of a patterned stimulus on a card or CRT monitor, adjacent to a uniform stimulus of the same mean chromaticity and luminance. Forced-choice preferential looking (FPL) is an adaptation of the preferential looking (PL) technique, in which the experimenter is blind to the stimulus position, and makes a decision as to whether the infant shows a preference for one side or the other by observing his behaviour. Behavioural aspects used in making this decision may include direction of first fixation, facial expression or duration of fixation, for example. Any factor or combination of factors may be chosen but must be used consistently throughout the trial. PL and FPL are used clinically in the assessment of infant visual acuity by means of Teller, Keeler and Cardiff cards, for example. In research on infant vision, stimuli are generally presented on CRT monitors. Both stimuli may be present side-by-side on the same screen, or on adjacent screens.

One difficulty with preferential looking techniques is that this type of behavioural response is not necessarily a reliable indicator of stimulus visibility (Banks and Dannemiller, 1987). This non-sensory factor hampers the transfer of information from the infant observer to the experimenter. In addition, young infants find re-fixation difficult and so may be unable to change fixation to the pattern. This factor changes with age, as re-fixation becomes easier from about three months of age, making comparisons with age unreliable (Atkinson, 1991, 1992).

Optokinetic nystagmus (OKN) is another technique which has been used in the assessment of infant vision. This involves a series of involuntary eye movements in response to gratings of specific spatial frequency moving rapidly across the visual field (Dobson and Teller, 1978). The eye movements include two phases: a slow fixation, or tracking of the stimulus,

followed by a rapid saccadic movement, or re-fixation on a more central part of the visual field. These reflex movements, which continue while the stimulus is moving, are used in OKN to determine the highest spatial frequency or lowest contrast which elicits a response movement. OKN movements are asymmetrical in neonates and become symmetrical at around 2 months of age, which is thought to reflect subcortical mediation of visual function before this age (Bronson, 1974; Atkinson, 1991, 1992).

3.3 Infant Visual Electrophysiology

Visual electrophysiology is used to determine the electrical response to a temporally modulated visual stimulus, recorded from the retina or visual cortex. Retinal responses are recorded by flash or pattern electroretinography (ERG), which provides information on the function of retinal photoreceptors. Specific responses from rods and cones may be elicited by using particular types of stimulation (Ikeda, 1993). Electrical responses from the visual cortex are visual evoked responses; when distinct components are elicited the response is known as a visual evoked potential (VEP).

The visual evoked response is widely used to investigate infant vision. A stimulus of known spatial and temporal parameters, usually presented on a CRT monitor, is viewed by the infant whose attention has been drawn to it by a noise or small toy. The visual evoked response is recorded to a range of patterned stimuli and to a uniform stimulus of the same mean luminance as the patterned stimuli. These responses may later be compared in order to determine which responses are elicited by visual stimuli and which are not significantly different to the unstimulated response, representing EEG noise levels. In this way, the experimenter is able to determine threshold, which is generally defined as the highest spatial frequency, or the lowest contrast, to which the visual system will respond.

Visual evoked responses may be recorded by transient or steady-state methods (Regan, 1982). Transient VEPs are recorded in response to a stimulus of sufficiently low temporal frequency to allow each response to be recorded without interference from subsequent responses. Steady-state

VEPs, which are elicited from stimuli of relatively high temporal frequency, overlap each other as the response to one stimulus has not terminated before the next begins. The transient method allows response morphology to be investigated, in addition to characteristics such as amplitude and latency. The steady-state VEP loses its morphology but may be recorded rapidly, and so has advantages in infant work.

One steady-state technique is known as the sweep VEP (Tyler et al, 1979) and has become widely used in the assessment of infant visual function. The stimulus for the sweep VEP is generated on a CRT monitor, and comprises gratings or checks which are counterphase modulated at a relatively high temporal frequency (3 to 20 Hz). During a recording period of 10 to 20 seconds, spatial stimulus parameters such as spatial frequency at a constant level of contrast or contrast at a constant spatial frequency, are changed every half second. In this way, the steady-state VEPs to a wide range of stimuli are recorded within a period of up to 20 seconds in adults and 10 seconds in infants, whose attention span is more limited. The clear advantage of this technique in infant work is that it can be completed relatively quickly. Its main disadvantage, as with all steady-state VEPs, is that response morphology is lost.

Describing and measuring a transient VEP is somewhat arbitrary and subjective, so that different experimenters may disagree, and inconsistencies may occur. The steady-state VEP is described unequivocally by Fourier analysis, in terms of amplitude and phase. The output of a Fourier analyser allows much less disagreement than the subjective analysis of the transient VEP. Both techniques have been and are currently used in the assessment of infant visual function, each being chosen for advantages which may be beneficial to a particular study. For an investigation of changes in response morphology and latency with age, the transient VEP is the method of choice, while for assessment of visual acuity and contrast sensitivity based on response amplitude the steady-state or sweep steady-state VEP may provide more reliable information.

3.4 Visual Acuity

Over the period from 1 to 7 months of age, VEP visual acuity has been found to increase from 1 cpd to the adult-like level of 30 cpd (Marg et al (1976). Similar VEP acuities were determined by Sokol (1978), while Banks and Salapatek (1978) measured acuities of 2.4 cpd at 1 month, 2.8 cpd at 2 months and 4.0 cpd at 3 months using FPL. Using the sweep VEP technique, Norcia and Tyler (1985) investigated the development of visual acuity over a 12-month period from birth. In this study of 197 infants, acuity was found to be 4.5 cpd at 1 month of age, increasing to an average of 20 cpd at 1 year (see figure 3.1). In this study, the adult mean of 24.3 cpd determined by the same method was approached by some infants at only 8 months of age.

It has been suggested that the difference between VEP and FPL estimates of infant visual acuity may be due to the criteria used in determining threshold by each method (Dobson and Teller, 1978). In VEP testing, threshold is determined according to the stimulus eliciting zero VEP amplitude, found by extrapolation (Campbell and Maffei, 1970; Morrone et al, 1990, 1993). Psychophysical thresholds, however, are generally based on stimuli yielding 70 to 75% correct responses from the observer. In adults, acuity and contrast sensitivity are similar when determined by either method (Norcia et al, 1990), suggesting that this factor does not entirely account for the differences found in infant measures.

Stimuli for VEP recordings are temporally modulated and as such may yield lower threshold estimates (higher sensitivity) than the stationary stimuli generally used in psychophysical tests. To test this hypothesis, Dobson and Teller (1978) used both static and temporally modulated stimuli to determine VEP visual acuity in two-month-old infants. They found similar estimates using both, suggesting that the type of stimulation used in electrophysiological work does not affect threshold measurements. Later work, however, (Sokol et al, 1992) has shown that VEP and FPL acuities measured in infants using temporally modulated stimuli are similar, and that differences emerge when different types of stimulation are used. This suggests that the use of temporally modulated stimuli in VEP studies yields higher acuity estimates than the use of static stimuli in FPL work.



Aston University

Content has been removed for copyright reasons

Figure 3.1

Group-averaged sweep VEP acuities with respect to chronological age from one month to one year (from Norcia and Tyler, 1985).

In addition, methods of threshold determination, immaturity of visuomotor areas and motivational factors may contribute (Banks and Dannemiller, 1987; Wilson, 1988).

3.5 Contrast Sensitivity

As described earlier, the sweep VEP method provides a rapid means of assessing visual function in infants, and this technique has been used to determine contrast sensitivity in infants (Norcia et al, 1989). Norcia et al (1990) used the sweep VEP method to measure contrast sensitivity and acuity in 51 infants from 1 week to 45 weeks of age. They found that contrast sensitivity to low spatial frequencies develops rapidly over the first two months of life, then reaches a plateau at around 10 weeks of age. Conversely, sensitivity to high spatial frequencies, close to visual acuity, was found to develop more gradually and steadily until around 30 weeks of age. Norcia et al suggest that this pattern of development may reflect the differential development of underlying post-receptoral mechanisms.

The contrast sensitivity function (CSF) in young infants has been found to change form significantly with age. At one month, the function is low-pass, while at 2 and 3 months of age it assumes the band-pass characteristic of the adult. This has been taken to illustrate a development of lateral inhibition between 1 and 2 months of age (Banks and Salapatek, 1976, 1978, 1981; Banks, 1983).

The representation of the CSF as the mean for a group of individuals has been criticised, however, as this type of function may mask wide inter-individual differences, found particularly in infant data (Peterzell et al, 1993, 1995). Movshon and Koirpes (1988) investigated the development of spatial contrast sensitivity in human and monkey infants by looking at individual and mean functions. They reanalysed the data of Banks and Salapatek (1978) in terms of individual rather than group-averaged results, and found that the CSF did not change shape, but was generally band-pass from 4 weeks of age, with wider inter-individual variations than shown by adult data.

Peterzell et al (1993, 1995) also illustrated the possible errors introduced by

the use of mean, or representative, rather than individual contrast sensitivity functions. They measured FPL contrast sensitivity longitudinally at 4, 6 and 8 months of age in 25 infants, and found some individual functions to be band-pass and some low-pass, while all representative functions were band-pass.

Contrast sensitivity differences at a range of spatial frequencies in individual infants have been used to demonstrate that multiple spatial channels exist in the visual system at 1, 2, 3 and 4 months of age (Peterzell et al, 1995). This is contrary to the finding of Banks and Ginsburg (1985) that multiple spatial channels are functional at 3 months but not at one-and-a-half months of age.

Spatial frequency-tuned channels in young infants have also been demonstrated using steady-state VEPs (Suter et al, 1994). After adapting 3, 6 and 12-week-old infants to specific spatial frequencies, VEP amplitude was attenuated to frequencies at or close to the adapted level, suggesting that multiple spatial frequency-tuned mechanisms exist in infants from as early as 3 weeks of age.

3.6 Infant Accommodation

Ocular accommodation in infants has been investigated by various means, including dynamic retinoscopy and photorefracton. Dynamic retinoscopy allows the freely accommodating eye to view a target of chosen viewing distance while retinoscopy is carried out. Photorefracton employs a xenon light source viewed by the infant, emitted from a fibre optic tip. Four cylindrical lenses are used to refract light returning from the subject's eye into the two principal meridians. In this way, the state of focus of each of the lights may be used to assess refractive error in each meridian. In the determination of accommodative ability, this technique is carried out on a freely accommodating eye at a range of viewing distances.

Early work on infant accommodation by Haynes et al (1965) using dynamic retinoscopy found that at less than one month of age infants are unable to accommodate, and that their ability improves with age, reaching adult

levels by 3 to 4 months. This work was repeated by Banks (1980), who found that at 3 to 5 weeks of age infants do show the ability to accommodate, although not as accurately as two and three-month-olds. Banks suggested that the difference between these results and earlier work may be due to stimulus differences. Haynes et al had used a small shield as a target, which may have been difficult for young infants to resolve at some viewing distances and may not have been an adequate stimulus for accommodation, while Banks used a larger stimulus comprising a checkerboard pattern.

A study of infant accommodation by Braddick et al (1979) using photorefracton at stimulus distances of 75cm and 150cm also suggests that infants are able to accommodate before one month of age. At this age, however, accommodation is more accurate at the closer viewing distance than at 150cm. In agreement with previous work, accuracy of accommodation was found to increase with age, becoming adult-like at both viewing distances by six months of age.

Two hypotheses for the inaccuracy of accommodation in young infants were proposed and tested by Banks (1980). The Motor Hypothesis suggests that accommodation is restricted by a physical inability to change focus, while the Sensory hypothesis argues that infants accommodate less accurately than adults because their reduced visual acuity offers a weak stimulus for accommodation. By determining that infants have a relatively large depth of focus, Banks showed that accommodative errors may exist in young infants without a significant reduction in acuity. This suggests that depth of focus allows objects to remain clear at a range of viewing distances without the need to accommodate, which is not fully consistent with either hypothesis, but may itself account for the limited accommodation demonstrated by young infants.

The Development of Chromatic Vision

3.7 Photopic Spectral Sensitivity

Spectral sensitivity in infants under light-adapted conditions has been determined using VEPs and psychophysical techniques. Dobson (1976) made use of a VEP latency increase with reduced stimulus luminance, to plot sensitivity to a range of eight test wavelengths, in five two-month-old infants and in two adults. Latency was used as an indicator of sensitivity, as it was found to be more reliable than amplitude, in its variation with luminance. The infants' results were compared to those of the adults, and showed relatively higher sensitivity to short-wavelength stimuli. At middle to long wavelengths, however, the infant and adult functions were similar. The possibility that this difference might be due to eccentric viewing by infants was rejected following an experiment in which central and eccentric viewing was compared in adults and found not to be significantly different. Rod contributions were also considered unlikely, as levels of VEP latency did not suggest scotopic involvement (Wooten, 1972). A more likely explanation was thought to be lower density of macular pigment in the infant than the adult eye.

Peeples and Teller (1978) used the forced-choice preferential looking method to determine photopic spectral sensitivity in two infants tested between the ages of 2 and 3 months post-term. Three adults were also tested psychophysically for comparison. In disagreement with Dobson (1976), they found that infant and adult spectral sensitivity functions were similar, and that infants showed relatively lower sensitivity to stimuli at the spectral extremes, but not to mid-spectral stimuli. They acknowledged that the differences between adult and infant results are slight, and that these findings are true only for the set of conditions used in their experiments. From the general similarity of sensitivity curves found in infants and adults, it was inferred that adult and infant brightness matches are similar under this set of conditions. Peeples and Teller stress that this may not be true of another set of adaptation conditions, and so brightness matches for infants should be determined independently, and not assumed to be the same as those of adults.

In agreement with Dobson (1976), Moskowitz-Cook (1979) found, also using visual evoked response latency, that infants up to 19 weeks of age showed relatively higher photopic sensitivity to short-wavelength stimuli. This was thought not to be due to differences in macular pigmentation or crystalline lens density, as the adults tested for comparison were young. Infants in the 19 to 22 week age group, however, showed the same shape sensitivity curve as adults, at all parts of the spectrum. In consideration of the possibility that extra-foveal cones and rods might contribute to sensitivity to light of shorter wavelengths, Moskowitz-Cook notes that foveal representation at the cortex far outweighs that of extra-foveal retina, and is closer to the scalp, in adults, but in young infants, lower skull resistance may allow deeper cortical responses to be recorded at the scalp. It is also possible that extra-foveal cones may make a relatively greater contribution to the evoked response in young infants, because foveal cones lag behind extra-foveal cones in their anatomical development (Youdelis and Hendrickson, 1986; Hendrickson, 1992).

Volbrecht and Werner (1987) determined photopic spectral sensitivity in nine infants aged four to six weeks, and in three adults for comparison. Test stimuli ranged from 400 to 550 nm, and were presented on a yellow adapting background. Steady-state VEPs were recorded in response to 2Hz modulation of each stimulus, in order to determine discrimination thresholds. In contrast to some previous findings described above, they found that sensitivity to short wavelength stimuli was similar in infants and adults.

Clavadetscher et al (1988) used the FPL method to determine photopic spectral sensitivity in 3- and 7-week-old infants. A range of five 8-degree test stimuli from 417 to 645 nm were presented against a 547 nm surround. The infants' spectral sensitivity curve followed that of the adult under scotopic conditions and under photopic conditions with eccentric fixation (30 degrees). It was concluded that rods may contribute to infants' spectral sensitivity under the conditions of the experiment (low photopic or mesopic light levels).

In a study of 42 infants aged 2 to 4 months and three adults, sensitivity to short-wavelength stimuli was elevated above the $V\lambda$ photopic function in both infants and adults (Bieber et al, 1995). This finding was thought to be partly due to inter-individual and age-related variations in ocular media density (Werner, 1982; Hansen and Fulton, 1989), which may explain the discrepant findings of previous studies.

3.8 Scotopic Spectral Sensitivity

Powers et al (1981) used the FPL technique to determine dark-adapted spectral sensitivity in infants at 1 and 3 months of age. Between these ages, the shape of the spectral sensitivity function remained constant, but shifted upwards at all wavelengths. One slight deviation from constant shape was a relatively greater sensitivity to short-wavelength light in 1-month-olds than 3-month-olds, although this was found not to be statistically significant. It was concluded that rods (the mediators of scotopic visual function) are functional by 1 month of age.

Brown (1986) used forced-choice preferential looking to measure increment threshold spectral sensitivity in eight 2-month-old infants. Broad-band stimuli classed as long wavelength (greater than 590 nm) and short wavelength (less than 540 nm) subtending 16 degrees were presented at 25 degrees in the retinal periphery. The infants were generally less sensitive than adults included for comparison, but the curve shapes for the two subject groups were similar indicating a similarity of scotopic spectral sensitivity in infants of this age and adults.

3.9 The Perception of Long and Middle Wavelength Stimuli in Infants

Chromatic sensitivity in young infants has been widely investigated, although much of the early work on this subject made use of adult heterochromatic brightness matches to remove luminance cues from the stimuli. This is an ineffective method of establishing isoluminance (see Chapter 1), but such studies are included here for completeness.

Hamer et al (1982) used pairs of lights in the Rayleigh region of the spectrum

to determine whether at least two photoreceptor types are functional in 1- 2- and 3-month-old infants. The FPL method was used to assess discrimination of a broad-band red or a 550 nm green from a yellow background, at a range of luminance differences including an adult brightness match. At four weeks of age, half of the infants were able to make a Rayleigh discrimination. In general, the ability to make Rayleigh discriminations increased with age, and was more significant for the red test field than for the green. Hamer et al considered the possibility that infants may be making use of the retinal periphery to make chromatic discriminations.

Using steady-state VEPs, Morrone et al (1990) compared red-green and luminance contrast sensitivity and visual acuity in eight infants over their first six months of age. They could elicit no chromatic response before 4 to 7 weeks of age using pattern-reversal stimuli of 0.1 cpd spatial frequency. The age at which the response first appeared was found to vary between infants. By 6 months of age, the response was adult-like, having shown a period of rapid development over the first 20 weeks of age. In general, chromatic responses showed a later onset but chromatic contrast sensitivity matured more rapidly than luminance contrast sensitivity.

Morrone et al suggest that, as cone contrast is considerably lower than physical chromatic contrast, the infant neural mechanism for the processing of these signals may be intact and functional at birth, but may have such poor contrast sensitivity that a physical contrast of greater than 100% would be required for perception of chromatic stimuli. This is a possible explanation of poor colour perception in young infants, but does not explain the difference in maturation rates of luminance and chromatic sensitivity. The authors point out that foveal cone immaturity is unlikely to account for limited colour vision, as long- and middle-wavelength-sensitive cones contribute heavily to the luminance channel, which shows sensitivity to contrast earlier. They suggest that different maturation rates of the parvocellular and magnocellular processing streams may be partly responsible for the difference between chromatic and luminance contrast sensitivity found in their study.

Further work (Burr et al, 1991; Morrone et al, 1993) substantiated these results. No visual evoked response to red-green isoluminant stimuli could be elicited before about 8 weeks of age, even at the low spatial frequencies of 0.1 and 0.2 cpd. Responses at higher spatial frequencies (0.7 and 1.0 cpd) could not be elicited before 14 weeks of age. At all ages, luminance contrast sensitivity was two to three times higher than chromatic contrast sensitivity at spatial frequencies of 0.1 and 0.4 cpd.

Burr et al (1996) again found that the two pathways develop at different rates, but that the evoked response to chromatic stimuli matures at a *slower* rate than that in response to luminance stimuli, in terms of response latency.

Using the transient VEP, Rudduck and Harding (1994) measured responses to red-green pattern-reversal stimuli at a spatial frequency of 0.25 cpd in 39 infants aged 1 to 13 weeks. In agreement with Morrone et al, they found that infants showed no response to isoluminant stimuli before the age of 7 weeks while all infants aged 8 weeks and older showed clear responses to all red-green stimuli at and around an adult isoluminant match.

Allen et al (1993), using the sweep VEP technique, obtained contrasting results to those of Morrone et al, in fourteen infants from 2 to 8 weeks of age. Red-green sinusoidal gratings of 0.8 cpd spatial frequency were phase-reversed at a temporal frequency of 3 Hz. Contrast sensitivity to this stimulus was determined in each infant at a range of red-green luminance ratios, including photometric isoluminance. In infants at all ages, chromatic contrast sensitivity was lower than the adult level, but responses were always obtained, even at photometric isoluminance. They also found that the ratio of chromatic to luminance contrast sensitivity was similar in infants and adults, suggesting that the two develop at the same rate. It was concluded that infants as young as 2 weeks of age are able to discriminate chromatic stimuli in the Rayleigh region. This implies that young infants must have functional long- and middle-wavelength-sensitive-cones, and the post-receptoral neurones required for processing of their signals.

This finding has been criticised on the grounds that the spatial frequency used may have produced significant chromatic aberration in the immature eye, and that only one infant was tested at this age. If present, chromatic aberration could cause a luminance artifact by placing the two chromatic stimuli in different focal planes (see Chapter 5) and so the stimulus may elicit a luminance response, even at isoluminance. However, Morrone et al (1993) could elicit no response to pattern-reversal isoluminant red-green stimuli of spatial frequency 0.7 or 1.0 cpd before 14 weeks of age, suggesting that these stimuli, of similar spatial parameters to those used by Allen et al (1993), were not contaminated by luminance artifacts.

Following the contrasting findings described above, Brown et al (1995) determined red-green and luminance contrast thresholds in 3-month-old infants, in an attempt to answer the question of whether chromatic and luminance contrast sensitivity are in the same ratio in infants and adults. If so, this would suggest that colour and luminance sensitivity in infants are both limited by a general insensitivity to contrast, consistent with the findings of Allen et al (1993). If not, chromatic sensitivity in infants may be reduced by selective insensitivity of the chromatic pathways, in agreement with Morrone et al (1993). Using the techniques of optokinetic nystagmus in infants, and two-alternative forced choice in adults, yellow-black (luminance) and red-green contrast sensitivity at a spatial frequency of 0.2 cpd was determined in 19 three-month-old infants and 9 adults. The difference between adult and infant chromatic-to-luminance contrast sensitivity ratios was not found to be statistically significant. This suggests that chromatic and luminance contrast sensitivity are not differentially affected in infants, and that poor colour perception in infants may be due to a general insensitivity to contrast.

The perception of moving isoluminant chromatic stimuli has been investigated in infants, at one and two months of age (Teller and Palmer, 1996). In this study, adults and two-month-old infants demonstrated direction discrimination of red-green stimuli at photometric isoluminance, but most one-month-olds failed in this task, suggesting that infants are able

to discriminate colour and motion in the same stimulus by about 2 months of age. The difference between sensitivity to moving luminance and chromatic stimuli was similar in infants and adults, in agreement with the findings of Brown et al (1995).

3.10 The Perception of Short Wavelength Stimuli in Infants

Teller et al (1978) used the FPL technique to determine whether 2-month-old infants could discriminate a range of wavelengths from white. At each wavelength, a single coloured bar was presented on a white background at a range of test/background brightness differences. Adult heterochromatic brightness matches had been used as a guide, so that the test and background should be of equal brightness for at least one of the presentations. Thus, it was assumed that if the infants could discriminate all of the presentations for a particular wavelength, they were able to do so on the basis of colour difference alone.

The 2-month-olds in this study could discriminate a wide spectral range from white, apart from yellow-green and purple stimuli. It was suggested that these hues may lie on an isochromatic zone, although the axis joining them was found to bear no similarity to classic deutan, protan or tritan axes. The possibility that these discrimination failures may be due to loss of attention, or other motivational factors, was also considered.

Chromatic adaptation was used by Pulos et al (1980) in an attempt to isolate the short-wavelength-sensitive mechanism in infants of 2 and 3 months of age. Adults were also tested psychophysically for comparison. Adults showed a change in the shape of the spectral sensitivity curve, as expected, under conditions of both yellow and blue adaptation. Conversely, 2-month-old infants showed no reduced sensitivity at particular parts of the spectrum when adapted to yellow, revealing no short-wavelength sensitive mechanism in young infants. 3-month-olds, however, showed an adult-like sensitivity reduction when adapted to a yellow background.

Varner et al (1985) made use of a tritan pair to investigate the perception of short-wavelength stimuli in infants, using forced-choice preferential

looking. Tritan pairs are pairs of lights which stimulate long- and middle-wavelength-sensitive cones equally. Thus, the presence of functional short-wavelength-sensitive cones and post-receptoral processing of their signals is required for discrimination of the two. Each pair was presented at a range of brightness differences including an adult heterochromatic brightness match. In this study, heterochromatic brightness matches were found to be approximately isoluminant. It was thought that adult observers may have used a minimally distinct border criterion, which could explain this surprising finding (see Chapter 1). The stimulus consisted of a 4-degree test field at a wavelength of 416 nm, and a 547 nm surround. In two out of six 4-week-olds, three out of five 7-week-olds and all of the six 2-month-olds, the full range of discriminations were made. This suggests that short-wavelength-sensitive cones are functional by 2 months of age, and that their maturation varies between individuals.

Adams et al (1991) speculate that poor discrimination of short-wavelength light in infants may reflect an immaturity of post-receptoral mechanisms, and that, if this is the case, infants may also show poor perception of yellow. A habituation-recovery paradigm was used to determine whether infants aged 1 to 6 days could distinguish test stimuli (565 and 595 nm) from a white background at a range of test/background luminance differences. Most (85%) of the infants tested were able to distinguish the 595 nm stimulus, while only half could distinguish the 565 nm stimulus. Taken in conjunction with their previous work (Adams and Maurer, 1984; Adams et al, 1990) these results indicate poor discrimination of yellow-green (565 nm) and blue (470 to 480 nm), while infants are able to discriminate other spectral stimuli. It was concluded that, as these spectral zones include blue and yellow, they may reflect post-receptoral immaturity of the blue-yellow opponent mechanism, possibly in conjunction with the immaturity of foveal cones.

Later work by Adams et al (1994) made use of a modified preferential looking technique, designed to minimise test periods for the investigation of chromatic discriminations in neonates. The young infants were initially tested to determine their sensitivity to luminance differences, then a large

or small range of stimuli was chosen. The small range would be chosen for an infant showing signs of low sensitivity to luminance differences. This allowed infants to be assessed using a minimal number of presentations, with the intention of completing the test before loss of attention.

74% of newborns (less than 7 days old) could distinguish red (660 nm) from an achromatic background at a range of luminance differences. 36% could distinguish green (520 nm), 25% yellow (580 nm) and 14% blue (475 nm). In general, the number of failures at each of the four wavelengths was found to reduce with age, until at 3 months all four stimuli could be distinguished from the achromatic background. The possibility that these results may imply a deficiency of the blue-yellow mechanism in young infants was considered. The authors made the point, however, that perception of green stimuli is also considerably reduced, so there is no clear distinction shown here between the efficiency of the red-green and blue-yellow pathways.

3.11 Restrictions on Spatial and Chromatic Infant Vision

It has been suggested (Bronson, 1974) that visual function during the first month of life is mediated by sub-cortical mechanisms, with cortical mechanisms becoming functional later. One example of sub-cortical control of visual function is the asymmetry of monocular OKN observed in infants less than 3 months of age. In monocular viewing, the stimulus is followed in the temporal-to-nasal (sub-cortically driven) direction, but not in the nasal-to-temporal (cortically driven) direction. OKN responses in hemispherectomised infants, however, have led to the suggestion that vision at an early age is under control of both sub-cortical and cortical mechanisms (Braddick et al, 1996).

Infants demonstrate responses to different types of visual stimuli at different ages, suggesting that the developmental time courses of the relevant neural circuitry may vary (Atkinson, 1992). For example, binocularity and re-fixation responses are not generally evident until about 3 months of age (Braddick, 1996), while infants are able to discriminate colour, directional movement and orientation by 6 to 8 weeks (Atkinson, 1992; Braddick, 1993). The presence of basic visual function from birth, and

in pre-term infants (Grose et al, 1989; Grose and Harding, 1990) in conjunction with the onset of responses to various types of visual stimuli at later ages, suggests that visual function is increasingly under cortical control over the first few months of life.

The *visual efficiency hypothesis* states that poor chromatic sensitivity in young infants is due to low visual efficiency in general, due to the immaturity of front-end properties, including optics and photoreceptors, and post-receptor mechanisms. Thus, infants may have a full complement of long-, medium- and short-wavelength-sensitive cones and the ability to process their signals, but these mechanisms may be relatively insensitive. This hypothesis is consistent with the findings of Allen et al (1993), Brown et al (1995) and Teller and Palmer (1996) that luminance and chromatic sensitivity are reduced in infants by an overall insensitivity of the visual system.

The *chromatic deficiency hypothesis* states that a lack of functional cones, or the inability to process their signals, explains poor chromatic discriminations by young infants. This is comparable to the colour-defective adult with a lack of long-, medium- or short-wavelength-sensitive cones causing protanopia, deuteranopia or tritanopia, respectively, and is consistent with the findings of Morrone et al (1990, 1993) that chromatic sensitivity is differentially affected by inefficiency of the chromatic mechanisms in the infant visual system.

The '*dark glasses*' hypothesis of infant vision is based on reduced quantum catch by the immature fovea, and suggests that infants require 350 times greater illumination to reach adult levels of spatial and chromatic vision (Banks and Bennett, 1988; see below). A number of studies have involved comparisons of infant visual function at different retinal illuminance levels, to test this hypothesis. Brown et al (1987) measured visual acuity at a range of luminance levels, for infants and adults. In adults, a range of retinal eccentricities and defocus were also applied. By comparing infant performance to that of adults under these conditions, they found that relatively poor spatial vision in infants is not solely due to refractive error,

foveal immaturity or overall light insensitivity, but probably to a combination of these factors.

Swanson and Birch (1990) found that at moderate spatial frequencies, temporal contrast sensitivity is low-pass in young infants, and is band-pass in adults. The low-pass function is not matched in adults at any retinal illuminance or spatial frequency, suggesting that reduced quantum catch cannot fully explain poor sensitivity in infants, and therefore that the dark glasses hypothesis does not fully explain limitations of infant vision. Further evidence against this hypothesis was provided by Allen et al (1992), who found that infants show no increase in sweep VEP acuity at luminance levels beyond 10 cd/m². Adults asymptote at about 100 cd/m², which is thought to represent a transition from scotopic to photopic function. The lower saturation level in infants suggests that higher retinal illuminance would not improve infant visual acuity, and therefore that the dark glasses hypothesis is incorrect.

Shannon et al (1996) measured sweep VEP contrast sensitivity in 2- and 3-month-olds at a range of luminance levels. It was found that the younger infants would require a 2000-fold increase in retinal illuminance to match adult sensitivity at a comparable spatial frequency, while only a 120-fold increase would be required for 3-month-olds. This suggests that at 2 months the dark glasses hypothesis does not entirely explain limitations of infant spatial vision, while at 3 months of age it may do.

Banks and Bennett (1988) point out that the dark-glasses hypothesis cannot fully explain limitations of chromatic vision, as cone sensitivity would become reduced by adaptation at similar luminance levels for infants and adults, so increased illumination would not improve the efficiency of infant cone function.

Banks and Bennett (1988) investigated the factors limiting spatial and chromatic vision in young infants, in an attempt to determine whether these deficits can be explained by the immaturity of front-end properties. This was achieved by using an ideal observer model with the optical and

foveal photoreceptor characteristics of the neonate. Optical characteristics included posterior nodal distance, pupil size, ocular media transmittance and optical transfer function. Foveal properties were based on the anatomical findings of Youdelis and Hendrickson (1986), and included inner segment size and shape, and outer segment length (see figure 3.2). Using these factors, the likelihood of quanta being caught by foveal photoreceptors and a resulting isomerizations taking place was calculated, and compared to that of the adult fovea.

The neonate's foveal cone inner segments are broader and shorter than those of the adult, and are not tapered (see figure 3.2) so have relatively poor waveguide properties. As a result, the effective foveal cone diameter in the young infant is that of the outer segment. In addition, the outer segment itself, where isomerizations takes place, is shorter than that of the adult. Taking inner and outer segment characteristics into account, the effective quanta-collecting area of the newborn fovea was found by Banks and Bennett to be 2%, compared to 65% in the adult fovea. They went on to investigate the effect of the difference in outer segment length in the neonate and adult fovea on the number of isomerizations carried out. They found a 10 to 1 difference in the number of isomerizations resulting from the same number of incident quanta in adults compared to infants. That is, ten times the number of quanta would need to be incident on the infant than the adult fovea, to allow the same number of isomerizations to take place in each. When the above factors were taken into account together with optical characteristics, it was found that 350 times more quanta are effectively absorbed by the adult than the infant fovea.

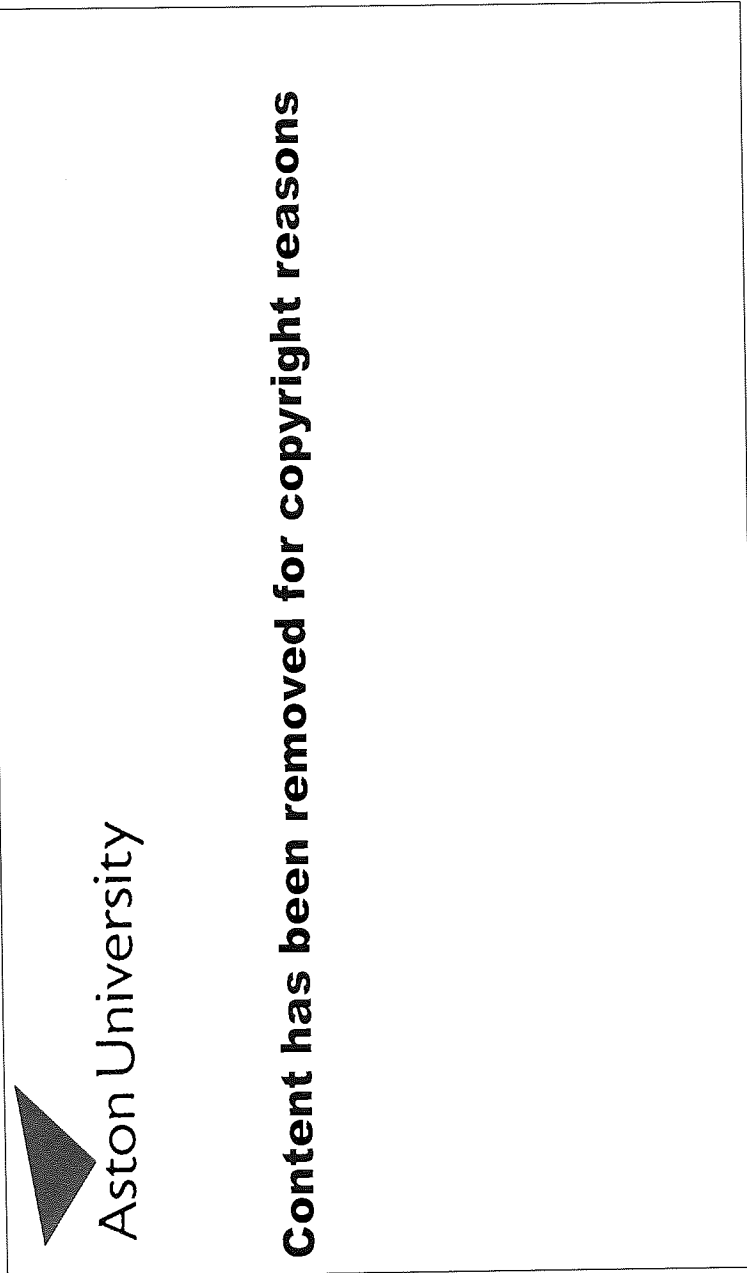


Figure 3.2
Neonate and adult foveal cone dimensions (from Banks and Bennett, 1988). The neonatal inner segment is not tapered, and the outer segment is much shorter than that of the adult.

The ideal observer model was then used to compare the achromatic contrast sensitivity function of the adult to that of the neonate. Poor achromatic contrast sensitivity in young infants was found to be mainly due to reduced effective quantum catch, while the remaining difference may be explained by post-receptoral factors.

In the same study, Banks and Bennett went on to investigate whether reduced chromatic contrast sensitivity in neonates can be explained by foveal photoreceptor immaturities. By comparing infant ideal observer chromatic discriminations to the results of other authors using real observers (Teller et al, 1978; Packer et al, 1984; Varner et al, 1985) they found that poor Rayleigh discriminations in young infants can be explained by the visual efficiency hypothesis. That is, the immaturity of front-end properties and post-receptoral mechanisms can account for neonates' inability to make Rayleigh discriminations. However, the visual efficiency hypothesis could not account for tritan discrimination failures in infants. Therefore, it was concluded that young infants may have insensitive short-wavelength-sensitive cones, or an inability to effectively process their signals post-receptorally.

Anatomical measurements of the neonate and infant fovea were used by Wilson (1988) to investigate the restrictions placed on spatial vision by the immature fovea. Infant acuity was computed according to the anatomical findings of Youdelis and Hendrickson (1986) and was found to be similar to published age-matched VEP acuities (Norcia and Tyler, 1985). Conversely, FPL acuity was not comparable to theoretical acuity until the age of 10 months and over. Wilson concluded from this that limits on psychophysically measured visual acuity at an early age represent constraints imposed by development of the visuo-motor association areas, rather than of the retino-striate visual pathway.

3.12 Rod Contributions to Colour Vision in Infants

Studies of infant colour vision require larger stimuli than those involving adults, as visual acuity is poor in infants less than six months of age, particularly for chromatic stimuli (Packer et al, 1984). Large test fields cannot

be restricted to the rod-free fovea, so rods may be stimulated in work on infant colour vision. It has been suggested, however, that the scotopic system in infants may saturate even under dark-adapted conditions, when large stimuli are used (Brown, 1988, 1990). This may be due to the pooling of responses over a large retinal area, saturating the post-receptoral pathways of the infant visual system (Brown, 1988).

Rods have been shown to contribute to colour perception in adults. McCann and Benton (1969) found that rods interact with long-wavelength sensitive cones to produce colour sensations. Montag and Boynton (1987) investigated colour perception under different viewing conditions in protanopes, deuteranopes and colour-normal adults. Using a 4-degree stimulus, all subjects demonstrated accurate colour naming. When the stimulus was reduced to 1 degree, however, the dichromats made errors while the colour-normal subjects continued to name colours accurately. In addition, short-wavelength-sensitive cone monochromats are able to accurately perform wavelength-discrimination tasks at mesopic luminance levels (Reitner et al, 1991). These results implicate the involvement of rods in wavelength discrimination under certain viewing conditions.

At mesopic levels then, chromatic discriminations may depend upon rod excitation in addition to that of cones. In the colour-normal observer, the presence of rod-generated signals in the two colour-opponent and one luminance channel results in different colour appearances at different levels of mesopic illumination. It does not, however, result in a colour sensation separate to those arising from cone signals (Montag and Boynton, 1987). Colour perception in the dichromatic observer, however, benefits from rod contributions, in providing a separate set of signals in all three post-receptoral channels. This may result in modulation of these channels by stimuli which excite the two remaining cone types equally. Thus, without rod input the stimuli would be indiscriminable to the dichromat. As explained earlier, it has been suggested that young infants may have a tritan defect (Banks and Bennett, 1988). They may, however be able to discriminate large stimuli at mesopic or low photopic levels, as rods may contribute to colour vision under these conditions.

3.13 Colour Vision in the Peripheral Visual Field

As the spectral sensitivity to short-wavelength stimuli has been shown to be elevated in the periphery (Wald, 1945), it has been suggested that tritan discriminations in infants may be due to the involvement of extra-foveal cones.

Graham et al (1975) measured spectral sensitivity at the fovea and at 10 degrees nasally and 25 and 45 degrees temporally. Their findings demonstrated the established increase to short wavelengths in the periphery, but they also showed that no significant further increase occurred beyond 10 degrees. These results suggest that the relative sensitivity increase to short wavelengths remains constant from 10 degrees to at least 45 degrees. In agreement with these findings, Kulikowski et al (1991) showed that the characteristics of the visual evoked response to chromatic stimuli subtending 16 degrees are similar to those subtending only 6 degrees, suggesting that the larger field elicits a response from a similar population of cortical cells. A larger signal-to-noise ratio was obtained with the larger field, suggesting that large chromatic stimuli may be more clinically viable than small-field chromatic stimuli.

Abramov and Gordon (1977) used heterochromatic flicker to measure spectral sensitivity at the fovea and at 45 degrees into the nasal periphery. They found a substantial relative increase in sensitivity to wavelengths less than 550 nm at 45 degrees compared to foveal presentation.

The requirement for large stimuli in infant studies of colour vision means that parafoveal and peripheral as well as foveal photoreceptors may be excited. As extra-foveal cones reach maturity earlier than foveal cones, chromatic discriminations in young infants may therefore be due at least in part to the presence of functional cones in the parafovea and near periphery.

3.14 The Genetic Basis of Defective Colour Vision

The colour-defective individual will confuse colours which the colour-normal observer is able to differentiate. This is because the nature of a

colour vision defect is such that one of the three types of photopigment is missing or anomalous. If missing, the defect is known as deuteranopia, protanopia or tritanopia. If the pigment is present but abnormal the defect is a deuteranomaly, protanomaly or tritanomaly. The two remaining normal cone types may be stimulated equally by two colours, which the dichromat may therefore be unable to discriminate. The colour-normal observer would be able to differentiate them because they would stimulate the third cone type to a different degree.

In humans, the gene sequences which code for long- and medium-wavelength-sensitive cone photopigment proteins are found on two adjacent loci on one arm of the 23rd chromosome pair, the sex chromosomes (Nathans et al, 1986a). Thus, the inheritance of defective colour vision is sex-linked. The gene sequence which encodes the short-wavelength-sensitive cone photopigment is found on autosome 7 and that which codes for rhodopsin on autosome 3. Defective colour vision in humans arises because the gene coding for a photopigment may be a mutation of the true gene, or may be absent altogether. A mutant gene will be dominated by a normal gene, if present, on the corresponding limb of the second X chromosome in females. One such gene is found on each of the pair of chromosomes. If the two genes are identical (for example, both coding for normal colour vision) they are a homozygous pair; if different they are heterozygous.

Females have two X sex chromosomes, so called because they each have four limbs. One of the gene pair exists on one of the chromosomes, and the other on the second chromosome. In the female, if a gene for defective colour vision (D) is present on one chromosome and a gene for normal colour vision (N) on the other (a heterozygous pair) the former is dominated by the latter, and the individual's colour vision is normal. This is a manifestation of the recessive nature of the gene for colour vision abnormality.

Tritanopia is not sex-linked, because the gene for short-wavelength-sensitive cones is located on an autosome. As a result, tritan defects are rare,

with an incidence of approximately 1 in 10000. The incidence of deutan and protan defects for comparison is 8% in males and 0.5% in females (Birch, 1993).

Males have one X chromosome and one Y chromosome. If a D gene exists on the X chromosome, there is no corresponding gene on the Y chromosome due to the absence of a fourth limb, and so the individual will have defective colour vision.

A homozygous female with both genes of the N type will have normal colour vision and will not be a carrier, while a homozygous female with both D genes will have defective colour vision and will be a carrier. This pattern of inheritance is illustrated by figure 3.3.

$$(a) \quad \begin{array}{c} \underline{X}X + XY \\ \underline{X}X \quad XY \quad \underline{X}X \quad \underline{X}Y \end{array}$$

$$(b) \quad \begin{array}{c} XX + \underline{X}Y \\ \underline{X}X \quad XY \quad \underline{X}X \quad XY \end{array}$$

$$(c) \quad \begin{array}{c} \underline{X}X + \underline{X}Y \\ \underline{X}X \quad XY \quad \underline{X}X \quad \underline{X}Y \end{array}$$

Figure 3.3

Examples of the mode of inheritance of the gene for defective colour vision. \underline{X} denotes the gene for defective colour vision; X denotes the absence of this gene.

(a) A carrier female and normal male produce 50 % carrier, 50 % normal females and 50 % colour-defective, 50 % normal males.

(b) A normal female and colour-defective male produce 100 % carrier females and 100 % normal males.

(c) A carrier female and colour-defective male produce 50 % carrier, 50 % colour-defective females and 50 % colour-defective, 50 % normal males.

Investigations into the genetics of colour vision have so far been concerned only with receptor photopigments, so the genetic basis of further stages of chromatic processing is poorly understood at present (Kaiser and Boynton, 1996). It has been hypothesised that the four types of gene, each of which codes for a different photopigment, arose from a common ancestor gene. To test this hypothesis, Nathans et al (1986b) analysed the amino-acid sequences of genes coding for each pigment in humans. Those which code for L and M photopigments were found to be over 98% identical in their amino-acid sequences, while they showed only 43% and 44% similarity to the gene for the S photopigment. Each of the three colour photopigment genes was 40% to 42% similar to similar to rhodopsin.

The almost identical gene sequences for L and M pigments may represent relatively recent duplication of the two from a single ancestor (Nathans et al, 1996b). A comparable situation has been demonstrated in monkeys. Old world monkeys have distinct gene loci on the X chromosome coding for L and M pigments, as is the case in humans. By contrast, New World monkeys have only one gene locus on the X chromosome, which encodes for a long-wavelength-sensitive pigment (Jacobs and Neitz, 1987). This implies that L and M pigments may have duplicated from a single L pigment 30 to 40 million years ago, coincident with the distinction of New and Old World monkeys (Nathans et al, 1986b). In humans, gene similarities may also suggest that rhodopsin, the S cone pigment and a gene coding for a long-wavelength-sensitive pigment diverged from one ancestral gene at around the same time, which is estimated to be 500 million years ago (Nathans et al, 1986b).

3.15 Colour Vision Screening in Infants and Children

Colour is used as an aid to learning and to provide a visually stimulating environment during the early developmental years (Alexander, 1975a,b; Mantyjarvi, 1991; Birch and Platts, 1993). The colour-defective infant may, therefore, be disadvantaged by an inability to make some colour discriminations. A number of colour vision screening tests have been designed for use with children and infants, and certain tests intended for

adults have been used with limited success in children.

The Ishihara pseudoisochromatic plates involve the recognition of numbers or tracing of a path. The path tracing task has proven unreliable for children (Birch and Platts, 1993) and the recognition of numbers is reliable only in those over six years of age (Mantjarvi, 1991). The Ishihara test for Unlettered Persons comprises shape identification (circles and squares) and simplified path tracing. This has proved successful for testing children from three to seven years of age (Birch and Platts, 1993).

The Velhagen Pflugertrident test is intended for young children and comprises pseudoisochromatic plates, each with an "illiterate E" in a certain orientation. This simplified task has proved surprisingly unreliable in young children (Mantjarvi, 1991). The Ohkuma test cards have a similar design, with Landolt C's in different orientations. This could theoretically be used successfully with young children, but has been found to have poor screening efficiency in adults (Birch and McKeever, 1993). The Farnsworth D15 test has proved confusing to young children (Alexander, 1975a,b) the 100 hue test may be assumed to present similar problems, as it is an extended version of the D15.

In contrast to the above, the Lanthony Tritan Album is intended for the detection of tritan defects, and has been performed reliably by children as young as 3 years of age (Mantjarvi, 1991).

3.16 Summary

Colour perception in infants has been investigated, using psychophysical and electrophysiological methods, in terms of photopic and scotopic spectral sensitivity, Rayleigh discriminations, tritan discriminations and anatomical considerations. Flawed methodology invalidated much of the early work on this subject, and definitive work is rare due to factors such as infants' attention.

Progress has been made, however, and it is now generally agreed that infants are able to make most chromatic discriminations by the age of three

months (Teller and Bornstein, 1987; Brown and Teller, 1989). Disagreement remains on a number of issues, including spectral sensitivity of infants in comparison to adults, the rates of development of luminance and chromatic mechanisms, and the age of onset of colour perception, making infant colour vision the subject of a great deal of continued interest.

CHAPTER 4

RATIONALE AND AIMS OF THE PRESENT STUDY

4.1 The Processing of Chromatic Information by the Infant Visual System

The processing of chromatic information begins at the retinal photoreceptors. Post-receptoral processing involves the inner retina, lateral geniculate nucleus and visual cortex. At photoreceptor level, foveal cone immaturity and cone contrast levels may play a part in limiting chromatic sensitivity in infants. Post-receptorally, the immaturity of chromatic- and luminance-processing mechanisms may restrict colour and spatial vision in infants. At present, it is unclear whether deficiencies of the chromatic mechanisms in particular are responsible for limiting chromatic sensitivity in infants.

The discrimination of isoluminant chromatic stimuli under photopic conditions demonstrates the presence of at least two functional cone types and the post-receptoral processing of their signals. A failure to discriminate such stimuli does not, however, demonstrate the absence of functional colour-opponent mechanisms, as the relatively poor effective cone contrast of chromatic, particularly red-green, stimuli and the poor waveguide properties of the immature foveal cone may limit chromatic sensitivity in infants.

It is thought that vision may be mediated at a subcortical level in the neonate, as indicated by the asymmetry of optokinetic nystagmus at an early age (Bronson, 1974; Atkinson, 1992). As the superior colliculus receives only magnocellular input (Schiller and Malpeli, 1977), it has been suggested that the parvocellular (colour-opponent) channels may not function until vision becomes cortically mediated, believed to be at about 2 to 3 months of age (Atkinson, 1984; Atkinson, 1992). Anatomically, the parvocellular units of the lateral geniculate nucleus are mature by about 6 months of age, while the magnocellular units are adult-like at the later age of 1 to 2 years (Hickey and Peduzzi, 1987). In the striate cortex, cells receiving parvocellular input are less metabolically active than those receiving magnocellular input in the neonate, while the opposite is true by 4 months of age (Wong-Riley et al,

1993).

Morrone et al (1990, 1993) and Rudduck and Harding (1994) found that the visual evoked response to isoluminant red-green stimuli is absent until about 8 weeks of age, while the response to luminance-modulated stimuli is present much earlier. Morrone et al also provided evidence to suggest that the red-green opponent and the luminance channels of the visual system develop at different rates, with the chromatic channel becoming functional later but developing more rapidly than the luminance channel in terms of contrast sensitivity. Later work by this group, however, (Burr et al, 1996) found that the evoked response to chromatic stimuli matures at a *slower* rate than that in response to luminance stimuli, in terms of response latency. These findings are generally in agreement with the chromatic deficiency hypothesis, that chromatic sensitivity in infants is limited by a deficiency of the chromatic mechanisms in particular.

In contrast, it has been proposed that chromatic and luminance systems do not develop independently, but that both are equally limited by an overall insensitivity of the infant visual system, due to the immaturity of foveal cones and post-receptoral processes. It is generally agreed that the immature fovea is not entirely responsible for limited vision in the neonate, and that post-receptoral factors may play a part. The findings of Allen et al (1993), Brown (1995) and Teller and Palmer (1996) are consistent with this, the visual efficiency hypothesis.

As described earlier, it is thought that chromatic sensitivity may be limited at an early age by cone contrast differences. Chromatic stimuli, Rayleigh stimuli in particular, offer low cone contrast levels due to the considerable spectral overlap of long- and medium-wavelength-sensitive cones (Bowmaker and Dartnall, 1980). The spectral overlap of short-wavelength-sensitive cones with other cone types is more modest. Luminance-modulated stimuli, however, offer much higher cone contrast levels, making the discrimination of such stimuli relatively easy (Brown et al, 1995).

In general, the findings of studies on infant colour vision have not been in agreement on either the age at which infants can make isoluminant chromatic discriminations, or on the rates of development of the colour-opponent and luminance pathways. These disagreements may be due to differences in stimulus type, investigative techniques and inaccuracies in the specification of infant age.

4.2 Investigative Techniques

Stimuli comprising medium to high spatial frequency components may offer luminance cues by introducing chromatic aberration. In addition, some early studies on chromatic vision in infants used adult brightness matches in an attempt to generate isoluminant stimuli. Heterochromatic stimuli rendered isoluminant by this technique have been found to stimulate the colour-opponent *and* luminance channels of the visual system. In studies of chromatic vision it is clearly very important to eliminate luminance cues, and so in most of the more recent investigations heterochromatic stimuli are designed to allow minimal or no modulation of the luminance channel, by using appropriate techniques to specify an isoluminant match as a first approximation for infants.

In electrophysiological studies, the transient visual evoked response to pattern-reversal chromatic stimulation is of the same morphology as the response to luminance-modulated stimuli (see Chapter 6). Thus, it may be difficult to identify response components which are generated by chromatic and not luminance elements in the stimulus when pattern-reversal stimuli are used. The transient evoked response to pattern-onset chromatic and luminance stimuli are of distinct morphology and so components in response to luminance elements in the stimulus may be easier to identify using this technique. In general, however, electrophysiological studies of chromatic vision in infants have used the steady-state VEP. This response may be more objectively analysed than the transient VEP and data is collected more rapidly. However, the steady-state response does not allow response morphology to be observed.

Chromatic vision in infants has been investigated using both

electrophysiological and behavioural techniques. Results from behavioural studies may be contaminated by non-sensory factors, such as lack of attention. Before about two months of age, infants find visual re-fixation difficult, and are able to re-fixate with ease by two to three months of age (Atkinson, 1992). Lack of attention and re-fixation difficulties may confound any study of infant vision, but may be a more significant factor in behavioural work, such as the forced-choice preferential looking technique, which makes the assumption that an infant viewing a patterned stimulus is able to discriminate that stimulus, and that if the stimulus is not preferred it is not discriminated.

4.3 Specification of Infant Age

The accurate specification of developmental age is clearly important when considering the age at which infants are able to discriminate certain visual stimuli. In human infants, it is generally not possible to know the precise date of conception, and thus the period of time over which the visual system has been developing. Infant age should, therefore, be specified in such a way that errors in the estimation of post-conceptual age are minimised. Most previous studies have specified infant age as post-natal age in infants born within two weeks of their term date of pregnancy. Disagreements over the age at which infants are able to make chromatic discriminations have involved differences of up to six weeks between studies. This discrepancy may be due to errors in the estimation of post-conceptual age, in addition to the methodological differences explained above.

4.4 Aims and Methods of the Present Study

The principal aim of the present study is to investigate the development of the colour-opponent visual pathway receiving input from short-wavelength-sensitive cones. This pathway is referred-to here as the S-cone opponent pathway, or channel. Development of this pathway is compared to development of the luminance and the red-green opponent pathway (also known here as the L-M pathway) in the same infants by recording evoked responses to a range of chromatic and luminance-modulated stimuli from infants, on a longitudinal basis.

Two types of chromatic stimuli are employed here, chosen to stimulate the S-cone opponent channel and the L-M opponent channel selectively. One heterochromatic pair is chosen to lie along a tritanopic confusion axis in CIE colour space, and is referred-to as the tritan stimulus. Tritan stimuli allow little or no modulation of the red-green colour-opponent channel, so this type of stimulation is intended to selectively stimulate the S-cone opponent pathway.

A second heterochromatic pair lie along an axis orthogonal to the tritan axis in CIE colour space. This is referred-to as the red-green stimulus and is intended to selectively stimulate the red-green colour-opponent channel, also known here as the L-M opponent channel, or pathway. Both types of heterochromatic stimuli are complementary and are rendered isoluminant using adult heterochromatic flicker photometry matches, in order to minimise luminance or brightness cues.

A luminance-modulated (green-black) stimulus is also employed, in order to elicit evoked responses from the luminance channel, for comparison with chromatic responses.

The age of onset of evoked responses significantly above EEG noise levels is used to signal the age, to the nearest week, at which each infant is first able to discriminate tritan stimuli without luminance cues. By comparing responses to the tritan, red-green and luminance-modulated stimuli, it is possible to determine whether infants are able to discriminate all types of stimuli at the same age. Observation of evoked responses beyond the age of onset is also of interest, as luminance and chromatic response characteristics change significantly with further maturation.

In this study, infant age is specified as post-term, which is defined as 40 weeks post-menstrual age, in order to minimise errors in the estimation of developmental age from conception. The visual evoked response is the chosen method by which to observe development, in order to avoid non-sensory factors inherent in behavioural work. The transient VEP is used in

preference to the steady-state VEP, so that response morphology may be observed.

The presentation mode for all stimuli used is pattern-onset, allowing morphologically distinct luminance and chromatic response components. This is verified by pilot work on adult subjects. Adult isoluminant matches are determined by heterochromatic flicker photometry, and are found to closely approximate photometric isoluminance. In adults and in the longitudinal study of infants, both types of chromatic stimuli are presented at photometric isoluminance and at a range of colour luminance ratios around this point, in order to observe response characteristics as luminance differences are introduced to the stimulus.

Evoked responses from the group of infants tested longitudinally are compared to those recorded from an infant with cystic fibrosis, encountered coincidentally among this group. This infant demonstrates abnormal responses to luminance and chromatic stimuli, by comparison with those elicited from healthy infants. The possibility that this finding may reflect a previously unreported cortical abnormality secondary to this illness is discussed.

CHAPTER 5

GENERAL METHODS

5.1 Computer-Generated Stimuli

Stimuli were generated using a Cambridge Research Systems VSG 2/2 graphics board with 14-bit DACs, and were presented on a 17-inch diameter CRT monitor (Eizo Flexscan 562-T) with a non-interlaced frame rate of 150 Hz and a line scan rate of 60 kHz. Chromaticity co-ordinates of the three phosphors measured using the Bentham PMC 3B spectroradiometer were as follows: Red $x=0.5842$, $y=0.3425$; Green $x=0.2772$, $y=0.5771$; Blue $x=0.1615$, $y=0.0768$. For each of the phosphors, a good level of stability with time was demonstrated by measuring co-ordinates at 10-minute intervals over a 90-minute period after switching the monitor on (see figures 5.1 to 5.3).

Programming was in the Borland C language. All stimuli were horizontal sinusoidal gratings and were generated at a range of luminance and chromatic contrasts. Spatial frequencies used were 0.2 cpd for infants and 1.0 cpd for adults, in order to avoid chromatic aberrations (Flitcroft, 1989) and to favour the colour-opponent pathways, which prefer low spatial frequencies (Mullen, 1985; Fiorentini et al, 1991). Initially, gratings were generated using the pure phosphors by presenting red and green 180 degrees out of phase for Red-Green gratings while Blue-Yellow gratings comprised a Blue-only stimulus in spatial antiphase with a Yellow stimulus, itself generated by setting red and green in phase (Arden et al, 1988). Isoluminant Blue-Yellow determined in this way was found by measurements of chromaticity co-ordinates to lie along a tritanopic confusion line in CIE colour space, with co-ordinates of $x=0.1615$, $y=0.0768$ for pure Blue and $x=0.4684$, $y=0.4255$ for pure Yellow. Stimuli on such an axis modulate short-wavelength-sensitive cones only, and not medium- or long-wavelength-sensitive cones (Wyszecki and Stiles, 1982).

This method, however, produced non-complementary stimuli which could not be rendered equal in both luminance and brightness (see Appendix 2).

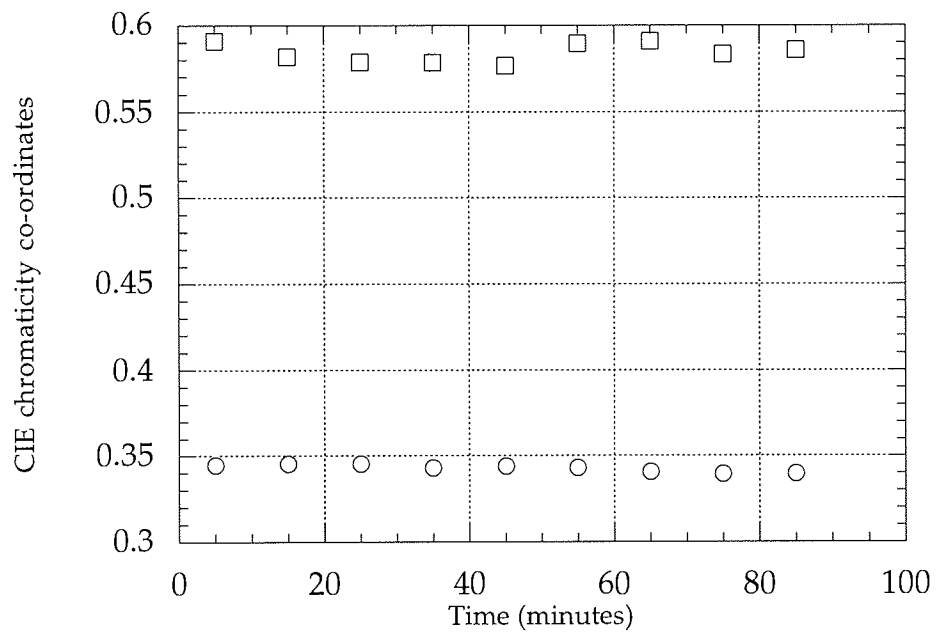


Figure 5.1
x (open squares) and y (open circles) CIE chromaticity co-ordinates of the red phosphor are shown with respect to time after switching the monitor on, at time zero.

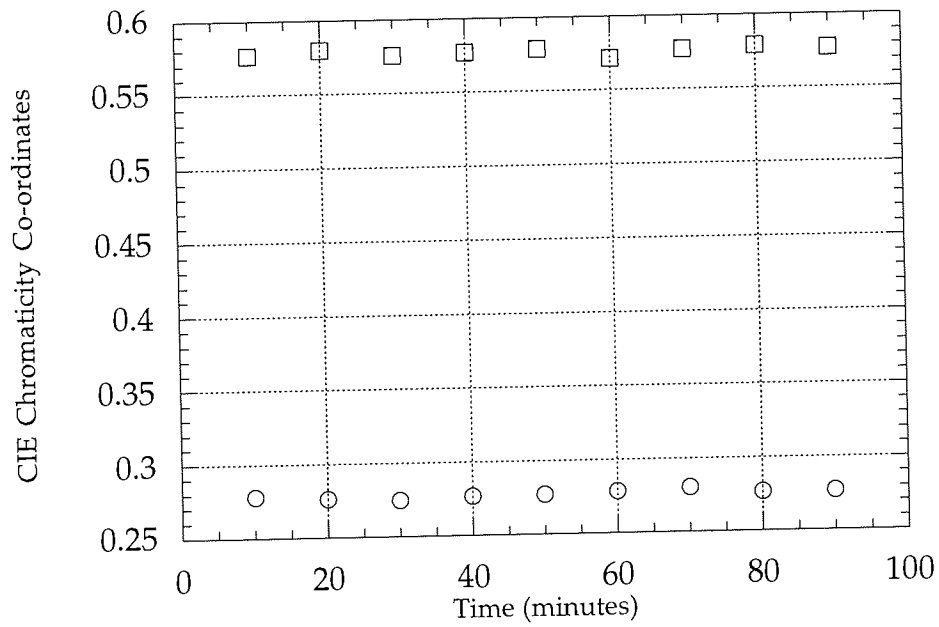


Figure 5.2
 x (open circles) and y (open squares) CIE chromaticity co-ordinates of the green phosphor are shown with respect to time after switching the monitor on, at time zero.

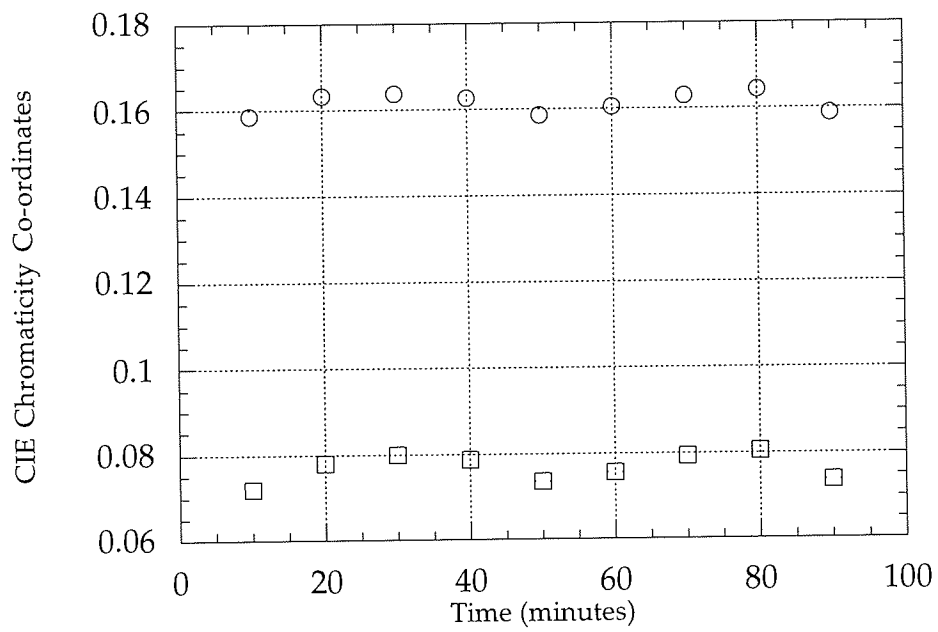


Figure 5.3
 x (open circles) and y (open squares) CIE chromaticity co-ordinates of the blue phosphor are shown with respect to time after switching the monitor on, at time zero.

Complementary stimuli along a tritanopic confusion axis and along an axis orthogonal to this in CIE colour space were generated by setting the appropriate chromaticity co-ordinates (Krauskopf et al, 1982; Flanagan et al, 1990; Rabin et al, 1994, Macaluso et al, 1995) using VSG software facilities. Accuracy of co-ordinates was verified using the Bentham spectroradiometer. The two types of chromatic stimuli generated in this way appeared Yellowish-Green/Purple and Red/Green (see figures 5.4 and 5.5) and were used for all experiments reported here. Such stimuli are less saturated than those generated at the extremities of the phosphor triangle formed by the three phosphors, but may be rendered equal in both luminance and brightness (Boynton and Kaiser, 1968).

5.2 Chromatic Luminance Ratios

The use of photometrically isoluminant chromatic stimuli has been criticised, as the stimuli may not be exactly isoluminant for each individual observer (Kulikowski et al, 1996; see also Switkes et al, 1996 for an alternative point of view). For this reason, chromatic stimuli used in the present study were presented at a range of luminance ratios, spanning photometric isoluminance. The range of chromatic stimuli varied from Yellowish-Green/Black (see figure 5.6) or Red/Black to Purple/Black or Green/Black, representing luminance ratios of 0.0 to 1.0, spanning physical isoluminance at a ratio of 0.5, following the method of Mullen (1985). At each ratio, a constant mean screen luminance of 20 cd/m² was maintained in order to minimise rod contributions to the evoked response (Wooten, 1972; Brown, 1988). The maximum luminance possible using the equipment described for generating chromatic stimuli was 40 cd/m². A mean of 20 cd/m² was used to allow this level to be maintained at all chromatic luminance ratios from 0.0 to 1.0. Luminance was measured using the Minolta LS 110 photometer.

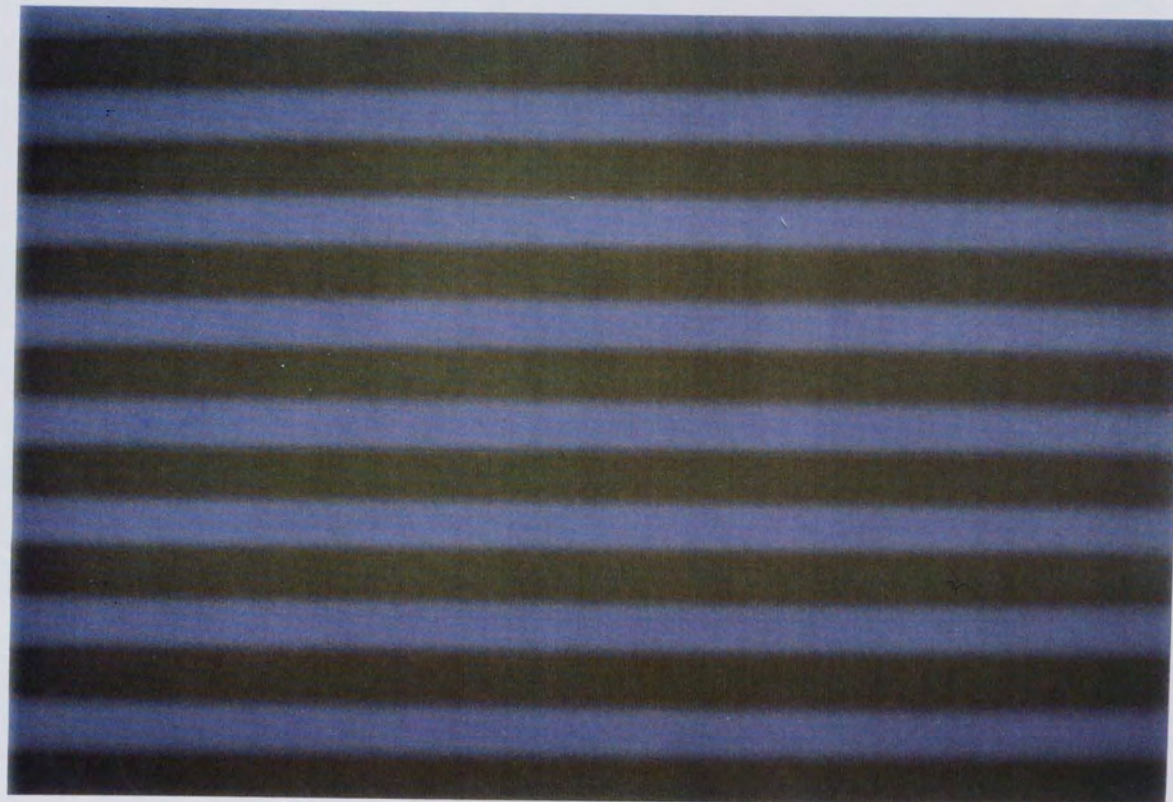


Figure 5.4
The photometrically isoluminant tritan stimulus (colour ratio 0.5) used in the present study is shown here at spatial frequency 1.0 cpd, viewing distance 100 cm (as viewed by adult subjects).

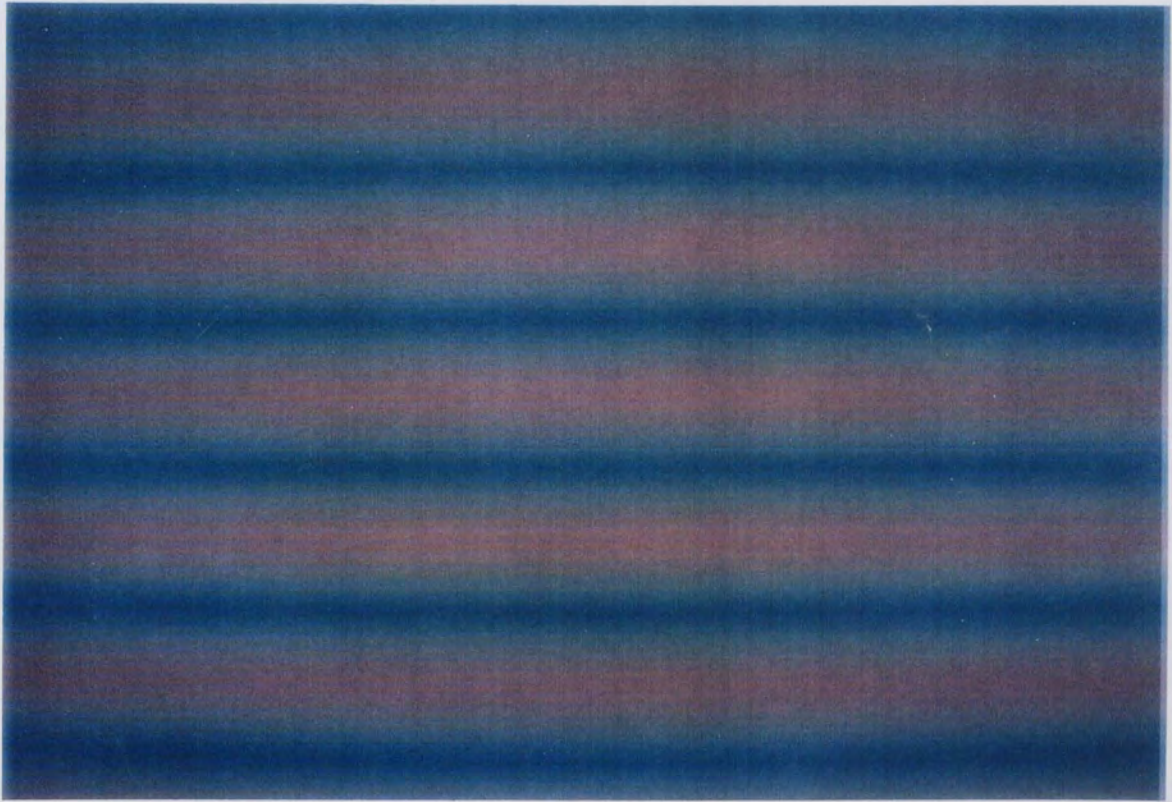


Figure 5.5
The photometrically isoluminant red-green stimulus (colour ratio 0.5) used in the present study is shown here at spatial frequency 0.2 cpd, viewing distance 40 cm (as seen by infant subjects).

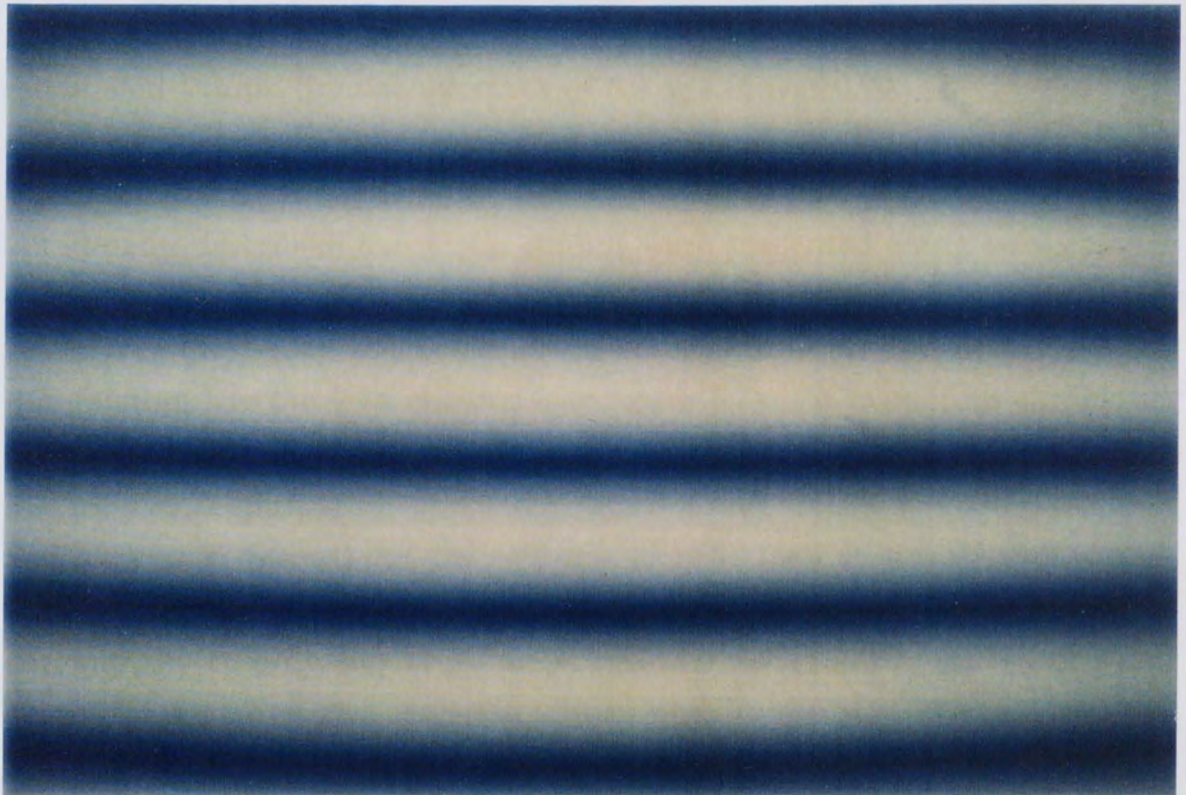


Figure 5.6
The luminance-modulated stimulus (colour ratio 1.0) used in the present study is shown here at spatial frequency 0.2 cpd, viewing distance 40 cm (as viewed by infant subjects).

The full range of luminance ratios used was: 0.0, 0.2, 0.4, 0.45, 0.5, 0.55, 0.6, 0.8, 1.0, presented in pseudo-random order. Between 0.4 and 0.6, small luminance steps were taken to ensure that the range included each individual's isoluminant point and to allow the accurate assessment of visual evoked response characteristics around physical isoluminance (Peeples and Teller, 1975; Burr et al, 1991; Rudduck and Harding, 1994). L-M- and S-cone contrasts afforded by each type of chromatic stimulus at maximum chromatic contrast, at each luminance ratio are shown in Table 5.1. These values were calculated using the Cole and Hine formula (1992), as described in Appendix 1. Michelson contrast of the luminance-modulated stimuli (luminance ratios of 0.0 or 1.0) was 0.90.

5.3 Chromatic Contrast Stimuli

As already described, chromatic stimuli were presented along two axes in CIE colour space: a tritanopic confusion axis intended to stimulate selectively the S-cone colour-opponent channel, and an axis orthogonal to this to stimulate the L-M channel (see figure 5.7). At maximum chromatic contrast, chromaticity co-ordinates were $x=0.36$, $y=0.45$ (greenish-yellow) and $x=0.26$, $y=0.22$ (purple) for the tritan stimulus and $x=0.38$, $y=0.275$ (red) and $x=0.23$, $y=0.35$ (green) for the orthogonal red-green stimulus. Stimuli at various levels of chromatic contrast were presented by calculating chromaticity co-ordinates at 5% steps between maximum (pure red or pure green, for example) and zero (the white point; $x=y=0.31$). The required co-ordinates were again specified using software facilities, and their accuracy was verified for each contrast level using the spectroradiometer. In this way, the chromatic difference between the two gratings could be varied, while maintaining constant mean luminance, in order to determine contrast thresholds and to assess visual evoked response characteristics at a range of chromatic contrasts.

Tritan Ratio	L	M	S
0.40	0.32	0.35	0.40
0.45	0.18	0.19	0.85
0.50	0.00	0.01	0.82
0.55	0.18	0.17	0.78
0.60	0.34	0.32	0.73

Red-Green Ratio	L	M	S
0.40	0.21	0.52	0.30
0.45	0.03	0.41	0.14
0.50	0.15	0.28	0.04
0.55	0.31	0.24	0.22
0.60	0.44	0.14	0.36

Table 5.1

L- M- and S-cone contrasts are shown for tritan and red-green stimuli of maximum physical contrast, at each colour ratio from 0.4 to 0.6. These values indicate that at isoluminance the tritan stimulus allows 82 % modulation of S-cones and zero modulation of L- and M-cones, and the red-green stimulus modulates S-cones by 4 %, L -cones by 15 % and 28 %. The maximum possible modulation of L- and M-cones is less than that of S-cones due to the spectral overlap of L- and M-cone sensitivity.

The effect of chromatic contrast change on CIE chromaticity co-ordinates is illustrated graphically by figure 5.7. Here, red-green stimuli, generated using the Red and Green screen phosphors, were changed from maximum to zero contrast in 10% steps to investigate the relationship between chromatic contrast and CIE chromaticity co-ordinates. Co-ordinates for luminance were measured at each contrast using the function spacecolorimeter. As the plot shows, the stimuli are most separated in CIE space at 100% and become of zero contrast.

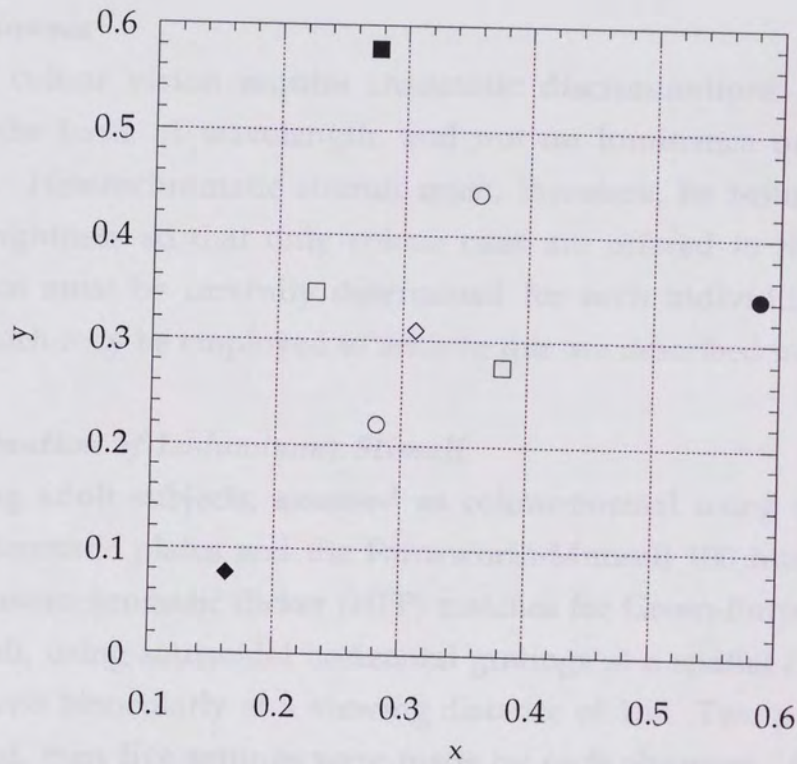


Figure 5.7

The colour axes used in the present study are shown in terms of their x and y CIE chromaticity co-ordinates. Extremities of the axes represent colours at maximum chromatic contrast and the origin (white point) zero contrast. Co-ordinates between these points represent intermediate chromatic contrasts. Filled circle=red phosphor; Filled square=green phosphor; Filled diamond=blue phosphor. Open circles = Tritan axis; Open squares = Red-Green axis. Open diamond = white point.

The effect of chromatic contrast changes on CIE chromaticity co-ordinates is illustrated graphically by figure 5.8. Here, red-green stimuli, generated using the Red and Green screen phosphors, were changed from maximum to zero contrast in 10% steps to investigate the relationship between chromatic contrast and CIE chromaticity co-ordinates. Co-ordinates and luminance were measured at each contrast using the Bentham spectroradiometer. As the plot shows, the stimuli are most separated in CIE space at 100% and coincide at zero contrast.

5.4 Isoluminance

Studies of colour vision require chromatic discriminations to be made purely on the basis of wavelength, and not on luminance or brightness differences. Heterochromatic stimuli must, therefore, be isoluminant and equal in brightness so that only colour cues are offered to the observer. Isoluminance must be carefully determined for each individual; different methods which may be employed to achieve this are described in Chapter 1.

5.5 Determination of Isoluminant Stimuli

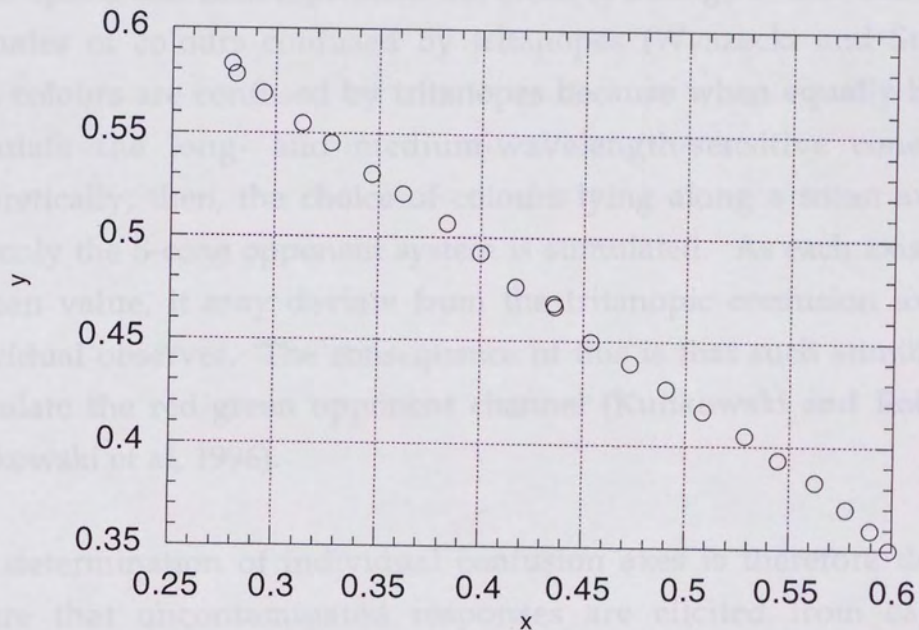
Three young adult subjects, assessed as colour-normal using the Ishihara pseudoisochromatic plates and the Farnsworth-Munsell 100 hue test, made a series of heterochromatic flicker (HFP) matches for Green-Purple and Red-Green stimuli, using sinusoidal horizontal gratings at a spatial frequency of 0.5 cpd viewed binocularly at a viewing distance of 1m. Two practice runs were allowed, then five settings were made by each observer. Adjustments to the chromatic luminance ratio were made directly by the observer, until a point of minimum perceived flicker was reached. For each setting, output values were recorded by the experimenter for subsequent calculation of the mean luminance of each colour grating at perceived isoluminance. As additive failures (see chapter 1) occur at between 11 and 22.6 Hz (Kaiser, 1991) and short-wavelength-sensitive cones may be compromised at temporal frequencies of 28Hz and above (Brindley et al, 1966; Stockman et al, 1993) the procedure was carried out at 20Hz and 30Hz for each subject, for comparison. No significant difference was found between the two, and 20Hz settings were used for determination of an isoluminant point.

The mean chromatic point determined by this method closely approximated photometric luminance, which was used to set the midpoint (luminance ratio 25) of the range of chromatic luminance stimuli from Yellow-Green/Black to Purple/Black or from Green/Black to Red/Black, as described earlier.

5.8 Choice of Colour Area and White Point

As described in Chapter 1, a number of tristimulus colour areas were used in EIT colour space, and each represents the mean of a range of area occupying approximately

Such colour areas were used to generate the colour stimuli. Theoretically, the choice of colour area used ensures that only a small number of colour areas are needed to describe the colour space. However, the colour area used in this study was chosen to ensure that the colour area used is representative of the colour space. The colour area used in this study was chosen to ensure that the colour area used is representative of the colour space.



The colour area used in this study was chosen to ensure that the colour area used is representative of the colour space. The colour area used in this study was chosen to ensure that the colour area used is representative of the colour space.

Mixed chromatic responses to patches are difficult elicited from both colour-opponent channels consist of two negativities, the earlier representing an L-M response and the later an S-cone response (Kukerewski and Kuffner, 1996). Once a chromatic response is elicited in infants, its nature in terms of colour opponent channels may be checked by looking for

Figure 5.8
x and y CIE chromaticity co-ordinates are shown for a red-green stimulus generated using the red and green phosphors, as the stimulus is reduced from maximum to zero chromatic contrast.

The mean isoluminant point determined by this method closely approximated photometric isoluminance, which was used to set the midpoint (luminance ratio 0.5) of the range of chromatic luminance stimuli from Yellowish-Green/Black to Purple/Black or from Green/Black to Red/Black, as described earlier.

5.6 Choice of Colour Axes and White Point

As described in Chapter 1, a number of tritanopic confusion axes exist in CIE colour space, and each represents the mean of a range of axes comprising coordinates of colours confused by tritanopes (Wyszecki and Stiles, 1982). Such colours are confused by tritanopes because when equally bright, they stimulate the long- and medium-wavelength-sensitive cones equally. Theoretically, then, the choice of colours lying along a tritan axis ensures that only the S-cone opponent system is stimulated. As each axis represents a mean value, it may deviate from the tritanopic confusion axis of each individual observer. The consequence of this is that such stimuli may also modulate the red-green opponent channel (Kulikowski and Robson, 1996; Kulikowski et al, 1996).

The determination of individual confusion axes is therefore desirable, to ensure that uncontaminated responses are elicited from each colour-opponent channel. This degree of accuracy in infants would require a level of attention which is rarely encountered at such a young age. In addition, when working with infants before the age of onset of visual evoked responses to isoluminant chromatic stimuli, the individual colour axis would need to be determined before visual evoked responses are demonstrated in infants, making this impossible to achieve.

Mixed chromatic responses to pattern-onset stimuli elicited from both colour-opponent channels consist of two negativities, the earlier representing an L-M response and the later an S-cone response (Kulikowski and Robson, 1996). Once a chromatic response is elicited in infants, its purity in terms of colour-opponent channels may be checked by looking for this characteristic.

Taking the above factors into account, standard colour axes (Wyszecki and Stiles, 1982; Krauskopf et al, 1982; Rabin et al, 1994) were used for the present study in order to generate isoluminant heterochromatic stimuli which elicit separable responses from each colour-opponent channel, and which are practical for infant work. Colour axes of this type may be set around any appropriate origin (Rabin et al, 1994), which may be any white point in colour space, so that stimuli are complementary. The white point for colour stimuli in the present study was of chromaticity co-ordinates $x=0.31$; $y=0.31$ and represents zero chromatic contrast, while extremities of each colour axis represent maximum chromatic contrast (see figure 5.7). This white point was chosen arbitrarily, and its neutral appearance was confirmed by three colour-normal adult observers. As described earlier, the accuracy of chromaticity co-ordinates was confirmed by spectroradiometry.

5.7 Chromatic Aberration

The refraction of light by any optical medium is related to wavelength, each wavelength of light effectively having a different refractive index. Short wavelength light is deviated more than that of medium or long wavelength. Thus, if a white stimulus is viewed, it will be dispersed into its constituent colours and light of short wavelength will have a shorter focal length than lights of longer wavelengths.

When heterochromatic stimuli are viewed, chromatic aberration has the effect of defocusing one colour with respect to the other. In addition, this relative defocus is known to be a stimulus for accommodation, so that contrast does not necessarily remain constant (Stone et al, 1993).

Heterochromatic stimuli rendered isoluminant in the object plane may no longer be isoluminant in the image plane (on the retina) due to relative defocus by chromatic aberration (Thibos et al, 1991). Studies requiring chromatic stimuli to be isoluminant may, therefore, be flawed by luminance intrusions.

Chromatic aberration effects increase with spatial frequency, being

negligible at low frequencies (Flitcroft, 1989). In the present study, heterochromatic stimuli were presented at a spatial frequency of 1.0 cpd for adults and 0.2 cpd for infants. This was intended to minimise the effects of chromatic aberration and to ensure that stimuli were within visual acuity limits for chromatic stimuli.

5.8 Pattern-Onset Stimuli

Once sinusoidal horizontal gratings had been generated in each colour, for either chromatic luminance or for chromatic contrast stimuli, an abrupt pattern-onset regime of presentation was established. The gratings were presented for a specified number of frames, then a uniform (unpatterned) stimulus of the same mean luminance and chromaticity as the pattern was presented for a further set number of frames.

The number of frames for stimulus onset and offset therefore determined the temporal frequency of the stimulus. The frame rate of the monitor used was 150 Hz (150 frames per second). A stimulus onset period of 15 frames (100 ms) followed by offset of 60 frames (400 ms) was presented twice per second, and so was at a temporal frequency of 2 Hz. This temporal duty cycle of 20% onset to offset was chosen to elicit a robust chromatic VEP (Rabin et al, 1994).

5.9 Determination of EEG Noise Levels

A control stimulus was generated for 'non-stimulus' recording, following each recording session. The purpose of a non-stimulus recording is to compare the visual evoked response to each pattern-onset stimulus with the response to a uniform screen of the same mean luminance. This stimulus was generated by presenting the same type of stimuli used for offset periods. Recording conditions were exactly the same as for pattern-onset stimuli.

Comparison of stimulus and non-stimulus recordings was carried out subjectively, but to allow a more accurate assessment the two were also compared in terms of signal-to-noise ratio. Using a software facility on the averaging equipment and a Borland C programme, the standard deviation

of response amplitude from baseline at 1000 points, at 0.5 ms intervals on a 500 ms sweep, was calculated for each recording. This value for the non-stimulus response was compared to that of each stimulus recording, to obtain a signal-to-noise ratio for each. Recordings with ratios of less than the arbitrarily chosen value of 1.5 were not regarded as evoked potentials, as these were not significantly greater than the EEG noise level (Kriss, 1993).

5.10 VEP Recording Procedure

Visual evoked potentials were recorded using the International 10-20 system of electrode positioning, from Oz referred to Cz (single channel), with Fz as earth. Scalp positions were abraded using Omniprep. Blenderm tape was used to fix silver silver-chloride 1cm disc electrodes in position. Collodion adhesive was used in addition to the tape in infants only. Resistance at each electrode position was tested prior to recording and was always below 8 kOhms.

VEPs were averaged from 50 recordings in adults and from at least 30 in infants, using the Medelec Sapphire 4E signal averager. Signals were bandpass filtered (1-50 Hz) and a sweep speed of 500 ms was specified on the averager. Each averaged response was repeated at least once to ensure that responses were reliable. The infants' attention was directed to the screen using a small bunch of keys. If attention was lost during recording averaging was paused, then continued when possible. The software was set to trigger averaging at the beginning of stimulus onset by sending a trigger pulse to the signal averager at this point of each presentation.

Viewing was always binocular, and was from a distance of 1m for adults. Infants were seated on a parent's lap (see figure 5.9) and viewed the stimulus from a distance of 40 cm, to avoid inaccuracy of accommodation beyond this distance in young infants (Banks, 1980). The angular subtense of the display was 40 deg horizontally by 32 deg vertically at a viewing distance of 40 cm, and 20 deg by 14 deg at 1m.

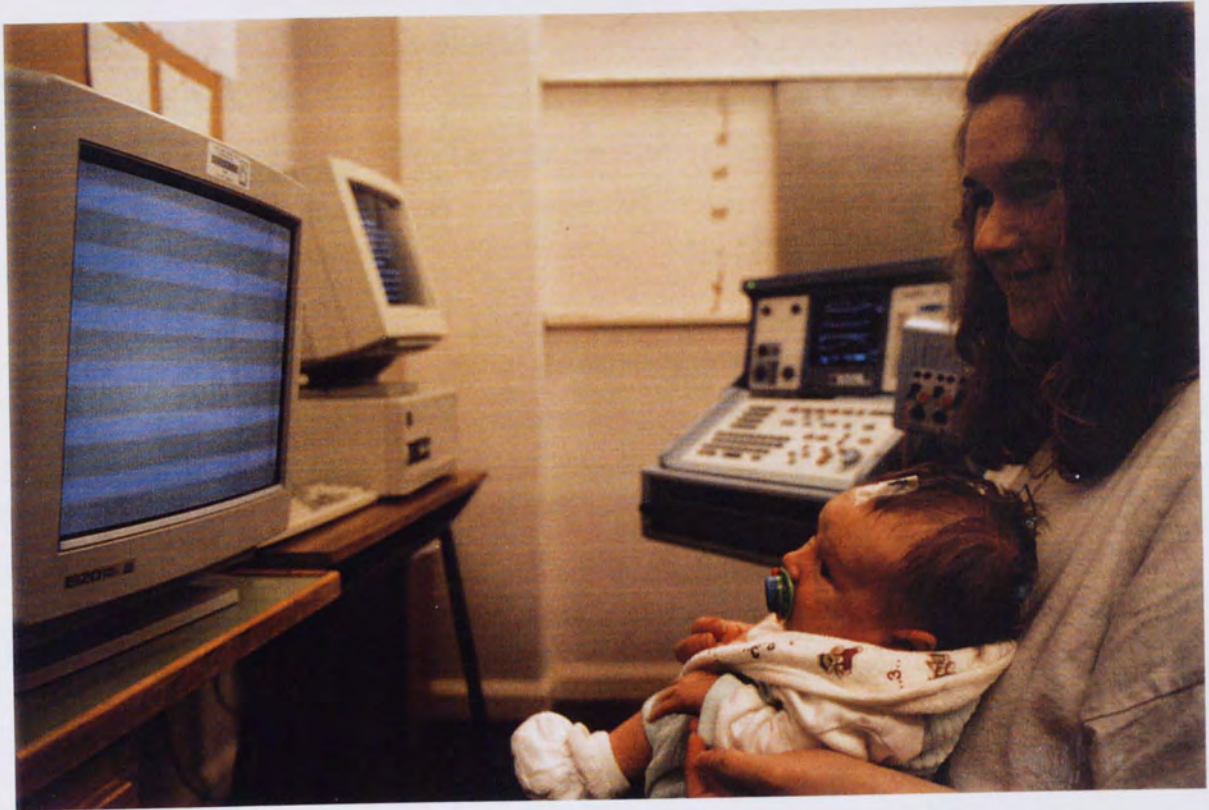


Figure 5.9
Infant BH is shown on his mother's lap watching the tritan stimulus, to illustrate the recording procedure used for infants.

5.11 Subjects

Infants were recruited from the patient population of the Newtown Health Centre ante-natal clinic and from the Aston University Nursery, both in Birmingham, by discussion with their parents. Adults were recruited from the student and staff population of Aston University Vision Sciences Department.

Exclusion criteria were significant refractive error, squint, amblyopia, ocular or systemic pathology and colour vision defects or family history of defective colour vision. An age limit of 39 was set for adult subjects, to avoid age-related changes in ocular media. Seventeen infants were recruited into the study. Five of these were subsequently excluded due to failure to complete tests, lack of co-operation, or inconsistency of results. Results from these five infants have not been reported here.

Of the twelve infants who completed the study, one (RH) was diagnosed with cystic fibrosis at the age of 13 weeks; results for this infant are reported in Chapter 8; results for the remaining eleven infants are reported in Chapters 7 and 9. Ten of the twelve infants were tested from 4 weeks post-term age, and tests were repeated at one to two weekly intervals until visual evoked responses to both types of chromatic stimuli were elicited at and around isoluminance. In most cases, intervals were of one week. In some instances, however, parents were unable to return exactly when required and up to two weeks passed between tests. Of these infants, five (DH, DC, JC, MB, PR) continued to attend up to three months of age, two of which (DH and MB) were also tested at 4, 5 and 6 months post-term. Two of the twelve infants (KB and AM) were tested for the first time at 3 months of age and were also tested at 4 and 5 months. All references to infant age are dated from term, which is taken as 40 weeks from the mother's last menstrual period.

Adults were screened for colour vision defects using the Ishihara pseudoisochromatic plates and the Farnsworth-Munsell 100-hue test under a standard Illuminant C (Kinnear, 1970). Visual acuity was assessed using the Snellen chart. In infants, refractive error was assessed by cycloplegic retinoscopy, using one drop of 1% cyclopentolate hydrochloride in each eye.

This was carried out after a session of VEP recording. Screening for ocular pathology and family history was by ophthalmoscopy and symptoms and history. A signed declaration of informed consent was obtained from each subject or parent prior to inclusion in the study.

The visual evoked response to chromatic stimulation has been widely studied in adults, in order to investigate the characteristics of the colour-opponent pathways of the visual system and to establish normative data for clinical comparisons. Stimulation has generally been either by pattern-reversal or pattern-onset, each of which have been found to give responses of distinct morphology to the same pattern stimuli. Response morphology is dependent not only on individual parameters such as spatial frequency, but also on whether grating or checkerboard stimulation is used (Murray and Speltridge, 1974; Murray et al, 1987).

Pattern-reversal checkerboard red-green stimuli were found by Thompson and Drasdo (1992) to produce a dominant negative peak at isoluminance. This response differed from the triphasic response to luminance-modulated stimuli, which comprised a dominant positivity flanked by negative going waves. Other workers, however (Berninger et al, 1989; Kubikowski et al, 1989, 1991) find that the pattern-reversal isoluminant chromatic and luminance contrast VEP are similar in morphology, each consisting of a major positivity at latencies of about 100ms and 140 ms respectively. These discrepant findings may be due to differences in spatial frequency used (Thompson and Drasdo, 1992).

Pattern-onset chromatic (luminance) stimulation also elicits a positive peak response component (Kubikowski et al, 1989). The peak latencies of pattern-onset isoluminant chromatic stimulation, however, comprise a negative component being longer in latency to blue-yellow or cyan stimulation than to red-green (Murray et al, 1987; Berninger et al, 1989; Kubikowski et al, 1989; Crognale et al, 1993; Korth et al, 1994; Rubin et al, 1994). This morphological distinction has been attributed to the different response characteristics of the phasic (transient) and tonic (sustained) cell types of the magnocellular and parvocellular systems respectively (Murray et al, 1987).

CHAPTER 6

THE ADULT CHROMATIC VEP

6.1 Introduction

The visual evoked response to chromatic stimulation has been widely studied in adults, in order to investigate the characteristics of the colour-opponent pathways of the visual system, and to establish normative data for clinical comparisons. Stimulation has generally been either by pattern-reversal or pattern-onset, each of which have been found to elicit responses of distinct morphology in the colour-normal human adult. Response morphology is dependent not only on mode of presentation (onset or reversal), but also on whether grating or checkerboard stimuli are used (Regan and Spekreijse, 1974; Murray et al, 1987).

Pattern-reversal checkerboard red-green stimuli were found by Thompson and Drasdo (1992) to produce a dominant negative peak at isoluminance. This response differed from the triphasic response to luminance-modulated stimuli, which comprised a dominant positivity flanked by negative-going waves. Other workers, however (Berninger et al, 1989; Kulikowski et al, 1989, 1991) find that the pattern-reversal isoluminant chromatic and luminance contrast VEP are similar in morphology, each consisting of a major positivity at latencies of about 100ms and 140 ms respectively. These discrepant findings may be due to differences in spatial frequency used (Thompson and Drasdo, 1992).

Pattern-onset achromatic (luminance) stimulation also elicits a positive peak response component (Kulikowski et al, 1989). The peak response to pattern-onset isoluminant chromatic stimulation, however, consists of a negative component, being longer in latency to blue-yellow or tritan stimulation than to red-green (Murray et al, 1987; Berninger et al, 1989; Kulikowski et al, 1989; Crognale et al, 1993; Korth et al, 1993; Rabin et al, 1994). This morphological distinction has been attributed to the different response characteristics of the phasic (transient) and tonic (sustained) cell types of the magnocellular and parvocellular systems respectively (Murray et al, 1987).

A second negative component in the evoked response to isoluminant chromatic stimulation, of approximately 60 ms longer latency than the major negativity, is elicited when pattern elements are introduced to the stimulus. This has led to the conclusion that the first negativity is a response to chromatic contrast, while the second is a response from cells not sensitive to colour but to pattern elements (Kulikowski et al, 1989). The negative response to isoluminant chromatic pattern-onset stimulation is widely accepted to be a response from parvocellular colour-opponent cells, and therefore is said to represent sustained activity, while positive components in the evoked response are thought to represent transient (magnocellular) activity (eg. Murray et al, 1987).

Generally, pattern onset-offset isoluminant stimuli have been found to elicit more robust VEPs than pattern-reversal stimuli. This difference is thought to be due to adaptation to the constantly presented pattern-reversal stimulation, while adaptation and recovery take place in the case of pattern onset-offset (Rabin et al, 1994). An optimal temporal duty cycle of 20% (Rabin et al, 1994) onset-to-offset have been determined by investigating responses to isoluminant stimuli of various onset-to-offset period ratios. This again suggests that a suitable recovery period between stimuli optimises the visual evoked response.

It has been suggested that stimuli comprising blue-yellow hues may elicit a bimodal response, indicating the involvement of more than one mechanism of the visual system (Kulikowski and Robson, 1996; Kulikowski et al, 1996). Blue-yellow stimuli may not lie along a tritanopic confusion axis (Krauskopf et al, 1982), and so may elicit responses not only from the S-cone opponent channel, as intended, but a mixed response from both colour-opponent channels. In this situation, the earlier peak would represent the red-green response while the later peak represents an S-cone response, generally found to be of longer latency.

When isoluminant chromatic stimuli are presented along protanopic, deuteranopic or tritanopic confusion axes, responses are severely reduced or

absent in dichromats (Shipley et al, 1965; Kinney and McKay, 1974; Crognale et al, 1993). This finding has been used clinically, and to confirm the effectiveness of colour confusion stimuli in stimulating distinct colour-opponent mechanisms (Rabin et al, 1994).

In the present study, visual evoked responses to isoluminant chromatic and to luminance-modulated stimuli were recorded from colour-normal adults, for comparison with those of infants. Responses were recorded to chromatic stimuli of maximum chromatic contrast at a range of luminance ratios and responses to isoluminant chromatic stimuli were also recorded at a range of chromatic contrasts from 80% to 10% of maximum, in an attempt to determine chromatic contrast thresholds.

Responses to chromatic stimuli of maximum contrast were required for comparison with those of infants. The selective stimulation of cells sensitive to chromatic and not luminance contrast is more effective at low chromatic contrast (Tootell et al, 1988). Responses to chromatic stimuli of relatively low contrast recorded from adults were useful in assessing whether components in the adult chromatic VEP were responses to chromatic or other elements in the stimuli.

6.2 Methods

Five adult subjects, three female, two male, aged 29 to 39 years were assessed as colour-normal using Ishihara pseudoisochromatic plates and the Farnsworth-Munsell 100-Hue test, under a standard Illuminant C light source. Relatively young subjects were chosen in order to avoid age-related ocular media density changes. All had 6/6 or better Snellen visual acuity in each eye.

Horizontal sinusoidal gratings of spatial frequency 1.0 cpd were generated as described in Chapter 5, and were viewed binocularly at a viewing distance of 1m. At this spatial frequency, 12.5 cycles were presented on the 17-inch diameter CRT monitor. Stimuli were presented along a tritanopic confusion axis (green-purple) and along an axis orthogonal to this (red-green) in CIE colour space, also described in Chapter 5. Isoluminance for

each colour pair was determined for three of the five colour-normal observers using heterochromatic flicker photometry at an alternation rate of 20Hz, and was found in all cases to closely approximate photometric isoluminance, as shown by figure 6.1.

Abrupt pattern-onset presentation was used at a temporal frequency of 2Hz, with a temporal duty cycle of 20%. This allowed an onset duration of 100ms and offset of 400ms. During offset periods, the stimulus was a uniform screen of the same mean luminance and mean chromaticity as the pattern.

Stimuli were presented at photometric isoluminance (colour luminance ratio 0.5) and at the following range of luminance ratios: 0.0, 0.2, 0.4, 0.45, 0.5, 0.55, 0.6, 0.8, 1.0. Here, 0.0 and 1.0 represent luminance-modulated chromatic stimuli such as green-black and red-black gratings. This range of colour luminance ratios was used for comparison with luminance and chromatic visual evoked responses in infants, and in order to investigate the behaviour of the adult VEP to pattern-onset isoluminant and luminance-modulated stimuli. Mean luminance for all stimuli was maintained at 20 cd/m², and was measured using the Minolta LS 110 photometer.

Photopic stimuli elicit evoked responses of different morphology, greater amplitude and shorter latency than those elicited under scotopic conditions (Wooten, 1972). Stimuli of moderate photopic luminance levels such as that used in the present study, may stimulate rods as well as cones. In order to investigate whether rods made a significant contribution to evoked responses from adults to stimuli used in this study, responses were recorded from one adult (VT) to isoluminant tritan and red-green stimuli at mean luminances of 20, 30 and 40 cd/m², the maximum luminance possible with the display used. Maximum chromatic contrast was used in stimuli presented to infants, so maximum contrast was also used for adults, as responses were to be compared in the two groups. In addition, chromatic stimuli were presented at a range of contrasts in an attempt to determine chromatic contrast thresholds, again for comparison with those of infants.

6.1.1 The peak visual evoked response to chromatic stimulation

(0.3) red-green or tritan chromatic stimulation consisted of a single reversivity at a latency of 113 to 183 ms after stimulus onset (see figures 6.2 to 6.5). At colour ratios away from isoluminance, this response component was found to decrease in latency (see figures 6.6 and 6.7). Responses to tritan stimulation peaked at a latency of 4 to 23 ms later than red-green responses, in four out of the five subjects (figure 6.8). In all subjects, responses to both types of chromatic stimulation were similar in amplitude ($p > 0.1$). This is in agreement with previous studies and is thought to reflect selective cortical magnification of the relatively small input from the S-cone opponent channel (Berninger et al., 1999).

6.1.2 Individual responses to pattern offset

The evoked response to pattern offset is illustrated by figure 6.9 (upper row). At isoluminance, the response was unimodal or bimodal. As luminance differences were introduced to the chromatic stimulus, however, a second, shorter offset burst as a first response became apparent. The second burst positivity of 100 ms to 120 ms after stimulus offset (figure 6.9, lower row, 20 to 30 ms lag). This component was verified as a response to stimulus offset by increasing the flash duration so that offset occurred first. The other response component was found to occur correspondingly later in the response (figure 6.7, lower row). The offset response became a single unimodal response as colour ratio approached 0.0 and 1.0 (chromatic stimulation and luminance ratio were 1.0 for one subject by figures 6.10 and 6.11. (However, the first subject, AE, FF and VT) demonstrated offset responses at colour ratios of 0.2 and 0.5 (very close to isoluminance), as well as at other colour ratios away from isoluminance. The remaining two subjects, J and VT, did not demonstrate offset responses at colour ratios of 0.0 to 0.5 and 0.5 to 1.0.

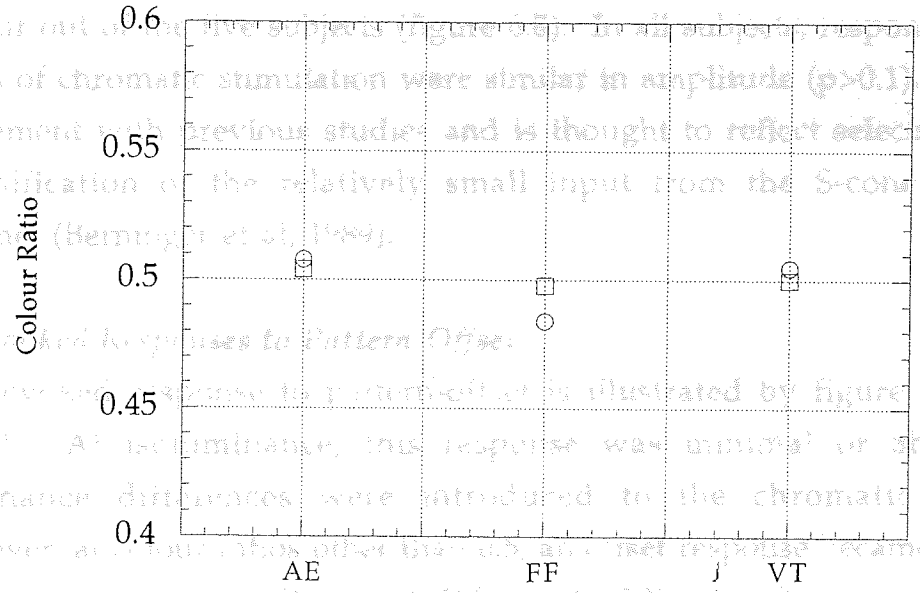


Figure 6.1. Colour ratios representing individual isoluminant points for three colour-normal adults, identified by their initials, determined by heterochromatic flicker photometry at a temporal frequency of 20 Hz. Photometric isoluminance is at a colour ratio of 0.5. Open circles represent tritan matches; open squares represent red-green matches.

Results and Discussion

6.3 Responses to Pattern-Onset Chromatic Stimuli

The peak visual evoked response to pattern-onset isoluminant (colour ratio 0.5) red-green or tritan chromatic stimulation consisted of a single negativity at a latency of 113 to 183 ms after stimulus onset (see figures 6.2 to 6.5). At colour ratios away from isoluminance, this response component was found to decrease in latency (see figures 6.6 and 6.7). Responses to tritan stimulation peaked at a latency of 4 to 23 ms later than red-green responses, in four out of the five subjects (figure 6.8). In all subjects, responses to both types of chromatic stimulation were similar in amplitude ($p>0.1$). This is in agreement with previous studies and is thought to reflect selective cortical magnification of the relatively small input from the S-cone opponent channel (Berninger et al, 1989).

6.4 Evoked Responses to Pattern-Offset

The evoked response to pattern-offset is illustrated by figure 6.9 (upper trace). At isoluminance, this response was minimal or absent. As luminance differences were introduced to the chromatic stimulus, however, at colour ratios other than 0.5, an offset response became apparent. This comprised a positivity at 100 ms to 120 ms after stimulus offset followed by a negativity 20 to 30 ms later. This component was verified as a response to stimulus offset by increasing the onset duration so that offset occurred later. The offset response component was found to occur correspondingly later in the response (figure 6.9, lower trace). The offset response increased in amplitude as colour ratios approached 0.0 and 1.0 (luminance-modulated stimulation), as shown for one subject by figures 6.10 and 6.11. Three of the five subjects (AE, FF and VT) demonstrated offset responses at colour ratios of 0.45 and 0.55, very close to isoluminance, as well as at other colour ratios away from isoluminance. The remaining two subjects (IH and RW) showed offset responses only at colour ratios of 0.0 to 0.4 and 0.6 to 1.0.

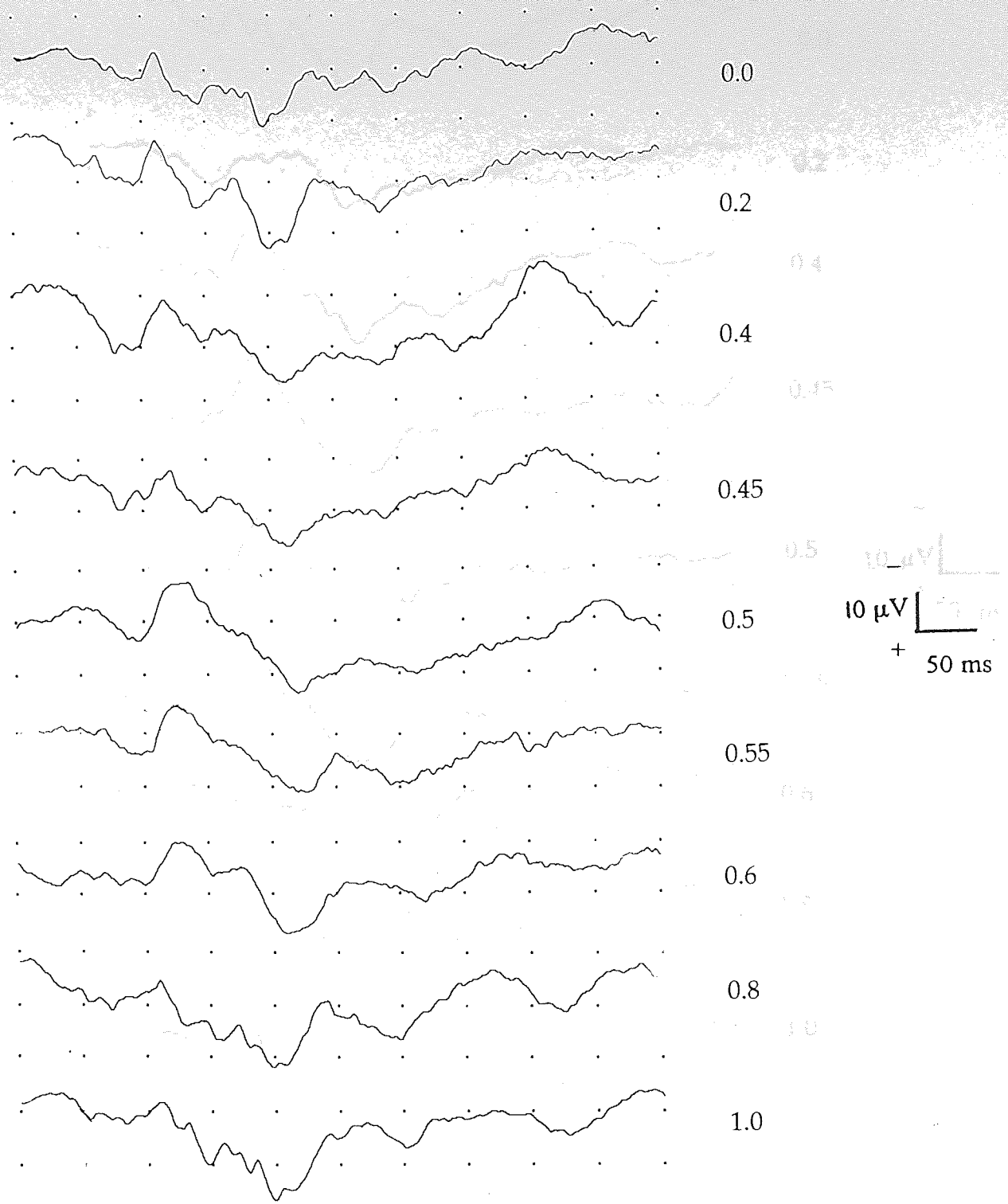


Figure 6.2.
 Visual evoked responses to tritan stimuli at the full range of colour ratios recorded from adult subject AE.

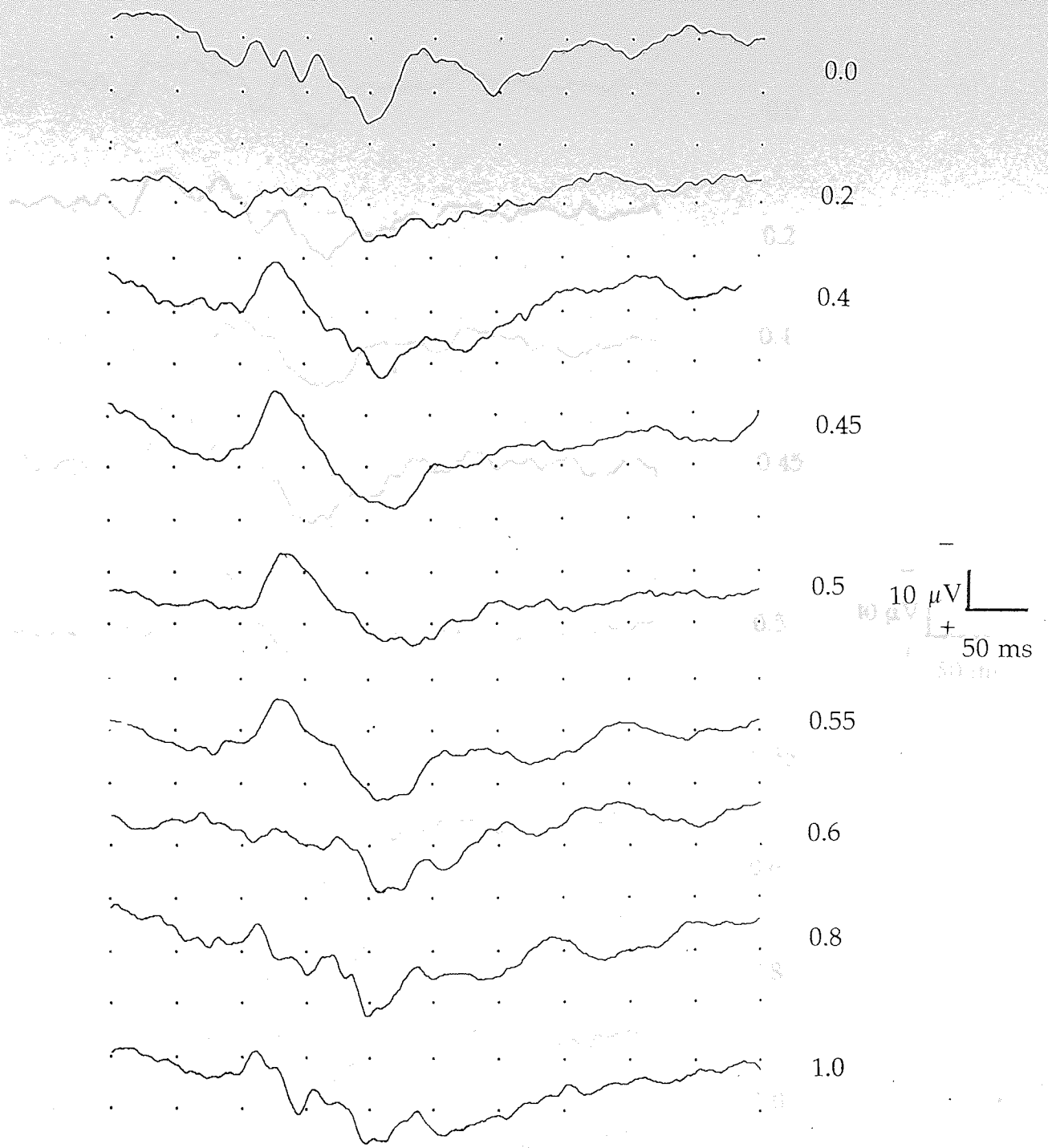


Figure 6.3.
 Visual evoked responses to red-green stimuli at the full range of colour ratios recorded from adult subject AE.

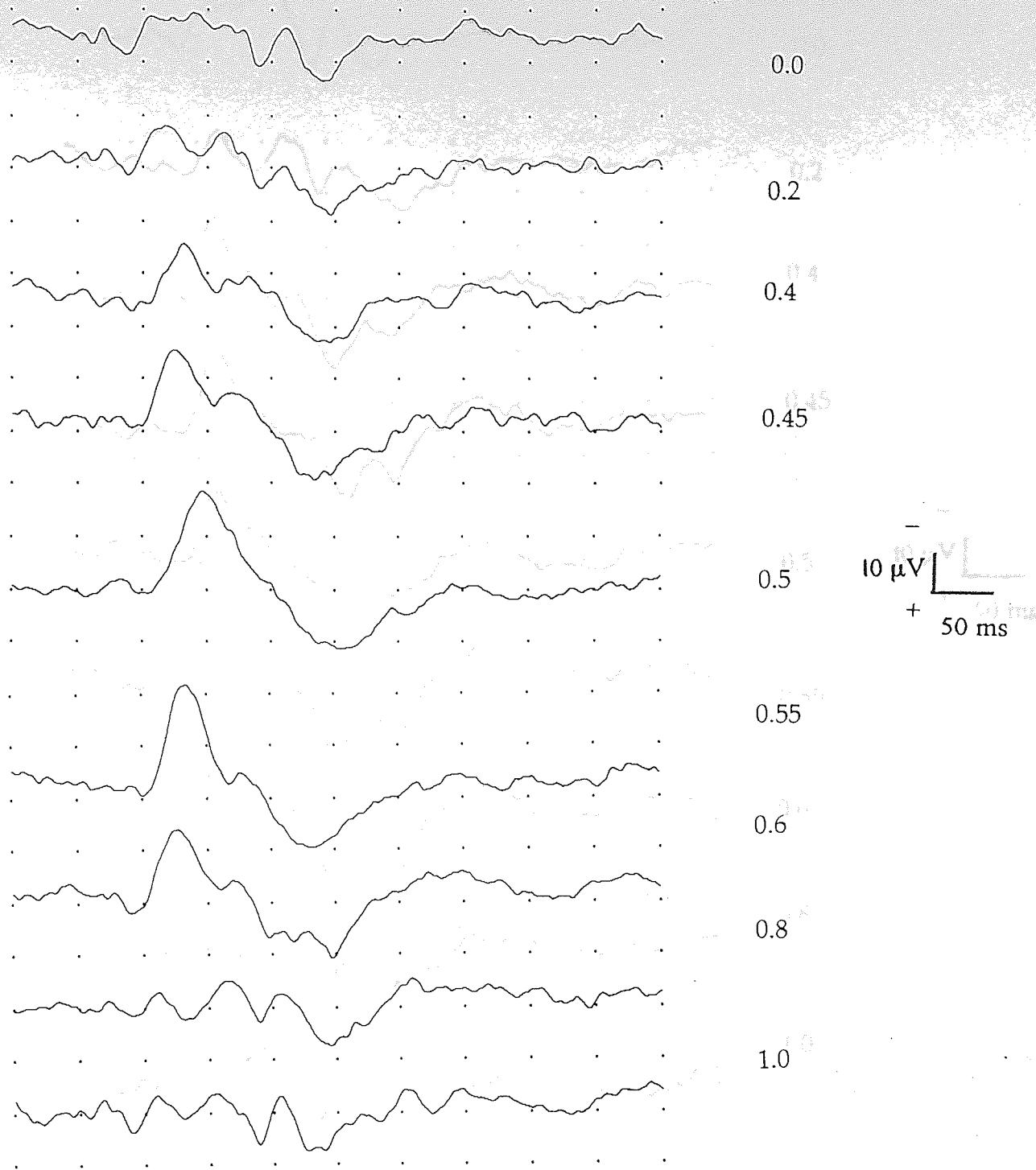


Figure 6.4.
 Visual evoked responses to tritan stimuli at the full range of colour ratios recorded from adult subject VT.

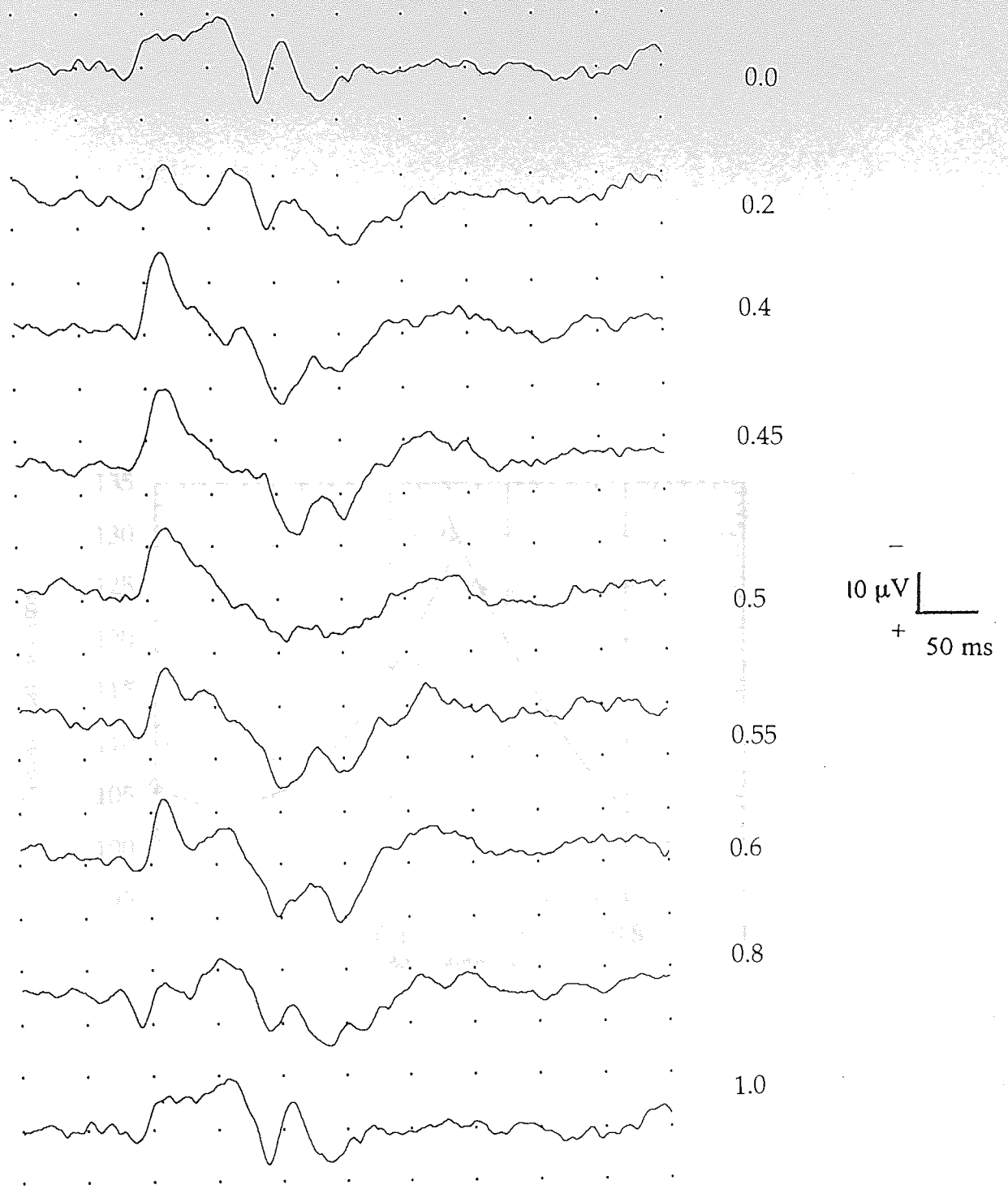


Figure 6.5. Visual evoked responses to red-green stimuli at the full range of colour ratios recorded from adult subject VT.

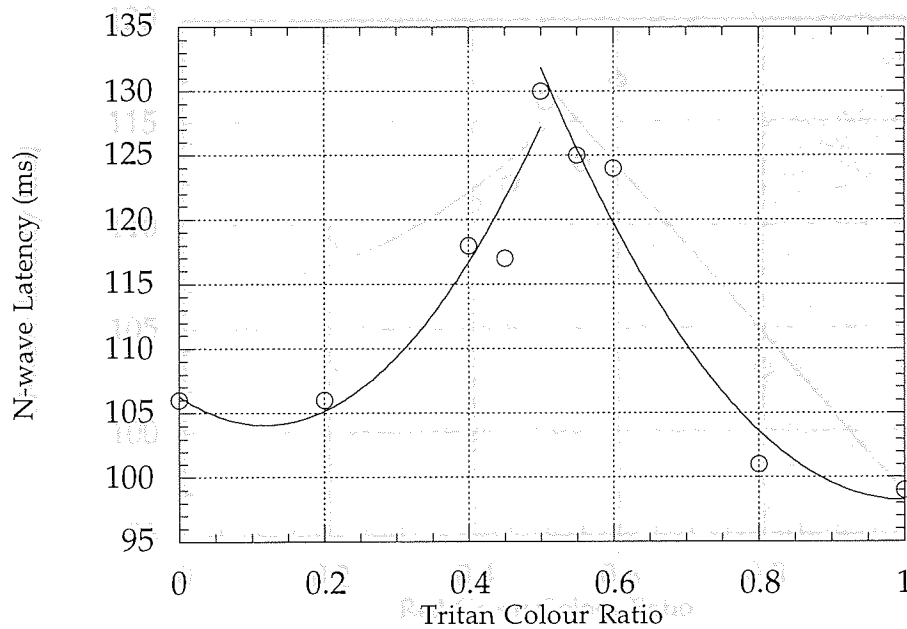


Figure 6.6.

Figure 6.6. Latency of the negative response to tritan stimulus onset is plotted against colour ratio for subject FF, showing an increase in latency towards isoluminance. Second-order polynomial functions are shown for data sets either side of isoluminance. These provided significantly better fits to the data than linear regression ($r=0.96$ for fit from 0.0 to 0.5; $r=0.98$ for fit from 0.5 to 1.0). This trend was present for all five adult subjects tested.

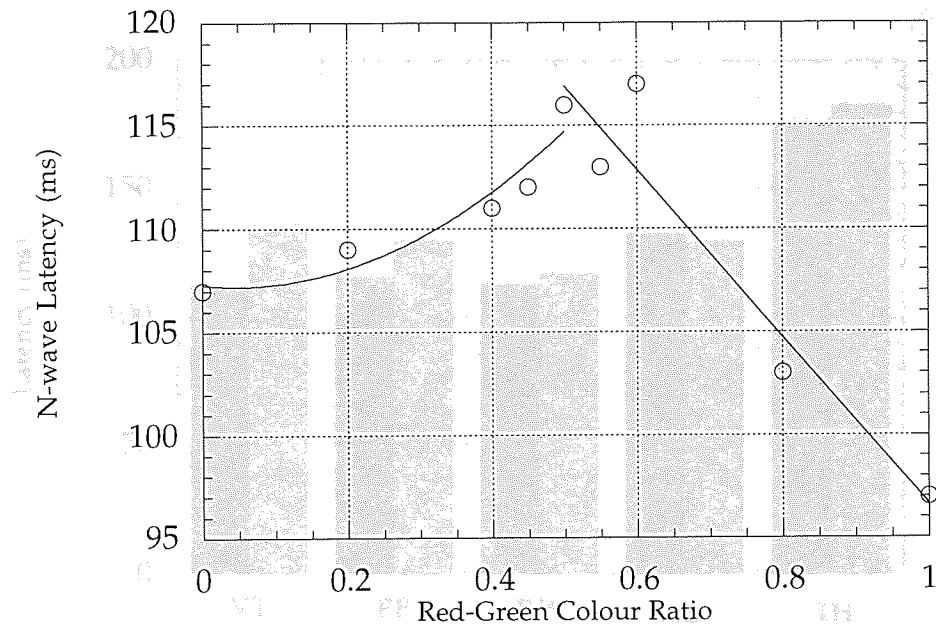


Figure 6.7.

The latency of the negative response to red-green stimulus onset is plotted against colour ratio, for subject FF, showing an increase in latency towards isoluminance. A second-order polynomial function is fit to the data from colour ratios of 0 to 0.5 ($r=0.94$); this provided a significantly better fit than a linear regression. The rest of the data is equally well represented by a linear function ($r=0.95$) there being no improvement with a polynomial fit in this case. This trend was present for all five adult subjects tested.

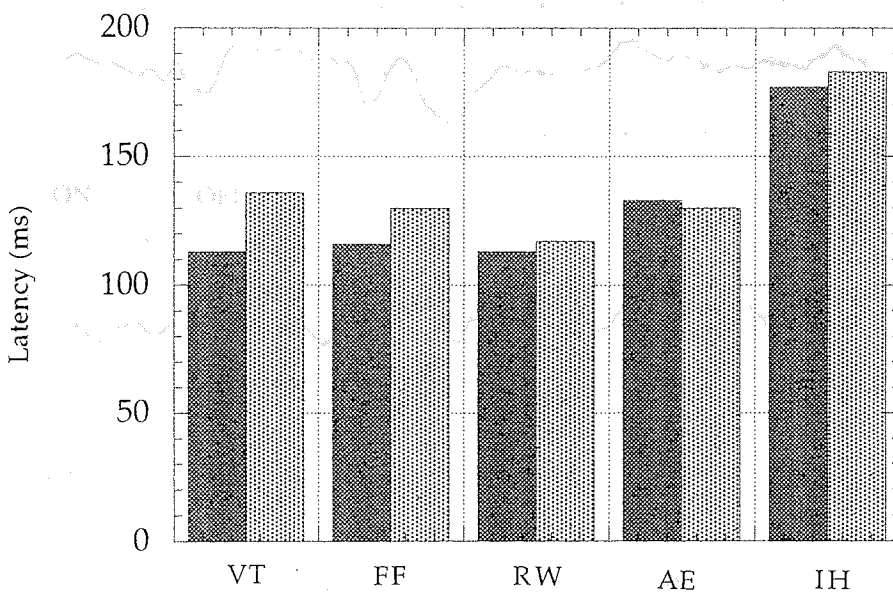


Figure 6.8.

The vertical axis shows latencies (ms) of the negative peak response to chromatic stimulus onset for red-green (darker columns) and tritan isoluminant stimuli. The mean of response latencies for red-green stimuli is 130.4 ms (standard deviation 27.3 ms) and for tritan responses 139.2 ms (standard deviation 25.5 ms). Subjects are identified by their initials.

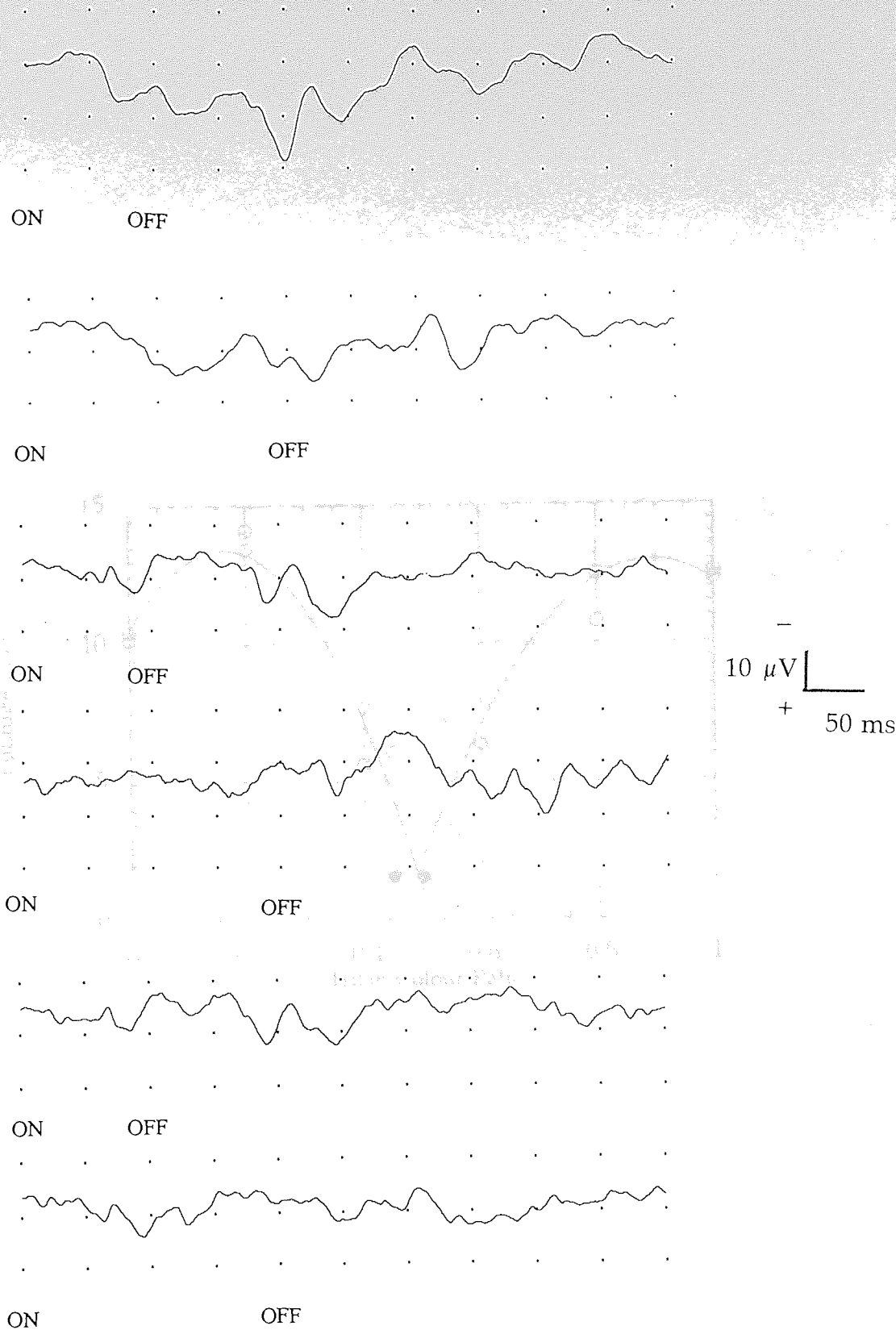


Figure 6.9. The visual evoked response to stimulus offset is demonstrated here by doubling the onset duration to 200 ms, so that stimulus offset occurs 100 ms later in the lower of each pair of traces than in the upper of each pair (Adult subject FF, top traces; RW, middle traces; VT, lowest traces). By increasing onset duration in this way, the temporal duty cycle changes from 1:4 to 1:1.5. Consequently, the onset response is diminished (see page 121) and the response as a whole differs in morphology.

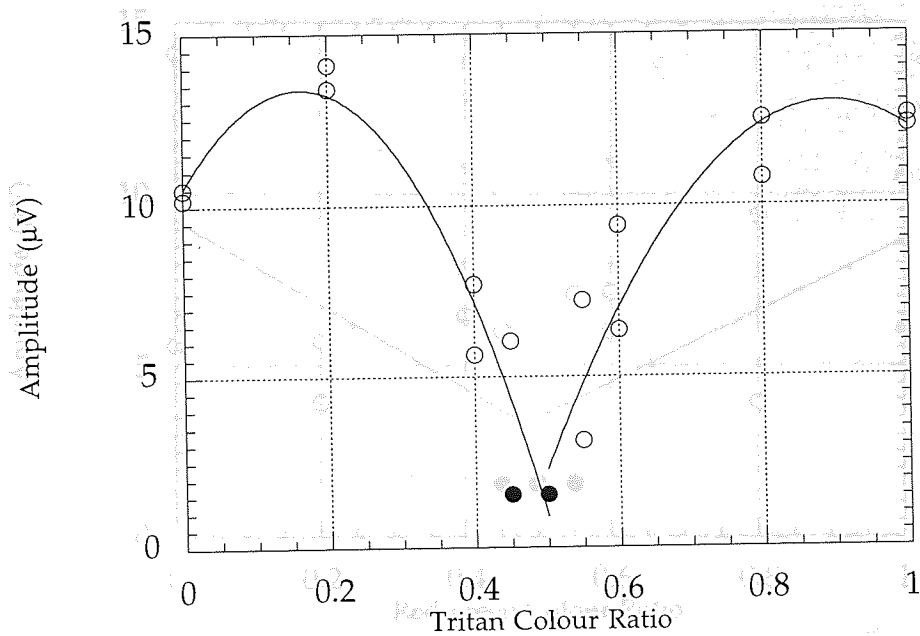


Figure 6.10. The amplitude of the visual evoked response to tritan stimulus offset is plotted here against colour ratio, for subject AE. Open circles indicate evoked responses significantly above EEG noise level; filled circles indicate those at or below this level. Second-order polynomial functions fit to each data set either side of isoluminance provided the best fit to the data ($r=0.96$ for fit from 0.0 to 0.5; $r=0.94$ for fit from 0.5 to 1.0). Four of the five adult subjects demonstrated the trend shown here with offset response amplitude reducing towards isoluminance.

6.5 The Response to Non-Isoluminant Chromatic Stimuli

The response to pattern-onset also changed considerably as luminance differences were introduced to the stimulus. As described earlier, the peak response to stimulus onset at isoluminance was a single negativity. At colour ratios other than 0.5, a second negative peak appeared on the descending limb of the onset response, at about 50 ms later than the first negativity (see figures 6.2 to 6.5). This component became more distinct with increasing luminance difference in the stimulus. As a result of changes to the onset and offset responses, the visual evoked response to luminance-modulated stimulation was found to be far more complex than the isoluminant response. This is in agreement with previous findings (Kulikowski et al, 1989) described earlier (see page 127) in a study of adult transient visual evoked responses to chromatic stimulation (red-green and blue-yellow). Two negative responses were elicited, one at a latency of 120 ms and one approximately 60 ms later. The first component was found to be a response to chromatic contrast while the second was in response to the pattern elements of the stimulus.

In the present study, the emergence of a second negativity which increases in definition with luminance difference in the stimulus suggests that the earlier negative component elicited at isoluminance is a response to chromatic contrast, while the second negative is a response to luminance stimulation. The first negative component is likely therefore to represent parvocellular activity and the second, magnocellular involvement.

Responses from subject VT at a range of chromatic contrasts (see figure 6.12) show that the second negativity is diminished at relatively low contrasts (10% and 20%), further implying that this component originates from cells not sensitive to colour contrast, as magnocellular and parvocellular neurones are selectively activated most effectively when low contrast stimuli are used (Tootell et al, 1988).

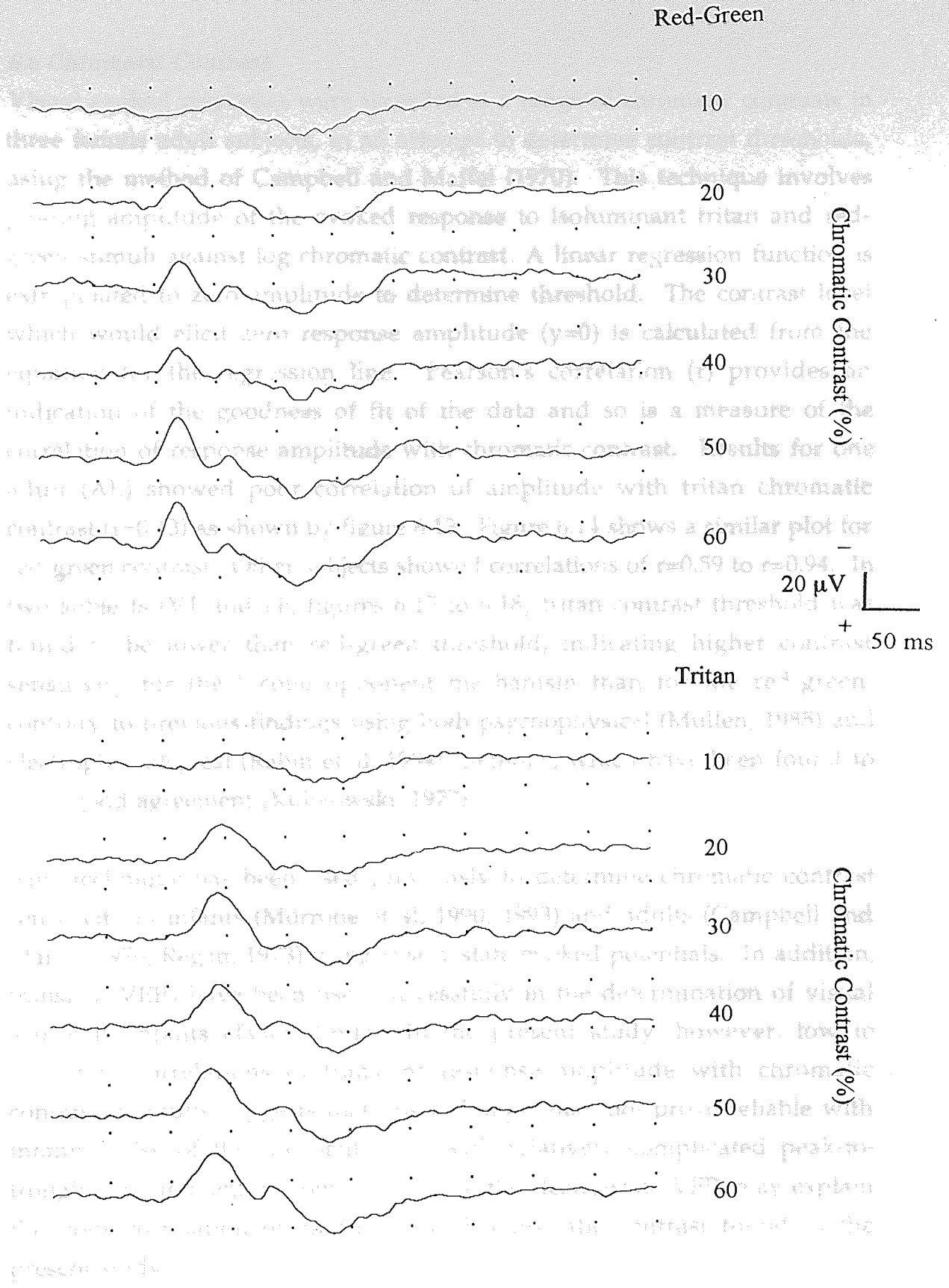
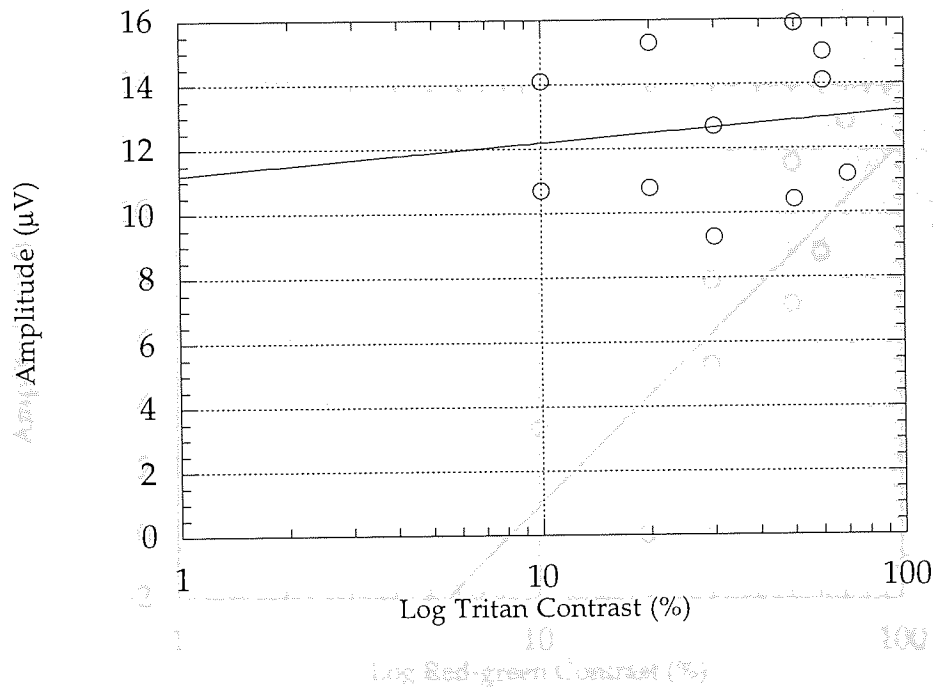


Figure 6.12. Visual evoked responses to isoluminant chromatic stimuli at a range of chromatic contrasts, recorded from adult subject VT.

6.6 Chromatic Contrast

Visual evoked responses were recorded at a range of chromatic contrasts in three female adult subjects, in an attempt to determine contrast thresholds, using the method of Campbell and Maffei (1970). This technique involves plotting amplitude of the evoked response to isoluminant tritan and red-green stimuli against log chromatic contrast. A linear regression function is extrapolated to zero amplitude to determine threshold. The contrast level which would elicit zero response amplitude ($y=0$) is calculated from the equation for the regression line. Pearson's correlation (r) provides an indication of the goodness of fit of the data and so is a measure of the correlation of response amplitude with chromatic contrast. Results for one adult (AE) showed poor correlation of amplitude with tritan chromatic contrast ($r=0.13$) as shown by figure 6.13. Figure 6.14 shows a similar plot for red-green contrast. Other subjects showed correlations of $r=0.59$ to $r=0.94$. In two subjects (VT and FF; figures 6.15 to 6.18) tritan contrast threshold was found to be lower than red-green threshold, indicating higher contrast sensitivity for the S-cone opponent mechanism than for the red-green, contrary to previous findings using both psychophysical (Mullen, 1985) and electrophysiological (Rabin et al, 1994) methods, which have been found to be in good agreement (Kulikowski, 1977).

This technique has been used previously to determine chromatic contrast sensitivity in infants (Morrone et al, 1990, 1993) and adults (Campbell and Maffei, 1970; Regan, 1973) using steady-state evoked potentials. In addition, transient VEPs have been used successfully in the determination of visual acuity in infants (Tyler, 1991). In the present study, however, low to moderate correlations of transient response amplitude with chromatic contrast in adults suggests that this technique may not prove reliable with infants. Use of the transient VEP, with relatively complicated peak-to-trough measurement by comparison with the steady-state VEP, may explain the poor correlation of amplitude with chromatic contrast found in the present study.



$$y = 11.198 + 0.99519 \log x$$

$$r = 0.13$$

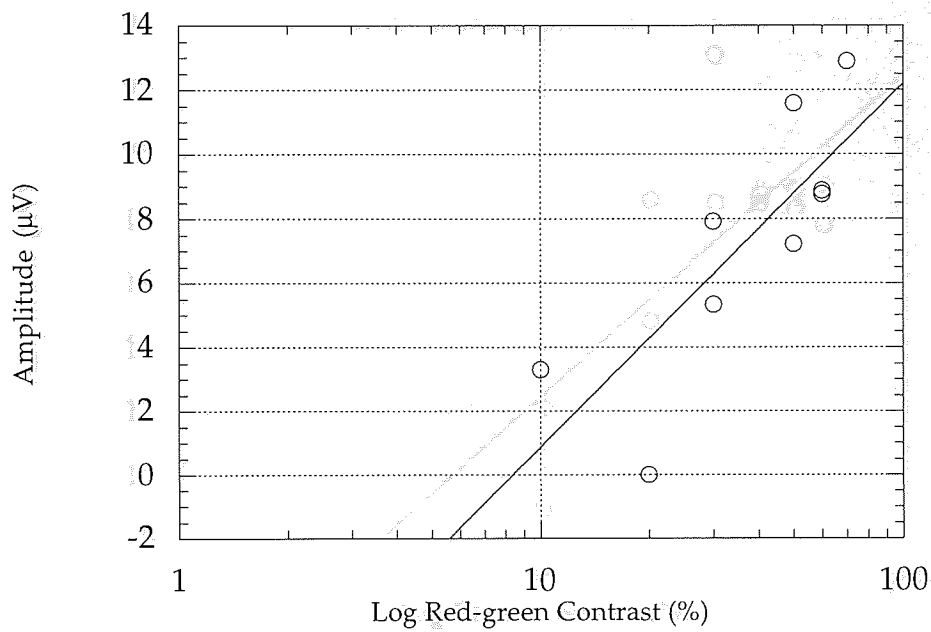
$$y = 10.17 + 11.337 \log x$$

$$r = 0.70$$

Contrast Threshold = 8.3%

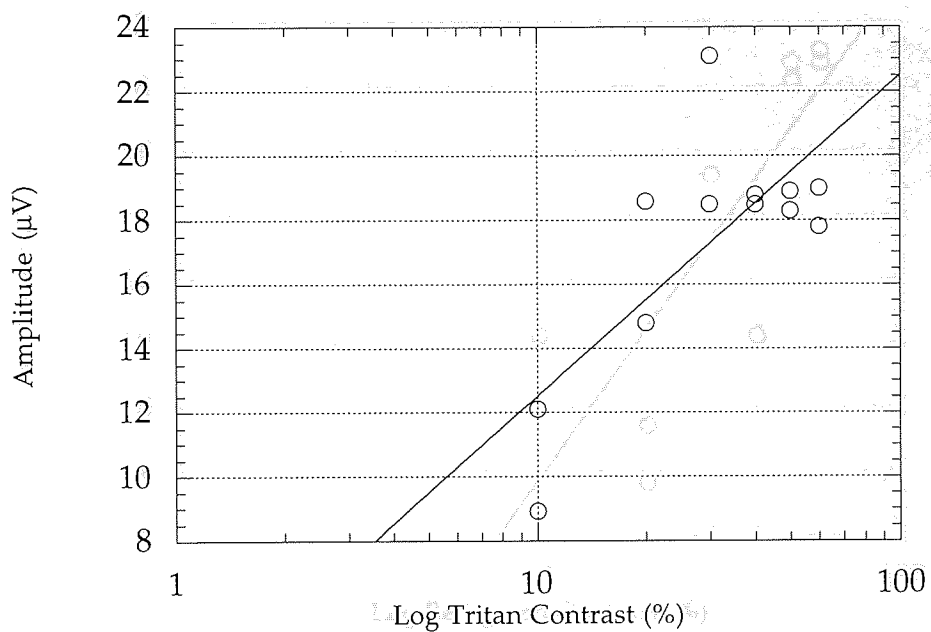
Figure 6.13.

Visual evoked response amplitude is plotted as a function of log tritan chromatic contrast, in an attempt to estimate tritan contrast threshold for subject AE. The solid line fit to the data is a linear regression function; r is the correlation coefficient. The equation shown is the equation for this line.



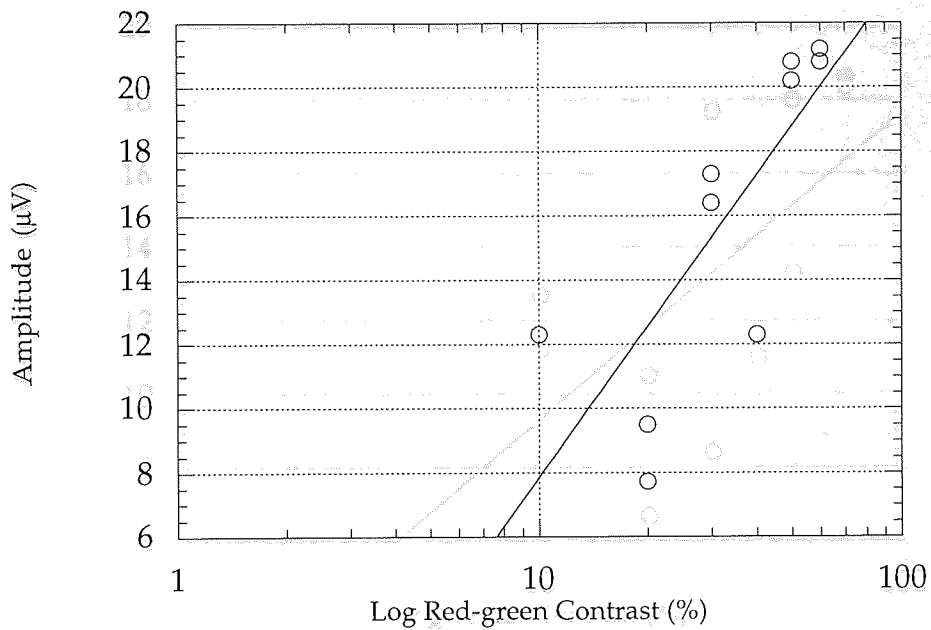
$y = -10.47 + 11.337 \log x$
 $r = 0.80$
 Contrast Threshold = 8.39%

Figure 6.14. Visual evoked response amplitude is plotted as a function of log red-green chromatic contrast, in order to estimate red-green contrast threshold for adult subject AE. The solid line fit to the data is a linear regression function; r is the correlation coefficient. The equation shown is the equation for this line, which was used to calculate contrast threshold.



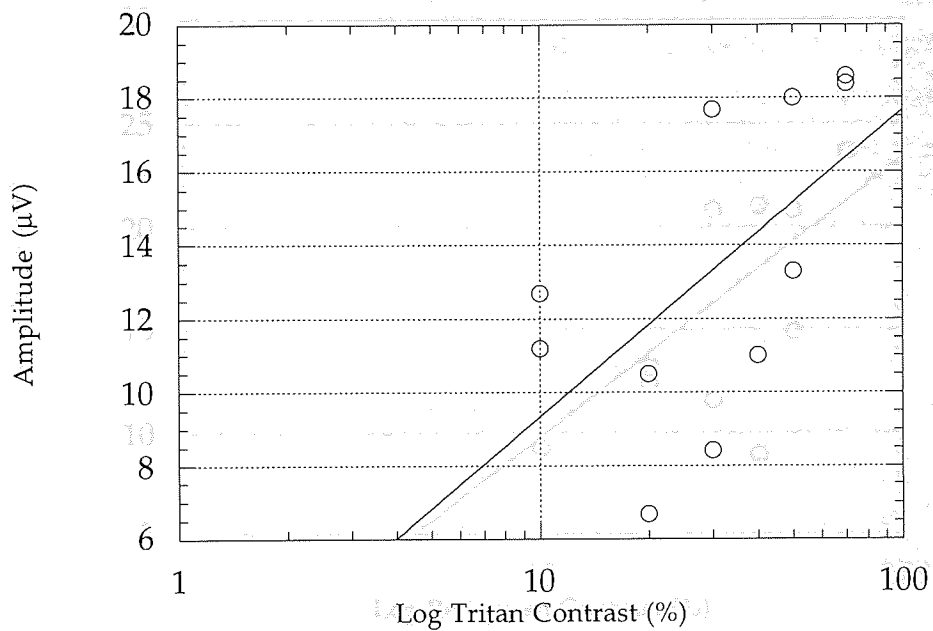
$y = -8.5005 + 16.58 \log x$
 $r = 0.94$
 Contrast Threshold = 3.26

Figure 6.15. Visual evoked response amplitude is plotted as a function of log tritan chromatic contrast, in an attempt to estimate tritan contrast threshold for subject VT. The solid line fit to the data is a linear regression function; r is the correlation coefficient. The equation shown is the equation for this line, which was used to calculate contrast threshold.



$y = -11.444 + 16.213 \log x$
 $r = 0.89$
 Contrast Threshold = 5.06

Figure 6.16. Visual evoked response amplitude is plotted as a function of log red-green chromatic contrast, in order to estimate red-green contrast threshold for subject VT. The solid line fit to the data is a linear regression function; r is the correlation coefficient. The equation shown is the equation for this line, which was used to calculate contrast threshold.

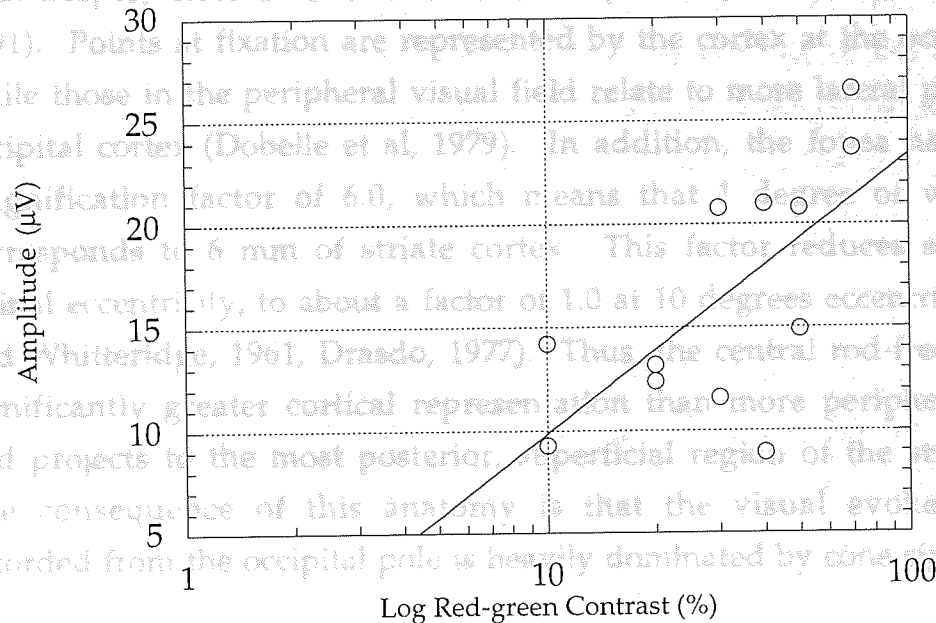


$y = 0.99172 + 8.3459 \log x$
 $r = 0.59$
 Contrast Threshold = 0.78

Figure 6.17. Visual evoked response amplitude is plotted as a function of log tritan chromatic contrast, in an attempt to estimate tritan contrast threshold for subject FF. The solid line fit to the data is a linear regression function; r is the correlation coefficient. The equation shown is the equation for this line, which was used to calculate contrast threshold.

have been identified (Woolsey, 1971). Under steady photopic conditions, respectively (Woolsey, 1971), the visual evoked response increases significantly in latency and is diminished in amplitude.

In human adults, the fovea is represented on the most posterior region of the striate cortex, with progressively more peripheral retina corresponding with deeper, more anterior striate cortex (Drasdo, 1977; Horton and Hoyt, 1991). Points of fixation are represented by the cortex at the occipital pole, while those in the peripheral visual field relate to more lateral points of the occipital cortex (Dobelle et al, 1979). In addition, the fovea has a cortical magnification factor of 6.0, which means that 1 degree of visual angle corresponds to 6 mm of striate cortex. This factor reduces steeply with retinal eccentricity, to about a factor of 1.0 at 10 degrees eccentricity (Daniel and Whitteridge, 1961; Drasdo, 1977). Thus, the central rod-free retina has significantly greater cortical representation than more peripheral regions, and projects to the most posterior, superficial region of the striate cortex. The consequence of this anatomy is that the visual evoked response recorded from the occipital pole is heavily dominated by cone signals.



The stimulus used in the present study subtended 20 deg by 14 deg at a viewing distance of 1 metre. The chromatic visual evoked response in $y = -3.6927 + 13.536 \log x$ $r = 0.66$ is not thought to depend upon stimulus size (Kulikowski et al, 1971). Contrast Threshold = 1.77. However, only the central 2.4 deg of the adult retina is rod-free, so it is possible that a stimulus of this size could excite rods as well as cones, thus contaminating the chromatic visual evoked response. The maximum mean luminance possible with the display system used in this study, over a luminance ratio range of 0.0 to 1.0, while maintaining a constant mean luminance level throughout, was 20 cd/m². In order to minimise the intrusion of rod signals in our visual evoked responses, this mean

Figure 6.18: was used for all stimuli

Visual evoked response amplitude is plotted as a function of log red-green chromatic contrast in order to estimate red-green contrast threshold, for subject FF. The solid line fit to the data is a linear regression function; r is the correlation coefficient. The equation shown is the equation for this line, which was used to calculate contrast threshold.

6.7 Intrusion of Rod Responses

Rod and cone contributions to the visual evoked response in human adults have been identified by recording from the occiput, under scotopic and photopic conditions, respectively (Wooten, 1972). Under scotopic conditions, the response increases significantly in latency and is diminished in amplitude.

In human adults, the fovea is represented on the most posterior region of the striate cortex, with progressively more peripheral retina corresponding with deeper, more anterior striate cortex (Drasdo, 1977; Horton and Hoyt, 1991). Points at fixation are represented by the cortex at the occipital pole, while those in the peripheral visual field relate to more lateral points of the occipital cortex (Dobelle et al, 1979). In addition, the fovea has a cortical magnification factor of 6.0, which means that 1 degree of visual angle corresponds to 6 mm of striate cortex. This factor reduces steeply with retinal eccentricity, to about a factor of 1.0 at 10 degrees eccentricity (Daniel and Whitteridge, 1961; Drasdo, 1977). Thus, the central rod-free retina has significantly greater cortical representation than more peripheral regions, and projects to the most posterior, superficial region of the striate cortex. The consequence of this anatomy is that the visual evoked response recorded from the occipital pole is heavily dominated by cone signals.

The stimulus used in the present study subtended 20 deg by 14 deg at a viewing distance of 1 metre. The chromatic visual evoked response in adults is not thought to depend upon stimulus size (Kulikowski et al, 1991). However, only the central 2.4 deg of the adult retina is rod-free, so it is possible that a stimulus of this size could excite rods as well as cones, thus contaminating the chromatic visual evoked response. The maximum mean luminance possible with the display system used in this study, over a luminance ratio range of 0.0 to 1.0, while maintaining a constant mean luminance level throughout, was 20 cd/m². In order to minimise the intrusion of rod signals in our visual evoked responses, this mean luminance was used for all stimuli.

For the anatomical reasons given above, it is unlikely that a signal recorded

from the occiput would be contaminated by rod responses. However, the rod system saturates at a luminance level approximately 2.0 log units brighter when stimuli are fixated steadily, as in the present study, than when flashed stimuli are used (Adelson, 1982). In addition, the rod system starts to saturate at a retinal illuminance of 100 scotopic trolands and is inactive at 2000 to 5000 scotopic trolands (Aguilar and Stiles, 1954). 100 scotopic trolands represents a stimulus mean luminance of 19 cd/m², assuming an average adult pupil diameter of 3.3 mm (Banks and Bennett, 1988). To demonstrate that there is no significant contribution from rod signals in the chromatic response recorded from adults in the present study at a mean luminance of 20 cd/m², the mean luminance of the isoluminant stimuli was increased to 30 and 40 cd/m², and any changes to characteristics of the response were noted. Responses were recorded using the same procedure as described earlier, to tritan and red-green stimuli at a colour ratio of 0.5.

Visual evoked responses recorded from subject VT to tritan and red-green isoluminant stimuli at 30 and 40 cd/m² are shown in figure 6.19. These responses are of similar morphology to those recorded at 20 cd/m² (see figures 6.4 and 6.5) comprising a peak negative component followed by a positive component. In figures 6.20 and 6.21, response amplitudes and latencies respectively are compared at each mean luminance level.

In terms of response amplitude, tritan responses were not significantly different at 20, 30 or 40 cd/m² ($p > 0.1$). The response to red-green stimulation at 20 cd/m² was of similar amplitude to that at 30 cd/m² ($p > 0.1$) but was of significantly greater amplitude than the response at 40 cd/m² ($p < 0.05$).

A comparison of response latencies shows that the response to isoluminant tritan stimulation at 20 cd/m² is of significantly longer latency than that at both higher mean luminance levels ($p < 0.05$). The response to red-green stimuli at 20 cd/m² is similar in latency ($p > 0.1$) to that at 30 cd/m², but is significantly greater than that at 40 cd/m² ($p < 0.05$).



Figure 6.19. Visual evoked responses to photometrically isoluminant tritan and red-green stimuli, at mean luminance levels of 30 and 40 cd/m^2 , recorded from subject VT. These may be compared with responses recorded from the same subject to both types of chromatic stimuli at 20 cd/m^2 in figures 6.4 and 6.5.

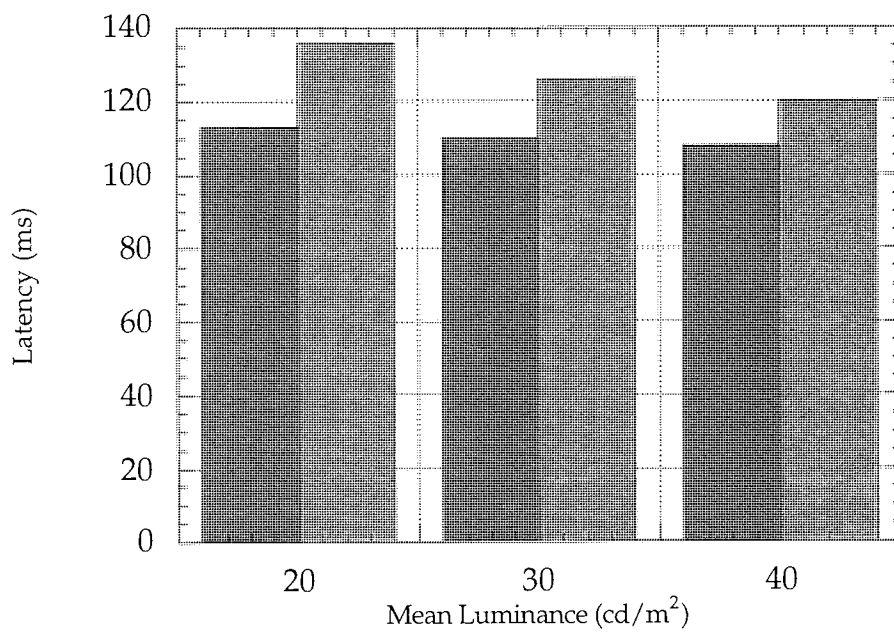


Figure 6.20. Latency of visual evoked responses recorded from subject VT are shown with respect to mean luminance, for photometrically isoluminant red-green (darker bars) and tritan (lighter bars) stimuli.

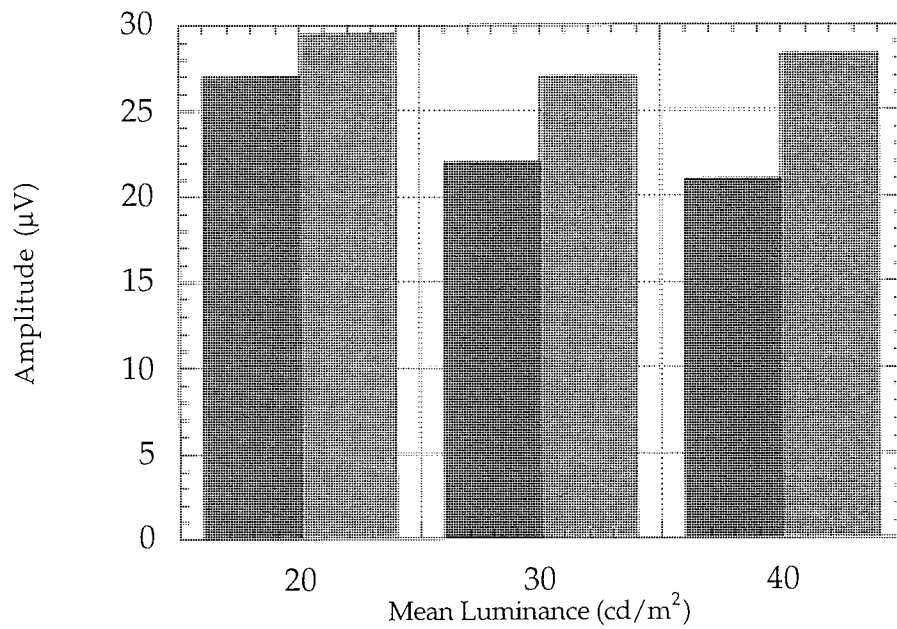


Figure 6.21. Amplitude of visual evoked responses recorded from subject VT are shown with respect to mean luminance, for photometrically isoluminant red-green (darker bars) and tritan (lighter bars) stimuli.

As described earlier, previous work has shown that visual evoked responses recorded from the occiput under scotopic conditions are of significantly longer latency and lower amplitude, and of different morphology than those recorded under photopic conditions. The occipital responses recorded here from an adult under different luminance levels are of similar morphology. Amplitude differs for the response to red-green stimulation only, at 20 and 40 cd/m². In this case, amplitude is greater at the lower luminance level, which suggests that the response at 20 cd/m² is not significantly contaminated by rod signals. Latency at 20 cd/m² is significantly longer than that at both higher mean luminances tested. The differences are not sufficiently high, however, to suggest that rod signals provide a significant contribution to the chromatic response at 20 cd/m² (Wooten, 1972). These results suggest that the visual evoked response to chromatic isoluminant stimulation at a mean luminance of 20 cd/m², recorded from the occiput in adults, is a photopic response with no significant contribution from rods.

Previously, when pattern-reversal chromatic stimulation has been used in infants the single positive component latency and amplitude have been used to define isoluminance for each individual as the colour ratio at which latency is at a maximum and amplitude is at a minimum (Ridduck and Harding, 1994). In the present study, the peak response component elicited at or close to isoluminance was a negativity which was not well defined at colour ratios away from isoluminance in all infants (see Results of this chapter). For this reason, latency and amplitude of this component could not be used in the estimation of isoluminance for infants. An earlier positive component (P₁₃₀) was elicited, the amplitude of which showed a correlation with colour ratio, being minimal at or close to photometric isoluminance and increasing as luminance differences were introduced in the stimulus. This component was therefore used to estimate isoluminance for both types of chromatic stimuli for each of a group of six infants.

CHAPTER 7

THE INFANT VISUAL EVOKED RESPONSE AT ISOLUMINANCE

7.1 Introduction

The characteristics of the visual evoked response in infants to pattern-onset chromatic stimuli at and around photometric isoluminance have not previously been studied. The pattern-reversal chromatic transient VEP in infants has been investigated previously (Rudduck and Harding, 1994). The peak response was found to be a positive component which increased in latency and decreased in amplitude towards isoluminance.

In adults, the peak visual evoked response to isoluminant chromatic pattern-reversing stimuli is a positivity, while the response to pattern-onset stimulation at isoluminance is a negative component (see Chapter 6). In the present study, visual evoked responses to pattern-onset chromatic stimulation were recorded at and around isoluminance in young infants in order to investigate response characteristics to these stimuli.

Previously, when pattern-reversal chromatic stimulation has been used in infants the single positive component latency and amplitude have been used to define isoluminance for each individual as the colour ratio at which latency is at a maximum and amplitude is at a minimum (Rudduck and Harding, 1994). In the present study, the peak response component elicited at or close to isoluminance was a negativity which was not well defined at colour ratios away from isoluminance in all infants (see Results of this chapter). For this reason, latency and amplitude of this component could not be used in the estimation of isoluminance for infants. An earlier positive component (P_{130}) was elicited, the amplitude of which showed a correlation with colour ratio, being minimal at or close to photometric isoluminance and increasing as luminance differences were introduced to the stimulus. This component was therefore used to estimate isoluminance for both types of chromatic stimuli, for each of a group of six infants.

7.2 Methods

Six infants (three male, three female; age range 6 to 10 weeks post-term) were included in this study. Stimuli, VEP recording technique, procedure and subject recruitment are as described in Chapter 5.

Visual evoked responses to a set of tritan and red-green stimuli from each infant, recorded at photometric isoluminance at 0.5, were recorded from each infant. For at least two sets of responses to these stimuli, the amplitude of the early positive response component (P₁₃₀) was measured and then plotted as a function of colour ratio. A second-order polynomial curve provided the best fit to each data set (see Results). The minimum of the curve may be described as a stationary point, at which the gradient is zero because the function is neither decreasing nor increasing at that point (Sherlock et al, 1982). Here, $dy/dx=0$, so the equation for the line may be differentiated once to determine the value of x at which the gradient equals zero. This value is the colour ratio at which the amplitude of the positive component is minimal, photometric isoluminance was calculated to estimate isoluminance for each chromatic stimulus, using the equation for the curve:

$$y = M0 + x (M1) + x^2 (M2)$$

where M0, M1 and M2 are gradient values given in the equation for each curve.

Example: value given is calculated as follows:

$$y = 70.944 - (260.24x) + (260.57x^2)$$

$$dy/dx = (-260.24) + 2(260.57x)$$

$$dy/dx = 0 \text{ (stationary point)}$$

$$0 = (-260.24) + 2(260.57x)$$

$$260.24 = 521.14x$$

$$x = 0.499$$

Therefore, in this example, the individual isoluminant point is at the colour ratio 0.499.

7.3 Results

As described earlier, the evoked response to non-isoluminant (colour ratios other than 0.5) chromatic stimuli demonstrated an early positive component, at a latency of about 130 ms after stimulus onset (P_{130}). At a young age, before the onset of a response at isoluminance, the visual evoked response recorded to isoluminant chromatic stimuli from each infant consisted of no clear components and was not significantly above noise levels. At a slightly later age, at and after the onset of an isoluminant response, the waveform consisted of a negative component at a latency of about 250 ms. This component was clear at and close to photometric isoluminance, but in some infants became less well defined at colour ratios away from isoluminance (0.4 and 0.6) as shown by the responses of infants MB and DH in figures 7.1 to 7.4.

This component was preceded by the earlier positivity, P_{130} . P_{130} was maximal at colour ratios away from isoluminance (0.4 and 0.6) and diminished towards photometric isoluminance at the colour ratio 0.5 (see figures 7.1 to 7.4).

Figures 7.5 to 7.16 show P_{130} amplitude plotted as a function of colour ratio, for at least two sets of responses to tritan and red-green colour ratios from 0.4 to 0.6, for the six infants included here. The solid line through each data set is a second-order polynomial curve; r is the correlation coefficient; the Minimum value given is calculated as described above in Methods and is taken as an estimate of isoluminance for each individual infant (see figure 7.17).



Figure 7.1. Visual evoked responses to tritan stimuli at the range of colour ratios shown recorded from infant DH at 6 weeks post term age. Responses to luminance-modulated stimulation and the non-stimulus condition are also shown for comparison.

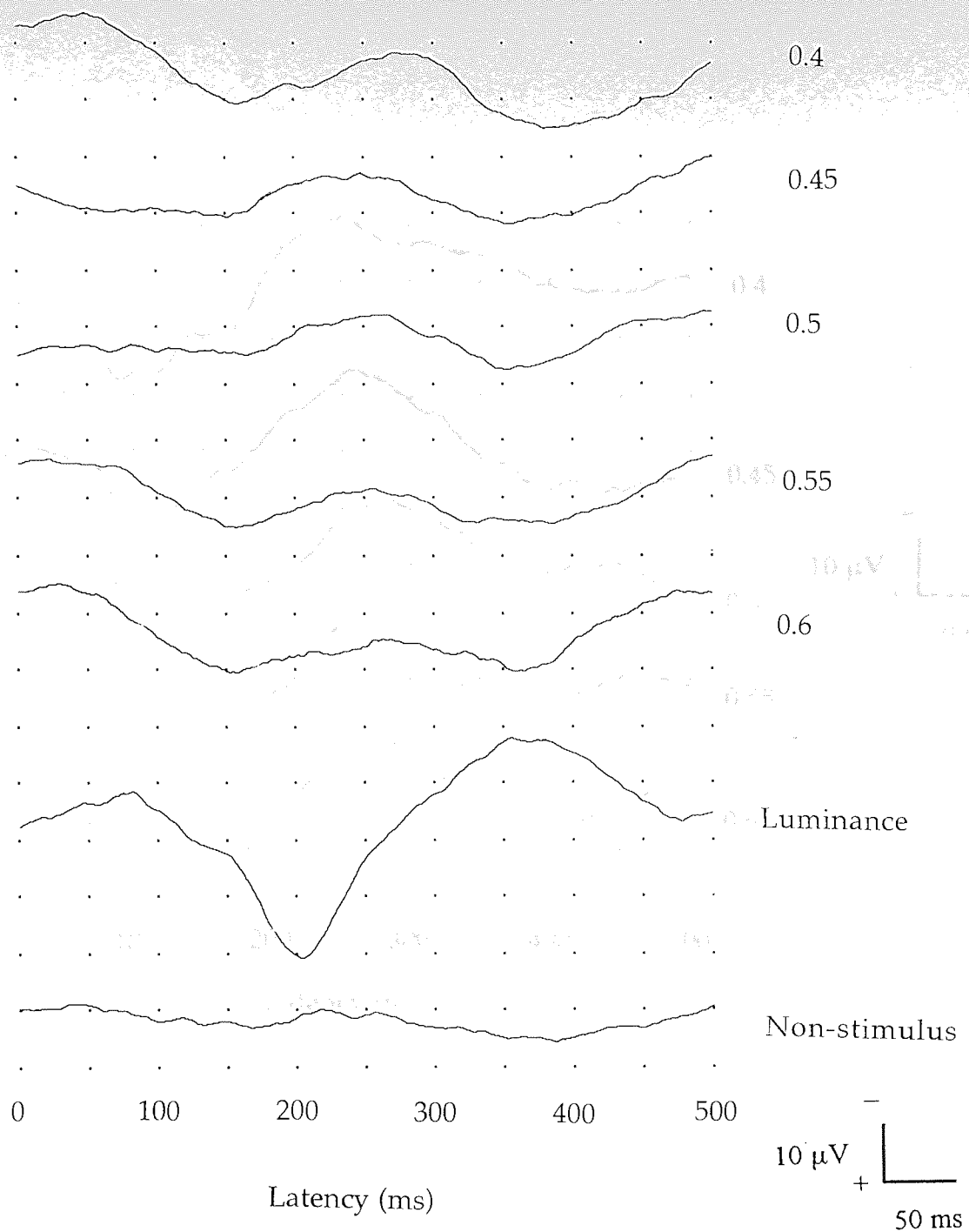


Figure 7.1.
 Visual evoked responses to tritan stimuli at the range of colour ratios shown, recorded from infant DH at 6 weeks post-term age. Responses to luminance-modulated stimulation and the non-stimulus condition are also shown for comparison.

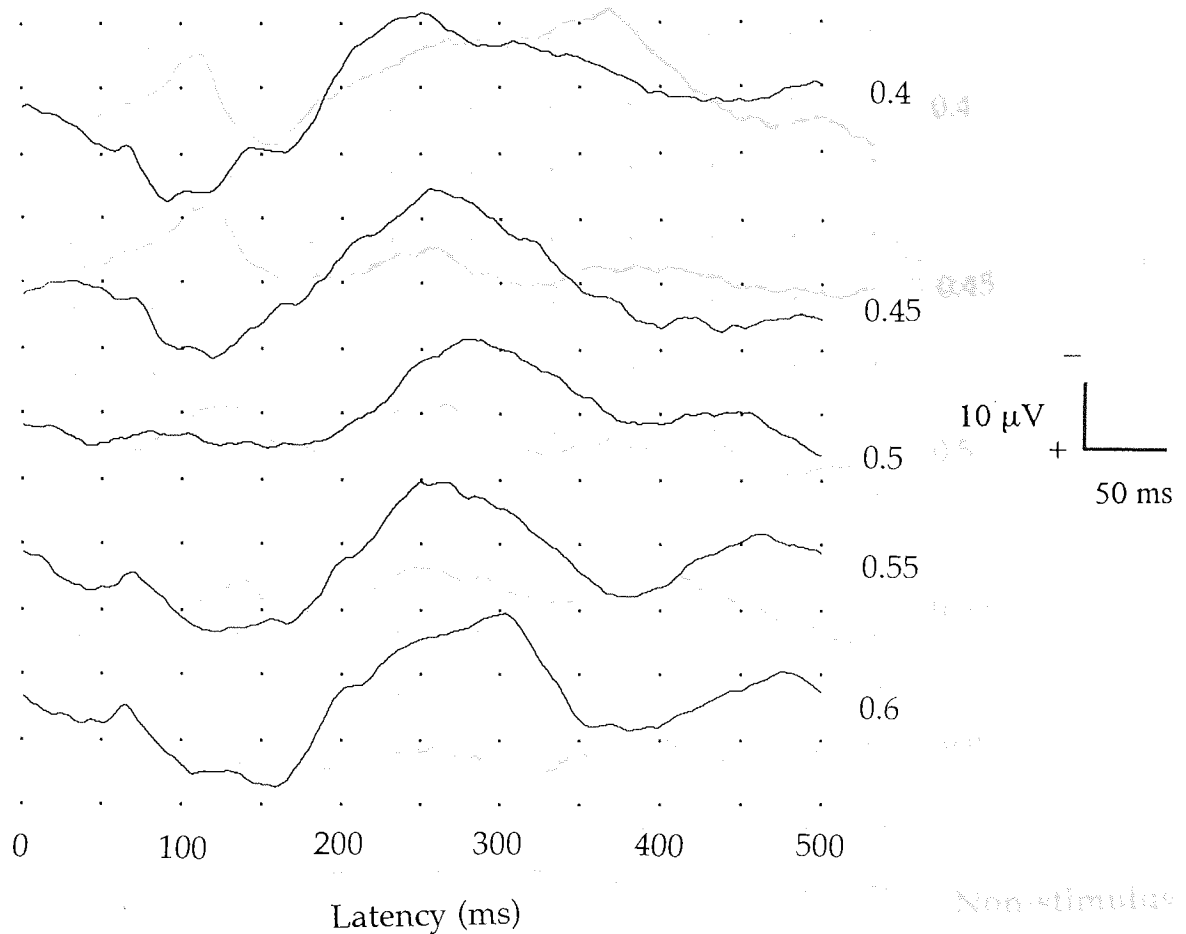


Figure 7.2.
 Visual evoked responses to red-green stimuli at the range of colour ratios shown, recorded from infant DH at 6 weeks post-term age.

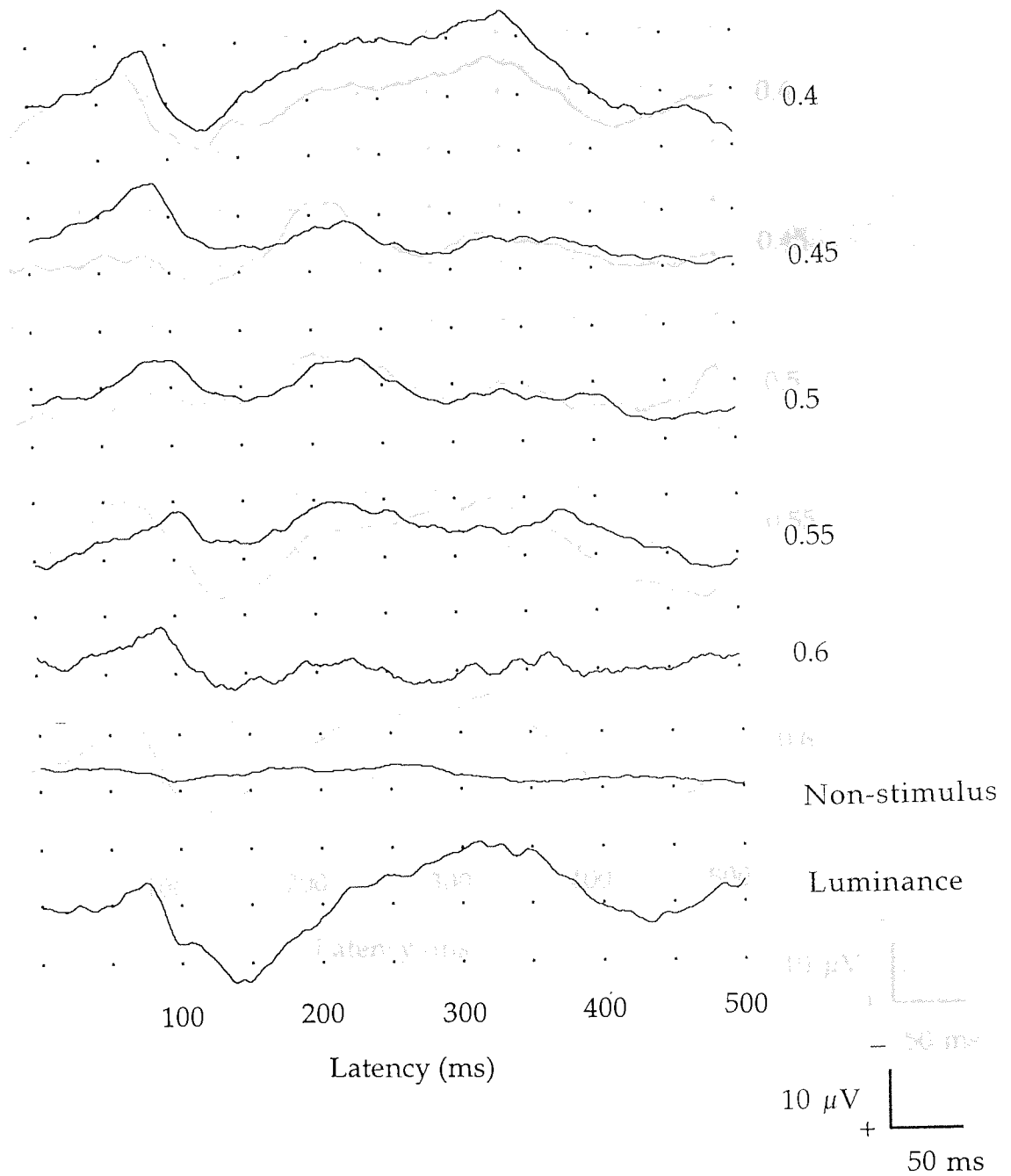


Figure 7.3. Visual evoked responses to tritan stimuli at the range of colour ratios shown, recorded from infant MB at 9 weeks post-term age. Responses to luminance-modulated stimulation and the non-stimulus condition are also shown for comparison.

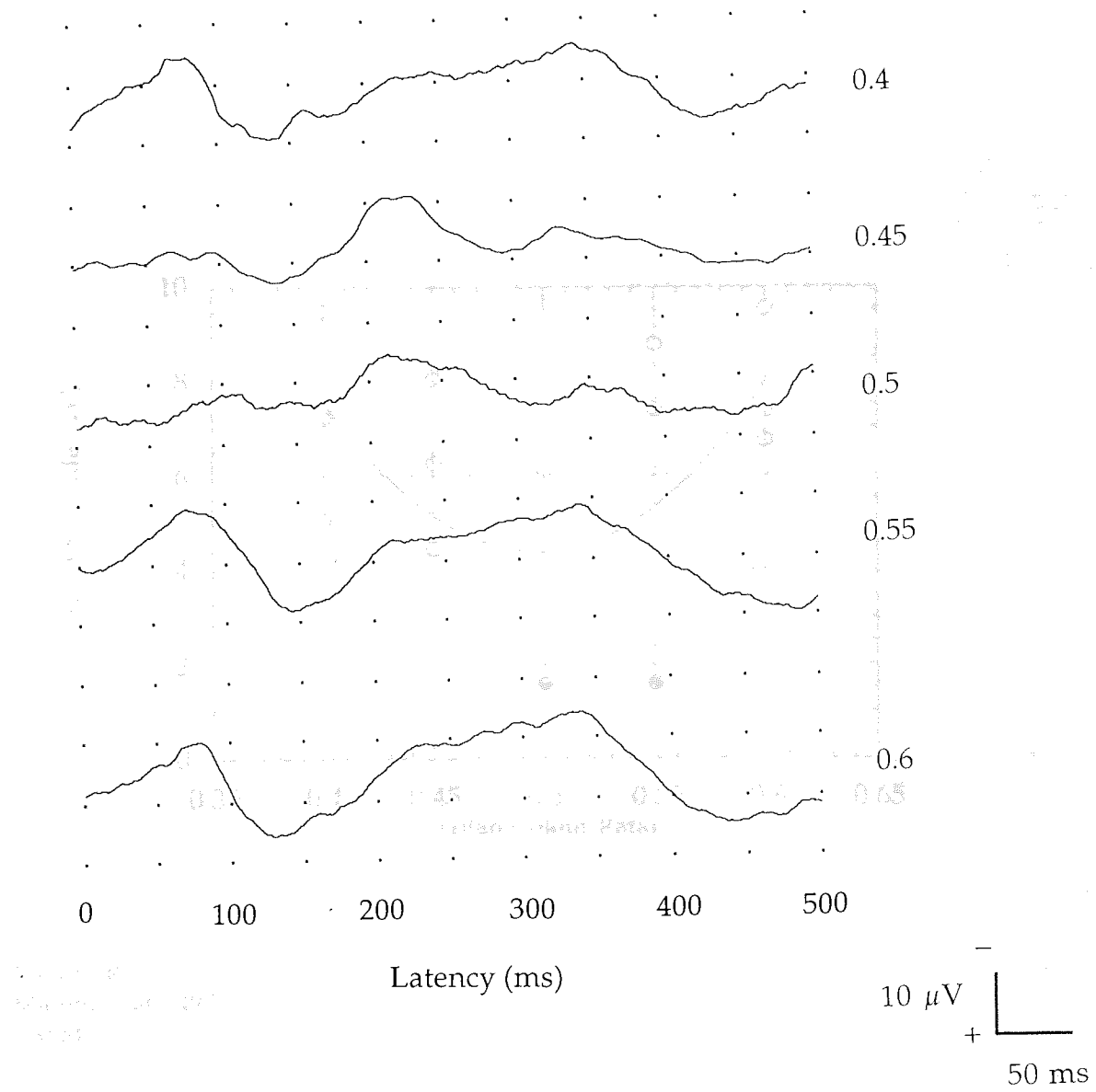
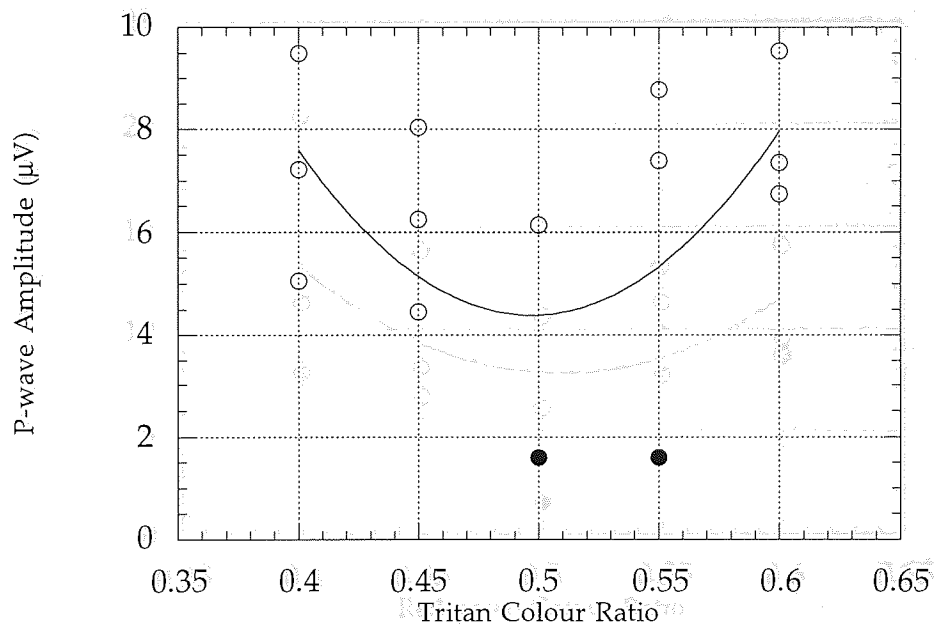
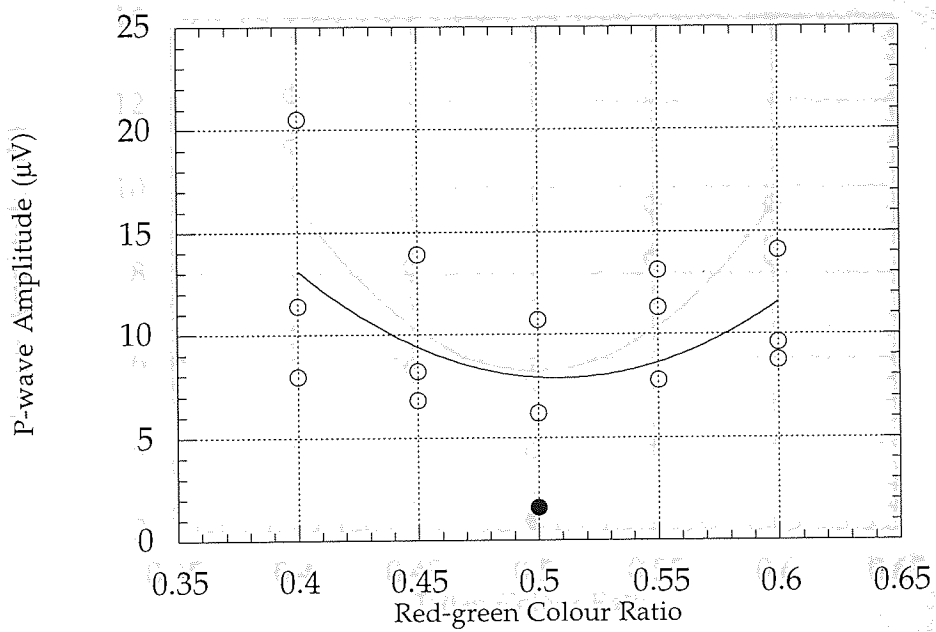


Figure 7.4. Visual evoked responses to red-green stimuli at the range of colour ratios shown, recorded from infant MB at 9 weeks post-term age.



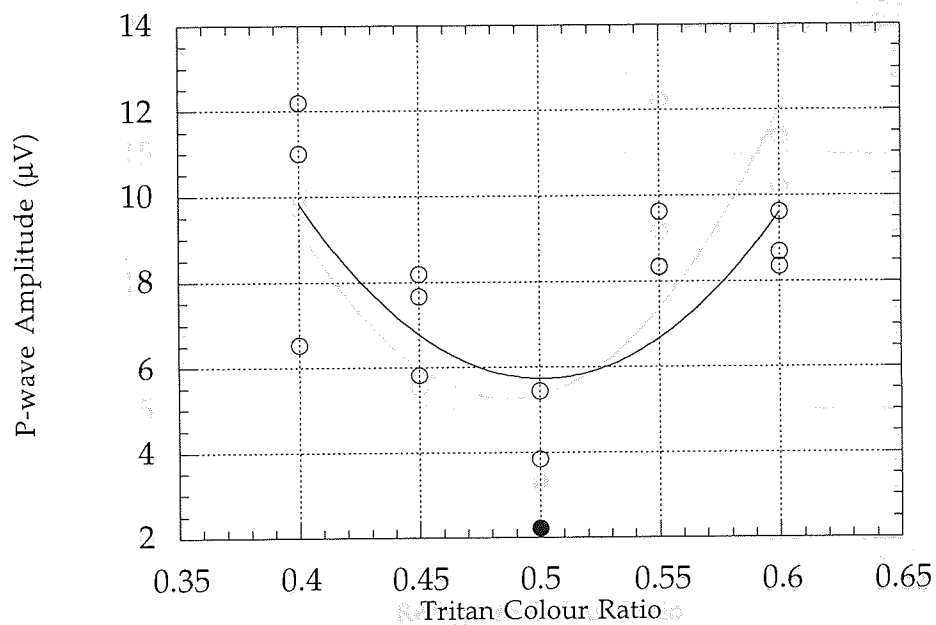
Infant PR
 Minimum at 0.509
 Infant PR
 Minimum at 0.497
 r=0.54

Figure 7.5.
 Mean amplitude of the early positive response component (P130) for three sets of visual evoked responses to tritan stimuli (infant PR). Open circles represent responses significantly above EEG noise; filled circles indicate responses at or below this level.



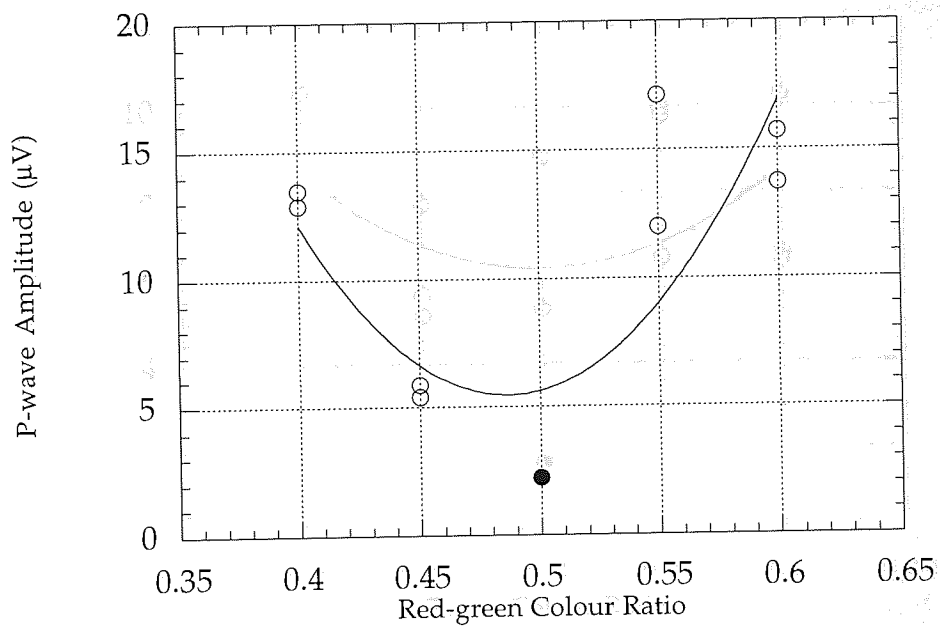
Infant PR
 Minimum at 0.509
 $r=0.46$
 Minimum at 0.509
 $r=0.46$

Figure 7.6
 Mean amplitude of the early positive response component (P130) for three sets of visual evoked responses to red-green stimuli (infant PR). Open circles represent responses significantly above EEG noise; filled circles indicate responses at or below this level.



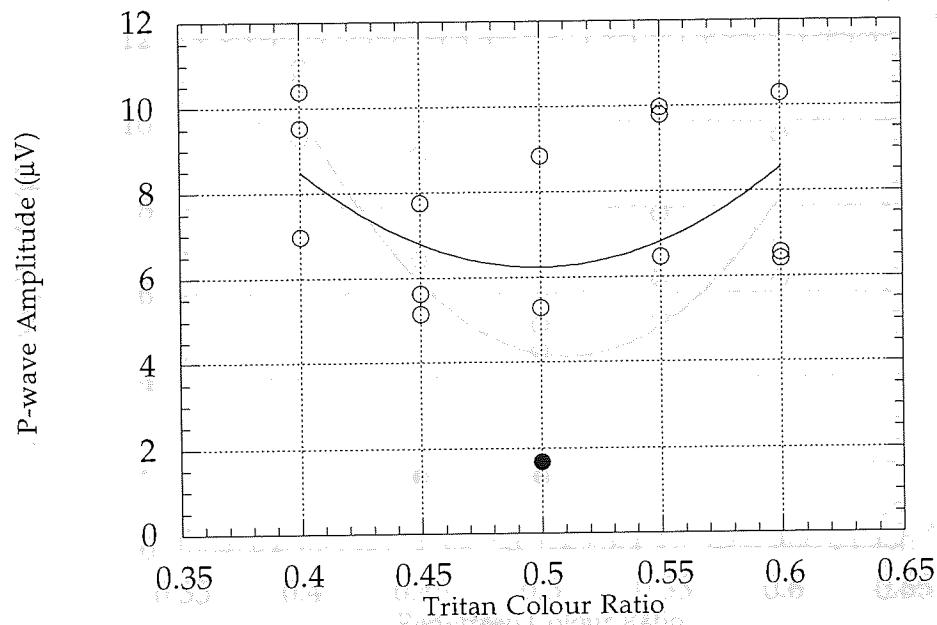
Infant MB
 Minimum at 0.501
 $r=0.66$

Figure 7.7
 Mean amplitude of the early positive response component (P130) for three sets of visual evoked responses to tritan stimuli (infant MB). Open circles represent responses significantly above EEG noise; filled circles indicate responses at or below this level.



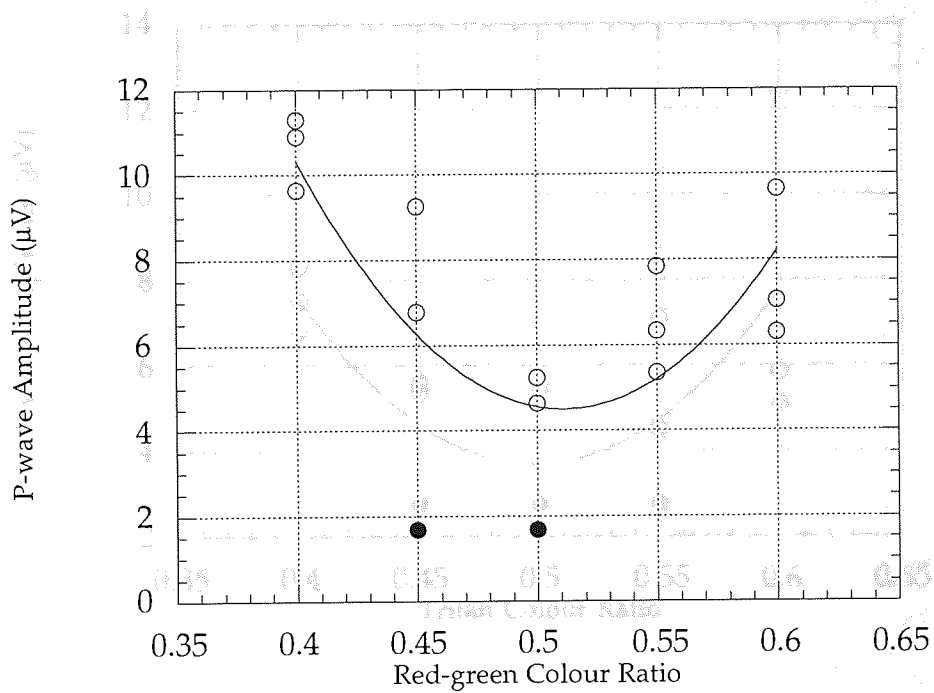
Infant MB
 Minimum at 0.487
 $r=0.77$

Figure 7.8
 Mean amplitude of the early positive response component (P₁₃₀) for two sets of visual evoked responses to red-green stimuli (infant MB). Open circles represent responses significantly above EEG noise; filled circles indicate responses at or below this level.



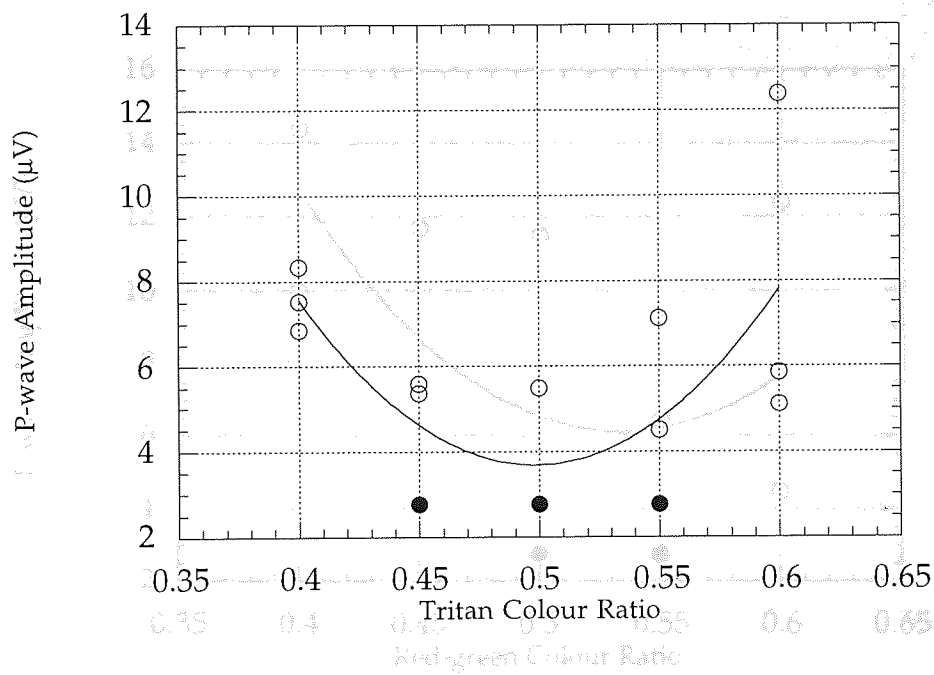
Infant AE
 Minimum at 0.499
 $r=0.40$

Figure 7.9
 Mean amplitude of the early positive response component (P130) for three sets of visual evoked responses to tritan stimuli (infant AE). Open circles represent responses significantly above EEG noise; filled circles indicate responses at or below this level.



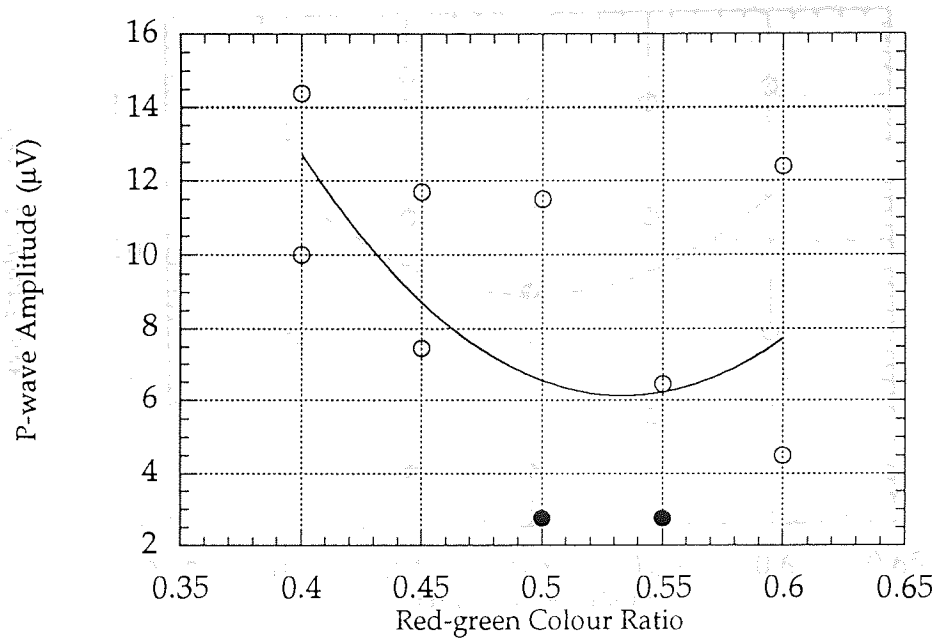
Infant OC
 Minimum at 0.495
 Infant AE
 Minimum at 0.511
 r=0.74

Figure 7.10
 Mean amplitude of the early positive response component (P130) for three sets of visual evoked responses to red-green stimuli (infant AE). Open circles represent responses significantly above EEG noise; filled circles indicate responses at or below this level.



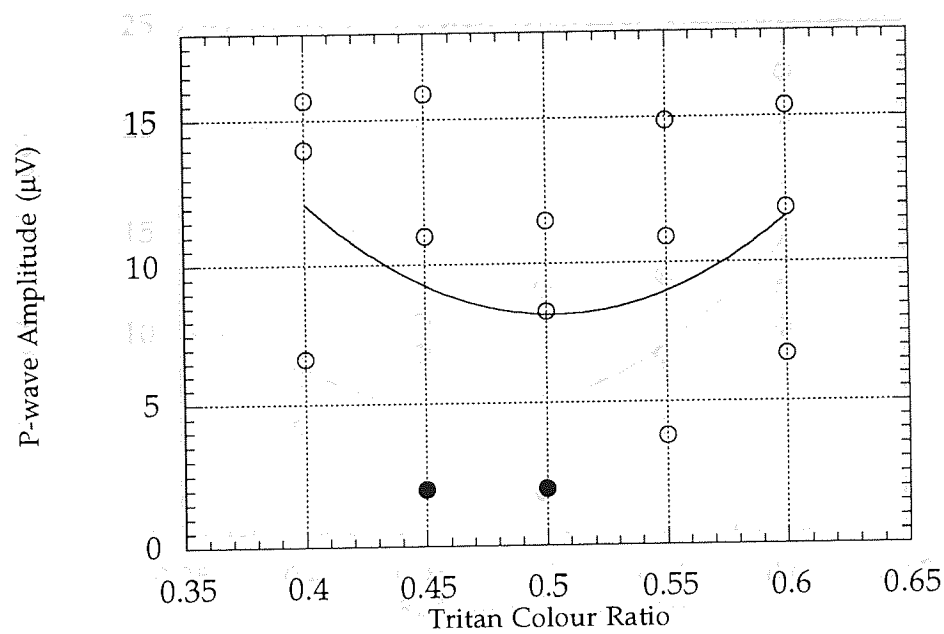
Infant DC
 Minimum at 0.498
 $r=0.67$

Figure 7.11
 Mean amplitude of the early positive response component (P130) for three sets of visual evoked responses to red-green stimuli (infant DC). Open circles represent responses significantly above EEG noise; filled circles indicate responses at or below this level.



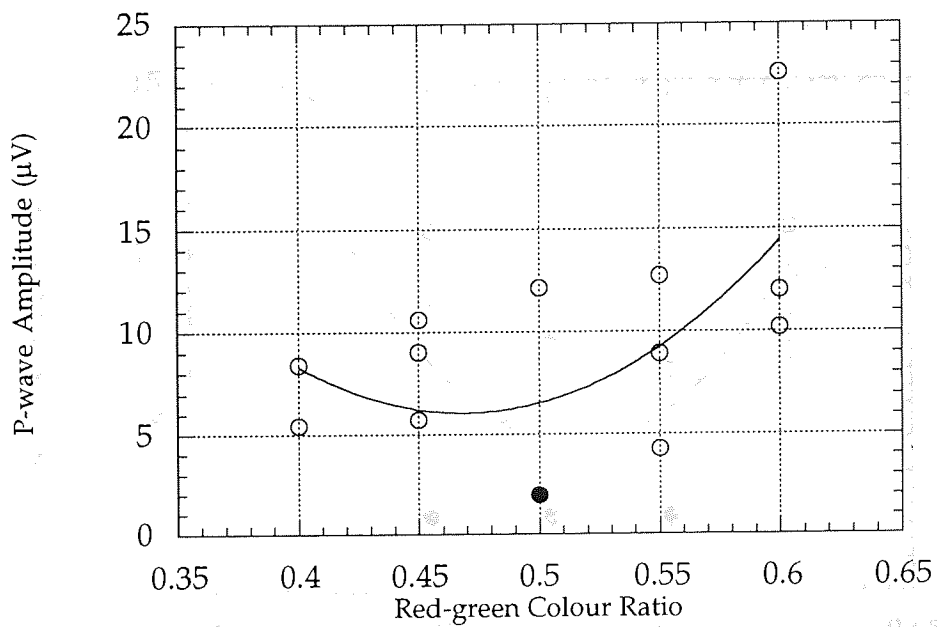
Infant DC
 Minimum at 0.53
 $r=0.59$

Figure 7.12
 Mean amplitude of the early positive response component (P_{130}) for two sets of visual evoked responses to red-green stimuli (infant DC). Open circles represent responses significantly above EEG noise; filled circles indicate responses at or below this level.



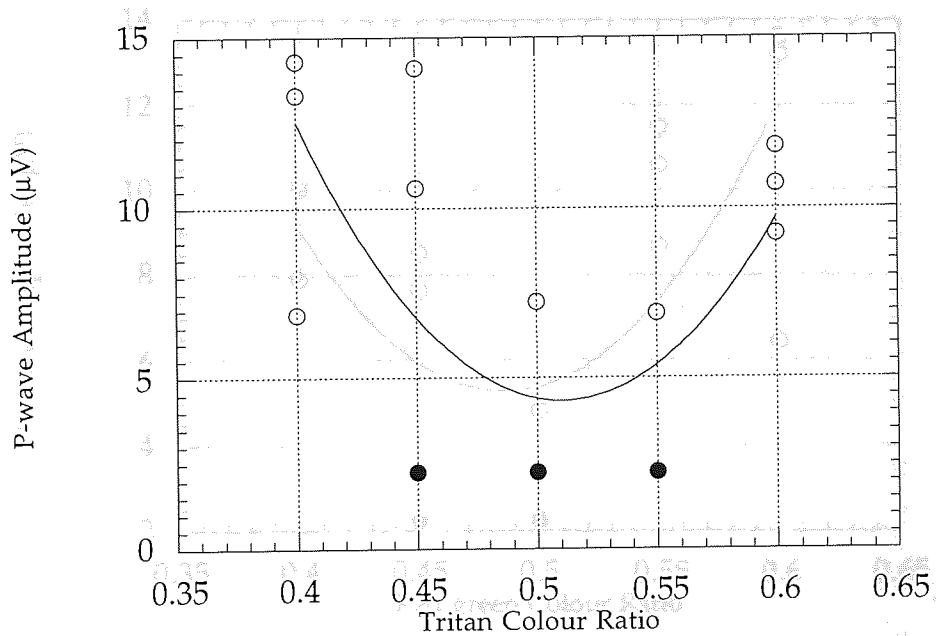
Infant DH
 Minimum at 0.504
 $r=0.33$

Figure 7.13
 Mean amplitude of the early positive response component (P130) for three sets of visual evoked responses to tritan stimuli (infant DH). Open circles represent responses significantly above EEG noise; filled circles indicate responses at or below this level.



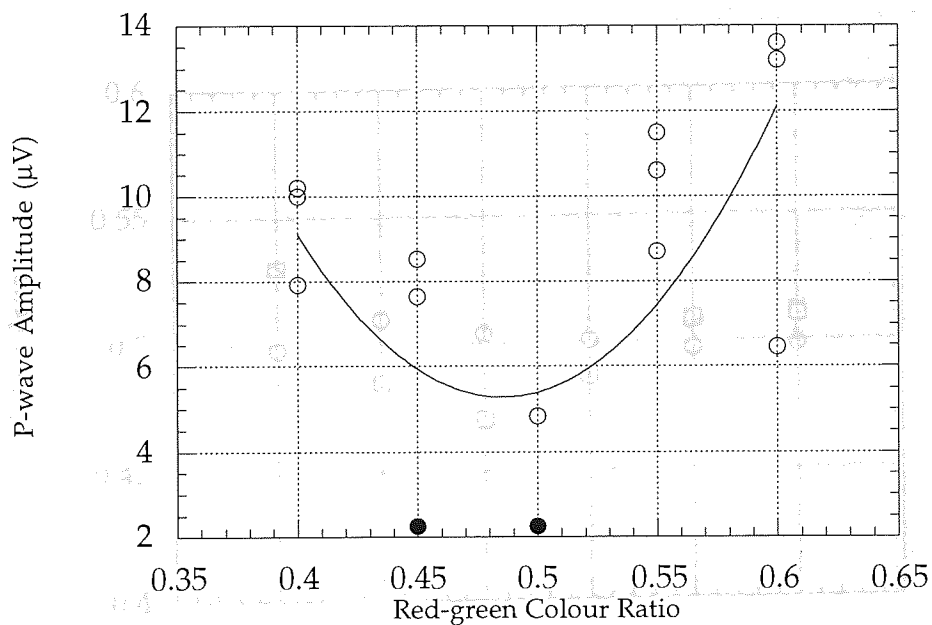
Infant DH
 Minimum at 0.47
 $r=0.60$

Figure 7.14
 Mean amplitude of the early positive response component (P₁₃₀) for three sets of visual evoked responses to red-green stimuli (infant DH). Open circles represent responses significantly above EEG noise; filled circles indicate responses at or below this level.



Subject JC2
 Minimum 0.51
 $r=0.66$

Figure 7.15
 Mean amplitude of the early positive response component (P130) for three sets of visual evoked responses to tritan stimuli (infant JC2). Open circles represent responses significantly above EEG noise; filled circles indicate responses at or below this level.



Infant JC2
 Minimum 0.485
 $r=0.67$

Figure 7.16: Mean amplitude of the early positive response component (P₁₃₀) for three sets of visual evoked responses to red-green stimuli (infant JC2). Open circles represent responses significantly above EEG noise; filled circles indicate responses at or below this level.

7.4 Luminance Adaptation

Luminance intrusions, such as those introduced by chromatic aberrations, may be a serious problem in studies of colour vision, particularly when short-wavelength stimuli are used. The factor may offer luminance cues to the observer, confounding one chromatic element with respect to the other two (see also, as discussed previously (see Chapter 5), low spatial frequency stimuli were used in the present study in an attempt to eliminate chromatic aberrations). However, it is possible that some contamination of the chromatic channels may occur. The presence of an early positive response to non-isoluminant colour ratios and the absence of this component at a later age to protoconic isoluminance suggests that luminance cues were successfully eliminated from the response.

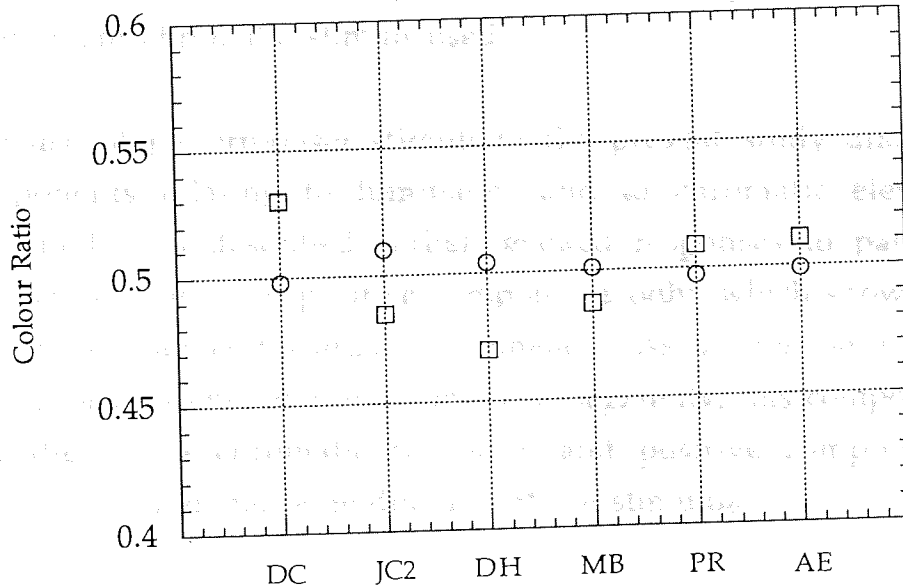


Figure 7.17.

Isoluminant points in terms of colour ratio for five infants estimated by the method described in the text are shown. Open squares represent red-green isoluminance and open circles represent tritan isoluminant points; subjects are identified by their initials.

Discussion

7.4 Luminance Artifacts

Luminance intrusions, such as those introduced by chromatic aberrations, are a potential problem in studies of colour vision, particularly when short-wavelength stimuli are used. This factor may offer luminance cues to the observer by defocusing one chromatic element with respect to the other (see Chapter 5). As discussed previously (see Chapter 5), low spatial frequency stimuli were used in the present study in an attempt to eliminate chromatic aberration. However, it is possible that some contamination of the chromatic stimulus may occur. The presence of an early positive component at non-isoluminant colour ratios and the absence of this component at or close to photometric isoluminance suggests that luminance cues of any origin were successfully eliminated from the isoluminant chromatic stimuli used.

The use of pattern-onset stimuli in the present study allows response components relating to luminance and to chromatic elements to be identified. As described earlier, evoked responses to pattern-reversal stimulation consist of positive components only, which show latency and amplitude changes towards isoluminance. As the response to chromatic pattern-onset stimulation in infants is a negativity, this component may be identified as a chromatic response, and positive components signify responses to luminance-modulation of the stimulus.

This situation parallels that found in adults, when luminance differences are introduced to chromatic pattern-onset stimuli (see Chapter 6). The peak visual evoked response to pattern-onset isoluminant chromatic stimuli in adults is a negative component and the peak response to luminance-modulated pattern-onset stimuli in adults is a positive component (see also Murray et al, 1987 and Berninger et al, 1989). In adults, as luminance differences are introduced to the chromatic stimulus, the response to pattern-onset becomes more complex, and the response to pattern-offset becomes larger in amplitude and better defined with increasing luminance difference. The response to pattern offset is not found in infants before

about 4 months of age (see Chapter 9) and so could not be observed in the infants investigated in the present study. Response morphology at isoluminance is thought to reflect parvocellular activity, and at colour ratios away from isoluminance the response is increasingly of magnocellular origin (Murray et al, 1987).

In infants, as we have seen, the peak evoked response to isoluminant chromatic pattern-onset stimuli is a negative component, with minimal or no positive components. As luminance differences are introduced to the chromatic stimulus, the response becomes more complex with an earlier positive component appearing, which increases in amplitude with luminance difference. This morphological change is also apparent at an earlier age, when the response to isoluminant chromatic stimuli consists of no distinct components, and P₁₃₀ appears as luminance differences are introduced to the stimuli (see figures 9.4 and 9.5).

The peak evoked response to luminance-modulated pattern-onset stimuli in infants is a positive component with minimal or no negative components. As in adults, this change in morphology of the evoked response appears to reflect underlying mechanisms; the negative response component elicited at isoluminance is the response to chromatic contrast, reflecting parvocellular activity, while the earlier positive component which increases in amplitude with luminance difference is the response to luminance contrast, and reflects magnocellular activity. Thus, morphology of the evoked response to chromatic pattern-onset stimulation may be used in infants, as in adults, to identify the activity of underlying luminance and chromatic mechanisms.

7.5 Infant Isoluminance

In some studies, photopic spectral sensitivity has been found to be elevated at short wavelengths in young infants with respect to adults (Dobson, 1976; Moskowitz-Cook, 1979), while others have found sensitivity to be similar in the two groups (Peeples and Teller, 1978; Volbrecht and Werner, 1987; Bieber et al, 1995). The relatively increased sensitivity to short-wavelength stimuli found by early studies (Dobson, 1976; Moskowitz-Cook, 1979) has

been attributed to the relatively low density of macular pigment at the immature fovea (Dobson, 1976; Bone et al, 1988) and to contributions from parafoveal cones (Moskowitz-Cook, 1979), as stimuli subtending 16 and 12 degrees respectively were used in these two studies. Other workers using large stimuli, however, have found similar short-wavelength sensitivity in infants and adults (Peeples and Teller, 1978), and Dobson (1976) could not elicit a similar effect using eccentric fixation, suggesting that relatively elevated sensitivity is not due to contributions from parafoveal cones. There is general agreement that infants and adults demonstrate similar spectral sensitivity curves at wavelengths above 500 nm (Dobson, 1976; Peeples and Teller, 1978; Moskowitz-Cook, 1979; Bieber et al, 1995).

Volbrecht and Werner (1987) determined sensitivity of short-wavelength-sensitive cones in 4- to 6-week-old infants and in adults using the visual evoked response to a 4-degree stimulus, and found similar sensitivity in the two groups. Sensitivity to short-wavelength stimuli was found to be elevated above the 2-degree $V\lambda$ function in 2- and 4-month-old infants and in adults by Bieber et al (1995), using the VEP. This elevation in adults as well as infants suggests that observers of all ages may deviate from the $V\lambda$ spectral sensitivity function, probably due to individual differences in ocular media density (Werner, 1982) and to relatively reduced macular pigment absorption of light at short wavelengths by a 5-degree stimulus, compared with the 2-degree stimulus used for the standard $V\lambda$ function (Bieber et al, 1982).

If infants are more sensitive than adults to short-wavelength stimuli, it is possible that a heterochromatic stimulus containing a short-wavelength element may not be isoluminant to infants at photometric isoluminance, the adult isoluminant match. This point may be illustrated as follows. In adults, contrast sensitivity is at a minimum at isoluminance, and increases at colour ratios away from this point (Mullen, 1985). Allen et al (1993) showed, using ideal observer theory, that protanopic or deuteranopic adult observers are least sensitive at a red-green colour ratio which is not at photometric isoluminance, as in the normal trichromatic individual, but at which the red element of the stimulus is more bright or less bright than the

green, respectively. They calculated that while the normal trichromatic ideal observer is least sensitive to contrast at a colour ratio of 0.5, the protanopic ideal observer is least sensitive to contrast at a red-green colour ratio of 0.62 using their particular stimulus. At this ratio, the remaining medium-wavelength-sensitive cone mechanism of the protanope would have equal quantum catch for the red and green elements of the stimulus and the observer would be unable to differentiate the two as the short-wavelength-sensitive cone mechanism is not involved in the discrimination of Rayleigh stimuli. Similarly, in the deuteranope, the colour ratio at which the long-wavelength-sensitive cone mechanism would be equally stimulated by the two chromatic elements was found to be 0.42.

A similar shift in isoluminance, or the colour ratio at which minimum contrast sensitivity is demonstrated, might also be expected in infants if spectral sensitivity is relatively elevated at certain regions of the visible spectrum, with respect to sensitivity in colour-normal adults, on which photometric isoluminance is based. If infants are relatively more sensitive than adults to short-wavelength stimuli, when viewing a photometrically isoluminant tritan stimulus, quantum catch will be relatively greater for the short-wavelength element of the stimulus than for the second chromatic element. Infant isoluminance for such a stimulus would therefore be expected to be shifted away from photometric isoluminance towards a colour ratio at which the short-wavelength element, such as the purple used in the present study, is less bright than the other element such as greenish-yellow. Infants of all ages are generally found to demonstrate adult-like photopic spectral sensitivity curves above 500 nm, so such a shift would not be expected when Rayleigh stimuli are used.

In the present study, isoluminance of tritan and red-green stimuli was found to be similar in infants and adults, as demonstrated by the lack of an early positive component at or close to photometric isoluminance, and by the estimation of individual isoluminant points (see figure 7.17). This suggests, in agreement with other studies (Volbrecht and Werner, 1987; Bieber et al, 1995), that infant spectral sensitivity is not significantly raised

with respect to adults, at short wavelengths. Discrepancies between these and some previous findings (Dobson, 1976; Moskowitz-Cook, 1979) may be due to individual variations in ocular media density (Werner, 1982), as suggested by Bieber et al (1995), and may also reflect macular pigment differences between individuals.

In the present study, the finding that infant and adult isoluminant points for both types of chromatic stimuli are similar may be useful in future studies on infant colour vision, as photometrically isoluminant matches may be used as a first approximation for individual isoluminance at an early age. The approximate nature of photometric luminance matches in infants and adults should be emphasised, however, as illustrated by inter-individual variations from the $V\lambda$ spectral sensitivity function.

In the intestinal mucosa, where β -carotene is converted by the action of β -carotene 15,15'-monooxygenase to retinaldehyde which is then reduced to retinol. Retinol is removed from the circulation by the liver, where it is stored, then released back into circulation as retinol bound to retinol binding protein (RBP) and transported in plasma to target tissues, including the retina (Goodman, 1988). In patients with liver disease, blood plasma levels of vitamin A and RBP have been found to be markedly reduced (Smith and Goodman, 1971). Patients with vitamin A deficiency show abnormal dark adaptation and rod and cone function, suggesting photoreceptor malfunction due to inadequate levels of retinol (Russell et al. 1975, Carney and Russell, 1980, Parham et al. 1980).

Fatty acids are also thought to be important for normal visual function. Docosahexaenoic acid (DHA) is a long-chain polyunsaturated fatty acid, which is formed in the adult human by desaturation and elongation of linolenic acid, one of the omega-6 essential fatty acids. Infants are less able than adults to carry out this process and so require dietary DHA, which is richly provided by breast milk but not by unsupplemented formula milk. DHA is found in high concentrations in the outer segment membranes of retinal photoreceptors and in the cerebral cortex and in much lower concentrations elsewhere in the body. This has led to the supposition that DHA may be essential for normal visual function, although this view has

CHAPTER 8

THE CHROMATIC AND LUMINANCE VEP IN INFANTS WITH FATTY ACID AND VITAMIN DEFICIENCY

8.1 Introduction

Infants with liver disorders demonstrate low blood plasma levels of essential fatty acids and vitamins A, D, E and K. Cystic fibrosis sufferers demonstrate similar deficiencies due to malabsorption and liver disease (Gotz and Stur, 1978; Warner, 1992). It is well established that vitamin A is essential for normal visual function. Vitamin A is a generic term used to describe retinol, which together with the protein opsin forms the photoreceptor rhodopsin, found in the outer segment membranes of rod photoreceptors. Dietary sources are converted to vitamin A in the intestinal mucosa, where β -carotene is converted by the action of two enzymes to retinaldehyde which is then reduced to retinol. Retinol is removed from the circulation by the liver, where it is stored, then released back into circulation as retinol bound to retinol binding protein (RBP) and transported in plasma to target tissues, including the retina (Goodman, 1988). In patients with liver disease, blood plasma levels of vitamin A and RBP have been found to be markedly reduced (Smith and Goodman, 1971). Patients with vitamin A deficiency show abnormal dark adaptation and rod and cone function, suggesting photoreceptor malfunction due to inadequate levels of retinol (Russell et al, 1973; Carney and Russell, 1980; Perlman et al, 1983).

Fatty acids are also thought to be important for normal visual function. Docosahexaenoic acid (DHA) is a long-chain polyunsaturated fatty acid, which is formed in the adult human by desaturation and elongation of linolenic acid, one of the omega-6 essential fatty acids. Infants are less able than adults to carry out this process and so require dietary DHA, which is richly provided by breast milk but not by unsupplemented formula milks. DHA is found in high concentrations in the outer segment membranes of retinal photoreceptors and in the cerebral cortex, and in much lower concentrations elsewhere in the body. This has led to the supposition that DHA may be essential for normal visual function, although its precise role

is unclear (Neuringer and Connor, 1986). It has been suggested that the presence of DHA in the phospholipid bilayer of the outer segment membranes of the rods and cones gives the cell membrane optimum thickness and fluidity for photochemical transduction to take place (Dratz et al, 1987).

The relationship between DHA and visual function has been widely investigated, with particular emphasis on full-term and pre-term infants, who may be susceptible to low levels of DHA in the diet at a period of rapid development of the visual pathway and of the cerebral cortex as a whole. Human infants fed DHA-deficient diets have significantly lower erythrocyte and cortical DHA levels than control infants, although no difference in retinal DHA has been found between the two groups (Makrides et al, 1994).

In general, significantly lower visual acuity, measured by both electrophysiological and behavioural techniques, is found in pre-term and full-term infants fed diets deficient in DHA than those fed breast milk or supplemented formula milk (Neuringer et al, 1984; Birch et al, 1992b; Birch et al, 1993; Makrides et al, 1993; Courage et al, 1995), although some work suggests that there is no significant difference in acuity between the two groups (Innis et al, 1994). In addition, the rod ERG shows higher thresholds and lower response amplitudes in infants on DHA-deficient diets than in those on breast milk or supplemented formula, while the cone ERG is unaffected in these infants (Uauy et al, 1990; Birch et al, 1992a). Measures of visual evoked response latency, however, have shown no significant difference between infants on supplemented and unsupplemented diets (Schweitzer et al, 1995).

In the present study, visual evoked responses to luminance and chromatic stimuli were recorded from ten infants with the principal aim of determining the age at which infants have functional S-cone pathways, and a secondary aim of comparing this with the development of L-M cone and luminance pathways (see Chapter 9). Nine of the ten infants demonstrated visual evoked potentials to luminance-modulated stimuli from the earliest age tested (4 weeks post-term) and responded to chromatic stimuli at and

around photometric isoluminance by 4 to 11 weeks post-term (see Chapter 9), in agreement with previous work on visual evoked responses in young infants (Morrone et al, 1993; Rudduck and Harding, 1994).

One male Caucasian infant (RH), included in the study as he was thought to be in good health by mother's report, showed no response to chromatic stimulation at any age from 4 to 12 weeks post-term, and absent or significantly delayed responses to luminance-modulated stimulation from 4 to 25 weeks post-term. Chromatic responses were not recorded beyond the age of 12 weeks, as reliable comparisons were not obtained in a group of healthy infants at this age (see Chapter 9).

In order to investigate this further, scotopic, photopic and fast-flicker ERGs were recorded from this infant, and were compared to those of a second group of control infants of comparable age range. At 11 weeks of age, cystic fibrosis was suspected in this infant by his general practitioner, and was diagnosed at 13 weeks.

In addition, photopic, fast-flicker and scotopic ERGs and visual evoked responses to flash and achromatic pattern-reversal stimulation were carried out on a group of 32 infants with liver disorders, in a cross-sectional study in collaboration with the Birmingham Children's Hospital. These infants are deficient in long-chain polyunsaturated fatty acids, including DHA. They received vitamin supplements but were not supplemented with fatty acids. ERG and achromatic (luminance) VEP results from these infants were compared with those of the second control group mentioned above, in order to further investigate the effects of fatty acid deficiency on visual function.

8.2 Methods

Three infant groups were included in this study:

Visual evoked responses to luminance and chromatic stimuli as described in Chapter 5 were recorded from a group of nine healthy infants. Results from these infants are reported in Chapter 9.

Photopic, Scotopic and fast-flicker ERGs and visual evoked responses to flash and achromatic pattern-reversal stimuli as described below were recorded from a group of 32 infants with liver disorders and fatty acid deficiency, in collaboration with the Birmingham Children's Hospital. Blood erythrocyte levels of DHA were determined in these infants by blood tests carried out and analysed by Children's Hospital staff on the same day as ERGs and VEPs, and were found to be significantly below normal in all of this group of infants.

Results from these infants were compared with those of a group of control infants using identical stimuli and recording procedures. Blood tests were not carried out on these infants. Infants fed different diets (breast vs bottle fed) have been found to have different levels of visual function (see introduction to this chapter) which is thought to be due to fatty acid deficiency. Within this group of normal infants, some were bottle-fed and some were breast fed. In order to determine whether these groups differed in their evoked response or ERG latencies, the two were compared, and showed no significant difference ($p > 0.1$ for all types of response).

All electrophysiological tests described were carried out on infant RH, the results of which were compared with those of both groups of control infants.

As with all subjects, a signed declaration of informed consent was obtained from a parent beforehand. Subject recruitment and exclusions are as described in Chapter 5. Infants with liver disorders were recruited by staff at the Birmingham Children's Hospital.

8.3 ERG Recording

ERGs were recorded using DTL fibre (Esakowitz et al, 1993) laid along the tear film below the lower eyelid of one eye, kept in position using a small piece of Blenderm tape on the side of the nose (Thompson and Drasdo, 1987). Recording was carried out on one eye only as this was an investigation of systemic rather than local ocular changes. Repeat tests were

carried out on the same eye. Unless otherwise stated, ERGs were recorded through natural (undilated) pupils. The DTL formed the active electrode and this was referred to an electrode on the outer canthus of the same eye; the earth electrode was positioned at Cz. White flash photopic, scotopic and 30 Hz flicker stimuli at a luminance of 200 cd/m² were chosen to elicit cone-dominated, rod-only and cone-only responses, respectively (Ikeda, 1993). The photopic ERG, at a temporal frequency of 0.9 Hz, was averaged from 8 sweeps, and the 30 Hz flicker ERG from 20 sweeps. The scotopic ERG was recorded following 10 minutes' dark adaptation, and was elicited by a single flash (not averaged) to avoid light adaptation. Resistance was below 8 kOhms for all ERG recordings. ERGs were recorded at least twice to ensure repeatability.

8.4 VEP Recording

The technique for recording VEPs to chromatic and luminance-modulated stimuli is described in Chapter 5.

Visual evoked responses to white flash stimuli and to square-wave achromatic pattern-reversing checks were recorded from O1 referred to C3 and Fz, and from O2 referred to C4 and Fz (four channels). Cz was used as earth and responses to both types of stimuli were averaged from 50 sweeps. White flash stimuli were presented at a temporal frequency of 0.9 Hz and a luminance of 100 cd/m². Pattern-reversing checks were presented at a temporal frequency of 1.1 Hz and an angular subtense of 0.5 degree at a viewing distance of 33 cm.

8.5 Schedule

Visual evoked responses to chromatic and luminance-modulated stimuli, as described in Chapter 5, were recorded from infant RH at weekly intervals from 4 to 6 then 8 to 12 weeks post-term age, and to luminance-modulated stimuli only at 19 and 25 weeks. Chromatic stimulation was not used at these later ages as reliable responses could not be elicited from control infants for comparison after 3 months of age (see Chapter 9). The schedule followed for these control infants is described in Chapter 5. ERGs were recorded at 12, 19 and 25 weeks only. At 25 weeks of age, all ERGs were

carried out first with a natural pupil and then the scotopic ERG was recorded with the pupil dilated using 1% cyclopentolate hcl.

Scotopic, photopic and fast-flicker ERGs and flash and achromatic pattern-reversal VEPs were recorded from control infants on a cross-sectional basis. Infants from the Children's Hospital were also seen on a cross-sectional basis.

Results

8.6 Cystic Fibrosis

Visual evoked responses recorded from infant RH to both types of chromatic stimulation (tritan and red-green) at and around photometric isoluminance showed no distinct components at any age from 4 to 12 weeks post-term, as illustrated for age 8 weeks by figures 8.1 and 8.2. By contrast, normal, healthy infants demonstrated evoked potentials to isoluminant chromatic stimulation from as early as 4 weeks post-term, and on average by 7 weeks for tritan stimuli and 9 weeks for red-green (see Chapter 9). Typical evoked responses to luminance and chromatic stimuli are shown for one infant (AE) in figures 8.3 and 8.4.

Luminance-modulated stimuli elicited responses of delayed latency from infant RH compared to those of age-matched healthy infants from 6 to 12 weeks post-term age. Evoked responses to luminance stimuli were indistinguishable from EEG noise levels as indicated by the non-stimulus condition before 6 weeks post-term age. The delay was statistically significant at the ages of 9, 10, 11, 12 and 19 weeks post-term ($p < 0.05$) but not at the earlier ages of 6 or 8 weeks ($p > 0.08$). As mentioned earlier, the chromatic response was not considered after 12 weeks, as most normal infants had demonstrated absent or diminished chromatic responses beyond 3 months of age, particularly to tritan stimulation, so no reliable comparison could be made (see Chapter 9).

Figure 8.5 shows luminance response latency with respect to age for infant RH and for the group of healthy infants for comparison. The responses of healthy infants to luminance-modulated stimuli reached a plateau of 120 to

130 ms latency by 11 to 12 weeks of age, while luminance responses from RH plateaued at about 200 ms by the same age. At 25 weeks post-term, the luminance response was again indistinguishable from noise. This is illustrated by figure 8.6, which also shows the comparable response from a healthy age-matched infant (AM).

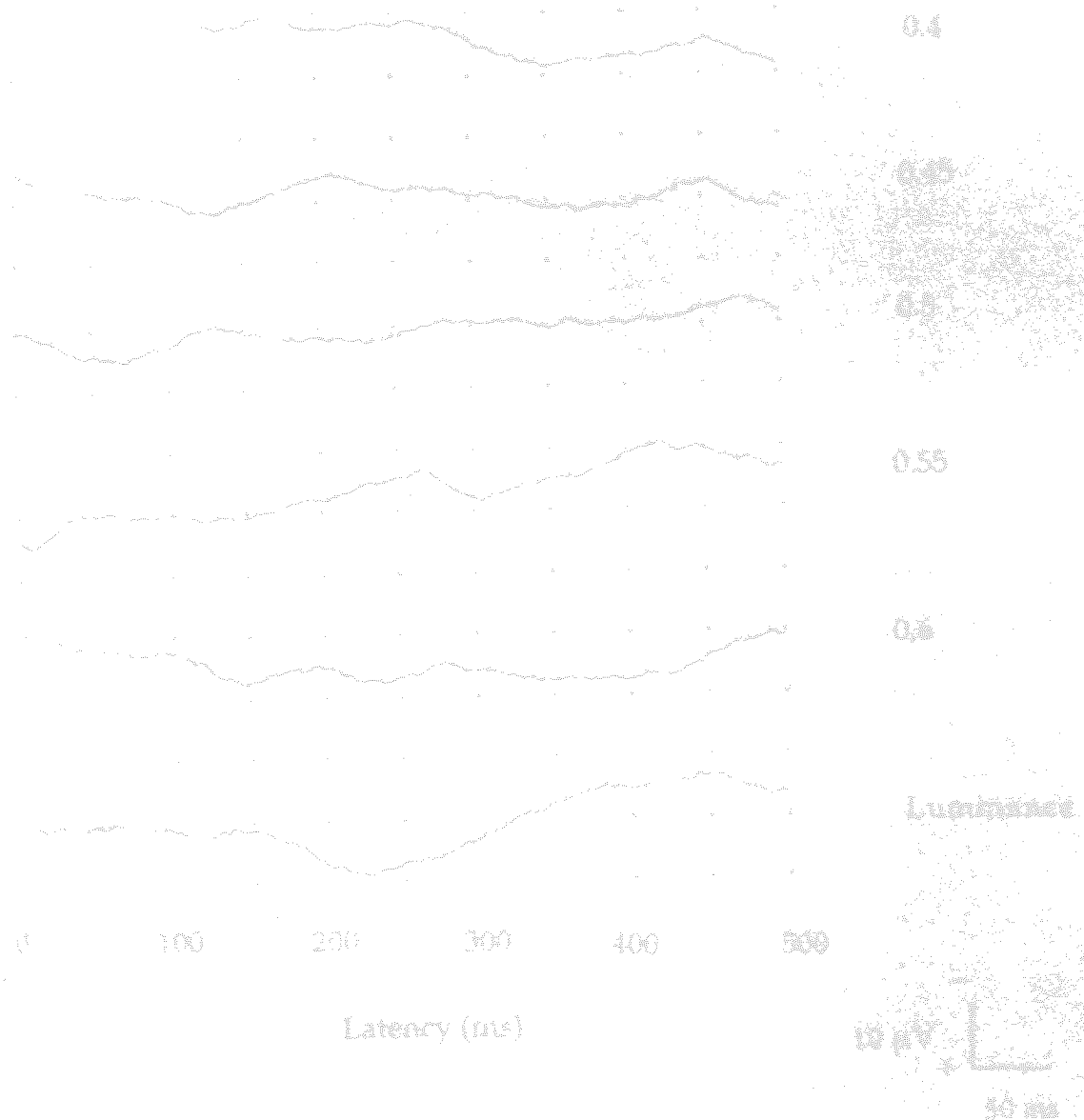


Figure 8.6
Visual evoked responses to pattern stimulation and around adult color response recorded from infant RH are shown, at 8 weeks post-term age. Also shown is the response to luminance modulated stimulation.

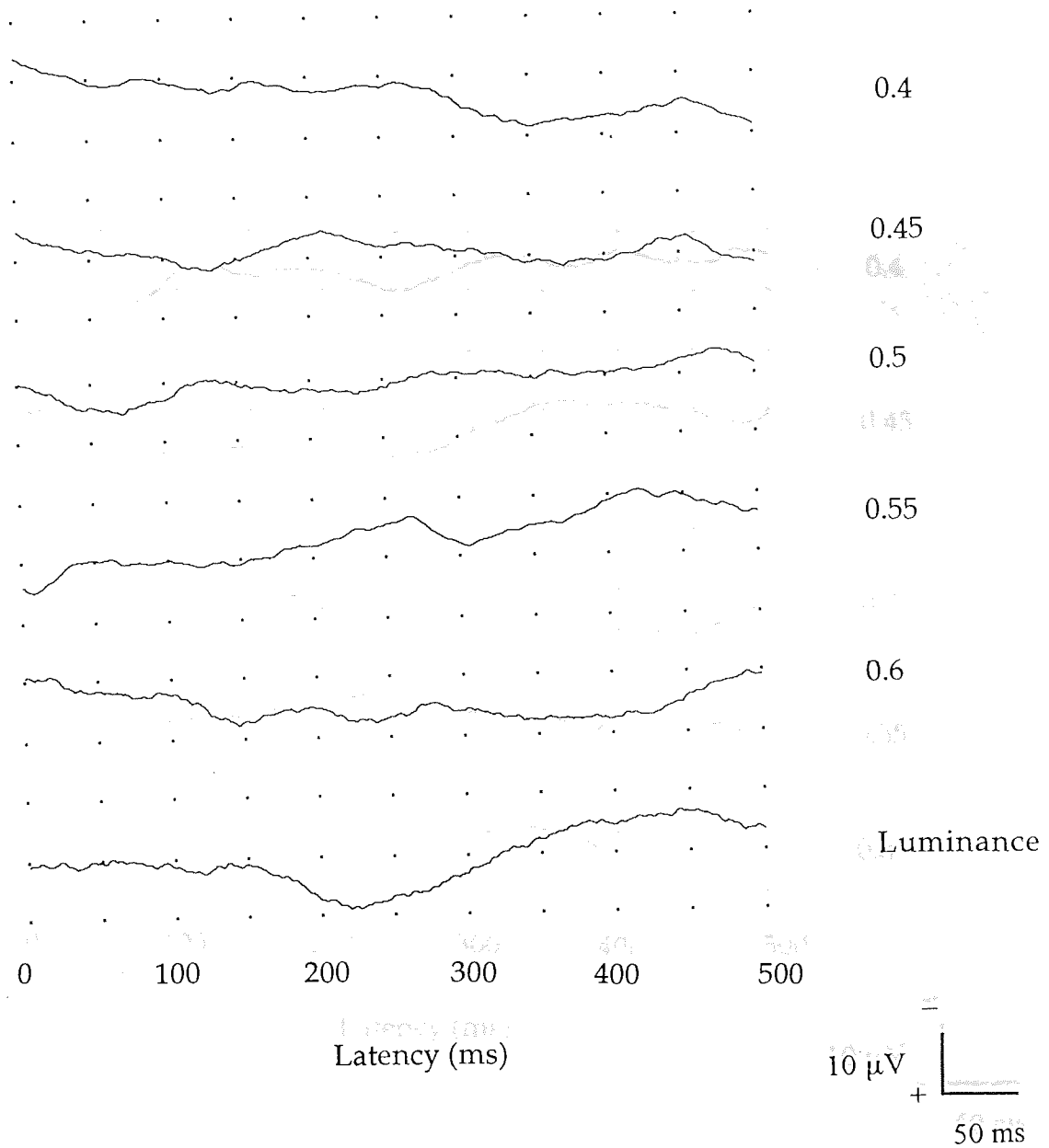


Figure 8.1. Visual evoked responses to tritan stimuli at and around adult isoluminance recorded from infant RH are shown, at 8 weeks post-term age. Also shown is the response to luminance-modulated stimulation.

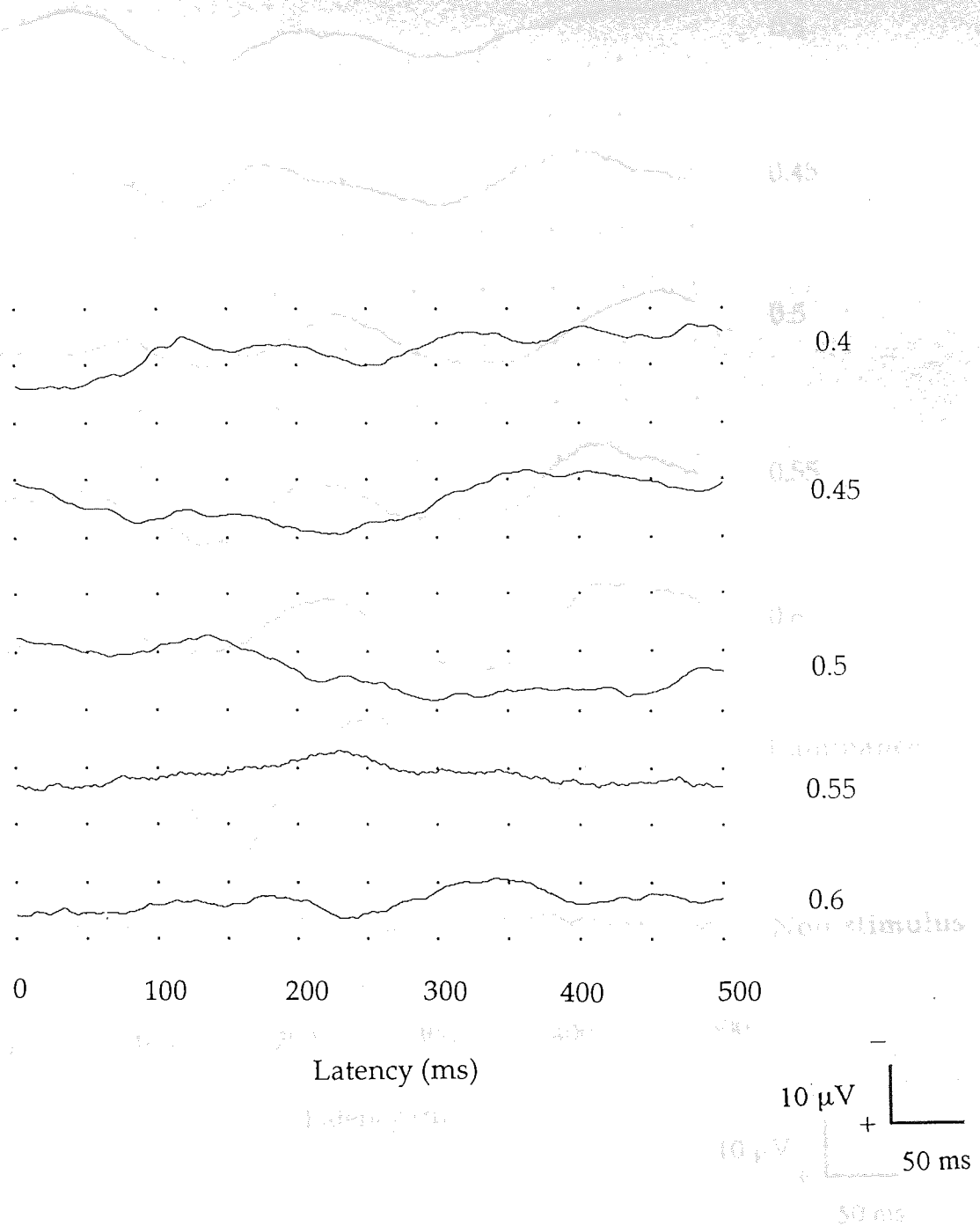


Figure 8.2. Visual evoked responses to red-green stimuli at and around the adult isoluminant match recorded from infant RH at 8 weeks post-term age are shown.

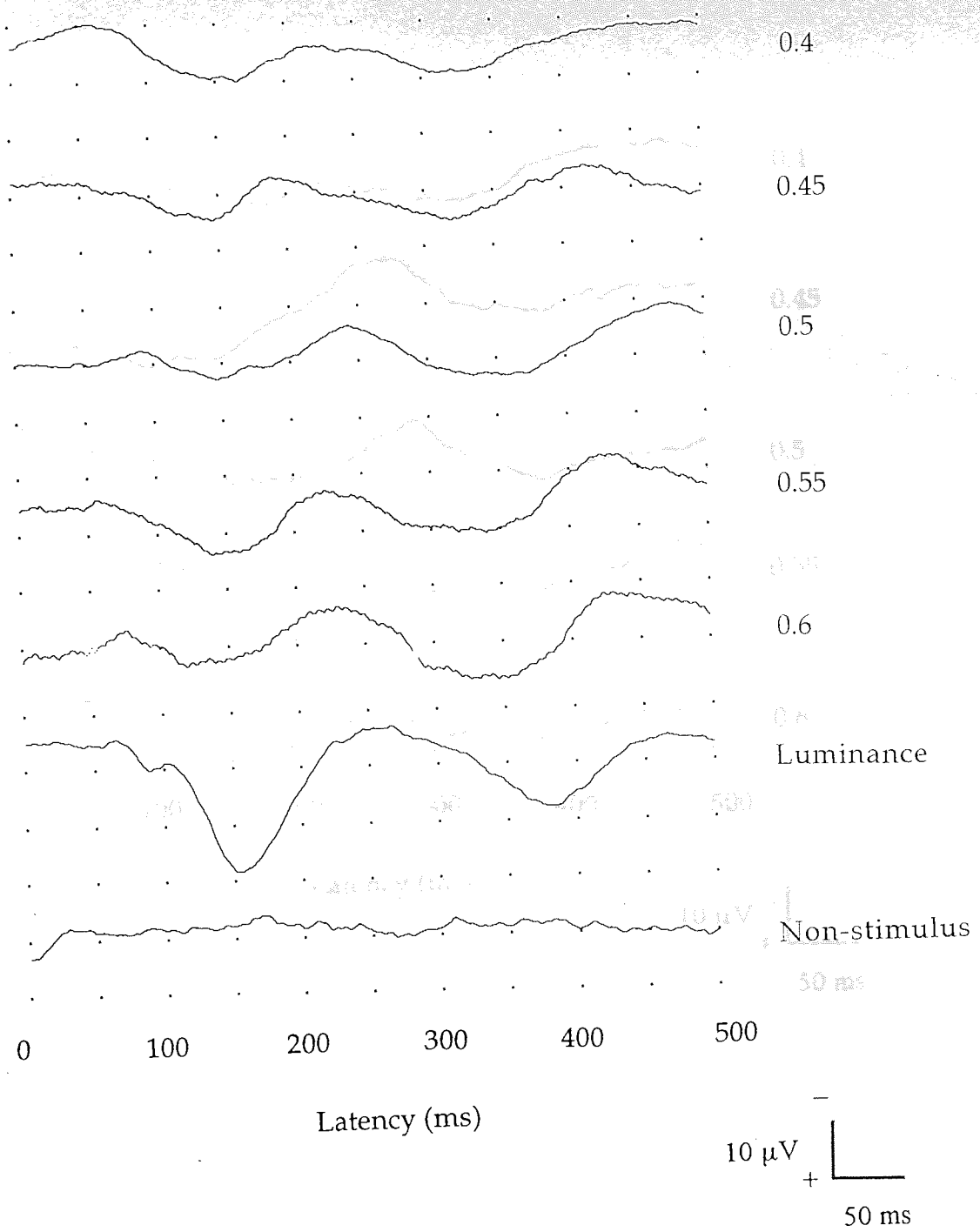


Figure 8.3. Visual evoked responses to tritan stimuli at the range of colour ratios shown, recorded from a healthy infant (AE) at 7 weeks (49 days) post-term age. Responses to luminance-modulated stimulation and the non-stimulus condition are also shown for comparison.

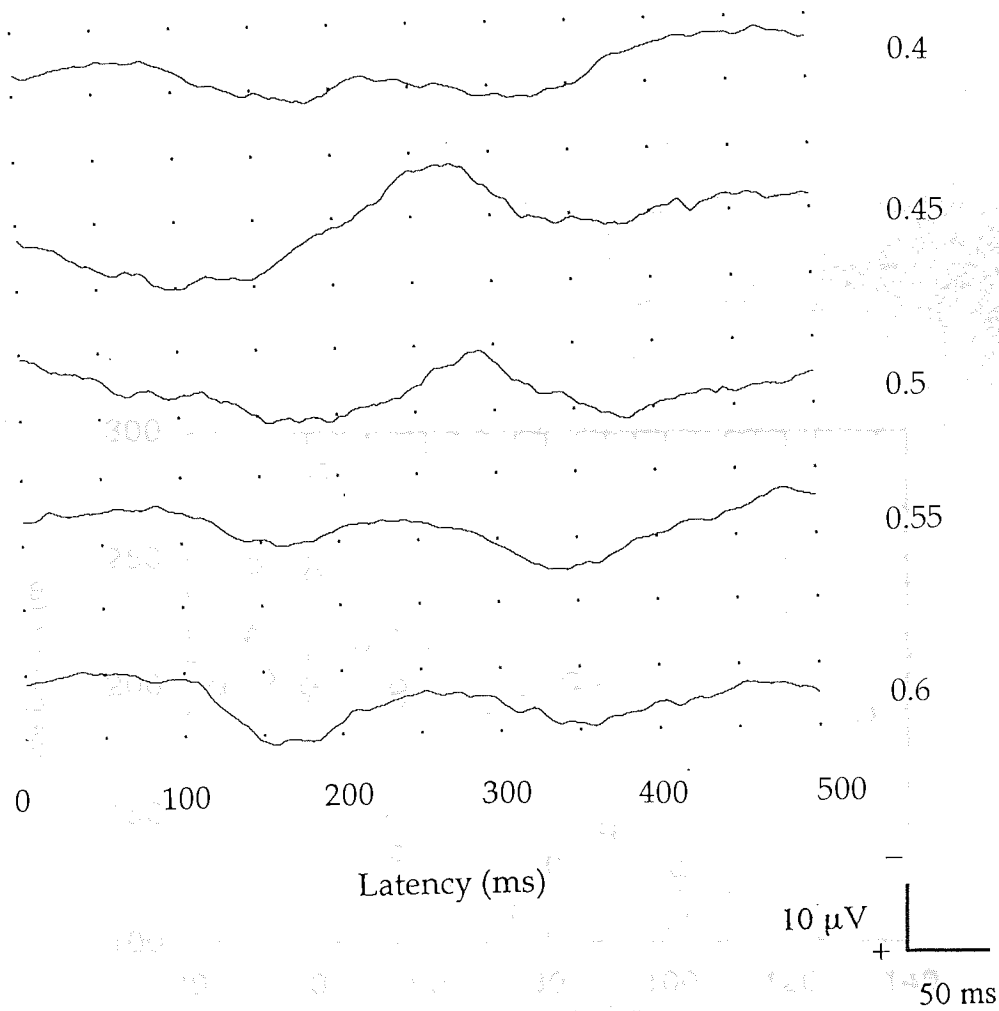


Figure 8.4.
 Visual evoked responses to red-green stimuli at the range of colour ratios shown, recorded from a healthy infant (AE) at 6 weeks (41 days) post-term age.

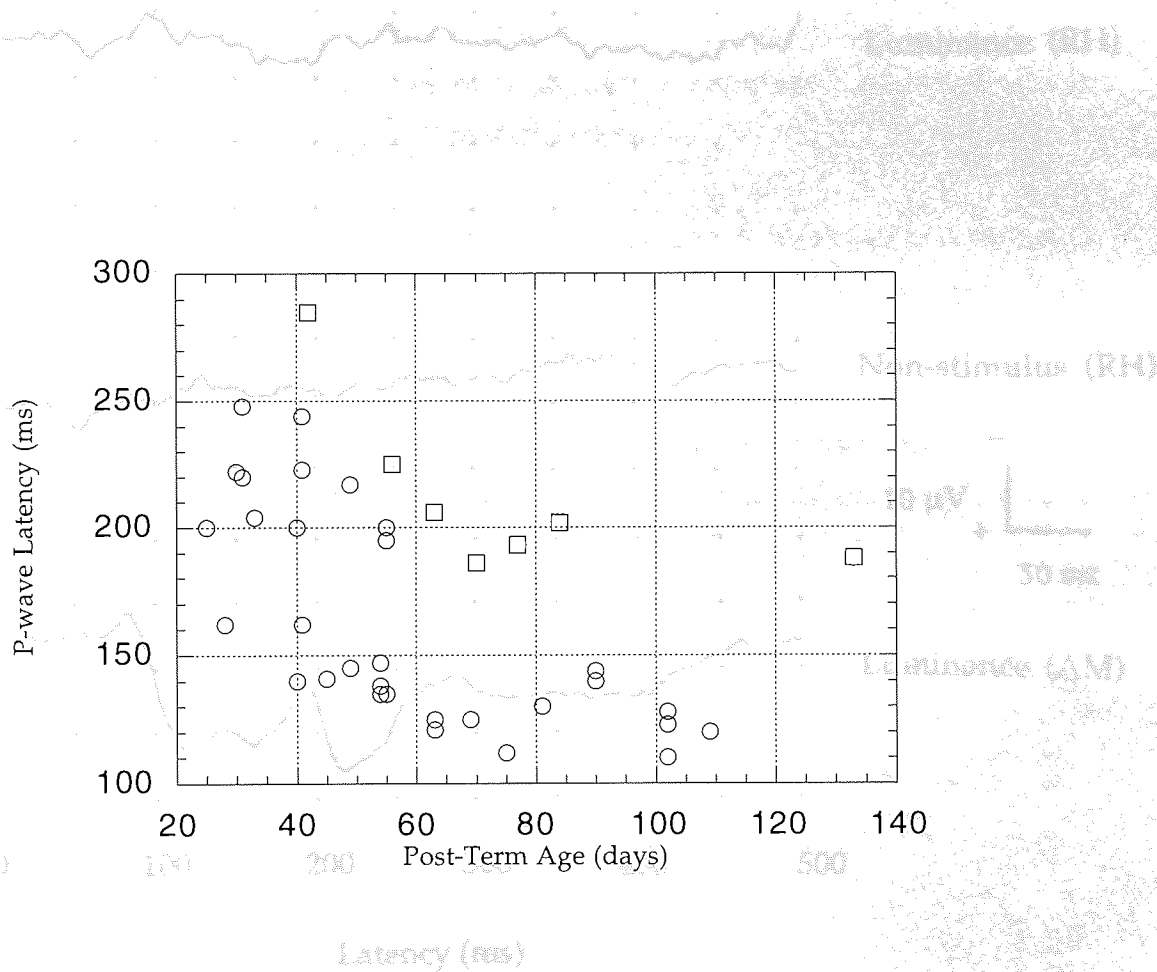


Figure 8.5. Visual evoked responses to luminance-modulated stimulation recorded from infant RH at 25 weeks post-term age (top trace) and to the non-stimulus condition. The evoked response to the stimulus is shown in the bottom trace. Positive peak response latencies to luminance stimuli are shown (open circles) with respect to the non-stimulus condition for the five normal infants tested up to three months post-term. Also shown are latencies of responses to the same stimulus recorded from infant RH (open squares).

absent in infant RH at this stage. When the luminance-modulated ERG demonstrates distinct a- and b-waves, ERGs under fast flicker (30 Hz) stimulation conditions recorded from infant RH show distinct a- and b-waves with no significant difference in latency to those of the age-matched normal infants ($p > 0.1$). In all cases, ERG recordings were carried out on eyes with a dilated pupil, so pupil size at the time of recording is unknown; consequently, response latencies only should be compared as differences in amplitude may be due to pupil size differences.

ERGs recorded from infant RH after diagnosis and 6 weeks of treatment of cystic fibrosis at the age of 19 weeks post term, are shown in figure 8.6. Response to photopic and 30 Hz stimulation are similar to those recorded from age-matched normal infants (figure 8.5). The scotopic ERG, by contrast to the situation before diagnosis, now shows distinct a- and b-waves of similar latencies to those recorded from age-matched normal infants (p > 0.1).

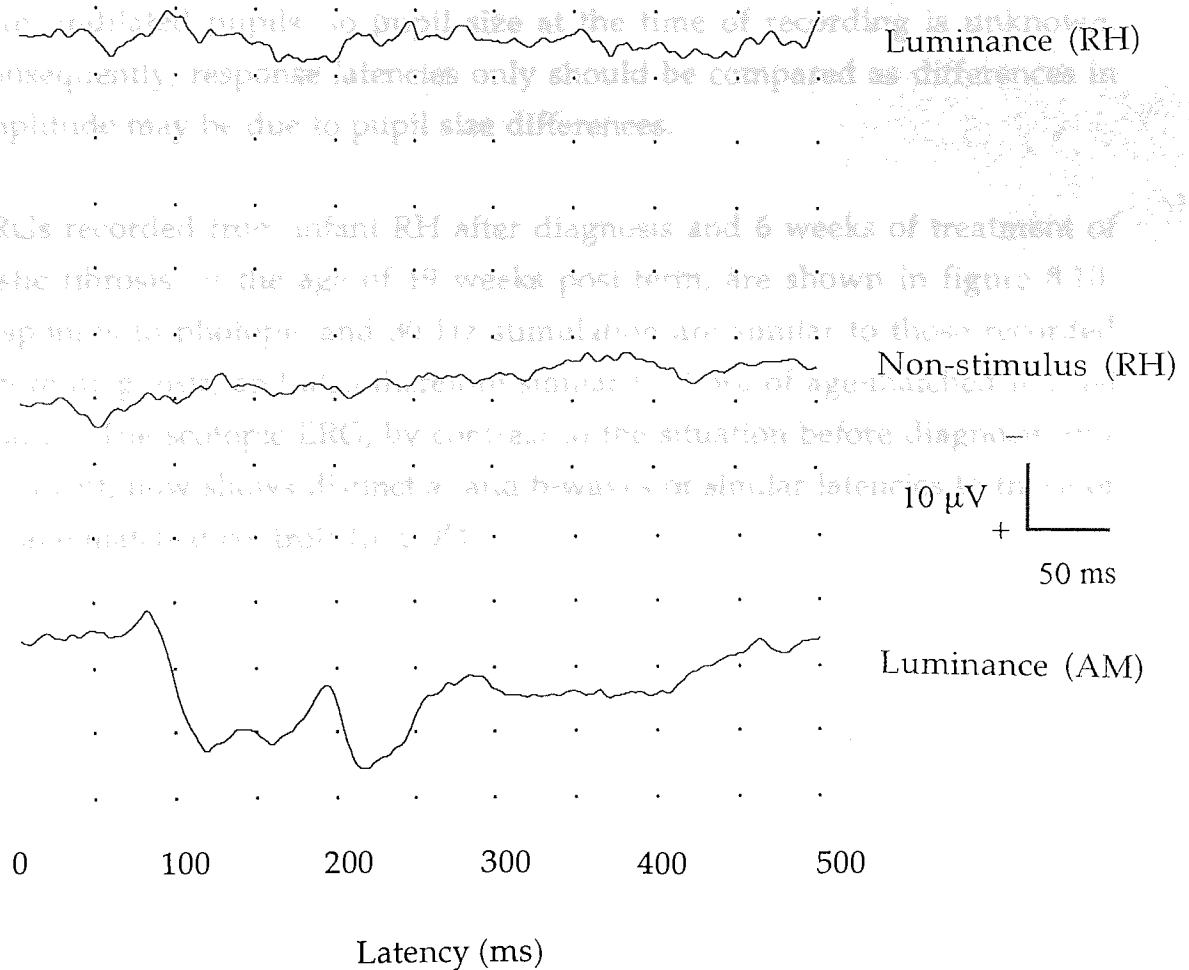


Figure 8.6. Visual evoked responses to luminance-modulated stimulation recorded from infant RH at 25 weeks post-term age (top trace) and to the non-stimulus condition. The evoked response to the same luminance stimulus recorded from a healthy infant (AM) at a comparable age (26 weeks post-term) is also shown for comparison (bottom trace).

ERGs recorded from infant RH at the age of 12 weeks post-term, before diagnosis and treatment of cystic fibrosis, and from healthy age-matched infants for comparison are shown in figures 8.7 to 8.9. Scotopic ERGs were absent in infant RH at this stage while the normal age-matched scotopic ERG demonstrates distinct a- and b-waves. ERGs under fast flicker (30 Hz) and photopic conditions recorded from infant RH show distinct a- and b-waves with no significant difference in latency to those of the age-matched normal infants ($p>0.1$). In all cases, ERG recordings were carried out on eyes with undilated pupils, so pupil size at the time of recording is unknown. Consequently, response latencies only should be compared as differences in amplitude may be due to pupil size differences.

ERGs recorded from infant RH after diagnosis and 6 weeks of treatment of cystic fibrosis, at the age of 19 weeks post-term, are shown in figure 8.10. Responses to photopic and 30 Hz stimulation are similar to those recorded before diagnosis, and also therefore similar to those of age-matched normal infants. The scotopic ERG, by contrast to the situation before diagnosis and treatment, now shows distinct a- and b-waves of similar latencies to those of the age-matched controls ($p>0.05$).



Figure 8.7.

Photopic ERGs are shown, recorded from infant RH (top) at 12 weeks post-term, age prior to diagnosis and treatment of cystic fibrosis, and from a healthy age-matched infant for comparison. Note that different time bases apply to each trace, so latency and amplitude values are also given.

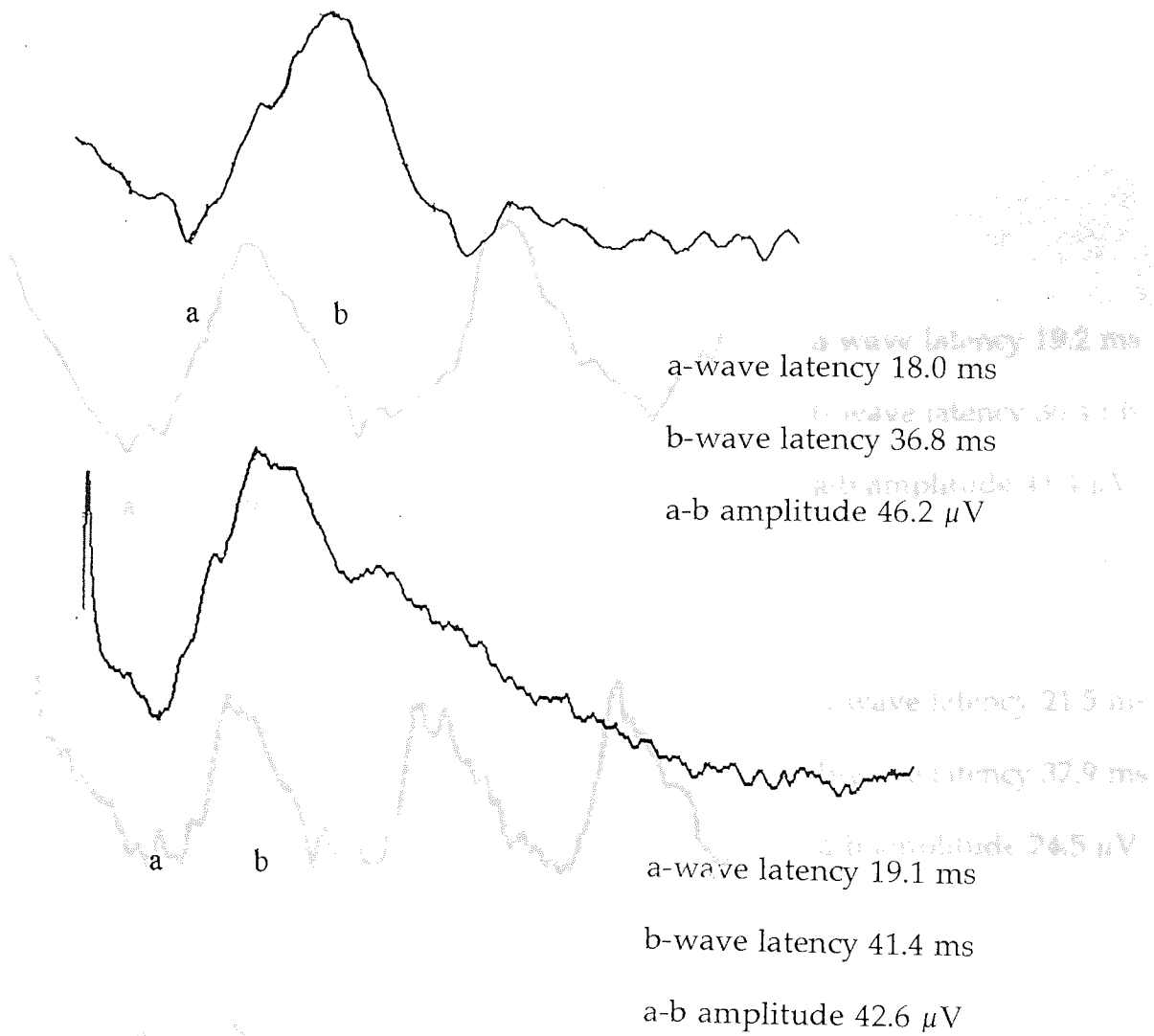


Figure 8.7.

Photopic ERGs are shown, recorded from infant RH (top) at 12 weeks post-term age, prior to diagnosis and treatment of cystic fibrosis and from a healthy age-matched infant for comparison. Note that different time bases apply to each trace, so latency and amplitude values are also given.

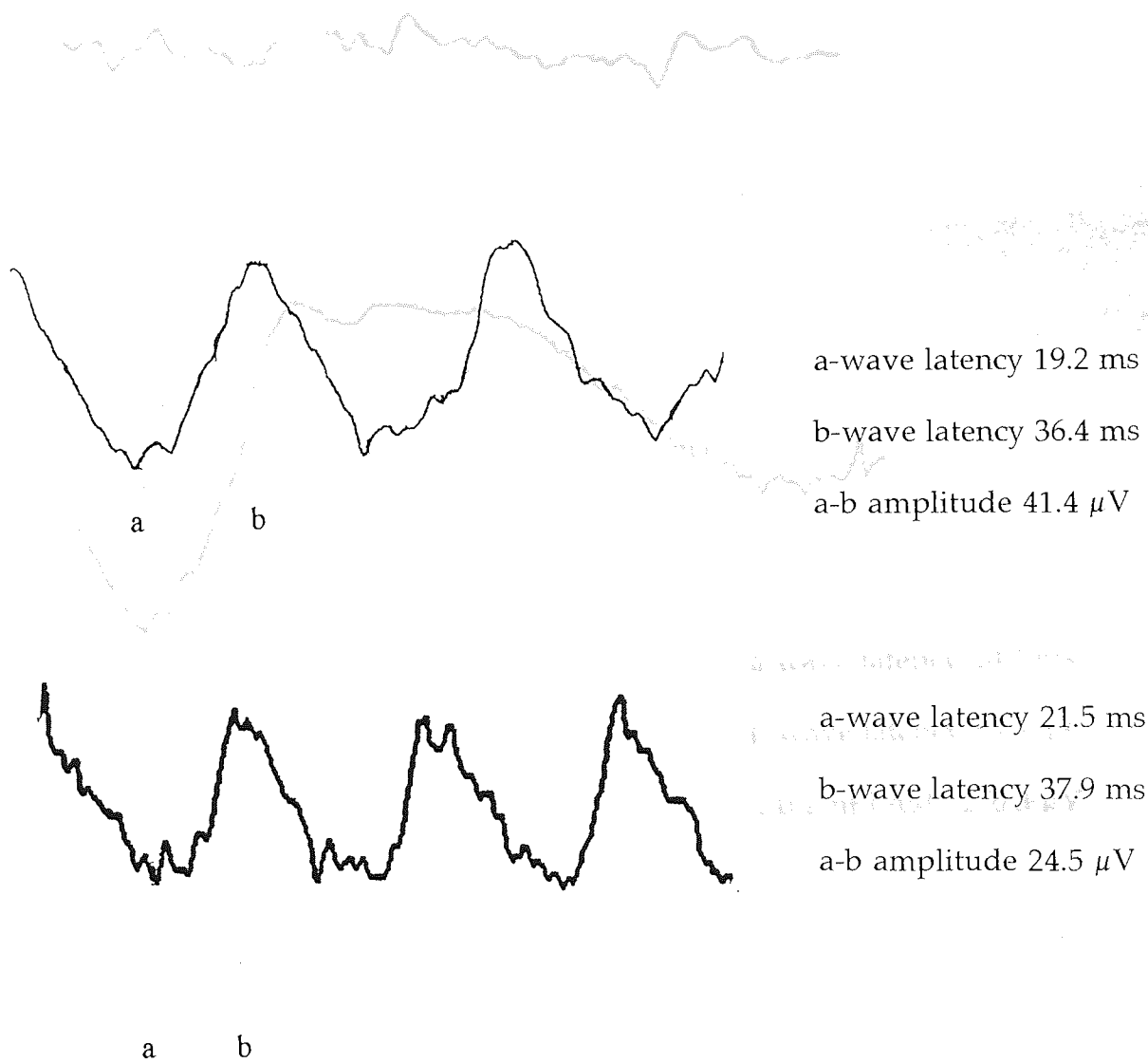


Figure 8.8.
 ERGs to 30 Hz flicker stimulation are shown, recorded from infant RH (top) at 12 weeks post-term, prior to diagnosis and treatment of cystic fibrosis and from a healthy age-matched infant for comparison. Note that different time bases apply to each trace, so latency and amplitude values are also given.

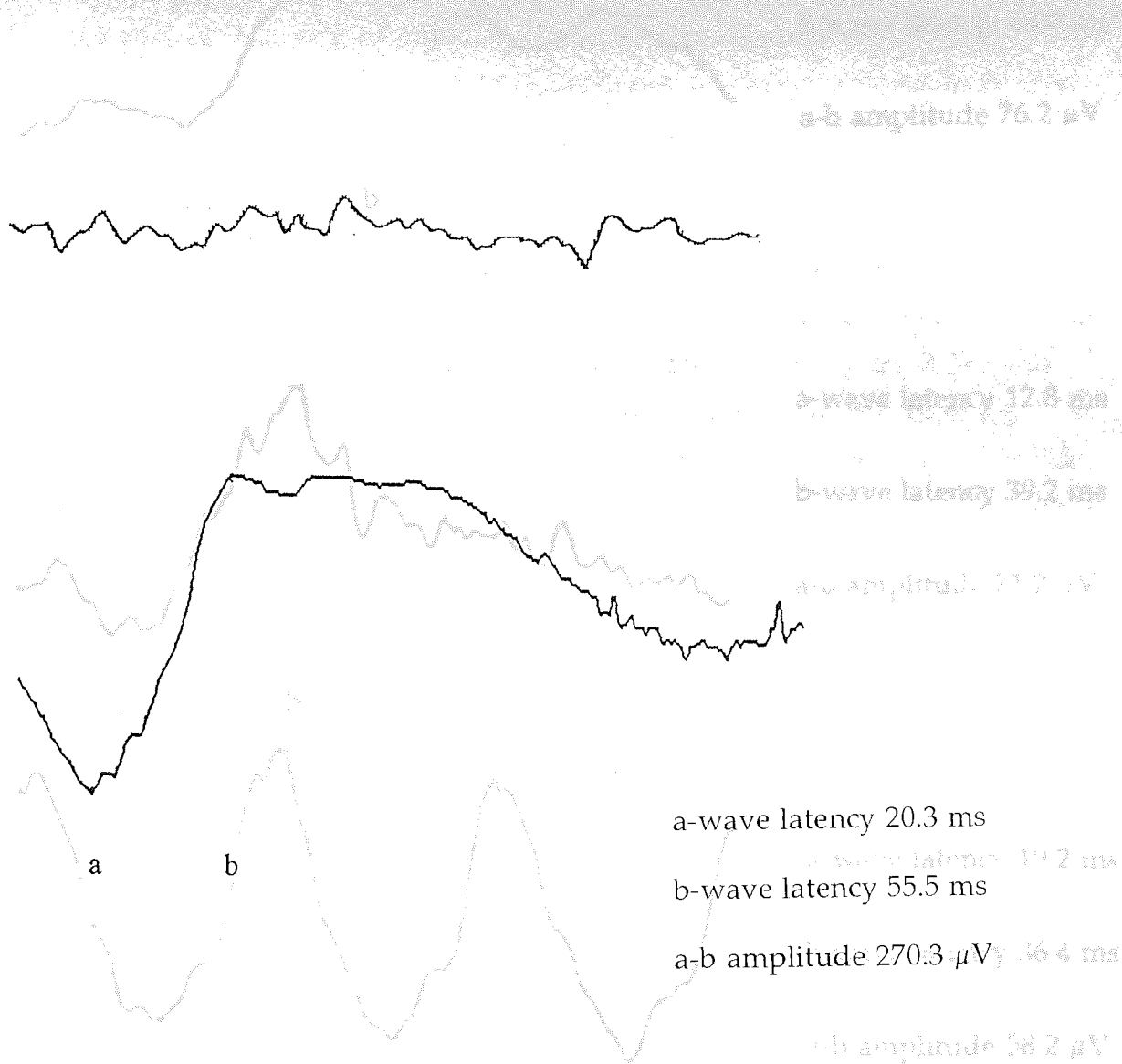


Figure 8.9.
 The scotopic ERG is shown, recorded from infant RH (top) at 12 weeks post-term, prior to diagnosis and treatment of cystic fibrosis, and from a healthy age-matched infant for comparison (lower trace).

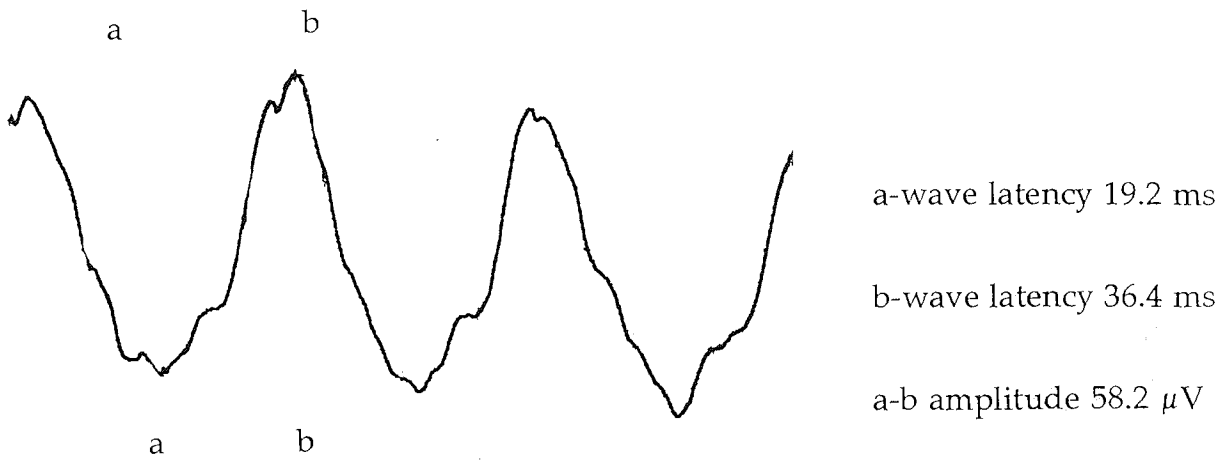
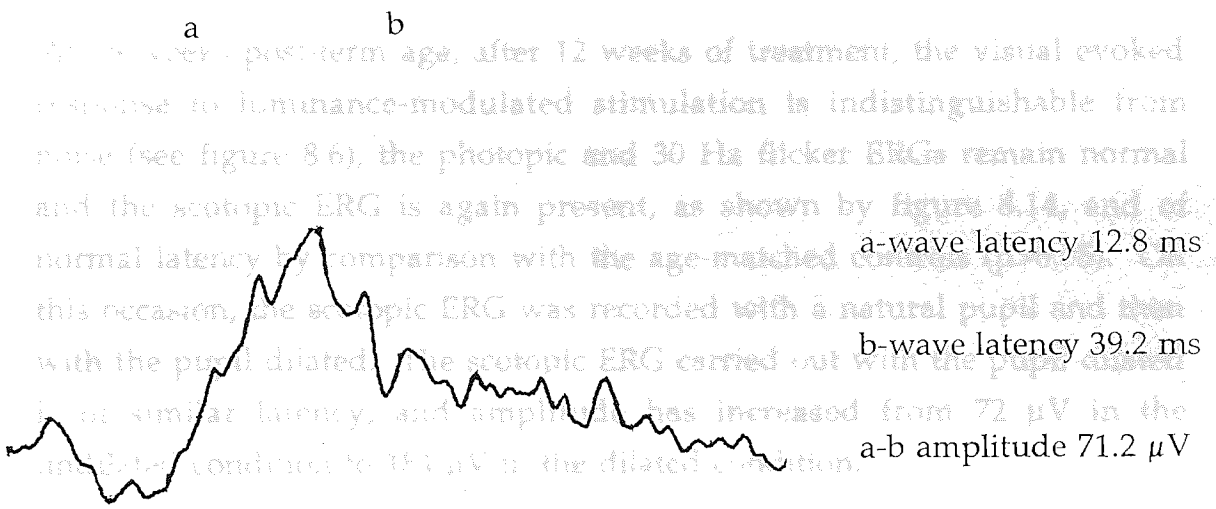


Figure 8.10. Scotopic, photopic and 30 Hz ERGs recorded from infant RH at the age of 19 weeks post-term after 6 weeks of treatment for cystic fibrosis.

Comparisons between ERGs from infant RH and from the control group are further illustrated by figures 8.11 to 8.13, which show b-wave latencies of photopic, 30 Hz and scotopic ERGs with respect to post-term age. For illustrative purposes, b-wave only, and not a-wave latencies have been plotted. All statistical comparisons apply to both a- and b-wave latencies.

At 25 weeks post-term age, after 12 weeks of treatment, the visual evoked response to luminance-modulated stimulation is indistinguishable from noise (see figure 8.6), the photopic and 30 Hz flicker ERGs remain normal and the scotopic ERG is again present, as shown by figure 8.14, and of normal latency by comparison with the age-matched controls ($p > 0.05$). On this occasion, the scotopic ERG was recorded with a natural pupil and then with the pupil dilated. The scotopic ERG carried out with the pupil dilated is of similar latency, and amplitude has increased from 72 μV in the undilated condition to 184 μV in the dilated condition.

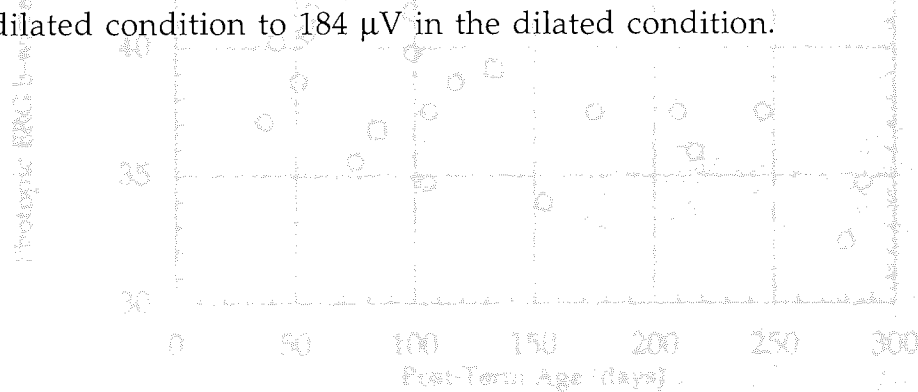


Figure 8.11

Photopic ERG b-wave latency is shown with respect to age for the group of healthy control children (open circles) and for normal 30 Hz flicker responses (open squares).

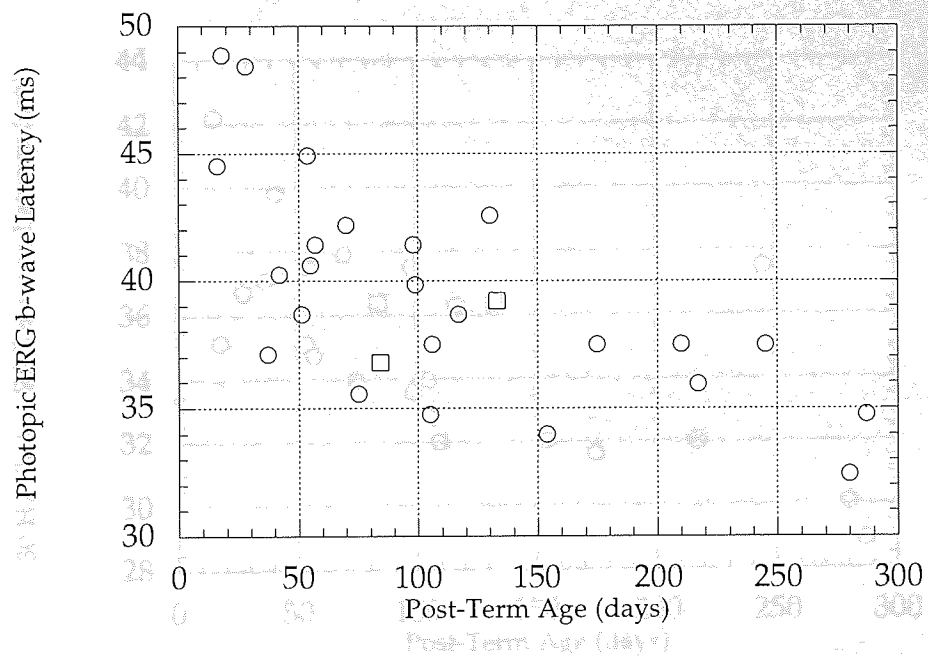


Figure 8.11. Photopic ERG b-wave latency (ms) is shown with respect to post-term age for the group of healthy control infants (open circles) and for infant RH (open squares) at 19 and 25 weeks of age.

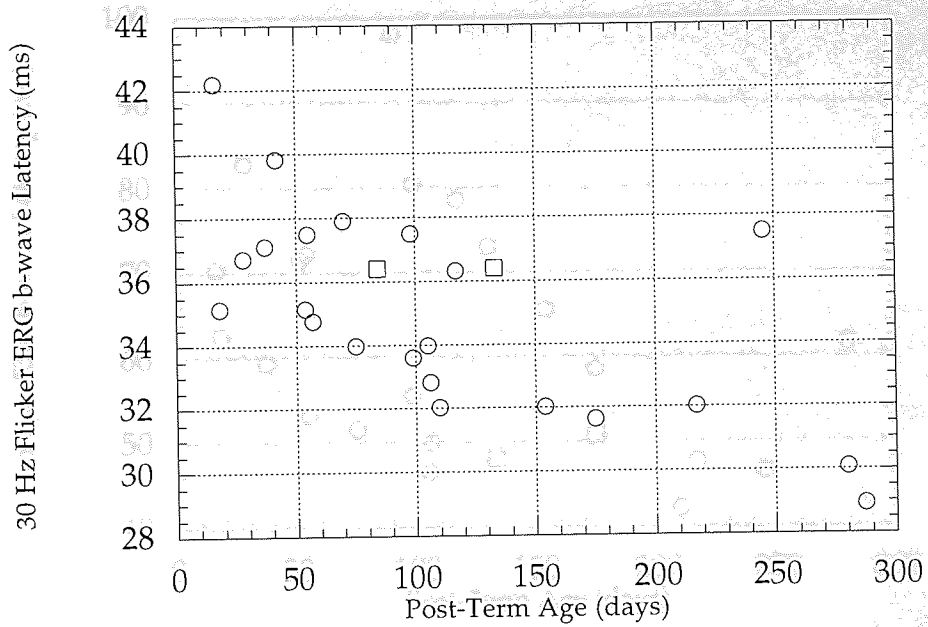


Figure 8.12. 30 Hz flicker ERG b-wave latency is shown with respect to post-term age for the group of healthy control infants (open circles) and for infant RH (open squares) at 19 and 25 weeks of age.

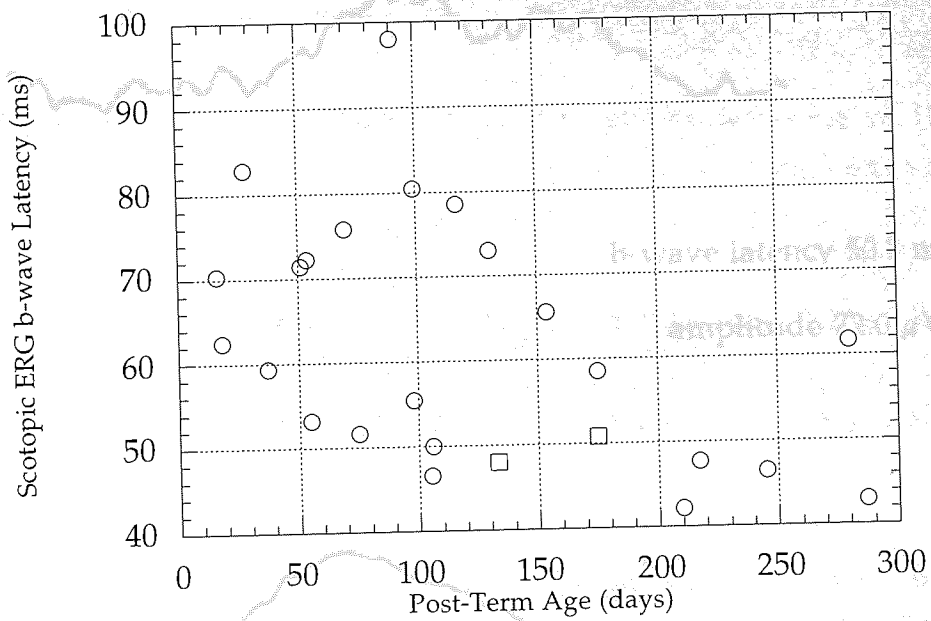


Figure 8.14

The scotopic ERG recorded from infant RH at 25 weeks post term age. The upper trace is the ERG recorded through a natural (undilated) pupil and the lower trace is the ERG recorded through a pupil dilated using 1% cyclopentolate. These different conditions are noted in the figure caption.

Figure 8.13

Scotopic ERG b-wave latencies are shown with respect to post-term age for the group of healthy control infants (open circles) and for infant RH at 19 and 25 weeks of age.

Hz flicker ERGs were present in all eyes of both eyes of all infants at all ages tested. Figure 8.13 shows latencies of the post-positive component of the evoked response to flash stimulation recorded from infants with liver disorders and from healthy control infants for comparison. The rate of maturation of the evoked response in terms of latency was compared in the two groups by analysis of variance. No significant difference in maturation rate was found between these two groups ($p > 0.1$). Latencies from both groups are approaching the adult level of about 20 ms by 6 months of age.

For the same infant groups, figure 8.14 shows latencies of the positive component of the evoked response to achromatic pattern-reversal stimulation. Again, by analysis of variance no significant difference was found between the two groups ($p > 0.1$) and responses from both groups are approaching adult latency levels of 300 ms by 6 months of age.

Mean \pm SD Hz and scotopic ERG b-wave latencies are shown with respect to age for the same two infant groups in figures 8.17 to 8.19. The rate of maturation of each type of ERG in terms of both b-wave and a-wave latency was similar in both groups ($p > 0.1$). Only one infant with liver disease demonstrated significantly delayed a-wave latency ($p < 0.05$). The photopic ERG amplitude in this infant was not significantly related ($p > 0.1$) and a- and b-wave amplitudes of the ERG to X-ray flicker stimulation were normal. In addition, one infant with liver disease demonstrated increased scotopic b-wave but not a-wave latency by comparison with control infants ($p < 0.05$).

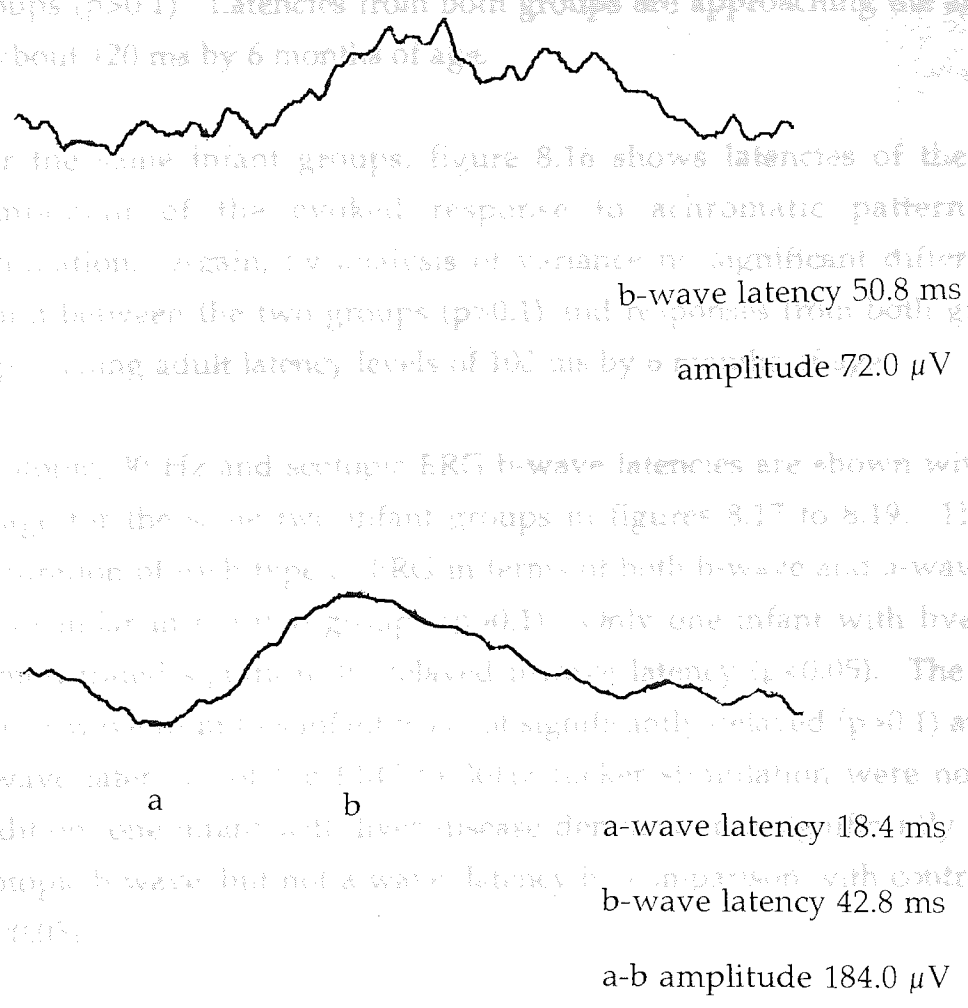


Figure 8.14. The scotopic ERG recorded from infant RH at 25 weeks post-term age. The upper trace is the ERG recorded through a natural (undilated) pupil and the lower trace is the ERG recorded through a pupil dilated using 1 % cyclopentolate hcl. These different conditions are reflected in the response amplitude differences.

8.7 Infants with Liver Disease

Flash and achromatic pattern-reversal VEPs and scotopic, photopic and 30 Hz flicker ERGs were present in all of the group of infants with liver disease at all ages tested. Figure 8.15 shows latencies of the peak positive component of the evoked response to flash stimulation, recorded from infants with liver disorders and from healthy control infants for comparison. The rate of maturation of the evoked response in terms of latency was compared in the two groups by analysis of variance. No significant difference in maturation rate was found between these two groups ($p>0.1$). Latencies from both groups are approaching the adult level of about 120 ms by 6 months of age.

For the same infant groups, figure 8.16 shows latencies of the positive component of the evoked response to achromatic pattern-reversal stimulation. Again, by analysis of variance no significant difference was found between the two groups ($p>0.1$) and responses from both groups are approaching adult latency levels of 100 ms by 6 months of age.

Photopic, 30 Hz and scotopic ERG b-wave latencies are shown with respect to age for the same two infant groups in figures 8.17 to 8.19. The rate of maturation of each type of ERG in terms of both b-wave and a-wave latency was similar in the two groups ($p>0.1$). Only one infant with liver disease demonstrated significantly delayed b-wave latency ($p<0.05$). The photopic ERG a-wave from this infant was not significantly delayed ($p>0.1$) and a- and b-wave latencies of the ERG to 30Hz flicker stimulation were normal. In addition, one infant with liver disease demonstrated significantly increased scotopic b-wave, but not a-wave, latency by comparison with control infants ($p<0.05$).

Figure 8.15

Latencies of b-wave component of the evoked response to brief white flash stimulation are shown with respect to age for infants with liver disease (open squares, mean 137.1 ms, standard deviation 15.1 ms) and healthy control infants (open circles, mean 136.6 ms, standard deviation 12.4 ms).

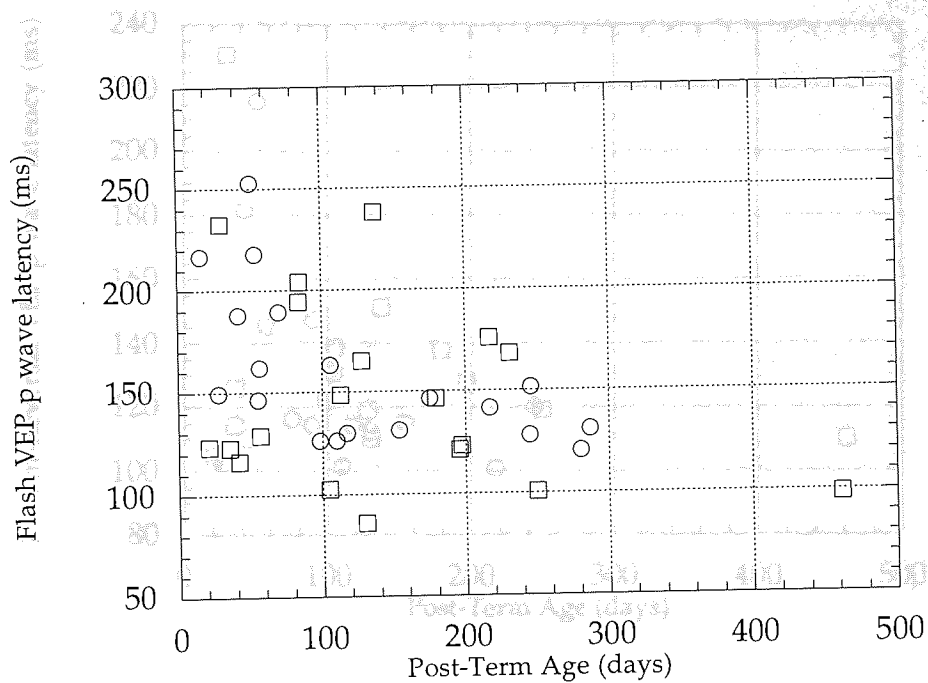


Figure 8.15
 Latencies of P-wave components of the evoked response to binocular white flash stimulation are shown with respect to age for infants with liver disease (open squares; mean 147.2 ms, standard deviation 45.1 ms) and healthy control infants (open circles; mean 158.8 ms, standard deviation 37.4 ms).

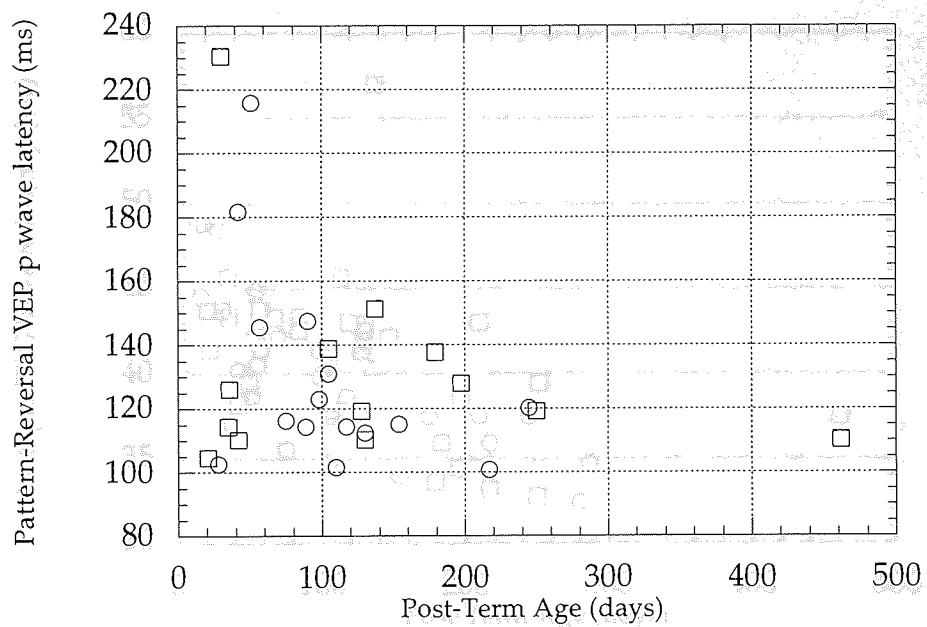


Figure 8.16
 p-wave latencies of the visual evoked response to binocular achromatic pattern-reversal stimulation are shown with respect to age for the group of infants with liver disease (open squares; mean 130 ms, standard deviation 32.9 ms) and the group of healthy control infants (open circles; mean 129.4 ms, standard deviation 32.0 ms).

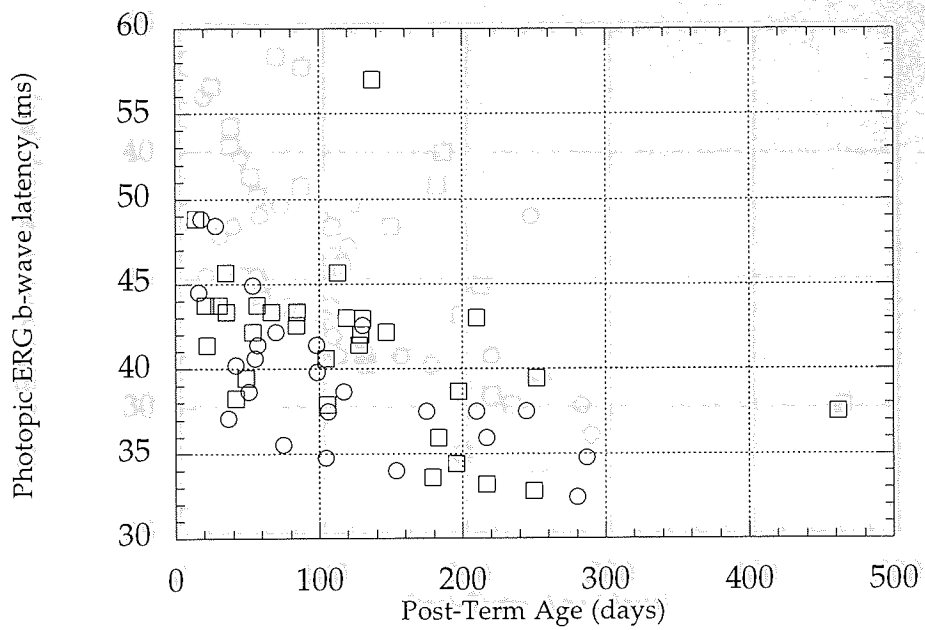


Figure 8.17
 Photopic ERG b-wave latencies are shown with respect to age for infants with liver disease (open squares; mean 41.3, standard deviation 4.9 ms) and a group of healthy control infants (open circles; mean 39.5, standard deviation 4.3 ms).

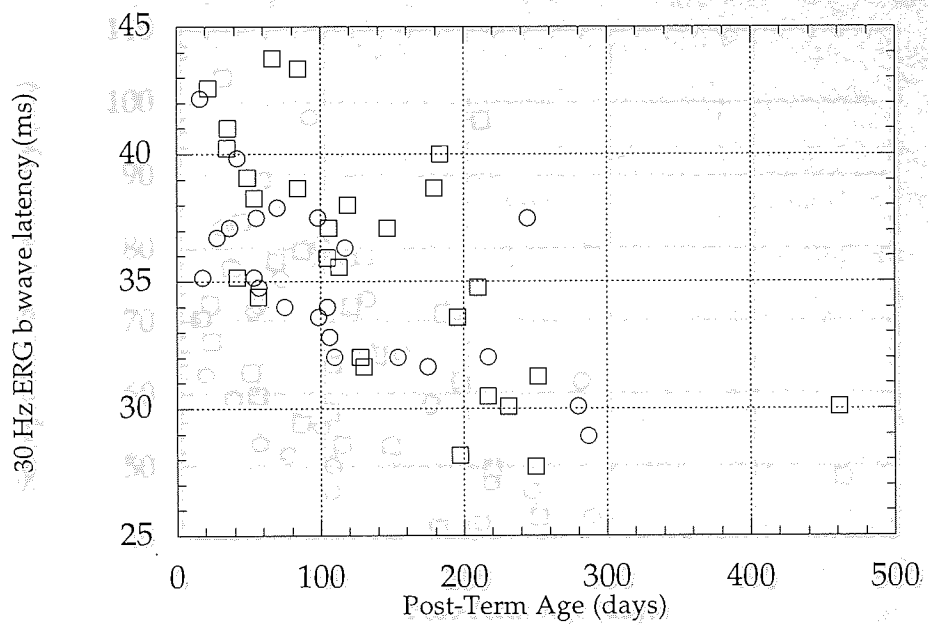


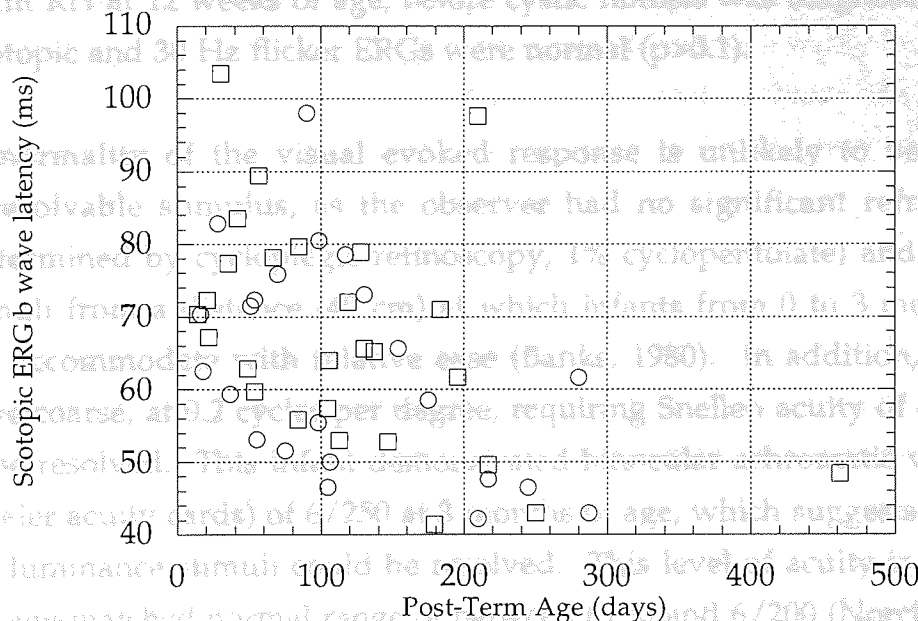
Figure 8.18
 30 Hz flicker ERG b-wave latencies are shown with respect to age for infants with liver disease (open squares; mean 35.9 ms, standard deviation 4.6 ms) and a group of healthy control infants (open circles; mean 34.9 ms, standard deviation 3.2 ms).

All of the nine healthy infants demonstrated normal responses to luminance-modulated stimulation at the earliest age tested, namely 4 weeks post-term. Visual evoked responses to luminance-modulated stimuli recorded from infant RH before and after treatment of cystic fibrosis were absent before 6 weeks post-term and were of significantly longer latency ($p < 0.05$) than those recorded from healthy age-matched infants after 8 weeks post-term. In addition, the scotopic ERG was absent in infant RH at 12 weeks of age, before cystic fibrosis was diagnosed, while the photopic and 30 Hz flicker ERGs were normal ($p > 0.1$).

Abnormalities of the visual evoked response is unlikely to be due to an unresolvable stimulus, as the observer had no significant refractive error (determined by cycloplegic retinoscopy, 1% cycloplegiate) and viewed the stimuli through a viewing aperture (1 cm), which infants from 0 to 3 months of age can accommodate with relative ease (Banks, 1980). In addition, the stimuli were coarse, at 0.3 cycles per degree, requiring Snellen acuity of only 6/1000 to be resolved. This acuity is similar to the minimum detectable visual acuity (Keeler acuity cards) of 6/250 at 4 months of age, which suggests that at least the luminance stimuli could be resolved. This level of acuity is just outside the age-matched normal range of between 6/60 and 6/200 (Norma and Fryck, 1985).

As described earlier (see Chapter 3) one of the advantages of the visual evoked response in the assessment of infant visual function is its objective nature. Responses are recorded only when the infant appears to be attentive to the stimulus, and the technique does not rely on behavioural responses. It is possible, however, that while the infant appears to be viewing the stimulus, it may be in poor focus due to lack of attention or interest. For example, the infant may actually be focused on a point in front of or behind the stimulus. This was controlled for in the present study by watching the infant's eyes to check for over-convergence or divergence during recording.

Figure 8.19
Scotopic ERG b-wave latencies are shown with respect to age for the infants with liver disease (open squares; 67.5 ms, standard deviation 15.5 ms) and healthy control infants (open circles; mean 62.9 ms, standard deviation 14.7 ms).



Discussion

8.8 Cystic Fibrosis

All of the nine healthy infants tested longitudinally demonstrated clear responses to luminance-modulated stimulation at the earliest age tested, namely 4 weeks post-term. Visual evoked responses to luminance-modulated stimuli recorded from infant RH before and after treatment of cystic fibrosis were absent before 6 weeks post-term and were of significantly longer latency ($p < 0.05$) than those recorded from healthy age-matched infants after 8 weeks post-term. In addition, the scotopic ERG was absent in infant RH at 12 weeks of age, before cystic fibrosis was diagnosed, while his photopic and 30 Hz flicker ERGs were normal ($p > 0.1$).

Abnormality of the visual evoked response is unlikely to be due to an unresolvable stimulus, as the observer had no significant refractive error (determined by cycloplegic retinoscopy, 1% cyclopentolate) and viewed the stimuli from a distance (40 cm) at which infants from 0 to 3 months of age can accommodate with relative ease (Banks, 1980). In addition, the stimuli were coarse, at 0.2 cycles per degree, requiring Snellen acuity of only 6/1000 to be resolved. This infant demonstrated binocular achromatic visual acuity (Keeler acuity cards) of 6/250 at 3 months of age, which suggests that at least the luminance stimuli could be resolved. This level of acuity is just outside the age-matched normal range of between 6/50 and 6/200 (Norcia and Tyler, 1985).

As described earlier (see Chapter 3) one of the advantages of the visual evoked response in the assessment of infant visual function is its objective nature. Responses are recorded only when the infant appears to be attentive to the stimulus, and the technique does not rely on behavioural responses. It is possible, however, that while the infant appears to be viewing the stimulus, it may be in poor focus due to lack of attention or interest. For example, the infant may actually be focused on a point in front of or behind the stimulus. This was controlled-for in the present study by watching the infant's eyes to check for over-convergence or divergence during recording. In addition, infant RH demonstrated abnormal evoked responses consistently to all stimuli at all test sessions. It is unlikely, therefore, that

abnormal responses reflect a temporary lack of attention.

The cause of VEP abnormalities in this infant is likely, then, to be of neural rather than optical origin, and may lie in the retina, the retino-striate visual pathway or the striate cortex (Wright et al, 1987). The visual evoked response recorded from the scalp over the striate cortex originates largely from the macula, heavily populated by foveal cones (Drasdo, 1977). As cone function was shown by the photopic and 30 Hz flicker ERGs to be unaffected in infant RH, abnormality of the retina is unlikely to have had a significant effect in reducing the cortical visual evoked response. In conjunction with the fact that in the healthy infant the cerebral cortex is richly supplied with DHA, this suggests that the post-receptor visual pathway may have been adversely affected in this infant as a result of malabsorption of fatty acids, reflected in his visual evoked responses to both luminance and chromatic stimuli.

The absence of any clear response component in the scotopic ERG of infant RH prior to treatment indicates that rod function was abnormal at this stage (Kriss, 1994). As described earlier, rod function may be adversely affected by low DHA concentrations or by low vitamin A levels, or a combination of these factors, both of which are characteristic of cystic fibrosis.

The restoration of scotopic ERGs recorded from infant RH at the age of 19 weeks post-term after 6 weeks of treatment suggests that dietary supplements during treatment provided substances necessary for the normal function of rod photoreceptors. Dietary supplements consisted of vitamins A, B1, B2, C, D, E and K. The essentiality of vitamin A in particular for normal dark adaptation suggests that supplements of this vitamin were at least partly responsible for the change in scotopic ERG after treatment.

Infants fed DHA-deficient diets have been found, post-mortem, to have low cortical DHA levels but normal retinal levels of DHA (Makrides et al, 1994), suggesting that retinal DHA may be maintained even when deficient in the diet. In the present study, infant RH demonstrated abnormal VEPs before

and during treatment, while ERGs were abnormal before treatment but normal afterwards. This indicates that the cortical requirement for DHA was not fulfilled by treatment, and that vitamin A deficiency prior to treatment may have been responsible for the absent scotopic ERG.

8.9 Infants with Liver Disease

As described previously, this group of infants had significantly reduced blood erythrocyte levels of DHA. As part of their treatment, they received vitamin supplements, but were not supplemented with fatty acids. In general, ERG and VEP latencies were not significantly different between these infants and healthy infants. The group of healthy infants did not have blood tests, so normal fatty acid and vitamin levels are assumed in these infants.

VEP and ERG abnormalities were not generally encountered in the group of infants with liver disease and fatty acid deficiency, although one infant showed significantly delayed scotopic ERG b-wave latency and another infant demonstrated significantly delayed photopic ERG b-wave latency (see results).

The present study has demonstrated abnormal visual evoked responses and scotopic electroretinograms in one young infant (RH) with cystic fibrosis before and after diagnosis and treatment, encountered coincidentally among a group of healthy infants. These abnormalities may be due to insufficient levels of essential fatty acids, vitamin A, or a combination of these with other factors. A group of infants with liver disorders showed no VEP abnormality, and in general no ERG abnormality. These infants were being treated for their condition, but were not given fatty acid supplements.

The fact that VEPs were abnormal in infant RH and not in the group being treated at the Children's Hospital may be due to general treatment administered to this latter group, allowing factors affecting visual function to fall above threshold levels for normal function, without the direct supplementation of fatty acids. The complete lack of any treatment in infant RH may have allowed these factors to fall below threshold, which

may vary between individuals, so that visual function became adversely affected, as reflected in his ERGs and VEPs. VEP abnormalities continued in this infant during treatment, at least for 12 weeks after the onset of treatment, which suggests that treatment may have been inadequate to restore normal visual function, or that the visual system takes longer than this period to return to normality.

During a sensitive period of development of the visual system, it is important that visual input is of good quality in order to prevent amblyopia. The most common forms of amblyopia are unilateral, in which visual input is degraded in one eye only, and so only one eye becomes amblyopic (Banks et al, 1975; Assaf, 1982; Mayer, 1989; Mitchell, 1990; Smith et al, 1991). Amblyopia can also occur bilaterally, however, in which case both eyes are affected by visual degradation (Stidwill, 1990). VEP abnormalities in infant RH suggest that it is important to monitor vision during the treatment of infants and young children with cystic fibrosis and other conditions in which vitamin and fatty acid deficiencies are encountered, in order to ensure that dietary supplementation is adequate for the prevention of abnormal visual function.

To determine optimum dietary treatment of infants with vitamin and fatty acid deficiency, this work should be followed by an investigation of the effects of dietary supplements on visual function in a group of such infants. In addition to visual acuity testing, visual electrophysiology may prove very useful in the assessment of vision and of the integrity of the visual pathway (Arden and Kolb, 1964) from retina to striate cortex in these patients.

CHAPTER 9

A LONGITUDINAL STUDY OF VISUAL EVOKED RESPONSES TO CHROMATIC STIMULI IN HUMAN INFANTS

9.1 Introduction

In general, infants less than two months of age demonstrate poor visual acuity (Norcia and Tyler, 1985; Brown et al, 1987), contrast sensitivity (Banks and Salapatek, 1978; Movshon and Kiorpes, 1988), motion sensitivity (Zanker and Mohn, 1993; Wattam-Bell, 1994, 1996) and colour vision (Varner et al, 1985; Allen et al, 1993; Morrone et al, 1990; 1993; Rudduck and Harding, 1994). There is no general agreement on why infants see poorly, although immaturity of foveal cones and of post-receptoral processes have been implicated (Youdelis and Hendrickson, 1986; Banks and Bennett, 1988).

In order to test the various hypotheses about infant vision (see Chapter 3) and to determine appropriate visual stimulation for infants, the development of human colour vision has been widely investigated, using both psychophysical and electrophysiological methods. However, there is disagreement on the age at which infants are able to discriminate colours in the Rayleigh region of the spectrum, without luminance cues. Some studies suggest that red-green discriminations are not possible until at least 8 weeks of age (Morrone et al, 1990; Rudduck and Harding, 1994) and that luminance- and chromatic-sensitive mechanisms develop at different rates (Morrone et al, 1993), while others find that such discriminations are possible at 2 weeks of age (Allen et al, 1993) and that the developmental rates of the two mechanisms are similar (Allen et al, 1993; Brown et al, 1995). Although widely debated in the literature, this discrepancy has not been satisfactorily explained. It is likely that it is partly explained by inter-individual variations, inaccuracies in estimating the term date of pregnancy and the use of inappropriate stimuli (see discussion).

The ability of infants to discriminate tritan stimuli (those stimulating long- and medium-wavelength-sensitive cones equally and therefore modulating only short-wavelength-sensitive cones) has been less thoroughly investigated. Early studies disagree on whether infants have functional

short-wavelength-sensitive cones and post-receptoral processing by two months of age (Pulos et al, 1980; Varner et al, 1985). Infants from two to three months of age have been found to show elevated photopic spectral sensitivity to short wavelengths compared with adults, while their sensitivity to medium and long wavelengths is similar to that of adults (Dobson, 1976; Moskowitz-Cook, 1979). More recent work, however, demonstrates similar sensitivity curves across the spectrum in infants and adults (Volbrecht and Werner, 1987). Such variations may reflect ocular media density differences between infants and adults (Werner, 1982).

The purpose of the present study was to investigate the development of the S-cone opponent pathway by recording transient visual evoked responses to tritan stimuli at and around the adult isoluminant match, in infants on a longitudinal basis from 4 weeks to a maximum of 6 months post-term age. For comparison, evoked responses to red-green and luminance-modulated stimuli were also recorded.

Methods

9.2 Subjects and Schedule

Nine subjects (6 male and 3 female) were investigated over a period from 4 weeks post-term to the age at which visual evoked potentials significantly above noise levels were recorded in response to all colour ratios for both types of colour stimuli and to luminance-modulated stimuli. Age for all infants is calculated from term date of pregnancy (40 weeks post-menstrual age) and is stated to the nearest week and in days, to allow maximum accuracy of developmental age specification. Tests were carried out on a weekly basis until evoked potentials were recorded to luminance-modulated stimuli and to tritan stimuli at all colour ratios, including photometric isoluminance, in order to observe the age of onset of a functional S-cone pathway in each infant. Tests were then carried out at intervals of one week (infants MB, JC1, AE, BH and PR), ten days (OG) and two weeks (DC, DH and JC2) until the onset of evoked potentials to both types of chromatic stimuli. Visual evoked responses to photometrically isoluminant tritan stimuli at a range of chromatic contrasts were also recorded in one of these infants (PR) at seven weeks post-term age.

Thereafter, visual evoked responses to luminance-modulated stimuli and to both types of chromatic stimuli at photometric isoluminance were recorded from five of these infants (MB, PR, DC, JC2 and DH) at intervals of two to three weeks, up to 3 months post-term age. Responses were also recorded at 4, 5 and 6 months of age, from two of these infants (DH and MB). In addition, responses to these stimuli were recorded from two female infants not included in the main study (AM and KB) at 3, 4 and 5 months of age.

9.3 Stimuli and Recording Parameters

See Chapter 5 for a full description of both types of chromatic stimuli and the luminance stimulus, calibration, spatial and temporal parameters, procedure and data analysis. Up to the age of onset of visual evoked potentials to luminance and both types of chromatic stimuli, responses were recorded to the non-stimulus condition and to stimuli at the following range of colour ratios: 0.4, 0.45, 0.5, 0.55, 0.6, 1.0. After the age of onset of evoked potentials to all stimuli, the stimulus range was reduced to tritan and red-green at photometric isoluminance, luminance-modulated stimuli and the non-stimulus condition.

Results

9.4 Responses to Luminance Stimuli

Visual evoked responses to luminance-modulated pattern-onset stimuli of spatial frequency 0.2 cpd were elicited from all nine infants at the earliest age tested, namely 4 weeks post-term. The luminance response at this age was a positivity of large amplitude peaking at a latency near 240 ms. A typical response to luminance stimulation at the age of 4 weeks is shown for one infant (MB) in Figure 9.1. Figures 9.2 and 9.3 show, for the five infants tested from 4 weeks to 3 months, the latency and amplitude of this positive component, plotted as a function of age. The latency showed a significant negative correlation with age ($r=0.74$; $p<0.001$) from about 240 ms at 4 weeks to 120 ms at 3 months, whereas the amplitude of the response changed little over this time ($r=0.36$; $P>0.05$).

By 3 months of age, the latency of the luminance response was approaching the adult-like value of approximately 120 ms (see Chapter 6). A non-linear (second-order polynomial) function provided a significantly better fit to the latency data than a linear function (p value from F ratio <0.05), while a non-linear function was not a significantly better fit to the amplitude data than a linear fit (p value from F ratio >0.05).

0 100 200 300 400 500
Latency (ms)

Figure 9.1

The visual evoked response from infant MB at 4 days (15 weeks) post-term age to luminance-modulated stimulation is shown (upper trace). The consists of a large positive component of latency approximately 240 ms after pattern onset. The non-stimulus response is also shown for comparison.

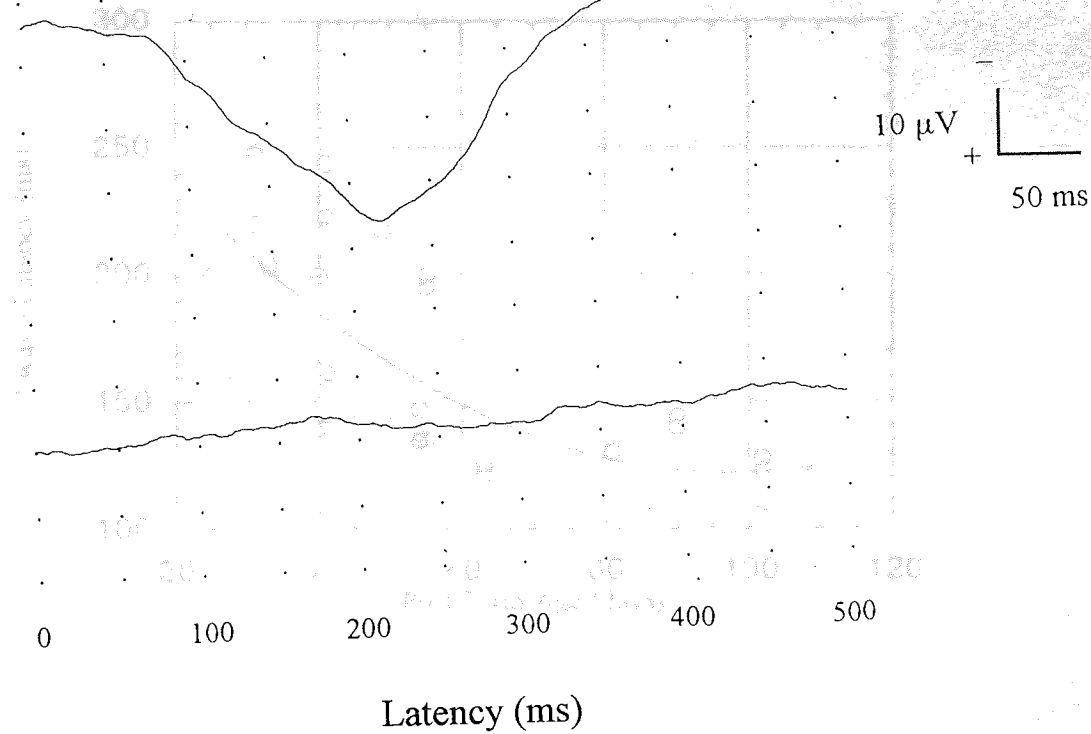


Figure 9.1. The visual evoked response from infant MB at 33 days (5 weeks) post-term age, to luminance-modulated stimulation is shown (upper trace). This consists of a large positive component of latency approximately 240 ms after pattern onset. The non-stimulus response is also shown for comparison.

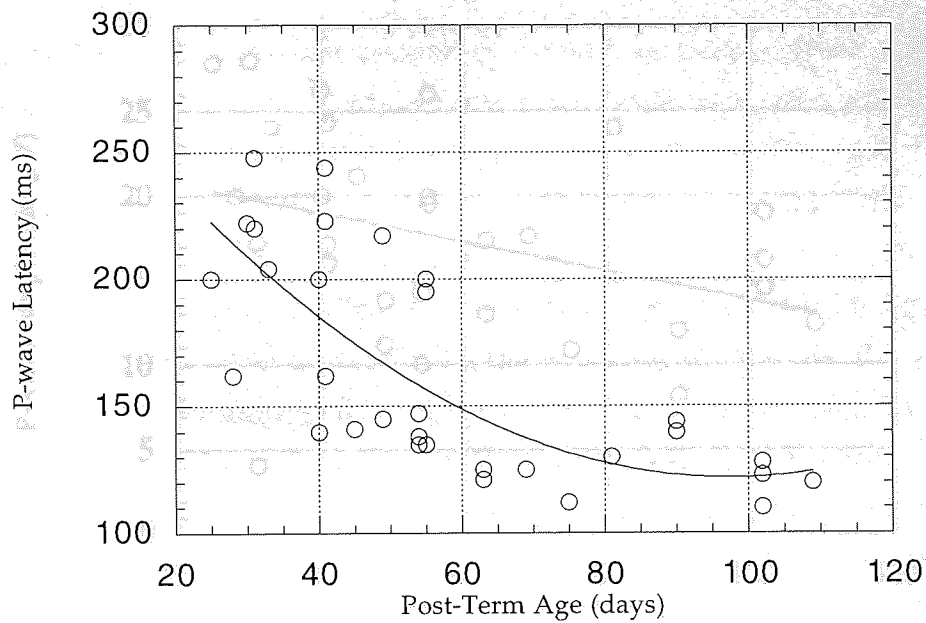


Figure 9.2

The latency of the positive peak response to luminance-modulated stimulation is shown with respect to post-term age in days for all of the five infants tested from 4 weeks to 3 months post-term age (MB, DH, DC, JC, PR). The regression function is the fit of a second-order polynomial ($r=0.74$) which provided a significantly better fit to the full data set than a linear function (P value from F ratio < 0.05), although the correlation is linear up to 80 days post-term age.

red-green) stimuli of 0.2 cpd spatial frequency at 2 weeks of age (see figures 9.4 and 9.5 showing traces with no response at isoluminance). For colour ratios on either side of photometric isoluminance, a positive potential was apparent, peaking near 130 to 150 ms. The absence or diminution of this positivity P₁₃₀ can be used to signal the presumed isoluminance point in an individual infant (see Chapter 7).

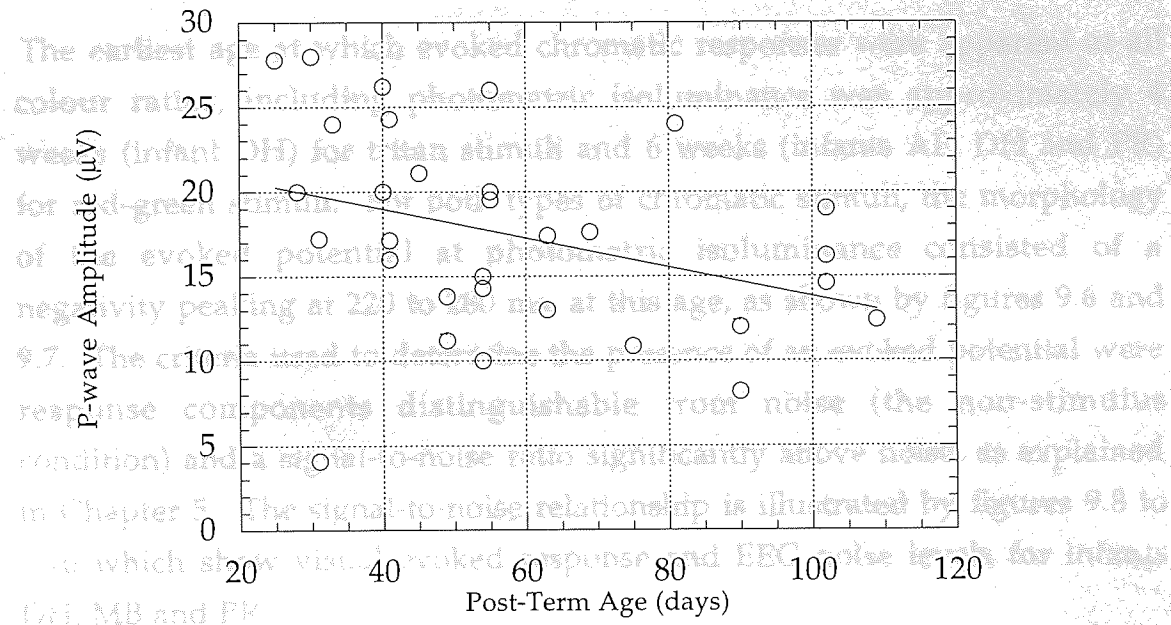


Figure 9.3. The amplitude of the positive peak response to luminance-modulated stimulation is shown with respect to post-term age in days for all of the five infants tested from 4 weeks to 3 months post-term age (MB, DH, DC, JC2, PR). The linear regression function ($r=0.36$) provided the best fit to the data in this case (p value from F ratio > 0.05).

9.5 Responses to Chromatic Stimuli

In eight of the nine infants, no evoked potential was apparent above the baseline noise level, to photometrically isoluminant chromatic (tritan or red-green) stimuli of 0.2 cpd spatial frequency at 4 weeks of age (see figures 9.4 and 9.5, showing traces with no response at isoluminance). For colour ratios either side of photometric isoluminance, a positive potential was apparent, peaking near 130 to 150 ms. The absence or diminution of this positivity P_{130} can be used to signal the presumed isoluminant point in an individual infant (see Chapter 7).

The earliest age at which evoked chromatic responses were apparent at all colour ratios, including photometric isoluminance was approximately 4 weeks (infant DH) for tritan stimuli and 6 weeks (infants AE, DH and PR) for red-green stimuli. For both types of chromatic stimuli, the morphology of the evoked potential at photometric isoluminance consisted of a negativity peaking at 220 to 280 ms, at this age, as shown by figures 9.6 and 9.7. The criteria used to determine the presence of an evoked potential were response components distinguishable from noise (the non-stimulus condition) and a signal-to-noise ratio significantly above noise, as explained in Chapter 5. The signal-to-noise relationship is illustrated by figures 9.8 to 9.10 which show visual evoked response and EEG noise levels for infants DH, MB and PR.



Figure 9.4
Visual evoked responses to tritan stimuli at and around the adult isoluminant match, recorded from infant MB at 38 days post-term age. The response at isoluminance is indistinguishable from noise, while traces around isoluminance exhibit a positive component of a latency of around 130 ms.

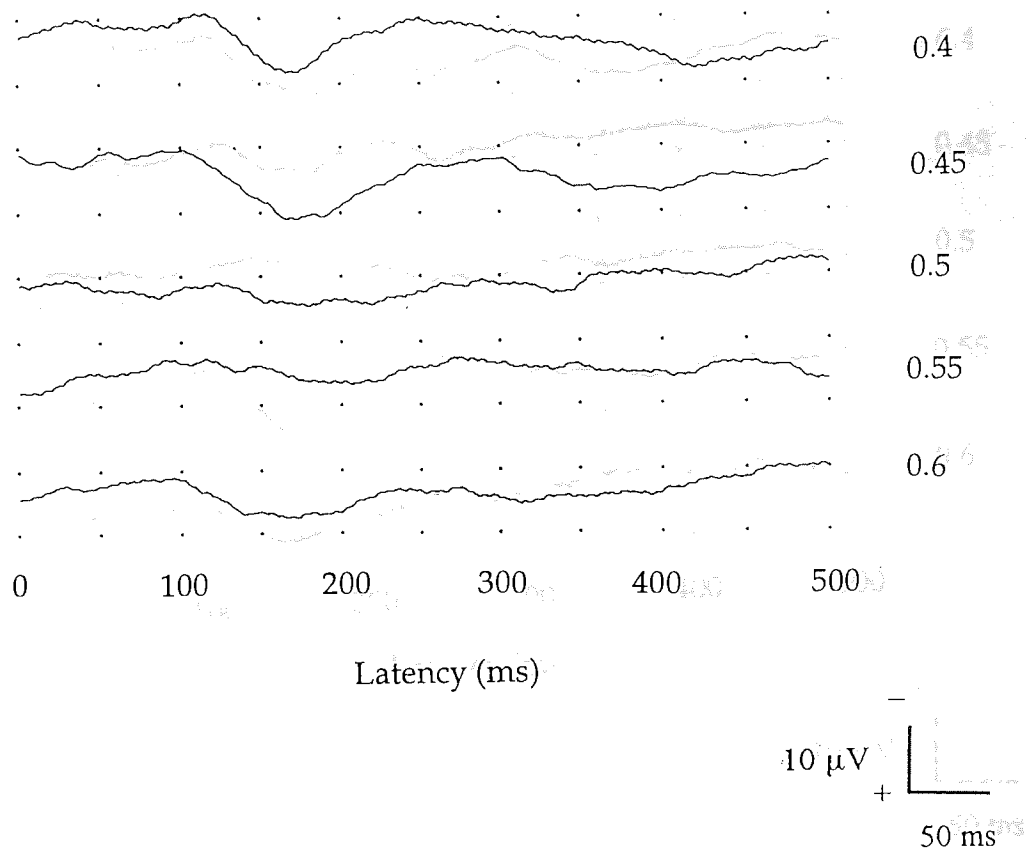


Figure 9.4

Visual evoked responses to tritan stimuli at and around the adult isoluminant match, recorded from infant MB at 28 days post-term age. The response at isoluminance is indistinguishable from noise, while those around isoluminance consist of a positive component at a latency of around 150 ms.

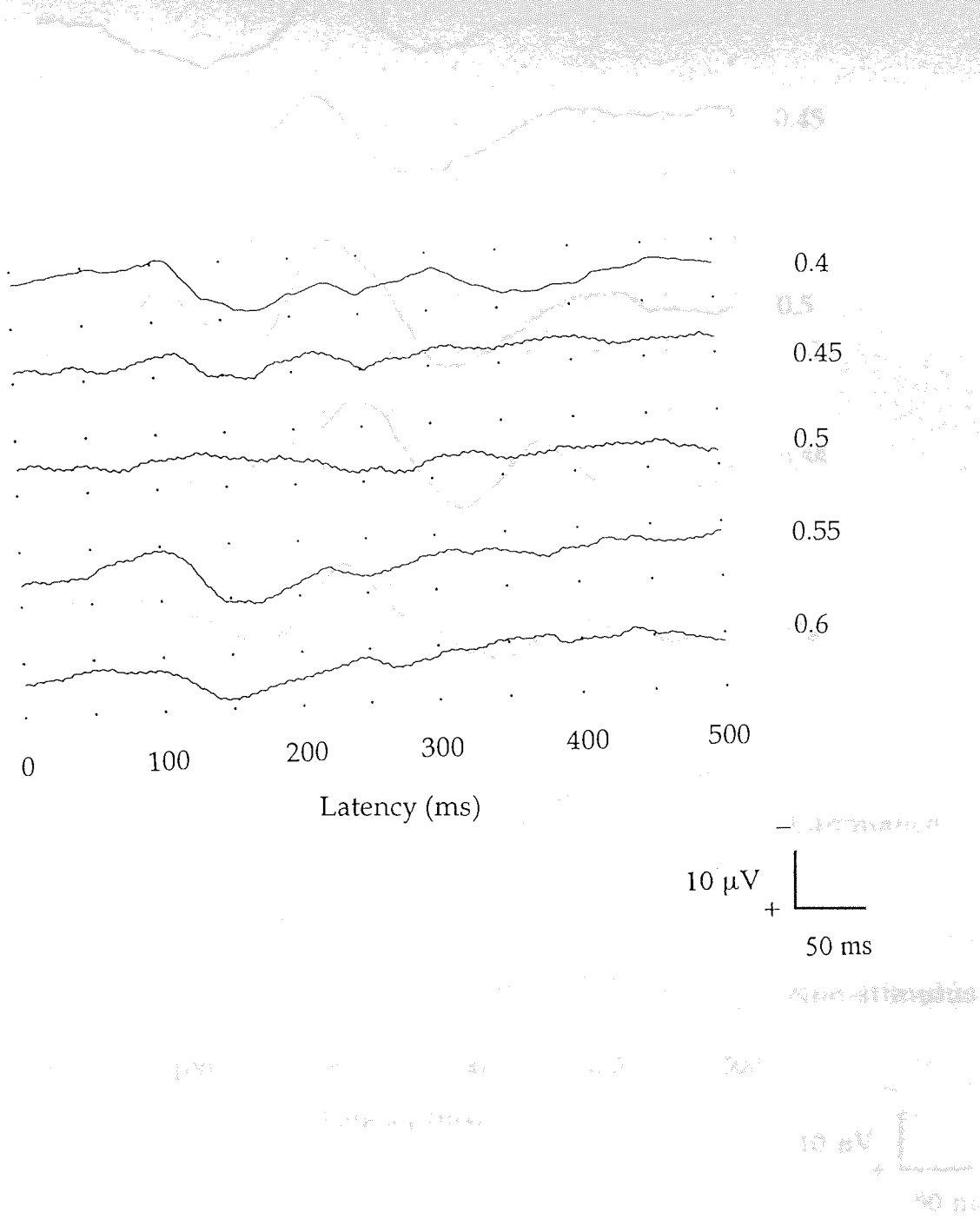


Figure 9.5 Visual evoked responses to red-green stimuli at and around the adult isoluminant match, recorded from infant MB at 28 days post-term age. The response at isoluminance is indistinguishable from noise, while those around isoluminance consist of a positive component at a latency of around 150 ms.

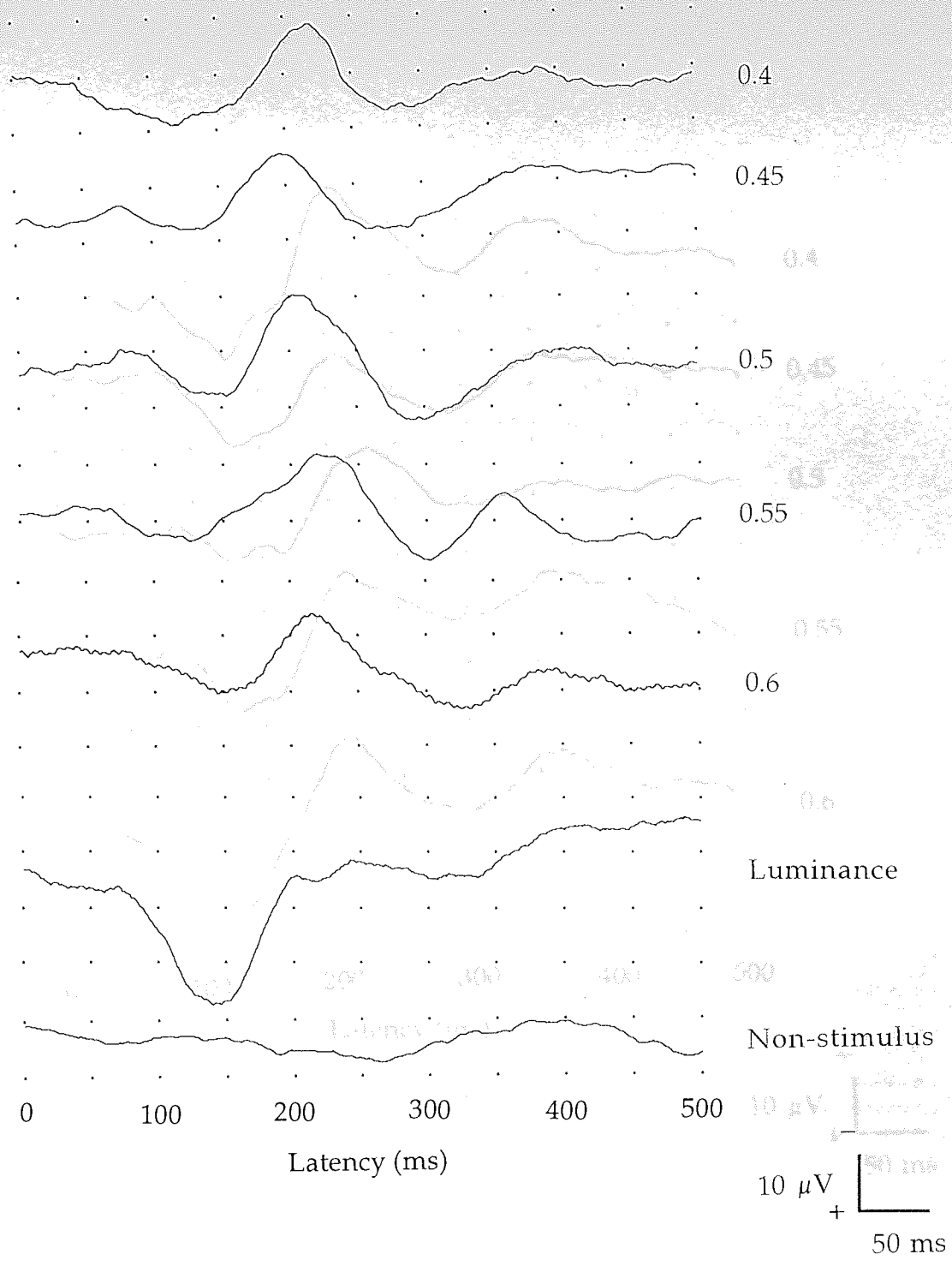
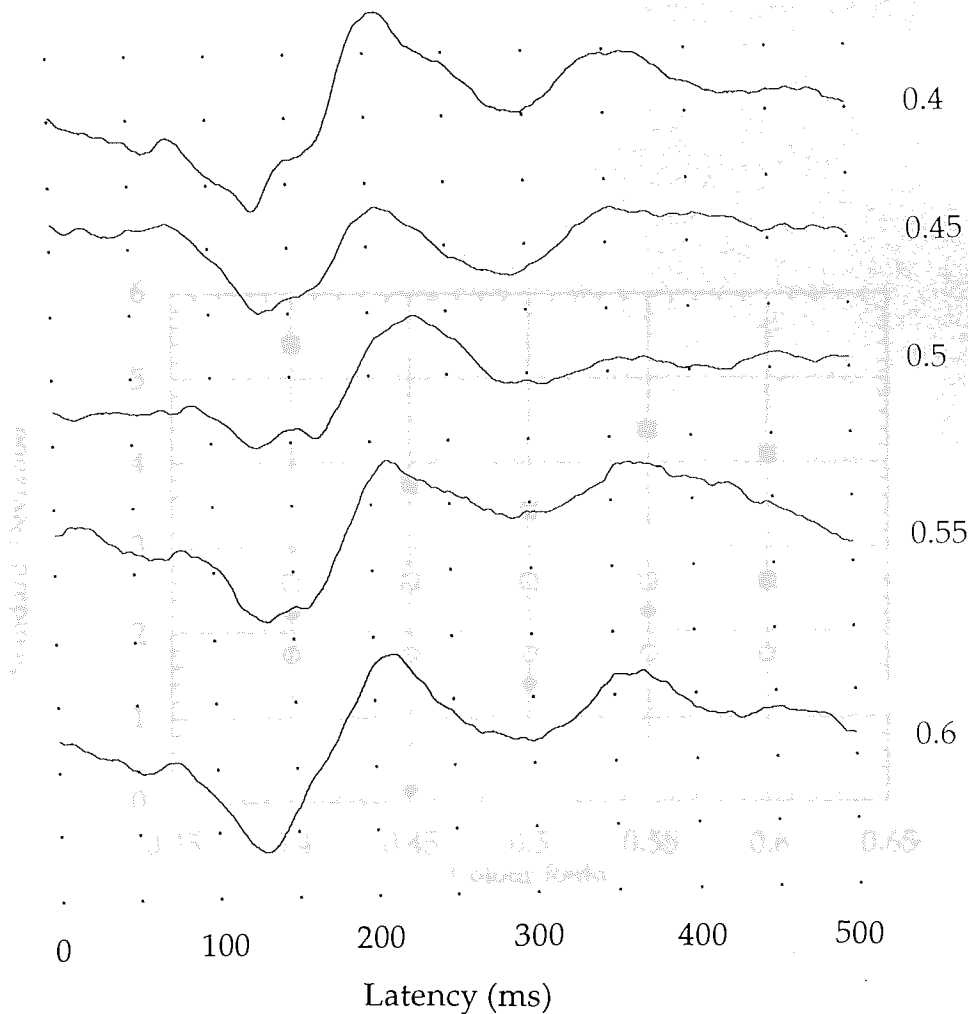


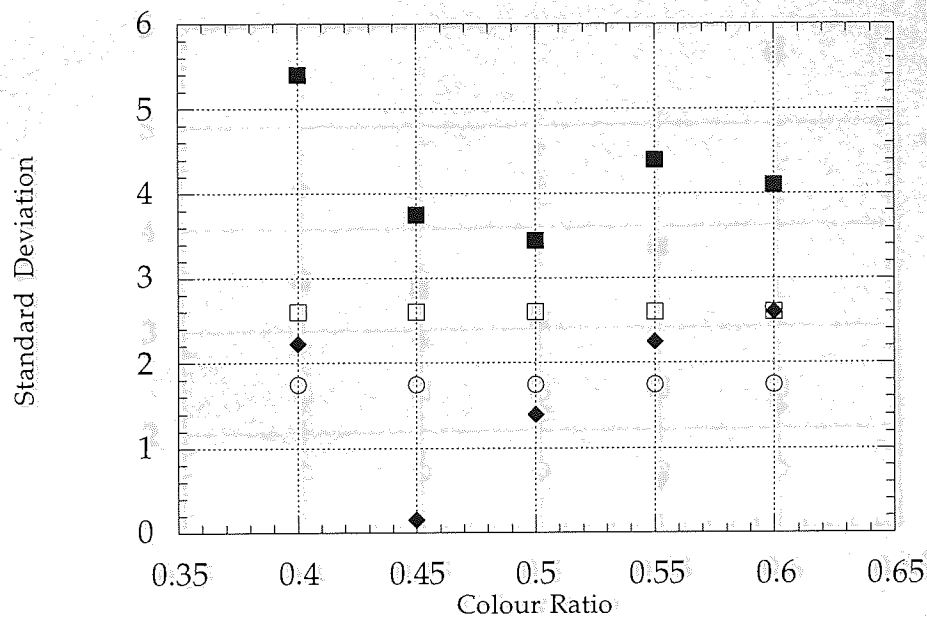
Figure 9.6
 Visual evoked responses recorded from infant PR at 45 days post-term age, in response to tritan stimuli at and around the adult isoluminant match (top five traces), to a luminance-modulated stimulus and the non-stimulus condition (lower two traces). All responses are significantly above noise levels (see also figure 9.10); chromatic responses consist of a negative component of latency 250 to 280 ms; some chromatic responses also demonstrate a positivity of latency around 150 ms. The peak response to luminance stimulation consists of a positive-going wave at 150 ms after stimulus onset (time zero).



Standard deviation (s.d.) values are shown by open circles from a baseline of the evoked response at each of 1000 points at 10 ms intervals over the response trace. In a 10 µV 50 ms scale assessment of evoked responses, standard deviation values were used to determine the presence or absence of responses significantly above noise levels. In figures 9.8 to 9.10, circles represent the standard deviation of the response in the non-stimulus condition, which is taken to indicate ERT noise levels; open squares represent 1.5 times this value, arbitrarily chosen to indicate a significant point above noise; filled squares represent the standard deviation of each of a set of ten responses recorded around the adult isoluminant match, and filled diamonds represent this value for the same responses to red-green stimuli.

Figure 9.7

Visual evoked responses recorded from infant PR at 45 days post-term age, in response to red-green stimuli at and around the adult isoluminant match. All responses are significantly above noise levels (see also figure 9.10); chromatic responses consist of a negative component of latency 250 to 280 ms; some chromatic responses also demonstrate a positivity of latency around 150 ms. The peak response to luminance stimulation consists of a positive-going wave at 150 ms after stimulus onset (time zero).



Standard deviation is calculated from the amplitude from baseline of the evoked response at each of 1000 points at 0.5 ms intervals on a 500 ms response trace. In addition to subjective assessment of evoked responses, standard deviation values were used to determine the presence or absence of responses significantly above noise levels. In figures 9.8 to 9.10, open circles represent the standard deviation of the response to the non-stimulus condition, which is taken to indicate EEG noise levels, open squares represent 1.5 times this value, arbitrarily chosen to indicate a significant point above noise, filled squares represent the standard deviation of each of a set of tritan responses at and around the adult isoluminant match, and filled diamonds represent this value for a set of responses to red-green stimuli.

Figure 9.8

Standard deviation values for EEG noise (open circles), 1.5 times this value (open squares) and for responses to tritan (filled squares) and red-green (filled diamonds) stimuli at and around adult isoluminance, recorded from infant DH at 25 days post-term age. In this case, responses to tritan but not red-green stimuli are significantly above EEG noise levels at all colour ratios.

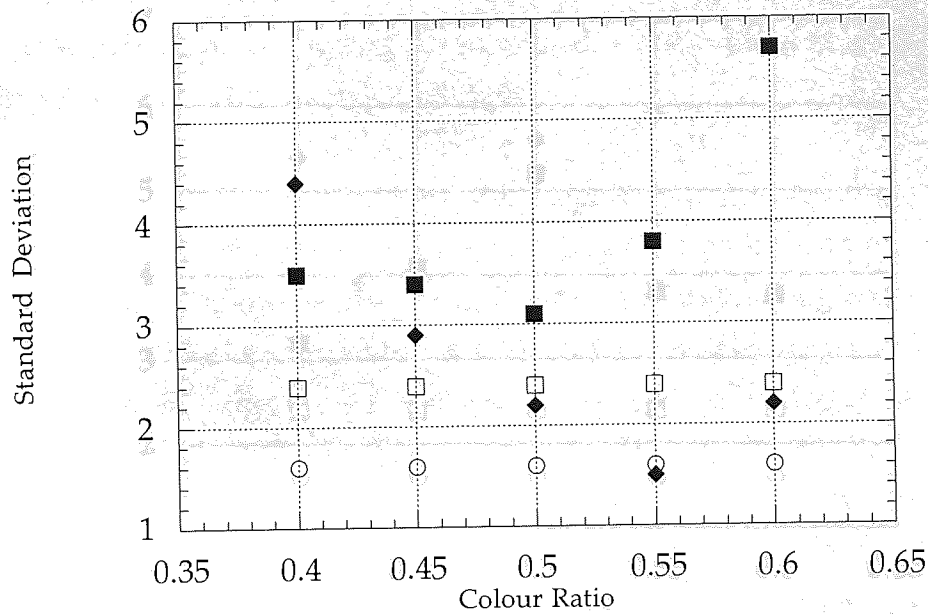


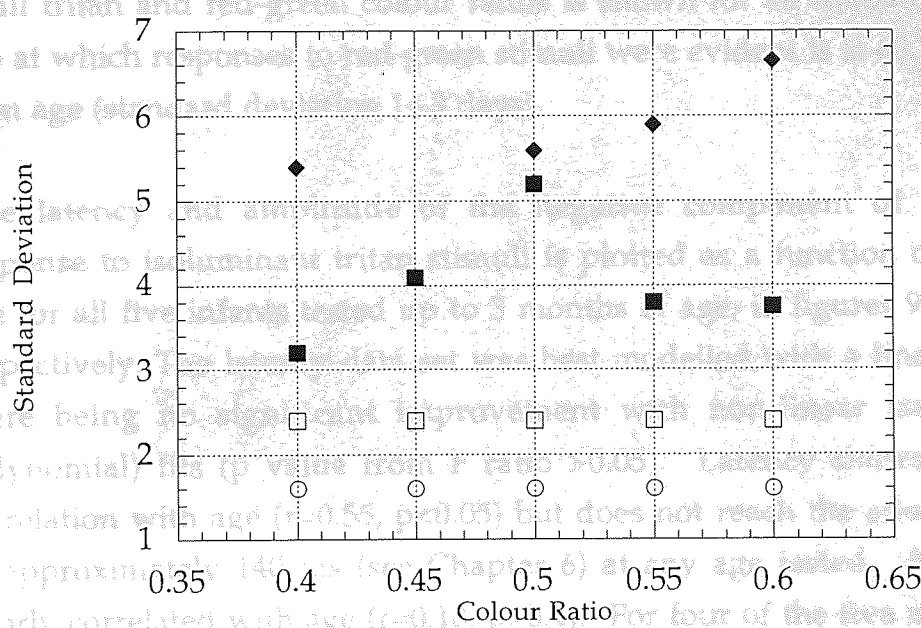
Figure 9.9) Standard deviation values for EEG noise (open circles), 1.5 times this value (open squares) and for responses to tritan (filled squares) and red-green (filled diamonds) stimuli at and around adult isoluminance, recorded from infant MB at 33 days post-term age. In this case, responses to tritan but not red-green stimuli are significantly above EEG noise levels at all colour ratios.

Critter Stimulus Level (Colour Ratio)

stimuli. Of the two remaining infants, All responded to red-green stimuli earlier than tritan stimuli and PR responded to both types of chromatic stimuli at the same age (45 days post-term). The mean age of onset of responses to tritan stimuli in this group of nine infants is 47.9 days post-term age (standard deviation 14.07 days). This is shown more clearly in figure 9.11, where the post-term age at which responses to both types appeared at all tritan and red-green colour ratios is shown for all subjects.

age at which responses to red-green stimuli were evoked at all colour ratios (standard deviation 14.31 days).

The latency and amplitude of the response to each of the tritan response to illuminant tritan stimuli is plotted as a function of post-term age for all five infants aged up to 3 months (figures 9.12 and 9.13 respectively). The best fit to the data was best modelled with a 3rd order polynomial (p value from F test) 70.00. Latency shows a negative correlation with age ($r = -0.55$, $p < 0.05$) but does not reach the adult-like value



approximately 140 ms (see Chapter 6) at any age tested. Amplitude is poorly correlated with age ($r = -0.12$, $p > 0.5$). For four of the five infants aged up to 3 months post-term evoked responses to illuminant tritan stimuli were indistinguishable from noise at this age; only infant PR evoked responses to all tritan stimuli distinguishable from noise significantly above noise levels at this age. This surprising finding is discussed later (see page 242-247 and 254).

Figure 9.10
Standard deviation values for EEG noise (open circles), 1.5 times this value (open squares) and for responses to tritan (filled squares) and red-green (filled diamonds) stimuli at and around adult isoluminance, recorded from infant PR at 45 days post-term age. In this case, responses to both tritan and red-green stimuli are significantly above EEG noise levels at all colour ratios.

With considerable inter-individual variation, seven of the nine infants demonstrated visual evoked potentials significantly above noise levels to tritan stimuli at all colour ratios at an earlier age than those to red-green stimuli. Of the two remaining infants, AE responded to red-green stimuli earlier than tritan stimuli and PR responded to both types of chromatic stimuli at the same age (45 days post-term). The mean age of onset of responses to tritan stimuli in this group of nine infants is 47.9 days post-term age (standard deviation 14.07 days). This is shown more clearly in figure 9.11, where the post-term age at which responses were first apparent at all tritan and red-green colour ratios is shown for all infants. The mean age at which responses to red-green stimuli were evident is 60.1 days post-term age (standard deviation 14.3 days).

The latency and amplitude of the negative component of the evoked response to isoluminant tritan stimuli is plotted as a function of post-term age for all five infants tested up to 3 months of age, in figures 9.12 and 9.13 respectively. The latency data set was best modelled with a linear function, there being no significant improvement with non-linear (second-order polynomial) fits (p value from F ratio >0.05). Latency shows a negative correlation with age ($r=0.55$, $p<0.05$) but does not reach the adult-like value of approximately 140 ms (see Chapter 6) at any age tested. Amplitude is poorly correlated with age ($r=0.18$, $p>0.1$). For four of the five infants tested up to 3 months post-term evoked responses to isoluminant tritan stimuli were indistinguishable from noise at this age; only infant PR demonstrated evoked responses to all tritan stimuli distinguishable from and significantly above noise levels at this age. This surprising finding is discussed later (see page 242-247 and 254).

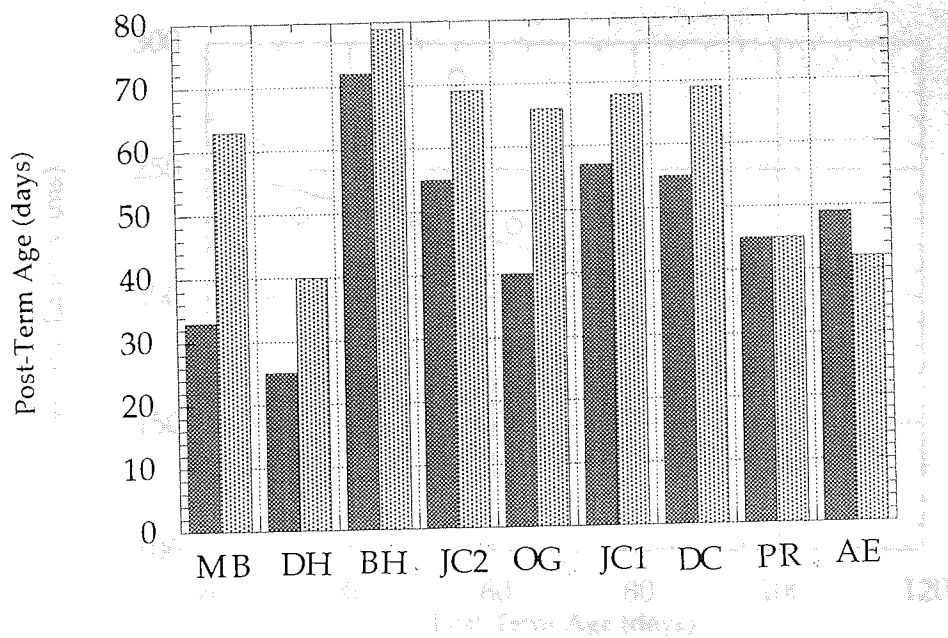


Figure 9.11.

The ordinate shows the post-term age of onset (days) of visual evoked responses significantly above noise levels to tritan (darker bars) and red-green (lighter bars) stimuli for each of the nine infants, indicated by their initials. The mean age of onset to tritan stimulation is 47.9 days post-term (standard deviation 14.07 days). The age at which responses to red-green stimuli were first evident is later in most infants (mean 60.11 days; standard deviation 14.3 days); this difference is statistically significant ($\chi^2 < 0.05$).

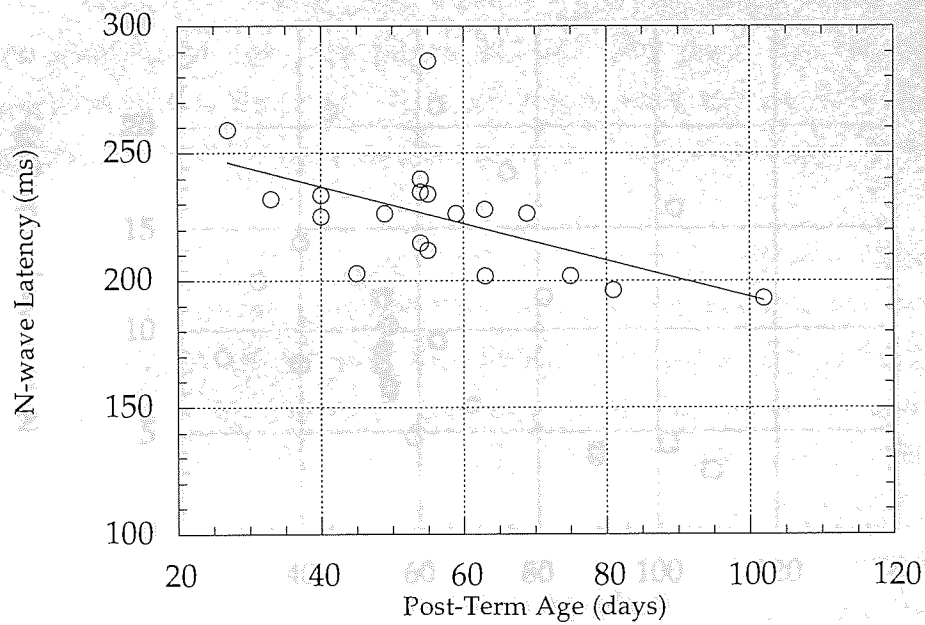


Figure 9.13

Figure 9.12. r_s represent the amplitude of the negative peak response to photometrically isoluminant tritan stimuli is shown with respect to post-term age for all of the five infants tested from 4 weeks to 3 months post-term age (MB, DH, DC, JC2, PR). The linear regression function ($r=0.55$) provided the best fit to the data (p value from F ratio > 0.05).

Post-term age in Figure 9.13. The amplitude of the negative peak response to photometrically isoluminant tritan stimuli is shown with respect to post-term age ($r=0.18$) for all five infants tested from 4 weeks to 3 months post-term age (MB, DH, DC, JC2, PR). Open squares indicate standard deviation of response amplitude for four of these infants in whom no response distinguishable from noise could be elicited to this stimulus at three months of age.

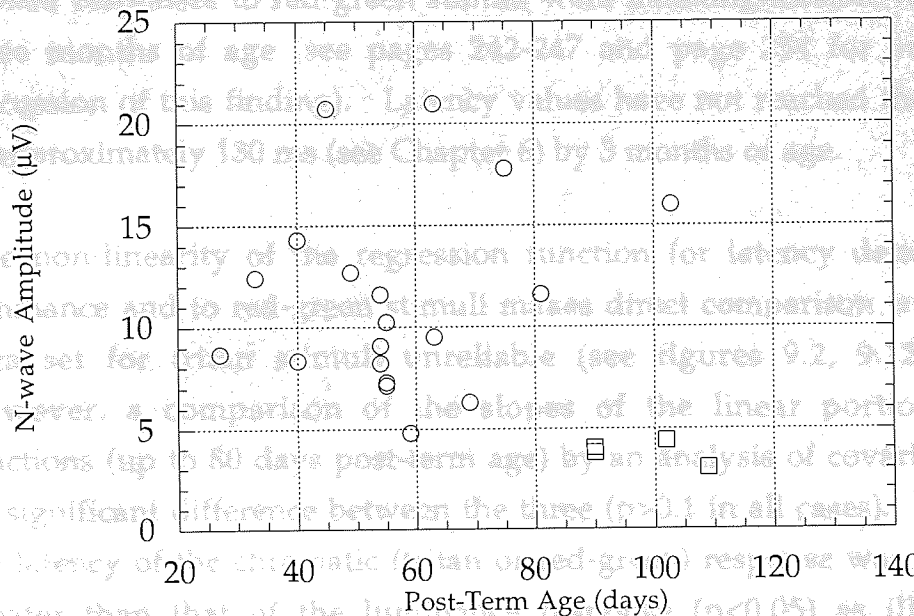


Figure 9.13. Open circles represent the amplitude of the negative peak response to photometrically isoluminant tritan stimuli is shown with respect to post-term age ($r=0.18$) for all five infants tested from 4 weeks to 3 months post-term age (MB, DH, DC, JC2, PR). Open squares indicate standard deviation of response amplitude for four of these infants in whom no response distinguishable from noise could be elicited to this stimulus at three months of age.

The latency and amplitude of the negative component of the evoked response to isoluminant red-green stimuli are plotted as a function of post-term age in figures 9.14 and 9.15 respectively. Data are shown for all five infants tested up to 3 months of age. A non-linear (second-order polynomial) function provided a significantly better fit to the latency data than a linear function (p value from F ratio test <0.05). Latency shows a significant negative correlation with age ($r=0.76$; $p<0.01$), but there is no significant effect of age on the amplitude of the evoked response ($r=0.15$; $p>0.1$). In three of the five infants tested over this period (MB, DH and JC2) evoked responses to red-green stimuli were indistinguishable from noise at three months of age (see pages 242-247 and page 254 for evidence and discussion of this finding). Latency values have not reached the adult level of approximately 130 ms (see Chapter 6) by 3 months of age.

The non-linearity of the regression function for latency data relating to luminance and to red-green stimuli makes direct comparison with the same data set for tritan stimuli unreliable (see figures 9.2, 9.12 and 9.14). However, a comparison of the slopes of the linear portions of these functions (up to 80 days post-term age) by an analysis of covariance reveals no significant difference between the three ($p>0.1$ in all cases). At each age, the latency of the chromatic (tritan or red-green) response was significantly greater than that of the luminance response ($p<0.05$) as illustrated by differences in elevation of the regression functions for each data set. There was no significant difference between the latency values at each age, for responses to red-green and tritan stimuli ($p>0.1$). The amplitude of the response to luminance-modulated stimuli was significantly greater than that of the response to tritan and to red-green stimuli ($p<0.05$), but there was no significant difference between response amplitudes for tritan and red-green stimuli ($p>0.1$).

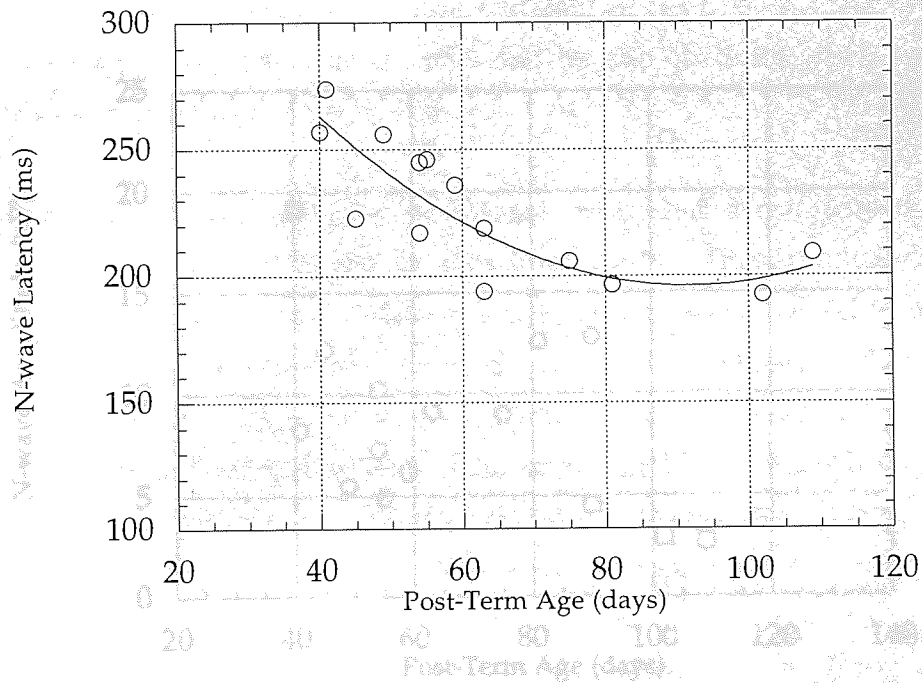


Figure 9.14

The latency of the negative peak response to photometrically isoluminant red-green stimuli is shown with respect to post-term age for all of the five infants tested from 4 weeks to 3 months post-term age (MB, DH, DC, JC2, PR). The regression function is the fit of a second order polynomial ($r=0.76$) which provided a significantly better fit to the data than a linear function (p value from F ratio test < 0.05).

chromatic contrasts of 10%, 20%, 40% and 80% as the minimum contrast specified by the chromaticity co-ordinates of the tritan stimulus (see Chapter 9). The results are shown in Figure 9.16. Note that the amplitude of the negative potential decreases with decreasing chromatic contrast, and is not evident for a contrast of 18%. A tritan chromatic contrast of 18% was chosen deliberately as it yields an S-cone contrast of 0.25, which approximates the mean L- to S-cone contrast of the human retina.

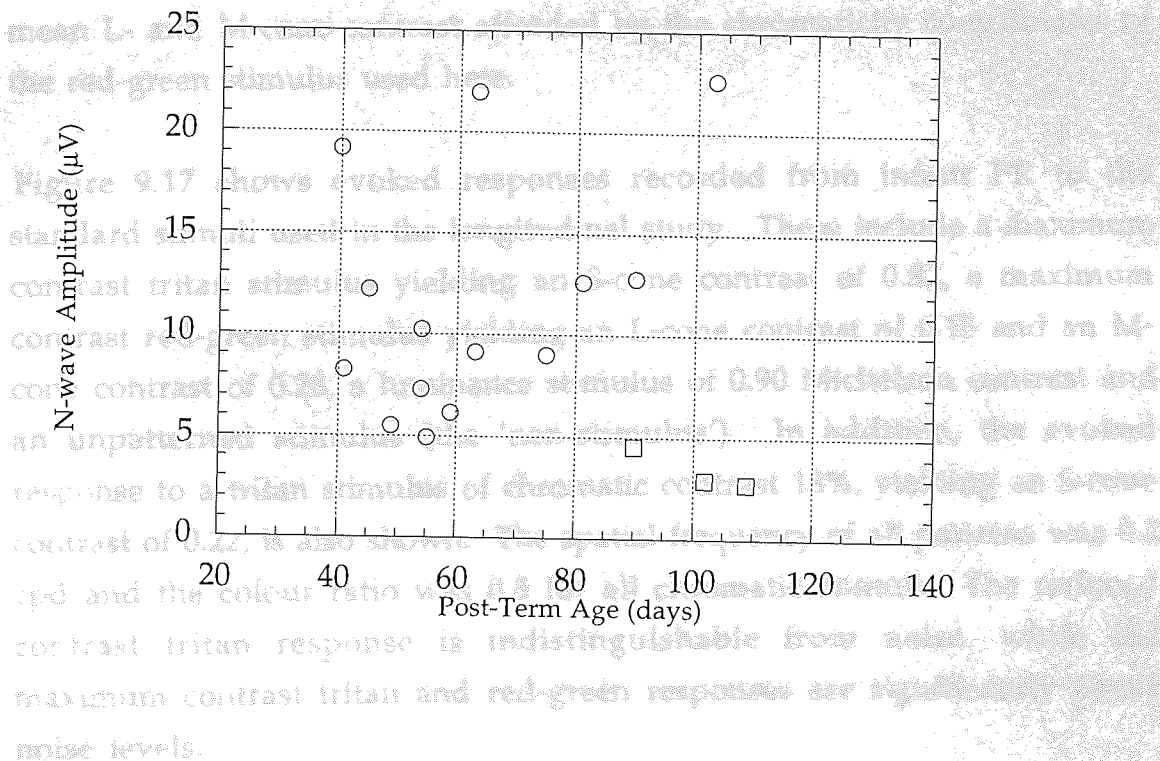


Figure 9.15

The amplitude of the negative peak response to photometrically isoluminant red-green stimuli is shown with respect to post-term age ($r=0.15$) for all five infants tested from 4 weeks to 3 months post-term age (MB, DH, DC, JC2, PR). Open squares indicate standard deviation of response amplitude for three of these infants in whom no response distinguishable from noise could be elicited to this stimulus at three months of age.

9.6 Responses to Lower Contrast Chromatic Stimuli

In one 7-week-old infant (PR), responses to photometrically isoluminant tritan stimuli (colour ratio 0.5) of spatial frequency 0.2 cpd were recorded at chromatic contrasts of 80%, 60%, 40% and 18% of the maximum contrast specified by the chromaticity co-ordinates of the tritan stimulus (see Chapter 5). The results are shown in figure 9.16. Note that the amplitude of the negative potential decreases with decreasing chromatic contrast, and is not evident for a contrast of 18%. A tritan chromatic contrast of 18% was chosen deliberately as it yields an S-cone contrast of 0.22, which approximates the mean L- and M-cone contrast afforded by the chromaticity co-ordinates of the red-green stimulus used here.

Figure 9.17 shows evoked responses recorded from infant PR to the standard stimuli used in the longitudinal study. These include a maximum contrast tritan stimulus yielding an S-cone contrast of 0.82, a maximum contrast red-green stimulus yielding an L-cone contrast of 0.15 and an M-cone contrast of 0.28, a luminance stimulus of 0.90 Michelson contrast and an unpatterned stimulus (the 'non-stimulus'). In addition, the evoked response to a tritan stimulus of chromatic contrast 18%, yielding an S-cone contrast of 0.22, is also shown. The spatial frequency of all patterns was 0.2 cpd and the colour ratio was 0.5 for all chromatic stimuli. The reduced contrast tritan response is indistinguishable from noise, while the maximum contrast tritan and red-green responses are significantly above noise levels.

Latency (ms)

Figure 9.16

Visual evoked responses to photometrically isoluminant tritan stimuli at a range of chromatic contrasts, recorded from infant PR at 54 days post-term age are shown. The top trace is the response to a tritan stimulus at 80% chromatic contrast, the second is 60% chromatic contrast and the third is 40% chromatic contrast. The bottom trace is the response to the tritan stimulus at 18% chromatic contrast; this represents an S-cone contrast of 0.22 which is equal the mean L-M cone contrast afforded by the red-green stimulus of maximum contrast. The evoked response diminishes with reducing contrast, and is indistinguishable from noise at the 18% contrast level.

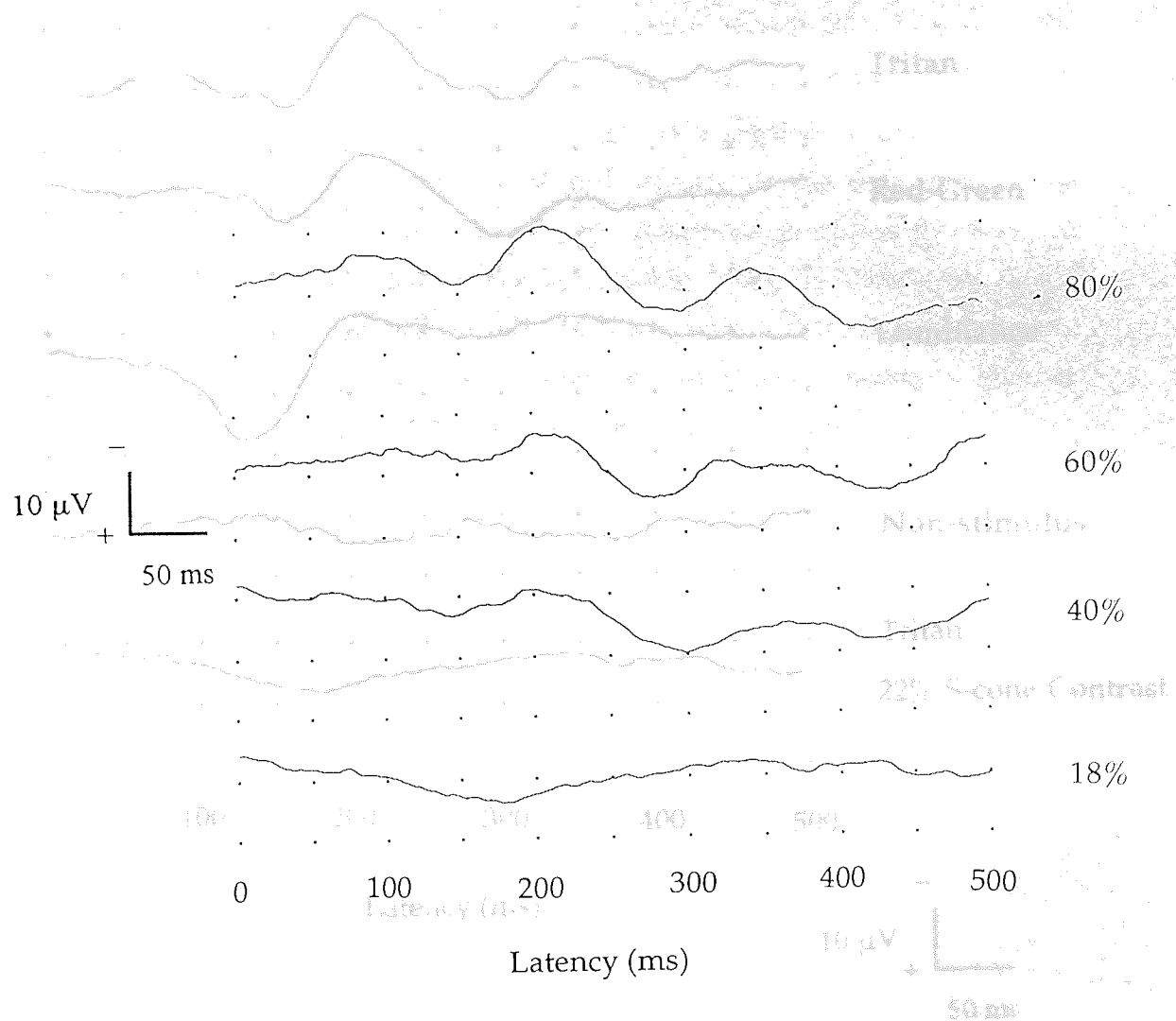


Figure 9.16

Visual evoked responses to photometrically isoluminant tritan stimuli at a range of chromatic contrasts, recorded from infant PR at 54 days post-term age are shown. The top trace is the response to a the tritan stimulus at 80 % chromatic contrast, the second to 60 % chromatic contrast and the third to 40 % chromatic contrast. The bottom trace is the response to the tritan stimulus at 18 % chromatic contrast; this represents an S-cone contrast of 22 % which equal the mean L-M cone contrast afforded by the red-green stimulus at maximum contrast. The evoked response diminishes with reducing contrast, and is indistinguishable from noise at the 18 % contrast level.

40 cd/m². The purpose of this was to investigate the possibility of contamination of the luminance from the level used throughout the study (30 cd/m²) to the maximum luminance possible with the monitor used (40 cd/m²). If response characteristics change significantly at a higher mean luminance, this may suggest the involvement of rod signals in the response. At the lower luminance level (see also Chapter 6), response morphology was not significantly different at either mean luminance level, as shown in Figure 9.18, and response latency and amplitude were similar at the two levels ($p > 0.1$), suggesting that the response at the lower luminance level is photopic, and is not significantly contaminated by rod signals.

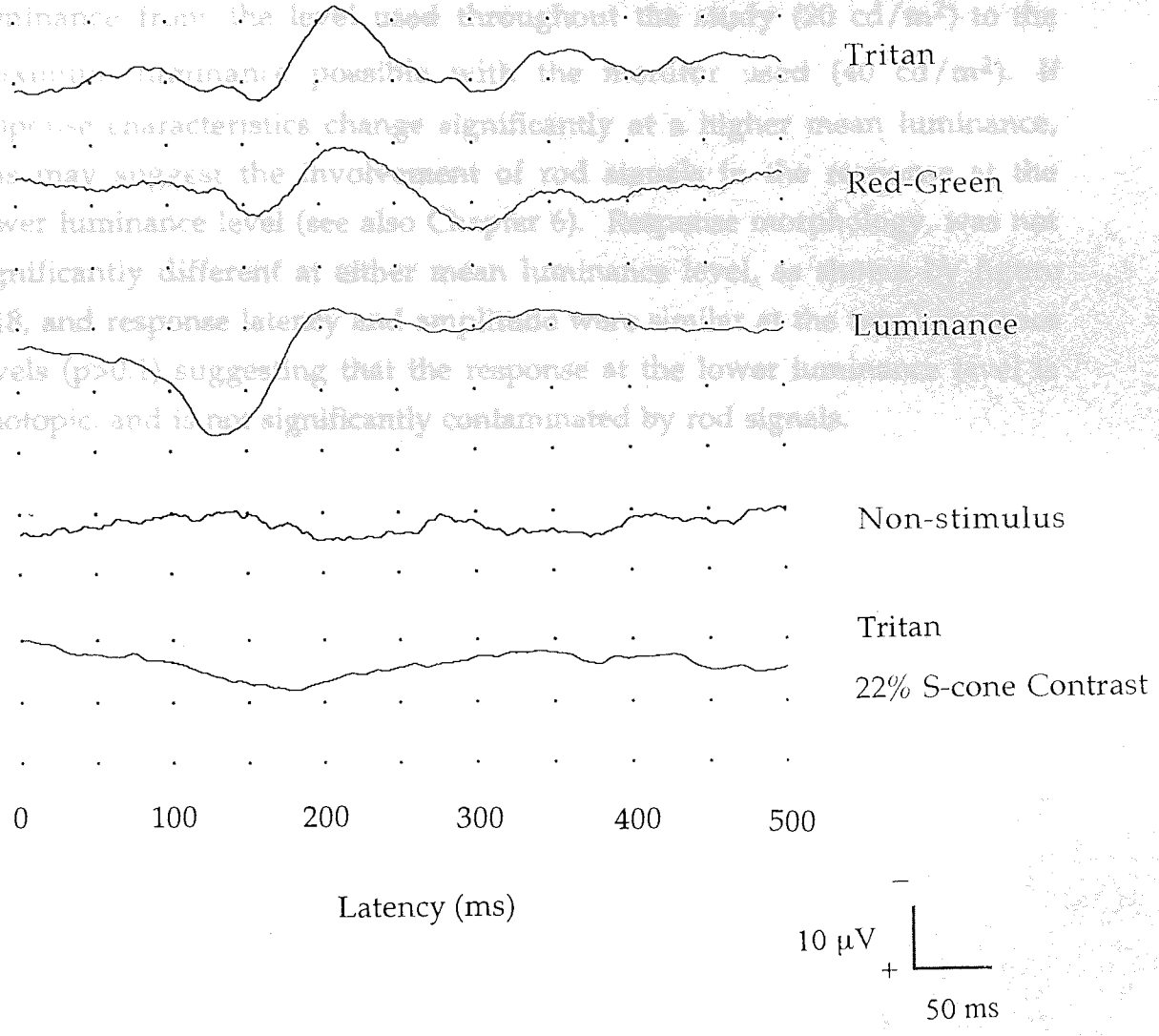


Figure 9.17
 Infant PR at 54 days post-term age. Visual evoked responses to photometrically isoluminant tritan and red-green stimuli at maximum chromatic contrast are shown (top two traces). The response to luminance stimulation and the non-stimulus condition are also shown, and the response to a tritan stimulus at 18 % chromatic contrast, representing the same mean contrast to the S-cones (22 %) as the red-green stimulus offers to the L and M cones at maximum contrast.

9.7 Evidence for the Photopic Nature of Responses to Chromatic Stimuli

In one infant (OG) at 7 weeks post-term, evoked responses to isoluminant tritan stimuli (colour ratio 0.5) were recorded at mean luminances of 20 and 40 cd/m². The purpose of this was to investigate the effect of increasing luminance from the level used throughout the study (20 cd/m²) to the maximum luminance possible with the monitor used (40 cd/m²). If response characteristics change significantly at a higher mean luminance, this may suggest the involvement of rod signals in the response at the lower luminance level (see also Chapter 6). Response morphology, was not significantly different at either mean luminance level, as shown by figure 9.18, and response latency and amplitude were similar at the two luminance levels ($p > 0.1$) suggesting that the response at the lower luminance level is photopic, and is not significantly contaminated by rod signals.

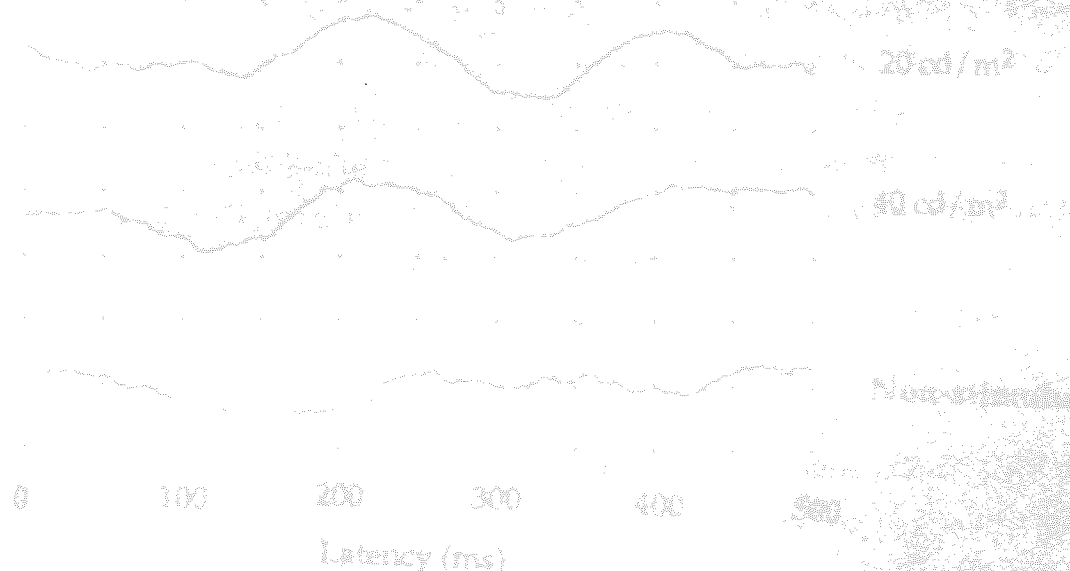


Figure 9.18

Visually evoked responses recorded from infant (OG) at 35 days post-term age to photometrically isoluminant tritan stimuli at 20 cd/m² (top trace) and 40 cd/m² luminance (trace). The response to the non-stimulus condition is the noise or comparison.

9.8 Evoked Responses at 3 to 6 Months of Age

From four of the five infants tested up to 3 months post-term, evoked responses to isoluminant tritan stimuli were unclear and in some cases were diminished from their previous values to noise levels at about 3 months of age; only infant PR demonstrated evoked potentials to both types of chromatic stimuli and to luminance stimuli significantly above noise levels. In three of the five infants, evoked responses to red-green stimuli were also indistinguishable from noise as indicated by the non-stimulus condition at this age. These findings are indicated by the open squares in figures 9.12 and 9.13 and are summarised in table 9.1.

In all infants, responses to luminance-modulated stimuli were distinguishable and significantly above noise levels at all ages tested. Latency and amplitude of the responses to luminance-modulated stimuli recorded from infants MB and DH up to six months of age are shown in figures 9.19 and 9.20. Figure 9.19 shows that the latency of the luminance response reaches adult-like values of approximately 120 ms by 4 to 5 months of age (see also Chapter 6). Figure 9.20 shows that the amplitude tends to reduce over the period from 4 weeks to about 4 months post-term age, reaching a minimum at 130.25 days, then begins to increase towards 6 months of age, at least for the two infants tested over this age range.

Figures 9.21 and 9.22 show responses recorded from infants MB and KB at 3 months post-term. In both cases, the tritan response is unclear, although it is significantly above EEG noise levels. The luminance response is well defined and significantly above noise. The response to isoluminant red-green stimuli is discernible in the case of KB, while MB shows no clear red-green response at this age (evoked potentials to red-green stimuli at the full range of colour ratios had been recorded from infant MB at the age of 9 weeks post-term).

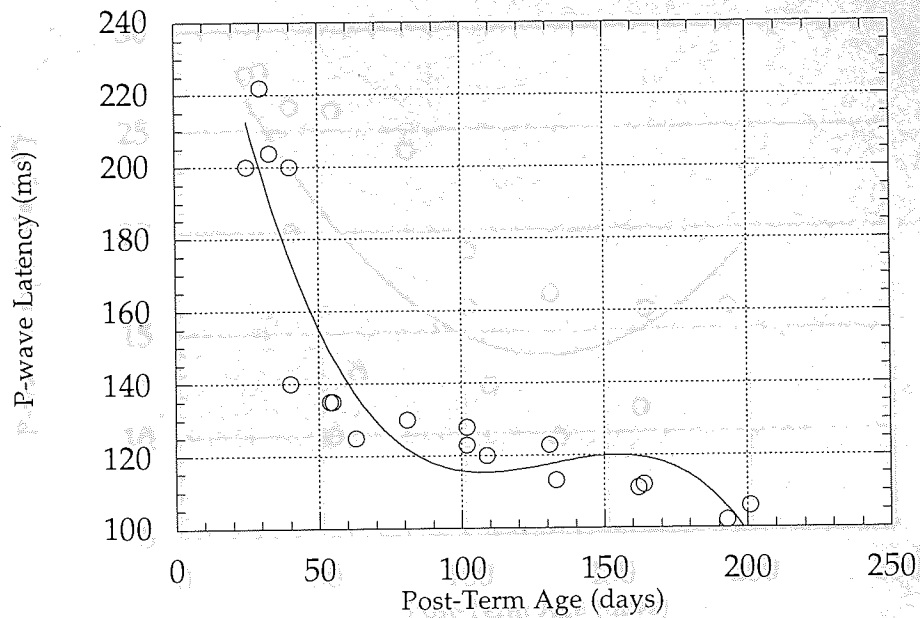


Figure 9.19
 The amplitude of the positive peak response to luminance stimulation is shown with respect to post-term age for the two infants (MB and DH) tested from 4 weeks to 6 months of age. The regression function ($r=0.92$) is the fit of a third order polynomial, which provides the best fit to the data (p value from F ratio test < 0.05).

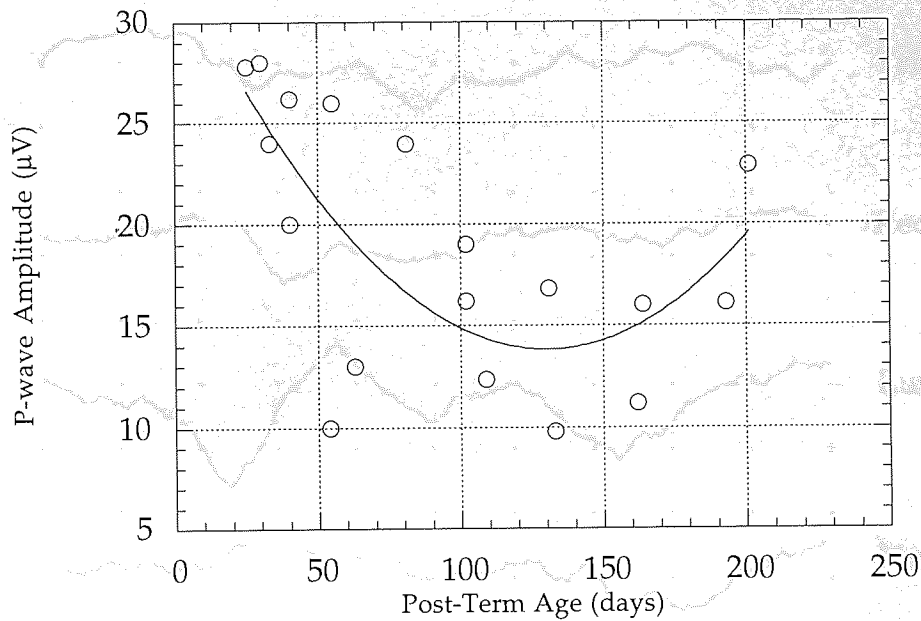


Figure 9.21

Visual evoked responses recorded from infant MB at 102 days post term age (approximately 3 months). The top trace is the response to photometrically isofluorescent Tritan stimulation, the second to a transient red-green stimulation, the third to a luminance-modulated stimulus and the bottom to a transient red-green stimulation.

Figure 9.20

The amplitude of the positive peak response to luminance stimulation is shown with respect to post-term age for the two infants (MB and DH) tested from 4 weeks to 6 months of age. The regression function ($r=0.70$) is the fit of a second order polynomial, which provides the best fit to the data (p value from F ratio test < 0.05). The amplitude reduces with age to reach a minimum at 130.25 days (approximately 4 months) post-term, then begins to increase with age.

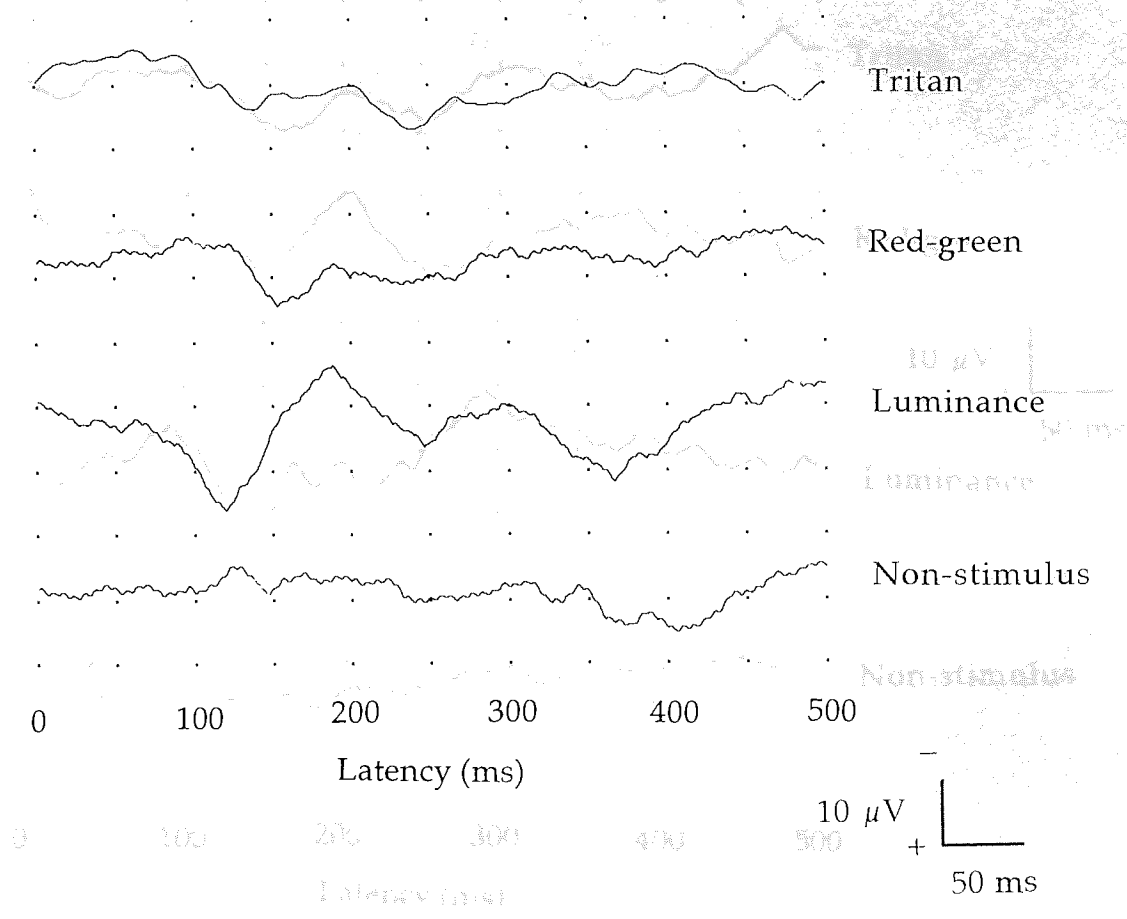


Figure 9.21
 Visual evoked responses recorded from infant MB at 102 days post-term age (approximately 3 months). The top trace is the response to photometrically isoluminant tritan stimulation, the second to isoluminant red-green stimulation, the third to a luminance-modulated stimulus and the bottom trace is the response to the non-stimulus condition. At this age in this infant, the responses to both types of chromatic stimulation are not clearly distinguishable from noise as indicated by the non-stimulus condition, and the morphology of the luminance stimulus is of increased complexity, when compared with a response to this type of stimulus at an earlier age (see figure 9.1).

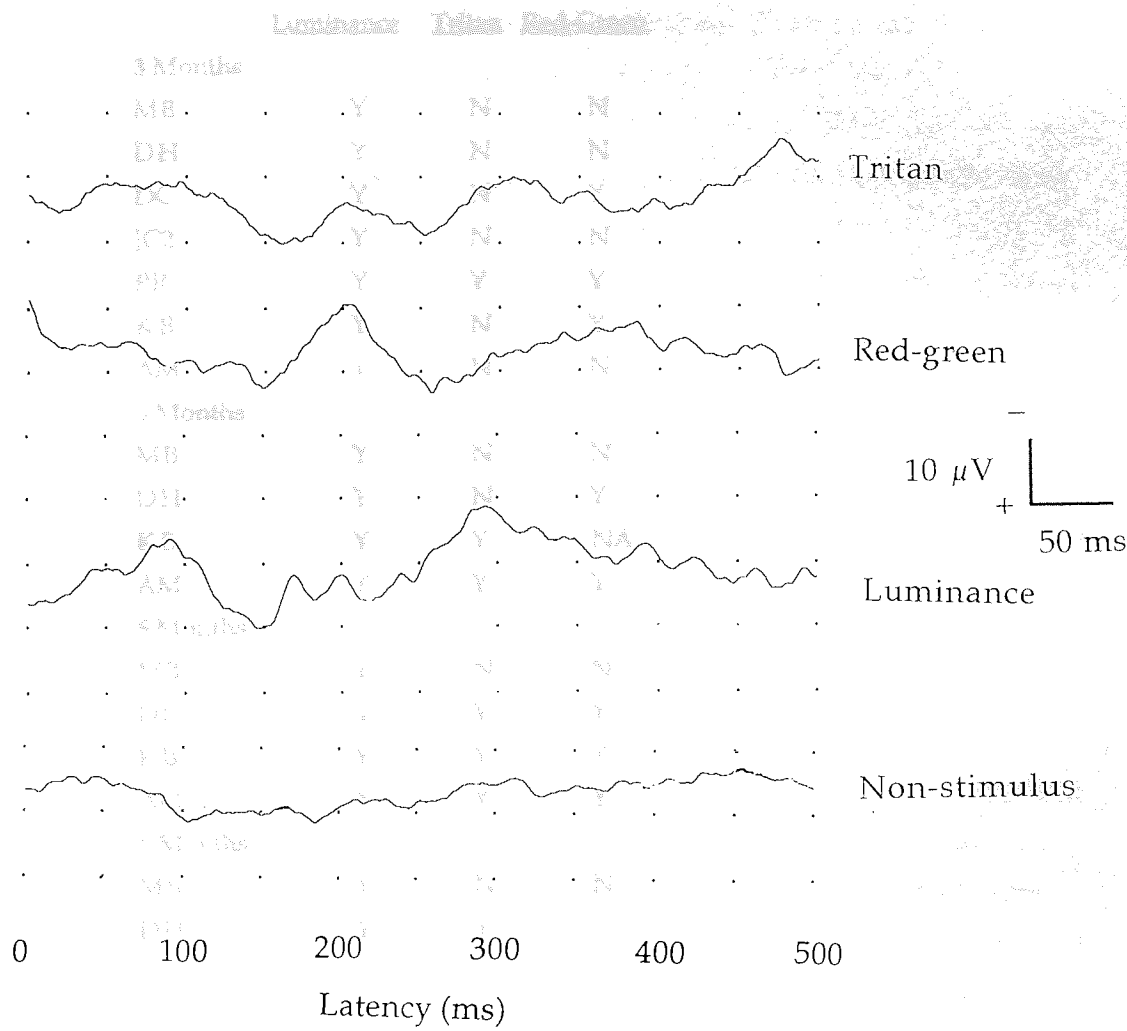


Figure 9.22
 Visual evoked responses recorded from infant KB at 3 months post-term age. The top trace is in response to photometrically isoluminant tritan stimulation, the second to isoluminant red-green stimulation and the third is a response to luminance-modulated stimulation. In this infant, the response to red-green stimulation is a clearly defined negativity at a latency of about 200 ms, while the tritan response is barely distinguishable from noise.

These results confirm that pattern-onset modulated stimuli (figure 9.1) are present in human infants from birth onwards post-term age (Moskowitz and Sokol, 1983; Harding et al, 1989; Mollich and Scharf, 1991). The response to high-frequency modulated pattern-onset stimuli by 3 to 6 months post-term age (figure 9.2) is shown in table 9.1.

	<u>Luminance</u>	<u>Tritan</u>	<u>Red-Green</u>
3 Months			
MB	Y	N	N
DH	Y	N	N
DC	Y	N	Y
JC2	Y	N	N
PR	Y	Y	Y
KB	Y	N	Y
AM	Y	N	N
4 Months			
MB	Y	N	N
DH	Y	N	Y
KB	Y	Y	NA
AM	Y	Y	Y
5 Months			
MB	Y	N	N
DH	Y	Y	Y
KB	Y	Y	Y
AM	Y	Y	Y

These findings are in contrast to those of Jägle et al (1980) who could find no consistent evidence for a functional short-wavelength-sensitive mechanism in 3-month-old infants, using chromatic adaptation and colour choice preferential looking. This was taken to suggest that the development of this mechanism may lag behind that of long- and medium-wavelength-sensitive mechanisms. Volbrecht and Werner (1967) suggest as a possible explanation for these discrepant findings that the background spectrum used by Perloe et al (1966) for adaptation of the remaining cone mechanisms may have been insufficiently bright for this purpose.

The present study did not rely on chromatic adaptation to isolate the short-

Table 9.1

For each infant tested up to and over the age of 3 months, this table indicates whether an evoked potential was present to each type of stimulation. Y=Yes, N=No; NA=Not applicable (no test carried out).

Discussion

9.9 Discrimination of Luminance and Chromatic Stimuli

These results confirm that visual evoked potentials to luminance-modulated stimuli (figure 9.1) are present in human infants by at least 4 weeks post-term age (Moskowitz and Sokol, 1983; Harding et al, 1989; McCulloch and Skarf, 1991). The response to luminance-modulated pattern-onset stimulation was adult-like (see Chapter 6) in terms of latency by 3 to 4 months post-term age (figures 9.2 and 9.19).

Responses to tritan stimuli at and around photometric isoluminance were present in infants by 4 to 10 weeks post-term (figures 9.6 and 9.11), implying the discrimination of stimuli along a tritanopic confusion axis without luminance cues. Such discriminations under photopic conditions require functional short-wavelength-sensitive cones and at least one other cone type, and functional post-receptoral processing of their signals. The findings of the present study suggest, therefore, that short-wavelength-sensitive cones in addition to at least one other cone type, and post-receptoral processing of their signals are functional by this age range, in general agreement with previous work (Varner et al, 1985; Volbrecht and Werner, 1987).

These findings are in contrast to those of Pulos et al (1980) who could find no consistent evidence for a functional short-wavelength-sensitive mechanism in 2-month-old infants, using chromatic adaptation and forced-choice preferential looking. This was taken to suggest that the development of this mechanism may lag behind that of long- and medium-wavelength-sensitive mechanisms. Volbrecht and Werner (1987) suggest as a possible explanation for these discrepant findings that the background stimulus used by Pulos et al (1980) for adaptation of the remaining cone mechanisms may have been insufficiently bright for this purpose.

The present study did not rely on chromatic adaptation to isolate the short-wavelength-sensitive mechanism, using tritan stimuli instead for this purpose. Varner et al (1985) also used tritan stimuli, and were able, using

forced-choice preferential looking, to demonstrate a functional short-wavelength-sensitive cone mechanism in 2-month-old infants, and in some 1-month-olds. The discrepancy between studies may be due to stimulus differences (Volbrecht and Werner, 1987). In addition, psychophysical and electrophysiological techniques are thought to tap different mechanisms of the visual system. This factor may partly explain the discrepancy between the findings of Pulos et al (1980) and those of the present study, in which visual evoked responses to tritan stimuli at a range of luminance ratios revealed a functional short-wavelength-sensitive cone mechanism in infants from 4 to 10 weeks post-term. This mechanism might not have been apparent using behavioural techniques, due to the contribution of non-sensory factors such as attention losses. Varner et al (1985), however, obtained similar findings to those of the present using a forced-choice paradigm, which suggests that these different techniques are not solely responsible for discrepant findings, and that other methodological factors such as stimulus type, may also contribute.

It has been suggested that, if vision is mediated subcortically in neonates (Bronson, 1974), there may be no evidence of a short-wavelength-sensitive mechanism in young infants, as the superior colliculus receives no input from short-wavelength-sensitive cones (Mollon, 1982; Atkinson, 1984, 1991). The superior colliculus receives no parvocellular input (Schiller and Malpeli, 1977) and input from long- and medium-wavelength-sensitive cones is magnocellular. Therefore, according to this hypothesis, short-wavelength and Rayleigh discriminations without luminance cues, mediated by the parvocellular system, should be equally affected at an early age, contrary to the findings of Pulos et al (1980).

Responses to red-green isoluminant stimuli were not present until 6 to 11 weeks post-term (figures 9.7 and 9.11), in agreement with previous studies using steady-state (Morrone et al, 1990, 1993) and transient (Rudduck and Harding, 1994) responses to pattern-reversal stimulation. There are at least two possible reasons why evoked responses to tritan stimuli were present, with wide inter-individual variations, approximately two weeks earlier than responses to red-green stimuli. It may be the case that the

development of the S-cone pathway precedes that of the L-M cone pathway. Alternatively, the difference may reflect the lower effective cone contrast at isoluminance for red-green stimuli compared with tritan stimuli when both are displayed at maximum chromatic contrast (see table 1, Chapter 5).

The absence of an evoked response to red-green stimuli at all luminance ratios at an early age does not imply the absence or deficiency of a functional L-M opponent pathway. One consequence of the considerable overlap of spectral sensitivity functions of long- and medium-wavelength-sensitive cones (see Chapter 1) is that each component colour of a heterochromatic stimulus, such as the red-green used in the present study, inevitably stimulate both L and M cone types and so the effective contrast of the stimulus for each cone type is relatively low. Much higher cone contrasts are possible for the short-wavelength-sensitive cone because its spectral sensitivity function has minimal overlap with that of the other cone types.

In the present study, evoked responses to tritan and red-green stimuli at a range of chromatic contrasts were recorded from one infant at 7 weeks post-term age (figures 9.16 and 9.17). Responses to tritan stimuli diminished at S-cone contrast levels close to the L-M cone contrast level afforded by the red-green stimulus at maximum physical contrast. This suggests that the discrimination of red-green stimuli is limited by the relatively low cone contrast affordable for L and M cones with red-green stimuli at maximum physical contrast, and that cone contrast differences are a likely explanation for the later onset of responses to red-green than to tritan stimuli.

Evoked responses to luminance-modulated stimuli were present in most infants at an earlier age than responses to isoluminant chromatic stimulation. A number of previous studies are in agreement with this (Morrone et al, 1990, 1993; Rudduck and Harding, 1994; Burr et al, 1996). In contrast to these findings, Allen et al (1993) report evoked responses to luminance-modulated and isoluminant red-green stimuli in all of a group of 14 infants, aged 2 to 8 weeks. In this particular study, results from only one infant at 2 weeks of age were included, the remaining results being from infants aged 5 to 8 weeks of age. Discrepant findings on the age of

onset of different visual functions may be due at least in part to inter-individual variations, because the exact period and rate of development from conception of each infant is unknown. The term date for pregnancy is calculated as 40 weeks from the first day of the mother's last menstrual period. Studies on infant vision generally specify infant age as the chronological age from birth, some specifying that birth date is within ten days to two weeks of calculated due term date (Swanson and Birch, 1990; Morrone et al, 1990, 1993; Allen et al, 1993; Zanker and Mohn, 1993). This two-week allowance introduces further errors in the estimation of the period of development from conception. In the present study, the age of each infant was defined as post-term, following the method of Rudduck and Harding (1994) to minimise these errors.

In general, the age at which infants are able to discriminate chromatic stimuli without luminance cues is later than the age at which luminance is detected. In the present study, all of the infants tested longitudinally demonstrated evoked responses to luminance-modulated stimuli from the earliest age tested (4 weeks post-term), while responses to chromatic stimuli without luminance cues were absent until, on average, 7 weeks post-term for tritan stimuli and 8.5 weeks post-term for red-green stimuli. This later age of onset of chromatic stimuli has also been found by previous workers (Morrone et al, 1990, 1993; Rudduck and Harding, 1994; Burr et al, 1996) and has been tentatively attributed to an earlier age of onset of functional magnocellular than parvocellular pathways (Burr et al, 1996). Morrone et al (1990, 1993) found that chromatic contrast sensitivity has a later age of onset but develops more rapidly than luminance contrast sensitivity. The same group, however (Burr et al, 1996), found that in terms of evoked response latency, the luminance channel develops more rapidly than the red-green colour-opponent channel.

In support of the chromatic deficiency hypothesis, Burr et al (1996) point to results from one infant at 8.5 weeks of age, from whom evoked responses to luminance stimuli are said to remain strong at contrast levels of about 14%, while responses to red-green isoluminant stimuli are diminished to noise levels at maximum physical contrast. The maximum L and M cone

contrasts using this type of stimulus, however, would be approximately 15% and 28% respectively, while the cone contrast for luminance stimuli is the same as the physical contrast level (Brown et al, 1995). Therefore, the possibility that luminance and chromatic discriminations in infants are limited by cone contrasts, and that poor luminance and chromatic sensitivity in infants is explained by the visual efficiency hypothesis, and not by a deficiency of the chromatic mechanisms in particular, cannot be dismissed.

In the present study, evoked responses to luminance stimulation were present in all infants from the earliest age tested, while responses to chromatic stimuli were absent at this age in 8 of the 9 infants tested longitudinally. As discussed earlier, cone contrast differences may explain the different ages of onset of discrimination of tritan and red-green stimuli. Cone contrast afforded by the luminance-modulated stimulus is equal to its Michelson contrast, at 90% in the present study. The S-cone contrast of the tritan stimulus at maximum physical contrast is 82%. This 8% cone contrast difference between the luminance and tritan stimuli is unlikely to explain the different ages of response onset observed in 8 of the 9 infants. This suggests that cone contrast is not the only factor in the later onset of responses to chromatic than luminance stimuli. As has been suggested previously (Burr et al, 1996), this difference may also reflect a later age of functional onset of parvocellular than magnocellular channels, supported by anatomical evidence of magnocellular units in the striate cortex being more metabolically active than parvocellular units in the neonate (Wong-Riley et al, 1993).

9.10 Development of Luminance and Chromatic Pathways

At each age from 4 weeks to approaching 3 months post-term, the latency of the peak chromatic (tritan and red-green) response is significantly greater than that of the luminance response (figures 9.2, 9.12 and 9.14). Latency values for tritan, red-green and luminance-modulated stimuli decrease with increasing age and the rate of decrease is similar for all three stimulus types. These results suggest, therefore, that the rate of development, reflected by evoked response latency changes, is similar for pathways

mediating chromatic information (red-green and tritan stimuli) and luminance information, at least up to 80 days post-term age.

Morrone et al (1990, 1993) and Burr et al (1996) find that chromatic and luminance sensitivity develop at different rates in infants. However, the pattern of development is unclear, as Morrone et al (1990, 1993) report more rapid development of chromatic than luminance sensitivity when evoked response amplitudes are taken into account, while Burr et al (1996) found latencies to chromatic and luminance stimuli to be similar until 10 weeks of age, after which luminance responses showed more rapid maturation than chromatic responses. It was thought that these different rates of development of chromatic and luminance evoked responses may represent different developmental patterns of parvocellular and magnocellular mechanisms, respectively, consistent with the chromatic deficiency hypothesis of infant colour vision. Evidence from other studies, however, suggests that chromatic sensitivity is reduced in infants by a general insensitivity of the visual system, and not of the chromatic mechanisms in particular (Allen et al, 1993; Brown et al, 1995; Teller and Palmer, 1996).

In the present study, the rates of latency decrease with age for the visual evoked responses to luminance, tritan and red-green stimuli were found to be similar, by an analysis of covariance. This analysis was carried out on data collected from infants up to 80 days post-term age, because all functions were linear over this period. Beyond this age, latencies of responses to luminance and red-green stimuli asymptoted, and so a second-order polynomial function provided the best fit to these data sets, while the function for responses to tritan stimuli remained linear. This difference between functions for responses to luminance and tritan stimuli may be assumed to indicate different developmental rates of their underlying mechanisms. However, less responses to tritan stimuli than to luminance-modulated stimuli were evident at 3 months of age, so the behaviour of these functions at about this age cannot be reliably compared. For this reason, functions were compared only up to 80 days post-term age, and no significant difference in rate of latency change with age was found between the three functions. Over the age range investigated here, this finding is in

agreement with the visual efficiency hypothesis, that chromatic sensitivity is reduced by a general insensitivity of the infant visual system and not by a deficiency of the chromatic mechanisms in particular.

9.11 Diminution of Responses at 3 Months Post-Term

The diminution of responses to isoluminant chromatic stimuli at 3 months of age may be due to a number of anatomical factors. The neonatal human skull is incomplete, with large anterior and posterior fontanelles (see Chapter 2). The situation of the posterior fontanelle coincides with the occiput (Oz), the scalp position at which the active electrode is placed in the present study and in many other studies of visual evoked responses in infants and adults. In adults, visual evoked responses recorded from the scalp over an area in which the skull is incomplete are larger in amplitude than those recorded from control adults with complete skulls (van der Broek, 1997). In addition, relatively high response amplitudes in neonates have been attributed partly to low resistance of the incomplete skull (Ellingson, 1958). Thus, closure of the posterior fontanelle, which occurs at 2 to 3 months of age (Soames, 1995) may partly explain the diminution of the evoked response recorded from the occiput at this age.

If fontanelle closure were the only factor responsible, all responses would be expected to be affected equally. The responses to chromatic stimulation are more significantly affected, however, than those to luminance stimulation, suggesting that other factors are involved. At 3 to 6 months of age, the density of macular pigment increases significantly (Bone et al, 1988; see Chapter 2). Macular pigment selectively absorbs short-wavelength light, and so its increased density may reduce the evoked response to tritan stimulation without having a significant effect on the response to red-green or luminance-modulated stimulation. In addition, rapid maturation of the cortex occurs during the first postnatal year, including myelination of the optic nerve (Magoon and Robb, 1981), development of the lateral geniculate nucleus (Hickey and Peduzzi, 1987) and the formation of synapses (Burkhalter et al, 1993). Anatomical changes such as these may result in changes to the evoked response recorded at the occiput, and may partly explain the diminution of responses to chromatic stimulation, and the

increased complexity of responses to luminance-modulated stimuli.

9.12 Intrusion of Rod Responses

The intrusion of rod responses may confound chromatic discrimination measures. This is particularly so in infants because it is necessary to use large, low spatial frequency stimuli to ensure that stimuli may be resolved. In addition, although it is generally agreed that VEPs recorded from the occipital pole (Oz) represent foveal cone activity (Daniel and Whitteridge, 1961; Drasdo, 1977; Horton and Hoyt, 1991), it is possible that extra-foveal signals, including those generated by rod activity, may be recorded from Oz in infants due to general cortical immaturity and the presence of skull fontanelles.

The scotopic and photopic visual evoked responses of adults differ markedly in terms of latency, amplitude and morphology (Wooten, 1972). In the present study, the morphology of the evoked response recorded in infants using pattern-onset chromatic stimuli is the same as that elicited in adults under photopic conditions (see Chapter 6). In addition, although small-field stimuli (<8 degrees) may not be sufficient to saturate rod activity, rod-initiated signals of infants may saturate with large-field stimuli (16 degrees) even under dark-adapted conditions (Brown, 1988, 1990). Therefore, the use of a photopic (20 cd/m²) display luminance and large-field stimuli (40 x 32 degrees) suggests that the evoked responses recorded in the present study were not contaminated by rod activity. The results obtained from infant OG at a mean luminance of 40 cd/m² further support the assumption that the responses to chromatic stimuli at 20 cd/m² in this study have no significant contribution from rods.

9.13 Colour Axes

In the present study, it is assumed that an appropriate tritanopic confusion axis for each infant was used. Tritanopic confusion axes in CIE colour space are calculated from group mean values (Wyszecki and Stiles, 1982) and may therefore be inappropriate for some individuals. In consequence, stimuli presented along a standard tritan axis may stimulate long- and medium-wavelength-sensitive cones unequally. Colour vision would need to be

functional, however, to allow determination of an individual's tritanopic confusion axis. This is clearly impossible with newborn infants, necessitating the use of standard colour axes.

9.14 Summary

The results of this study show that infants are able to discriminate colours along a tritanopic confusion axis without luminance cues by 4 to 10 weeks post-term age. This implies that short-wavelength-sensitive cones, the S-cone pathway and at least one other cone type are functional by 4 to 10 weeks. Wide inter-individual variations may be due to the inevitable inaccuracy in determining post-conceptual age in human infants. In addition, these results suggest that the S-cone pathway, the L-M cone pathway and the luminance pathway develop at a similar rate, at least up to 80 days post-term age. This similarity is consistent with the visual efficiency hypothesis, while the later age of onset of responses to chromatic than luminance stimuli may at least partly reflect a later age of functional onset of parvocellular than magnocellular channels.

A deficiency of the chromatic post-receptoral mechanisms may, therefore, partly explain the later age of onset of responses to chromatic than luminance stimuli, while general insensitivity of the visual system restricts both luminance and chromatic sensitivity after the age of onset, at least up to 80 days of age.

The diminution of responses to chromatic stimulation at about 3 months of age may be due to a combination of anatomical factors. Recognition of the fact that this change occurs is important because the absence of responses in infants beyond this age could be taken to indicate that infants are unable to discriminate isoluminant chromatic stimuli. This is clearly not the case, as in the present study evoked responses to tritan and red-green stimuli at and around the adult isoluminant match are elicited from infants at 1 to 2 months post-term age.

CHAPTER 10

GENERAL DISCUSSION

10.1 The Infant Visual Evoked Response around Isoluminance

This is the first study of visual evoked responses to pattern-onset tritan and red-green stimuli in human infants. This type of stimulus presentation has demonstrated a distinct morphological change as luminance differences are introduced to the chromatic stimulus, which parallels the situation found in adults by previous workers and in the present study. This change in morphology proved useful in identifying luminance contributions to the evoked response, and was used to estimate individual isoluminance in each of a group of six infants. Infants demonstrated similar isoluminant points to those of adults, and therefore to photometric isoluminance, for both types of chromatic stimuli. This suggests that infant spectral sensitivity is similar to that of adults not only at medium and long wavelengths, as is well established, but also at short wavelengths, which has been the subject of some controversy. Similar spectral sensitivity in infants and adults indicates that photometric isoluminance may be used as a first approximation to that of infants, for tritan as well as red-green stimuli.

10.2 The Maturation of Visual Evoked Responses to Chromatic and Luminance-Modulated Stimulation

Evoked responses to tritan stimuli at all colour ratios were present one to two weeks earlier than to red-green stimuli, in most infants. Responses to chromatic stimuli at a range of chromatic contrasts demonstrate that this difference reflects the relatively low contrast of L and M cones, and not a developmental lag of the L-M opponent channel.

Wide inter-individual variations were encountered in the age of onset of evoked responses to both types of chromatic stimulus. This is probably due to inaccuracies in the estimation of developmental age from conception, which may explain discrepant findings on the earliest age at which infants are able to discriminate chromatic stimuli, widely debated in the literature.

In the present study, evoked responses to luminance stimuli were present

in all infants from the earliest age tested, while responses to chromatic stimuli were absent at this age in 8 of the 9 infants tested longitudinally. While cone contrast differences may explain the later onset of responses to red-green than to tritan stimuli, they do not entirely explain the relatively early onset of responses to luminance-modulated stimuli, as the cone contrasts of maximum contrast tritan stimuli and luminance-modulated stimuli are similar. This difference may reflect a later age of functional onset of post-receptoral processing of chromatic than luminance signals, and is supported by anatomical evidence of earlier onset of magnocellular than parvocellular function in the striate cortex (Wong-Riley et al, 1993).

These conclusions are not totally in agreement with any of the existing hypotheses on chromatic sensitivity in infants. Similar rates of development of luminance and colour-opponent pathways in terms of evoked response latency support the visual efficiency hypothesis, that chromatic vision in infants is limited by a general insensitivity of the visual system, and not by a deficiency of the colour-opponent pathways in particular. This insensitivity is thought to be due at least in part to the immaturity of foveal cones and post-receptoral processing in the neonate (Youdelis and Hendrickson, 1986; Banks and Bennett, 1988). In the present study, this similarity is demonstrated from the age of onset of chromatic evoked responses, to 80 days post-term age, after which chromatic responses were no longer reliable. The later age of onset of responses to isoluminant chromatic than to luminance stimuli, however, is likely to be due to a later age of functional onset of post-receptoral processing of chromatic than of luminance signals.

Subcortical mediation of vision in young infants would allow behavioural responses to luminance stimuli at an earlier age than those to isoluminant chromatic stimuli, because the colour-opponent (parvocellular) pathways have no input to the superior colliculus. The visual evoked response recorded from the cortex, however, is dominated by cortical activity. In the present study, an earlier age of onset of cortical evoked responses to luminance stimuli than to isoluminant chromatic stimuli, which cannot be fully explained by cone contrast differences, may reflect a later age of

functional onset of cortical processing of chromatic than luminance information. In conjunction, these results suggest that chromatic vision in young infants is limited by the relatively later age of functional onset of colour-opponent (parvocellular) mechanisms, while the two are equally affected by foveal and post-receptorial immaturity after this age, at least up to 80 days (11.5 weeks) post-term.

10.3 The Diminution of Evoked Responses at 3 Months of Age

Responses to photometrically isoluminant chromatic stimuli became diminished at about 3 months of age, while responses to luminance stimuli became more complex at about this age. These changes may be due to anatomical factors such as the closure of the posterior fontanelle, the development of cortical synapses and increased density of macular pigment. Some previous studies of the visual evoked response to chromatic stimuli in infants have not continued past 2 to 3 months of age (Allen et al, 1993; Rudduck and Harding, 1994) and so this diminution would not have been noted. Morrone et al (1990, 1993) and Burr et al (1996) have reported visual evoked potentials to isoluminant red-green stimuli in infants up to 7 months of age. As explained previously, the evoked response to tritan stimuli in the present study was more significantly diminished at 3 months than the response to red-green stimuli. This difference, which may be due to increased density of macular pigment, could explain why no diminution was observed in responses to red-green stimuli by Morrone et al (1990, 1993) and Burr et al (1996). To date, no other study has reported on maturation of the transient evoked response to pattern-onset tritan stimuli, so the consistency of this finding is not known at present.

One alternative explanation for the diminution of evoked responses to chromatic stimuli at about 3 months of age could be that the response before this age reflects the involvement of parafoveal cones, becoming less apparent as anatomical changes occur, so that the occipital response becomes less diffuse and more foveal with anatomical changes at this age. This is unlikely to be the case, however, as estimated isoluminant points in infants were found to be similar to those of adults. If the discrimination of short-wavelength stimuli were mediated by parafoveal cones at an early age,

elevated sensitivity to short-wavelengths would be expected (Moskowitz-Cook, 1979), resulting in a shift away from photometric isoluminance.

The diminution of responses to chromatic stimulation at about 3 months of age is likely, therefore, to be due to a combination of anatomical factors. Recognition of the fact that this change occurs is important because the absence of responses in infants beyond this age could be taken to indicate that infants are unable to discriminate isoluminant chromatic stimuli. This is clearly not the case, as in the present study evoked responses to tritan and red-green stimuli at and around the adult isoluminant match are elicited from infants at 1 to 2 months post-term age.

10.4 Scotopic vs Photopic Mechanisms

Chromatic discriminations in monochromats, demonstrated by previous studies, imply the use of rods together with a single cone type. In the present study, evoked potentials to chromatic stimuli are assumed to reflect the presence of at least two functional cone types and the post-receptoral processing of their signals. Chromatic stimuli were presented at the maximum luminance level possible to maintain constant mean luminance at the full range of colour luminance ratios, in order to minimise rod activity. It is feasible, however, that signals from one cone type only, in addition to those of rods, could be compared to allow such discriminations, as is the case in monochromats.

Evoked responses recorded from the occiput in adults are dominated by foveal cone signals, as a result of cortical magnification. In infants, the anatomy of the visual cortex and the lower resistance of the skull (Ellingson, 1958) may allow deeper responses, including those of rods, known to be functional in one-month-old infants (Werner, 1982), to be recorded at the occiput.

There are at least two reasons to believe that this is not the case in the present study. Firstly, responses to chromatic stimuli in infants were found to be of similar morphology to those of adults, and response characteristics in both infants and adults did not change when the chromatic stimuli were

increased in brightness. The scotopic evoked response differs from the photopic response in latency, amplitude and morphology (Wooten, 1972). The similarity of evoked responses to chromatic stimuli in infants and adults suggests that the response was dominated by similar factors in both cases, and therefore that the response in infants was not significantly contaminated by rod signals.

Secondly, further evidence is provided by the estimation of isoluminance in a group of six infants. Scotopic spectral sensitivity is shifted towards short wavelengths, by comparison with photopic sensitivity. If rods made a significant contribution to the chromatic evoked response, therefore, a shift away from photometric isoluminance would be expected. Isoluminant points for both types of chromatic stimuli in infants, however, were found to be similar to photometric isoluminance, suggesting that chromatic discriminations were made possible by the presence of two functional cone types, rather than by rods.

10.5 Abnormal Evoked Responses

Evoked responses to chromatic and luminance stimuli recorded from one infant with cystic fibrosis were abnormal by comparison to those of healthy infants over the same age range. In addition, scotopic ERGs were absent prior to treatment of this condition, indicating abnormal rod function. Visual evoked response abnormalities are likely to reflect abnormal function of post-receptoral luminance and chromatic channels. Photoreceptor abnormality is not likely to have affected the evoked response, as photopic ERGs were normal at all ages in this infant, and the evoked response remained abnormal in the presence of a normal scotopic ERG after treatment. VEP abnormalities are unlikely to reflect a lack of attention to the stimuli, as this finding occurred consistently in response to all stimuli at all test sessions.

This previously unreported finding has implications for visual development in infants with cystic fibrosis. Further investigation is required, to determine whether visual function is abnormal in a larger number of such infants, and whether appropriate treatment restores visual

function to normal levels.

10.6 Conclusions

Short-wavelength-sensitive cones and the S-cone opponent neural pathway are functional by 4 to 10 weeks post-term age. The age of onset shows considerable inter-individual variation, and the likely explanation for this is that precise developmental age from conception is generally unknown in human infants. Function of the L-M opponent pathway is demonstrated at the slightly later age range of 6 to 11 weeks post-term. This difference between the two colour-opponent pathways is due at least in part to the considerable spectral overlap of L and M cones.

During the first two to three months of post-natal development, the colour-opponent and luminance post-receptor pathways mature at similar rates. Colour-opponent pathways are functional at a later age, however, than the luminance pathway, and this difference does not appear to be entirely due to cone contrast levels.

Taken together, the findings of this study demonstrate that, in the neonate, chromatic mechanisms are more limited than luminance mechanisms, but that after the age of functional onset all post-receptor pathways are limited to a similar degree. This pattern of maturation may reflect different stages of anatomical development of the retino-striate visual pathway, and abnormal patterns of maturation may occur in the presence of certain systemic pathological conditions.

Adelson, Edward H. Saturation and Adaptation in the Visual System. *Journal of Vision Research*. 1982; 22: 1299-1312.

Aguldas, M.; Stiles, W. S. Saturation of the Rod Mechanism of the Retina at High Levels of Stimulation. *Optica Acta*. 1954; 1(1): 59-63.

Alexander, Kenneth R. Color Vision Testing in Young Children: A Review. *American Journal of Optometry and Physiological Optics*. 1975a; 52: 332-335.

Alexander, Kenneth R. The Munsell Pediatric Color Perception Test as a Color Vision Screener: A Comparative Study. *American Journal of Optometry and Physiological Optics*. 1975b; 52: 318-319.

List of References

- Abramov, Israel; Gordon, James. Color Vision in the Peripheral Retina. 1. Spectral Sensitivity. *Journal of the Optical Society of America*. 1977; 67(2): 195-201.
- Abramov, Israel; Gordon, James; Hendrickson, Anita; Hainline, Louise; Dobson, Velma; LaBossiere, Eileen. Retina of the Newborn Human Infant. *Science*. 1982; 217: 265-267.
- Adams, R. J.; Maurer, D. Detection of Contrast by the Newborn and 2-Month-Old Infant. *Infant Behaviour and Development*. 1984; 7: 415-422.
- Adams, R. J.; Maurer, D.; Cashin, H. The Influence of Stimulus Size on Newborns' Discrimination of Chromatic from Achromatic Stimuli. *Vision Research*. 1990; 30: 2023-2030.
- Adams, Russell J.; Courage, Mary L.; Mercer, Michele E. Deficiencies in Human Neonates' Color Vision: Photoreceptoral and Neural Explanations. *Behavioural Brain Research*. 1991; 43: 109-114.
- Adams, Russell J.; Courage, Mary L.; Mercer, Michele E. Systematic Measurement of Human Neonatal Color Vision. *Vision Research*. 1994; 34(13): 1691-1701.
- Adelson, Edward H. Saturation and Adaptation in the Rod System. *Vision Research*. 1982; 22: 1299-1312.
- Aguilar, M.; Stiles, W. S. Saturation of the Rod Mechanism of the Retina at High Levels of Stimulation. *Optica Acta*. 1954; 1(1): 59-65.
- Alexander, Kenneth R. Color Vision Testing in Young Children: A Review. *American Journal of Optometry and Physiological Optics*. 1975a; 52: 332-337.
- Alexander, Kenneth R. The Titmus Pediatric Color Perception Test as a Color Vision Screener: A Comparative Study. *American Journal of Optometry and Physiological Optics*. 1975b; 52: 338-342.

Allen, Dale; Banks, Martin S.; Norcia, Anthony M. Does Chromatic Sensitivity Develop More Slowly Than Luminance Sensitivity? *Vision Research*. 1993; 33(17): 2553-2562.

Allen, Dale; Bennett, Patrick J.; Banks, Martin S. The Effects of Luminance on FPL and VEP Acuity in Human Infants. *Vision Research*. 1992; 32(11): 2005-2012.

Anstis, S.; Cavanagh, P. A Minimum Motion Technique for Judging Equiluminance *In Colour Vision Eds J.D. Mollon and L.T. Sharpe*. London: Academic Press; 1983.

Arden, G. B.; Gunduz, K.; Perry, S. Colour Vision Testing with a Computer Graphics System. *Clinical Vision Science*. 1988; 2(4): 303-320.

Arden, G. R.; Kolb, Helga. Electrophysiological Investigations in Retinal Metabolic Disease: Their Range and Application. *Experimental Eye Research*. 1964; 3: 334-347.

Arey, L. B. *Developmental Anatomy, a Textbook and Laboratory Manual of Embryology* 7th Ed. Philadelphia: Saunders; 1974.

Assaf, Ahmad A. The Sensitive Period: Transfer of Fixation after Occlusion for Strabismic Amblyopia. *British Journal of Ophthalmology*. 1982; 66: 64-70.

Atkinson, J. Early Visual Development: Differential Functioning of Parvocellular and Magnocellular Pathways. *Eye*. 1992; 6: 129-135.

Atkinson, J. Human Visual Development over the First 6 Months of Life: A Review and a Hypothesis. *Human Neurobiology*. 1984; 3(61-74).

Atkinson, J. Review of Human Visual Development: Crowding and Dyslexia *In Vision and Visual Dysfunction Vol. 13 Ed J.R. Cronley-Dillon*. Basingstoke: MacMillan Press Ltd.; 1991.

Banks, Martin S. The Development of Visual Accommodation During Early Infancy. *Child Development*. 1980; 51: 646-666.

Banks, Martin S. The Development of Spatial and Temporal Contrast Sensitivity. *Current Eye Research*. 1983; 2(3): 191-198.

Banks, Martin S.; Aslin, Richard N.; Letson, Robert D. Sensitive Period for the Development of Human Binocular Vision. *Science*. 1975; 190: 675-677.

Banks, Martin S.; Bennett, Patrick J. Optical and Photoreceptor Immaturities Limit the Spatial and Chromatic Vision of Human Neonates. *Journal of the Optical Society of America A*. 1988; 5(12): 2059-2079.

Banks, Martin S.; Dannemiller, James L. Infant Visual Psychophysics *In Handbook of Infant Perception, Volume 1*. New York: Academic Press; 1987.

Banks, Martin S.; Ginsburg, Arthur P. Infant Visual Preferences: A Review and New Theoretical Treatment *In Advances in Child Development and Behaviour Vol. 19*. New York: Academic Press; 1985.

Banks, Martin S.; Salapatek, Philip. Acuity and Contrast Sensitivity in 1-, 2-, and 3-Month-Old Human Infants. *Investigative Ophthalmology and Visual Science*. 1978; 17(4): 361-365.

Banks, Martin S.; Salapatek, Philip. Contrast Sensitivity Function of the Infant Visual System. *Vision Research*. 1976; 16: 867-869.

Banks, Martin S.; Salapatek, Philip. Infant Pattern Vision: A New Approach Based on the Contrast Sensitivity Function. *Journal of Experimental Child Psychology*. 1981; 31: 1-45.

Bembridge, B. A. The Problem of Myelination in the Central Nervous System with Special Reference to the Optic Nerve. *Transactions of the Ophthalmological Society UK*. 1956; 76: 311-322.

Berninger, T. A.; Arden, G. B.; Hogg, C. R.; Frumkes, T. Separable Evoked Retinal and Cortical Potentials from Each Major Visual Pathway: Preliminary Results. *British Journal of Ophthalmology*. 1989; 73: 502-511.

Bieber, Michelle L.; Volbrecht, Vicki J.; Werner, John S. Spectral Efficiency Measured by Heterochromatic Flicker Photometry is Similar in Human Infants and Adults. *Vision Research*. 1995; 35(10): 1385-1392.

Birch, David G.; Birch, Eileen E.; Hoffman, Dennis R.; Uauy, Ricardo D. Retinal Development in Very-Low-Birth-Weight Infants Fed Diets Differing in Omega-3 Fatty Acids. *Investigative Ophthalmology and Visual Science*. 1992b; 33(8): 2365-2375.

Birch, Eileen; Birch, David; Hoffman, Dennis; Hale, Linda; Everett, Mary; Uauy, Ricardo. Breast-Feeding and Optimal Visual Development. *Journal of Pediatric Ophthalmology and Strabismus*. 1993; 30: 33-38.

Birch, Eileen E.; Birch, David G.; Hoffman, Dennis R.; Uauy, Ricardo. Dietary Essential Fatty Acid Supply and Visual Acuity Development. *Investigative Ophthalmology and Visual Science*. 1992a; 33(11): 3242-3253.

Birch, J.; Platts, C. E. Colour Vision Screening in Children: an Evaluation of Three Pseudoisochromatic Tests. *Ophthalmic and Physiological Optics*. 1993; 13: 344-349.

Birch, Jennifer. *Diagnosis of Defective Colour Vision*. Oxford: Oxford University Press; 1993.

Birch, Jennifer; McKeever, Lisa M. Survey of the Accuracy of New Pseudoisochromatic Plates. *Ophthalmic and Physiological Optics*. 1993; 13: 35-40.

Boettner, Edward A.; Wolter, J. Transmission of the Ocular Media. *Investigative Ophthalmology*. 1962; 1(6): 776-783.

Bone, Richard A.; Landrum, John T.; Fernandez, Lilia; Tarsis, Sara L. Analysis of the Macular Pigment by HPLC: Retinal Distribution and Age Study. *Investigative Ophthalmology and Visual Science*. 1988; 29(6): 843-849.

Bowmaker, J. K.; Dartnall, H. J. A. Visual Pigments of Rods and Cones in a Human Retina. *Journal of Physiology*. 1980; 298: 501-511.

Boynton, Robert M.; Kaiser, Peter K. Vision: The Additivity Law Made to Work for Heterochromatic Photometry with Bipartite Fields. *Science*. 1968; 161: 366-368.

- Braddick, Oliver. Binocularity in Infancy. *Eye*. 1996; 10: 182-188.
- Braddick, Oliver. Orientation and Motion-Selective Mechanisms in Infants *In Infant Vision: Basic and Clinical Research* Ed K. Simons. Oxford: Oxford University Press; 1993.
- Braddick, Oliver; Atkinson, Janette; French, Jennifer. A Photorefractive Study of Infant Accommodation. *Vision Research*. 1979; 19: 1319-1330.
- Braddick, Oliver; Atkinson, Janette; Hood, Bruce. Striate Cortex, Extrastriate Cortex and Colliculus: Some New Approaches *In Infant Vision* Eds F. Vital-Durand, J. Atkinson and O. Braddick. Oxford: Oxford University Press; 1996.
- Brindley, G. S.; DuCroz, J. J.; Rushton, W. A. H. The Flicker Fusion Frequency of the Blue-Sensitive Mechanism of Colour Vision. *Journal of Physiology*. 1966; 183: 497-500.
- Bronson, Gordon. The Postnatal Growth of Visual Capacity. *Child Development*. 1974; 45: 873-890.
- Brown, Angela M. Development of Visual Sensitivity to Light and Color Vision in Human Infants: A Critical Review. *Vision Research*. 1990; 30(8): 1159-1188.
- Brown, Angela M. Saturation of Rod-Initiated Signals in 2-Month-Old Human Infants. *Journal of the Optical Society of America A*. 1988; 5(12): 2145-2158.
- Brown, Angela M. Scotopic Sensitivity of the Two-Month-Old Human Infant. *Vision Research*. 1986; 26(5): 707-710.
- Brown, Angela M.; Dobson, Velma; Maier, Jennifer. Visual Acuity of Human Infants at Scotopic, Mesopic and Photopic Luminances. *Vision Research*. 1987; 27(10): 1845-1858.
- Brown, Angela M.; Lindsey, Delwin T.; McSweeney, Elaine M.; Walters, Melissa M. Infant Luminance and Chromatic Contrast Sensitivity: Optokinetic Nystagmus Data on 3-Month-Olds. *Vision Research*. 1995; 35(22): 3145-3160.

Brown, Angela M.; Teller, Davida Y. Chromatic Opponency in 3-Month-Old Human Infants. *Vision Research*. 1989; 29(1): 37-45.

Burkhalter, Andreas; Bernardo, Kerry L.; Charles, Vinod. Development of Local Circuits in Human Visual Cortex. *The Journal of Neuroscience*. 1993; 13(5): 1916-1931.

Burr, David C.; Morrone, M. C.; Fiorentini, Adriana. Development of Infant Contrast Sensitivity and Acuity for Coloured Patterns *In From Pigments to Perception Eds A. Valberg and B.B. Lee*. New York: Plenum Press; 1991.

Burr, David C.; Morrone M.C.; Fiorentini, Adriana. Spatial and Temporal Properties of Infant Colour Vision *In Infant Vision Eds F. Vital-Durand, J. Atkinson and O. Braddick*. Oxford: Oxford University Press; 1996.

Campbell, F. W.; Maffei, L. Electrophysiological Evidence for the Existence of Orientation and Size Detectors in the Human Visual System. *Journal of Physiology*. 1970; 207: 635-652.

Capilla, P.; Aguilar, M. Red-Green Flicker Resolution as a Function of Heterochromatic Luminous Modulation. *Ophthalmic and Physiological Optics*. 1993; 13: 183-185.

Carden, D.; Hilken, H.; Butler, S. R.; Kulikowski, J. J. Lesions of Primate Visual Area V4 Produce Long-Lasting Deficits to Colour Constancy. *The Irish Journal of Psychology*. 1992; 13(4): 455-472.

Carney, Elizabeth A.; Russell, Robert M. Correlation of Dark Adaptation Test Results with Serum Vitamin A Levels in Diseased Adults. *Journal of Nutrition*. 1980; 110: 552-557.

Clavadetscher, John E.; Brown, Angela M.; Ankrum, Corlene; Teller, Davida Y. Spectral Sensitivity and Chromatic Discriminations in 3- and 7-Week-Old Human Infants. *Journal of the Optical Society of America A*. 1988; 5(12): 2093-2105.

Cole, Graeme R.; Hine Trevor. Computation of Cone Contrasts for Color Vision Research. *Behavior Research Methods, Instruments, and Computers*. 1992; 24(1): 22-27.

Coren, Stanley; Girgus, Joan S. Density of Human Lens Pigmentation: *In Vivo* Measures Over an Extended Age Range. *Vision Research*. 1972; 12: 343-346.

Courage, M.; Friel, J.; Andrew, W.; McCloy, U.; Adams, R. Dietary Fatty Acids and the Development of Visual Acuity in Human Infants. *Investigative Ophthalmology and Visual Science*. 1995; 36(4): S48.

Cowan, W. M. The Development of the Brain. *Scientific American*. 1979; 241: 107-116.

Crognale, Michael A.; Switkes, Eugene; Rabin, Jeff; Schneck, Marilyn E.; Haegerstrom-Portnoy, Gunilla; Adams, Anthony J. Application of the Spatiochromatic Visual Evoked Potential to Detection of Congenital and Acquired Color-Vision Deficiencies. *Journal of the Optical Society of America A*. 1993; 10(8): 1818-1825.

Daniel, P. M.; Whitteridge, D. The Representation of the Visual Field on the Cerebral Cortex in Monkeys. *Journal of Physiology*. 1961; 159: 203-221.

DeMonasterio, F. M.; Gouras, P. Functional Properties of Ganglion Cells of the Rhesus Monkey Retina. *Journal of Physiology*. 1975; 251: 167-195.

Derrington, A. M.; Krauskopf, J.; Lennie, P. Chromatic Mechanisms in Lateral Geniculate Nucleus of Macaque. *Journal of Physiology*. 1984; 357: 241-265.

Desimone, Robert; Schein, Stanley J.; Moran, Jeffrey; Ungerleider, Leslie G. Contour, Color and Shape Analysis Beyond the Striate Cortex. *Vision Research*. 1985; 25(3): 441-452.

DeValois, R. L.; Pease, P. L. Contours and Contrast: Response of Monkey Lateral Geniculate Nucleus Cells to Luminance and Color Figures. *Science*. 1971; 171: 694-696.

Diaz-Araya, Claudia; Provis, Jan M. Evidence of Photoreceptor Migration during Early Foveal Development: A Quantitative Analysis of Human Fetal Retinae. *Visual Neuroscience*. 1992; 8: 505-514.

Dobelle, W. H.; Turkel, Joseph; Henderson, David C.; Evans, Jerald R. Mapping the Representation of the Visual Field by Electrical Stimulation of Human Visual Cortex. *American Journal of Ophthalmology*. 1979; 88: 727-735.

Dobson, Velma. Spectral Sensitivity of the 2-Month Infant as Measured by the Visually Evoked Cortical Potential. *Vision Research*. 1976; 16: 367-374.

Dobson, Velma; Teller, Davida Y. Visual Acuity in Human Infants: A Review and Comparison of Behavioural and Electrophysiological Studies. *Vision Research*. 1978; 18: 1469-1483.

Dow, Bruce M. Colour Vision *In* Vol 4 of *Vision and Visual Dysfunction* Ed A.G. Leventhal *Series* Ed J.R. Cronley-Dillon. Oxford: MacMillan Press; 1991.

Drasdo, N. The Neural Representation of Visual Space. *Nature*. 1977; 266(5602): 554-556.

Dratz, E. A.; Ryba, N.; Watts, A. Studies of the Essential Role of Docosahexaenoic Acid (DHA), 22:omega3, in Visual Excitation. *Investigative Ophthalmology and Visual Science*. 1987; 28: S96.

Duke-Elder, S. The Anatomy of the Visual System *In* *System of Ophthalmology* Vol 2. London: Kimpton; 1961.

D'Zmura, M.; Lennie, P. Shared Pathways for Rod and Cone Vision. *Vision Research*. 1986; 26(8): 1273-1280.

Ellingson, R. J. Electroencephalograms of Normal, Full-term Newborns immediately after birth with observations on Arousal and Visual Evoked Responses. *Electroencephalography and Clinical Neurophysiology*. 1958; 10: 31-50.

Esakowitz, L.; Kriss, A.; Shawkat, F. A Comparison of Flash Electroretinograms Recorded from Burian Allen, Jet, C-Glide, Gold Foil, DTL and Skin Electrodes. *Eye*. 1993; 7: 169-171.

Estevez, O.; Spekreijse, H. The "Silent Substitution" Method in Visual Research. *Vision Research*. 1982; 22: 681-691.

Fantz, R. L. Visual Perception from Birth as Shown by Pattern Selectivity. *Annals of the New York Academy of Sciences*. 1965; 118: 793-814.

Ferrera, Vincent P.; Nealey, Tara A.; Maunsell John H.R. Mixed Parvocellular and Magnocellular Geniculate Signals in Visual Area V4. *Nature*. 1992; 358: 756-758.

Ferrera, Vincent P.; Nealey, Tata A.; Maunsell, John H. R. Responses in Macaque Visual Area V4 Following Inactivation of the Parvocellular and Magnocellular LGN Lesions. *The Journal of Neuroscience*. 1994; 14(4): 2080-2088.

Fiorentini, Adriana; Burr, David C.; Morrone, M. C. Temporal Characteristics of Colour Vision: VEP and Psychophysical Measurements *In From Pigments to Perception Eds A. Valberg and B.B. Lee*. New York: Plenum Press; 1991.

Flanagan, Patrick; Cavanagh, Patrick; Favreau, Olga. Independent Orientation-selective Mechanisms for the Cardinal Directions of Colour Space. *Vision Research*. 1990; 30(5): 769-778.

Flitcroft, D. I. The Interactions Between Chromatic Aberration, Defocus and Stimulus Chromaticity: Implications for Visual Physiology and Colorimetry. *Vision Research*. 1989; 29(3): 349-360.

Ford, E. H. R. The Growth of the Foetal Skull. *Journal of Anatomy*. 1956; 90: 63-72.

Goodman, DeWitt S. Vitamin A Metabolism and the Liver *In The Liver: Biology and Pathobiology 2nd Edition Eds I.M. Arias, W.B. Jacoby, H. Popper, D. Schachter and D.A. Shafritz*. New York: Raven Press; 1988.

- Gotz, M. H.; Stur, O. B. Recent Advances in Cystic Fibrosis Research *In* Monographs in Paediatrics Vol 10 *Eds* F. Falkner, N. Kretchmer and E. Rossi. Basel: Karger; 1978.
- Gouras, P. Identification of Cone Mechanisms in Monkey Ganglion Cells. *Journal of Physiology*. 1968; 199: 533-547.
- Gouras, P. Cortical Mechanisms of Colour Vision *In* Vol 6 of Vision and Visual Dysfunction *Ed* P. Gouras *Series Ed* J.R. Cronley-Dillon. Oxford: MacMillan Press; 1991.
- Gouras, P.; Kruger, J. Responses of Cells in Foveal Visual Cortex of the Monkey to Pure Colour Contrast. *Journal of Neurophysiology*. 1979; 42: 850-860.
- Gouras, P.; Zrenner, E. Enhancement of Luminance Flicker by Color-Opponent Mechanisms. *Science*. 1979; 205: 587-589.
- Graham, Ben V.; Holland, Richard; Sparks, David L. Relative Spectral Sensitivity to Short Wavelength Light in the Peripheral Visual Field. *Vision Research*. 1975; 15: 313-316.
- Grose, J.; Harding, G. F. A.; Wilton, A. Y.; Bissenden, J. G. The Maturation of the Pattern Reversal VEP and Flash ERG in Pre-Term Infants. *Clinical Vision Science*. 1989; 4(3): 239-246.
- Grose, Jillian; Harding, Graham. The Development of Refractive Error and Pattern Visually Evoked Potentials in Pre-Term Infants. *Clinical Vision Science*. 1990; 5(4): 375-382.
- Ham, William T.; Ruffolo, John J.; Mueller, H. A.; Clarke, A. M.; Moon, M. E. Histologic Analysis of Photochemical Lesions Produced in Rhesus Retina by Short-Wavelength-Light. *Investigative Ophthalmology and Visual Science*. 1978; 17(10): 1029-1035.
- Hamer, Russell D.; Alexander, Kenneth R.; Teller, Davida Y. Rayleigh Discriminations in Young Human Infants. *Vision Research*. 1982; 22: 575-587.

- Hansen, Ronald M.; Fulton, Anne B. Psychophysical Estimates of Ocular Media Density of Human Infants. *Vision Research*. 1989; 29(6): 687-690.
- Harding, G. F. A.; Grose, J.; Wilton, A.; Bissenden, J. G. The Pattern Reversal VEP in Short-Gestation Infants. *Electroencephalography and Clinical Neurophysiology*. 1989; 74: 76-80.
- Haynes, H.; White, B. L.; Held, R. Visual Accommodation in Human Infants. *Science*. 1965; 148: 528-530.
- Hendrickson, Anita. A Morphological Comparison of Foveal Development in Man and Monkey. *Eye*. 1992; 6: 136-144.
- Hendrickson, Anita E.; Youdelis, Cristine. The Morphological Development of the Human Fovea. *Ophthalmology*. 1984; 91(6): 603-612.
- Hickey, T. L.; Peduzzi, J. D. Structure and Development of the Visual System *In Handbook of Infant Perception, Volume 1*. New York: Academic Press; 1987.
- Horton, Jonathan C.; Hoyt, William F. The Representation of the Visual Field in Human Striate Cortex. *Archives of Ophthalmology*. 1991; 109: 816-824.
- Hubel, David H. *Eye, Brain and Vision*. New York: Scientific American Library; 1988.
- Hubel, David H. *Eye, Brain and Vision*. New York: Scientific American Library; 1995.
- Hubel, David H.; Livingstone, Margaret S. Complex-unoriented Cells in a Subregion of Primate Area 18. *Nature*. 1985; 315: 325-327.
- Ikeda, Hisako. Clinical Electroretinography *In Evoked Potentials in Clinical Testing*. Singapore *Ed* A.M. Halliday: Longman; 1993.
- Innis, Sheila M.; Nelson, Carolanne M.; Rioux, M. F.; King, D. J. Development of Visual Acuity in Relation to Plasma and Erythrocyte

omega-6 and omega-3 Fatty Acids in Healthy Term Gestation Infants. *American Journal of Clinical Nutrition*. 1994; 60: 347-352.

Jacobs, Gerald H.; Neitz, Jay. Inheritance of Color Vision in a New World Monkey. *Proceedings of the National Academy of Science, USA*. 1987; 84: 2545-2549.

Kaiser, P. K.; Boynton, R. M. *Human Color Vision*. Washington D.C.: Optical Society of America; 1996.

Kaiser, Peter K. Visual Photometry: Relating Psychophysics to Some Aspects of Neurophysiology *In From Pigments to Perception Eds A. Valberg and B.B. Lee*. New York: Plenum Press; 1991.

Kingdom, Frederick A. A.; Mullen, Kathy T. Separating Colour and Luminance Information in the Visual System. *Spatial Vision*. 1995; 9(2): 191-219.

Kinnear, P. R. Proposals for Scoring and Assessing the 100-Hue Test. *Vision Research*. 1970; 10: 423-433.

Kinney, Jo Ann S.; McKay, Christine L. Test of Color-Defective Vision Using the Visual Evoked Response. *Journal of the Optical Society of America*. 1974; 64(9): 1244-1250.

Korth, M.; Nguyen, N. X.; Rix, R.; Sembritzki, O. Interactions of Spectral, Spatial, and Temporal Mechanisms in the Human Pattern Visual Evoked Potential. *Vision Research*. 1993; 33(17): 2397-2411.

Krauskopf, John; Williams, David R.; Heeley, David W. Cardinal Directions of Color Space. *Vision Research*. 1982; 22: 1123-1131.

Kriss, A. Recording Technique *In Evoked Potentials in Clinical Testing Ed A.M. Halliday*. Singapore: Longman; 1993.

Kriss, A. Skin ERGs: Their Effectiveness in Paediatric Visual Assessment, Confounding Factors, and Comparison with ERGs Recorded Using Various Types of Corneal Electrode. *International Journal of Psychophysiology*. 1994; 16: 137-146.

Kruger, J.; Gouras, P. Spectral Selectivity of Cells and its Dependence on Slit Length in Monkey Visual Cortex. *Journal of Neurophysiology*. 1980; 43: 1055-1069.

Kulikowski, J. J. On the Nature of Visual Evoked Potentials, Unit Responses and Psychophysics *In From Pigments to Perception Eds A. Valberg and B.B. Lee*. New York: Plenum Press; 1991.

Kulikowski, J. J. Visual Evoked Potentials as a Measure of Visibility *In Visual Evoked Potentials in Man: New Developments Ed J.E. Desmedt*. Oxford: Clarendon Press; 1977.

Kulikowski, J. J.; Murray, I. J.; Russell, M. H. A. Effect of Stimulus Size on Chromatic and Achromatic VEPs *In Colour Vision Deficiencies X Eds B. Drum, J.D. Moreland and A. Serra*. Dordrecht: Kluwer Academic; 1991.

Kulikowski, J. J.; Murray, I. J.; Parry, N. R. A. Electrophysiological Correlates of Chromatic-Opponent and Achromatic Stimulation in Man *In Colour Vision Deficiencies IX Eds B. Drum and G. Verriest*. Dordrecht: Kluwer Academic; 1989.

Kulikowski, J. J.; Robson, A. G. Selectivity and Variability of Visual Cortical Responses to Chromatic Stimulation. *Investigative Ophthalmology and Visual Science*. 1996; 37(3): S670.

Kulikowski, J. J.; Robson, Anthony G.; McKeefry, Declan J. Specificity and Selectivity of Chromatic Visual Evoked Potentials. *Vision Research*. 1996; 36(21): 3397-3401.

Kulikowski, J. J.; Walsh, V. Colour Vision: Isolating Mechanisms in Overlapping Streams *In Progress in Brain Research Vol. 95 Eds T.P. Hicks, S. Molotchnikoff and T. Ono*. London: Elsevier Science; 1993.

Kulikowski, J. J.; Walsh, V. Limits of Vision *In Vision and Visual Dysfunction Eds J.J. Kulikowski, V. Walsh and I.J. Murray*. London: Macmillan Press; 1991.

Lee, B. B.; Valberg, A.; Tigwell, D. A.; Tryti, J. An Account of Spectrally Opponent Neurons in Macaque Lateral Geniculate Nucleus to

Successive Contrast. Proceedings of the Royal Society of London B. 1987; 230: 293-314.

Lennie, Peter; D'Zmura, Michael. Mechanisms of Color Vision. CRC Critical Reviews in Neurobiology. 1988; 3(4): 333-400.

Lennie, Peter; Krauskopf, John; Sclar, Gary. Chromatic Mechanisms in Striate Cortex of Macaque. The Journal of Neuroscience. 1990; 10(2): 649-669.

Leventhal, Audie G.; Rodieck, R. W.; Dreher, B. Retinal Ganglion Cell Classes in the Old World Monkey: Morphology and Central Projections. Science. 1981; 213: 1139-1142.

Livingstone, Margaret S.; Hubel, David H. Specificity of Cortico-cortical Connections in Monkey Visual System. Nature. 1983; 304: 531-534.

Logothetis, N. K.; Schiller, P. H.; Charles, E. R.; Hurlbert, A. C. Perceptual Deficits and the Activity of the Color-Opponent and Broad-Band Pathways at Isoluminance. Science. 1990; 247: 214-217.

Macaluso, Claudio; Baratta, Giovanni; Lamedica, Alessandro; Luani, Davide; Cordella, Marco. Visual Evoked Cortical Potentials and Psychophysical Determination of Color Contrast Thresholds Along Different Chromatic Axis. Documenta Ophthalmologica. 1995; 90: 201-209.

Macleod, D. I. A.; Boynton, Robert M. Chromaticity Diagram Showing Cone Excitation by Stimuli of Equal Luminance. Journal of the Optical Society of America. 1979; 69(8): 1183-1186.

Magoon, Elbert H.; Robb, Richard M. Development of Myelin in Human Optic Nerve and Tract. Archives of Ophthalmology. 1981; 99: 655-659.

Makrides, M.; Simmer, K.; Goggin, M.; Gibson, R. A. Erythrocyte Docosahexaenoic Acid Correlates with the Visual Response of Healthy, Term Infants. Pediatric Research. 1993; 33(4): 425-427.

Makrides, Maria; Neumann, Mark A.; Byard, Roger W.; Simmer, Karen; Gibson, Robert A. Fatty Acid Composition of Brain, Retina, and

Erythrocytes in Breast- and Formula-fed Infants. *American Journal of Clinical Nutrition*. 1994; 60: 189-194.

Mallet, R. The Management of Binocular Vision Anomalies *In Optometry* Eds K. Edwards and R. Llewellyn. London: Butterworths; 1988.

Mann, I. C. The Development of the Human Eye. London: British Medical Association; 1964.

Mantylarvi, Maija. Colour Vision Testing in Pre-School-Aged Children. *Ophthalmologica*. 1991; 202: 147-151.

Marg, Elwin; Freeman, Donald N.; Peltzman, Philip; Goldstein, Phillip J. Visual Acuity Development in Human Infants: Evoked Potential Measurements. *Investigative Ophthalmology*. 1976; 15(2): 150-153.

Maunsell, J. H. R.; Nealey, T. A.; DePriest, D. D. Magnocellular and Parvocellular Contributions to Responses in the Middle Temporal Visual Area (MT) of the Macaque Monkey. *Journal of Neuroscience*. 1990; 10: 3323-3334.

Mayer, D. L.; Moore, Bruce; Robb, Richard M. Assessment of Vision and Amblyopia by Preferential Looking Tests after Early Surgery for Unilateral Congenital Cataracts. *Journal of Pediatric Ophthalmology and Strabismus*. 1989; 26(2): 61-68.

McCann, John J.; Benton, Jeanne L. Interaction of the Long-Wave Cones and the Rods to Produce Color Sensations. *Journal of the Optical Society of America*. 1969; 59(1): 103-107.

McCulloch, Daphne L.; Skarf, B. Development of the Human Visual System: Monocular and Binocular Pattern VEP Latency. *Investigative Ophthalmology and Visual Science*. 1991; 32(8): 2372-2381.

Merigan, William H. P and M Pathway Specialization in the Macaque *In From Pigments to Perception* Eds A. Valberg and B.B. Lee. New York: Plenum Press; 1991.

Michael, G. R. Color Vision Mechanisms in Monkey Striate Cortex: Dual-Opponent Cells with Concentric Receptive Fields. *Journal of Neurophysiology*. 1978; 41: 572-588.

Mitchell, D. E. Sensitive Periods in Visual Development: Insights Gained from Studies of Recovery of Visual Function in Cats Following Early Monocular Deprivation or Cortical Lesions *In Vision: Coding and Efficiency* Ed C. Blakemore. Cambridge: Cambridge University Press; 1990.

Mollon, J. Color Vision *In Annual Review of Psychology* Volume 33 Eds Rosenzweig, Mark R//Porter, Lyman W. California: Annual Reviews Inc; 1982.

Montag, Ethan D.; Boynton, Robert M. Rod Influence in Dichromatic Surface Color Perception. *Vision Research*. 1987; 27(12): 2153-2162.

Morrone, M. C.; Burr, David C.; Fiorentini, Adriana. Development of Contrast Sensitivity and Acuity of the Infant Colour System. *Proceedings of the Royal Society of London B*. 1990; 242: 134-139.

Morrone, M. C.; Burr, David C.; Fiorentini, Adriana. Development of Infant Contrast Sensitivity to Chromatic Stimuli. *Vision Research*. 1993; 33(17): 2535-2552.

Moskowitz-Cook, Anne. The Development of Photopic Spectral Sensitivity in Human Infants. *Vision Research*. 1979; 19: 1133-1142.

Moskowitz, Anne; Sokol, Samuel. Developmental Changes in the Human Visual System as Reflected by the Latency of the Pattern Reversal VEP. *Electroencephalography and Clinical Neurophysiology*. 1983; 56: 1-15.

Movshon, J. A.; Kiorpes, Lynne. Analysis of the Development of Spatial Contrast Sensitivity in Monkey and Human Infants. *Journal of the Optical Society of America A*. 1988; 5(12): 2166-2172.

Mullen, K. T.; Kingdom, F. A. A., Colour Contrast in Form Perception *In Vision and Visual Dysfunction* Vol 6 Ed P. Gouras. Oxford: MacMillan; 1991.

Mullen, Kathy T. The Contrast Sensitivity of Human Colour Vision to Red-Green and Blue-Yellow Chromatic Gratings. *Journal of Physiology*. 1985; 359: 381-400.

Murray, I. J.; Parry, N. R. A.; Carden, D.; Kulikowski, J. J. Human Visual Evoked Potentials to Chromatic and Achromatic Gratings. *Clinical Vision Science*. 1987; 1(3): 231-244.

Nathans, Jeremy; Piantanida, Thomas P.; Eddy, Roger L.; Shows, Thomas B.; Hogness, David S. Molecular Genetics of Inherited Variation in Human Color Vision. *Science*. 1986a 1; 232: 203-210.

Nathans, Jeremy; Thomas, Darcy; Hogness, David S. Molecular Genetics of Human Color Vision: The Genes Encoding Blue, Green and Red Pigments. *Science*. 1986b 2; 232: 193-202.

Neuringer, Martha; Connor, William E.; Van Petten, Cyma; Barstad, Louise. Dietary Omega-3 Fatty Acid Deficiency and Visual Loss in Infant Rhesus Monkeys. *Journal of Clinical investigation*. 1984; 73: 272-276.

Neuringer, Martha; Connor, William E. n-3 Fatty Acids in the Brain and Retina: Evidence for Their Essentiality. *Nutrition Reviews*. 1986; 44(9): 285-294.

Norcia, Anthony M.; Tyler, Christopher W.; Hamer, Russell D. Development of Contrast Sensitivity in the Human Infant. *Vision Research*. 1990; 30(10): 1475-1486.

Norcia, Anthony M.; Tyler, Christopher W.; Hamer, Russel D.; Wesemann, Wolfgang. Measurement of Spatial Contrast Sensitivity with the Swept Contrast VEP. *Vision Research*. 1989; 29(5): 627-637.

Norcia, Anthony M.; Tyler, Christopher W. Spatial Frequency Sweep VEP: Visual Acuity During the First Year of Life. *Vision Research*. 1985; 25(10): 1399-1408.

Norren, Dirk V.; Vos, Johannes J. Spectral Transmission of the Human Ocular Media. *Vision Research*. 1974; 14: 1237-1244.

Packer, Orin; Hartmann, E. E.; Teller, Davida Y. Infant Color Vision: The Effect of Test Field Size on Rayleigh Discriminations. *Vision Research*. 1984; 24(10): 1247-1260.

Pease, Paul L.; Adams, Anthony J.; Nuccio, Edward. Optical Density of Human Macular Pigment. *Vision Research*. 1987; 27(5): 705-710.

Peeples, David R.; Teller, Davida Y. Color Vision and Brightness Discrimination in Two-Month-Old Human Infants. *Science*. 1975; 189: 1102-1103.

Peeples, David R.; Teller, Davida Y. White-Adapted Photopic Spectral Sensitivity in Human Infants. *Vision Research*. 1978; 18: 49-53.

Perlman, I.; Barzilai, D.; Haim, T.; Schramek, A. Night Vision in a Case of Vitamin A Deficiency due to Malabsorption. *British Journal of Ophthalmology*. 1983; 67: 37-42.

Peterzell, David H.; Werner, John S.; Kaplan, Peter S. Individual Differences in Contrast Sensitivity Functions: the First Four Months of Life in Humans. *Vision Research*. 1993; 33(3): 381-396.

Peterzell, David H.; Werner, John S.; Kaplan Peter S. Individual Differences in Contrast Sensitivity Functions: Longitudinal Study of 4-, 6- and 8-Month-Old Human Infants. *Vision Research*. 1995; 35(7): 961-979.

Pokorny, Joel; Smith, Vivianne C.; Lutze, Margaret. Heterochromatic Modulation Photometry. *Journal of the Optical Society of America A*. 1989; 6(10): 1618-1623.

Powers, Maureen K.; Schneck, Marilyn; Teller, Davida Y. Spectral Sensitivity of Human Infants at Absolute Visual Threshold. *Vision Research*. 1981; 21: 1005-1016.

Pritchard, J. J.; Scott, J. H.; Girgis, F. G. The Structure and Development of Cranial and Facial Sutures. *Journal of Anatomy*. 1956; 90: 73-87.

Pulos, Elizabeth; Teller, Davida Y.; Buck, Steven L. Infant Color Vision: A Search for Short-Wavelength-Sensitive Mechanisms by Means of Chromatic Adaptation. *Vision Research*. 1980; 20: 485-493.

Rabin, Jeff; Switkes, Eugene; Crognale, Michael; Schneck, Marilyn E.; Adams, Anthony J. Visual Evoked Potentials in Three-Dimensional Color Space: Correlates of Spatio-chromatic Processing. *Vision Research*. 1994; 34(20): 2657-2671.

Reading, Veronica M.; Weale, R. A. Macular Pigment and Chromatic Aberration. *Journal of the Optical Society of America*. 1974; 64(2): 231-234.

Regan, D. Comparison of Transient and Steady-State Methods *In* Evoked Potentials *Ed* I. Bodis-Wollner. New York: New York Academy of Sciences; 1982.

Regan, D. Evoked Potentials Specific to Spatial Patterns of Luminance and Colour. *Vision Research*. 1973; 13: 2381-2402.

Regan, D.; Spekreijse, H. Evoked Potential Indications of Colour Blindness. *Vision Research*. 1974; 14: 89-95.

Reid, R. C.; Shapley, Robert M. Spatial Structure of Cone Inputs to Receptive Fields in Primate Lateral Geniculate Nucleus. *Nature*. 1992; 356: 716-717.

Reitner, Andreas; Sharpe, Lindsay T.; Zrenner, Eberhart. Wavelength Discrimination with only Rods and Blue Cones *In* From Pigments to Perception *Eds* A. Valberg and B.B. Lee. New York: Plenum Press; 1991.

Robb, Richard M. Regional Changes in Retinal Pigment Epithelial Cell Density During Ocular Development. *Investigative Ophthalmology and Visual Science*. 1985; 26(5): 614-620.

Robinson, S. R.; Hendrickson, A. Shifting Relationships Between Photoreceptors and Pigment Epithelial Cells in Monkey Retina: Implications for the Development of Retinal Topography. *Visual Neuroscience*. 1995; 12: 767-778.

Rodiek, R. W. Which Cells Code for Colour? *In* From Pigments to Perception *Eds* A. Valberg and B.B. Lee. New York: Plenum Press; 1991.

Rudduck, Gillian A.; Harding, Graham F. A. Visual Electrophysiology to Achromatic and Chromatic Stimuli in Premature and Full Term Infants. *International Journal of Psychophysiology*. 1994; 16: 209-218.

Russell, Robert M.; Smith, Vivianne C.; Multack, Richard; Krill, Alex E.; Rosenberg, Irwin H. Dark-Adaptation Testing for Diagnosis of Subclinical Vitamin-A Deficiency and Evaluation of Therapy. *The Lancet*. 1973; 2: 1161-1164.

Schiller, P. H.; Logothetis, N. K.; Charles, E. R. Functions of the Color-Opponent and Broad-Band Channels of the Visual System. *Nature*. 1990; 343: 68-70.

Schiller, P. H.; Malpeli, J. G.; Schein, S. J. Composition of Geniculostriate Input to Superior Colliculus of the Rhesus Monkey. *Journal of Neurophysiology*. 1979; 42(4): 1124-1133.

Schiller, P. H.; Malpeli, J. G. Functional Specificity of Lateral Geniculate Nucleus Laminae of the Rhesus Monkey. *Journal of Neurophysiology*. 1978; 41: 788-797.

Schiller, Peter H. The Color-Opponent and Broad-Band Channels of the Primate Visual System *In From Pigments to Perception Eds A. Valberg and B.B. Lee*. New York: Plenum Press; 1991.

Schiller, Peter H.; Malpeli, Joseph G. Properties and Tectal Projections of Monkey Retinal Ganglion Cells. *Journal of Neurophysiology*. 1977; 40(2): 428-445.

Schweitzer, F. C.; Prager, T. C.; Zou, Y.; Ruiz, R. S.; Chen, H.; Anderson, R. E.; Jensen, C. L.; Heird, W. C. Effect of 18:3 omega-3 Intake on Pattern Visual Evoked Potentials in Term Infants. *Investigative Ophthalmology and Visual Science*. 1995; 36(4): S48.

Shannon, Elizabeth; Skoczenski, Ann M.; Banks, Martin S. Retinal Illuminance and Contrast Sensitivity in Human Infants. *Vision Research*. 1996; 36(1): 67-76.

Shatz, Carla. The Developing Brain. *Scientific American*. 1992 Sep: 35-41.

Sherlock, A. J.; Roebuck, E. M.; Godfrey, M. G. *Calculus: Pure and Applied*. London: Edward Arnold; 1987.

Shiple, T.; Jones, R. W.; Fry, A. Evoked Visual Potentials and Human Colour Vision. *Science*. 1965; 150: 1162-1164.

Shipp, S.; Zeki, S. Segregation of Pathways Leading from Area V2 to Areas V4 and V5 of Macaque Monkey Visual Cortex. *Nature*. 1985; 315: 322-324.

Smith, Frank Rees; Goodman, DeWitt S. The Effects of Diseases of the Liver, Thyroid, and Kidneys on the Transport of Vitamin A in Human Plasma. *The Journal of Clinical Investigation*. 1971; 50: 2426-2436.

Smith, J. C.; Atkinson, J.; Anker, S.; Moore, A. T. A Prospective Study of Binocularity and Amblyopia in Strabismic Infants Before and After Corrective Surgery: Implications for the Human Critical Period. *Clinical Vision Science*. 1991; 6(5): 335-353.

Smith, V. C.; Pokorny, J. Spectral Sensitivity of the Foveal Cone Photopigments Between 400 and 500 nm. *Vision Research*. 1975; 15: 161-171.

Snodderley, D. M.; Auran, James D.; Delori, Francois C. The Macular Pigment. 2. Spatial Distribution in Primate Retinas. *Investigative Ophthalmology and Visual Science*. 1984a; 25(6): 674-685.

Snodderley, D. M.; Brown, Paul K.; Delori, Francois C.; Auran, James D. The Macular Pigment. 1. Absorbance Spectra, Localization, and Discrimination from Other Yellow Pigments in Primate Retinas. *Investigative Ophthalmology and Visual Science*. 1984b; 25(6): 660-673.

Soames, R. W. *Cranial Characteristics at Different Ages In Grays Anatomy*. London: Churchill Livingstone; 1995.

Sokol, S.; Moskowitz, A.; McCormack, G. Infant VEP and Preferential Looking Acuity Measured with Phase Alternating Gratings. *Investigative Ophthalmology and Visual Science*. 1992; 33(11): 3156-3161.

Sokol, Samuel. Measurement of Infant Visual Acuity from Pattern Reversal Evoked Potentials. *Vision Research*. 1978; 18: 33-39.

Stidwill, D. *Orthoptic Assessment and Management*. Oxford: Blackwell; 1990.

Stockman, Andrew; MacLeod, Donald I. A.; Lebrun, Stewart J. Faster Than the Eye Can See: Blue Cones Respond to Rapid Flicker. *Journal of the Optical Society of America A*. 1993; 10(6): 1396-1402.

Stone, Debra; Mathews, Steven; Kruger, Philip B. Accommodation and Chromatic Aberration: Effect of Spatial Frequency. *Ophthalmic and Physiological Optics*. 1993; 13: 244-252.

Suter, Penelope S.; Suter, Steve; Roessler, Jacqueline S.; Parker, Kerrie L. Spatial-Frequency-Tuned Channels in Early Infancy: VEP Evidence. *Vision Research*. 1994; 34(6): 737-745.

Swanson, William H.; Birch, Eileen E. Infant Spatiotemporal Vision: Dependence of Spatial Contrast Sensitivity on Temporal Frequency. *Vision Research*. 1990; 30(7): 1033-1048.

Switkes, Eugene; Crognale, Michael; Rabin, Jeff; Schneck, Marilyn E.; Adams, Anthony J. Reply to "Specificity and Selectivity of Chromatic Visual Evoked Potentials". *Vision Research*. 1996; 36(21): 3403-3405.

Teller, D. Y. The Forced-Choice Preferential Looking Procedure: A Psychophysical Technique for use with Human Infants. *Infant Behaviour and Development*. 1979; 2: 135-153.

Teller, Davida Y.; Bornstein, Marc H. Infant Color Vision and Color Perception *In Handbook of Infant Perception, Volume 1*. New York: Academic Press; 1987.

Teller, Davida Y.; Palmer, John. Infant Color Vision: Motion Nulls for Red/Green vs Luminance-modulated Stimuli in Infants and Adults. *Vision Research*. 1996; 36(7): 955-974.

Teller, Davida Y.; Peeples, David R.; Sekel, Michael. Discrimination of Chromatic from White Light by Two-Month-Old Human Infants. *Vision Research*. 1978; 18: 41-48.

Thibos, Larry N.; Bradley, Arthur; Zhang, Xiaoxiao. Effect of Ocular Chromatic Aberration on Monocular Visual Performance. *Optometry and Vision Science*. 1991; 68(8): 599-607.

Thompson, D. A.; Drasdo, N. An Improved Method for Using the DTL Fibre in Electroretinography. *Ophthalmic and Physiological Optics*. 1987; 7(3): 315-319.

Thompson, Dorothy A.; Drasdo, Neville. Colour, Contrast and the Visual Evoked Potential. *Ophthalmic and Physiological Optics*. 1992; 12: 225-228.

Tootell, Roger B. H.; Silverman, Martin S.; Hamilton, Susan L.; DeValois, Russell L.; Switkes, Eugene. Functional Anatomy of Macaque Striate Cortex. 3. Color. *The Journal of Neuroscience*. 1988; 8(5): 1569-1593.

Tyler, Christopher W. Visual Acuity Estimation in Infants by Visual Evoked Cortical Potentials *In Principles and Practice of Clinical Electrophysiology of Vision* Eds J.R. Heckenlively and G.B. Arden. London: Mosby; 1991.

Tyler, Christopher W.; Apkarian, Patricia; Levi, Dennis M.; Nakayama, K. Rapid Assessment of Visual Function: an Electronic Sweep Technique for the Pattern Visual Evoked Potential. *Investigative Ophthalmology and Visual Science*. 1979; 18(7): 703-713.

Uauy, Ricardo D.; Birch, David G.; Birch, Eileen E.; Tyson, Jon E.; Hoffman, Dennis R. Effect of Dietary Omega-3 Fatty Acids on Retinal Function of Very-Low-Birth-Weight Neonates. *Pediatric Research*. 1990; 28(5): 485-492.

Ueno, Takehiro. Sustained and Transient Properties of Chromatic and Luminance Systems. *Vision Research*. 1992; 32(6): 1055-1065.

van der Broek, S. P. Volume Conduction Effects in EEG and MEG, unpublished PhD Thesis. The Netherlands: University of Twente; 1997.

Varner, D.; Cook, James E.; Schneck, Marilyn E.; McDonald, Mary Alice; Teller, Davida Y. Tritan Discriminations by 1- and 2-Months-Old Human Infants. *Vision Research*. 1985; 25(6): 821-831.

Vautin, R. G.; Dow, B. M. Color Cell Groups in Foveal Striate Cortex of the Behaving Macaque. *Journal of Neurophysiology*. 1985; 54(2): 273-292.

Volbrecht, Vicki J.; Werner, John S. Isolation of Short-Wavelength-Sensitive Cone Photoreceptors in 4-6-Week-Old Human Infants. *Vision Research*. 1987; 27(3): 469-478.

Vos, J. J.; Walraven, P. L. On the Derivation of the Foveal Receptor Primaries. *Vision Research*. 1970; 11: 799-818.

Wald, G. Human Vision and the Spectrum. *Science*. 1945; 101: 653-658.

Walsh, V.; Carden, D.; Butler, S. R.; Kulikowski, J. J. The Effects of V4 Lesions on the Visual Abilities of Macaques: Hue Discrimination and Colour Constancy. *Behavioural Brain Research*. 1993; 53: 51-62.

Walsh, V.; Kulikowski, J. J.; Butler, S. R.; Carden, D. The Effects of Lesions of Area V4 on the Visual Abilities of Macaques: Colour Categorization. *Behavioural Brain Research*. 1992; 52: 81-89.

Warner, J. O. *British Medical Bulletin 48: Cystic Fibrosis*. New York: Churchill Livingstone; 1992.

Wattam-Bell, John. Coherence Thresholds for Discrimination of Motion Direction in Infants. *Vision Research*. 1994; 34(7): 877-883.

Wattam-Bell, John R. B. Development of Visual Motion Processing *In* Infant Vision *Eds* F. Vital-Durand, J. Atkinson and O. Braddick. Oxford: Oxford University Press; 1996.

Werner, J. S. Development of Scotopic Sensitivity and the Absorption Spectrum of the Human Ocular Media. *Journal of the Optical Society of America*. 1982; 72: 247-258.

Werner, John S.; Donnelly, Seaneen K.; Kliegl, Reinhold. Aging and Human Macular Pigment Density. *Vision Research*. 1987; 27(2): 257-268.

Wiesel, T. N.; Hubel, D. H. Effects of Visual Deprivation on Morphology and Physiology of Cells in the Cat's Lateral Geniculate Body. *Journal of Neurophysiology*. 1963; 26: 978-993.

Wiesel, T. N.; Hubel, D. H. Spatial and Chromatic Interactions in the Lateral Geniculate Body of the Rhesus Monkey. *Journal of Neurophysiology*. 1966; 29: 1115-1156.

Wiesel, Torsten N. Postnatal Development of the Visual Cortex and the Influence of Environment. *Nature*. 1982; 299: 583-591.

Williams, P.; Warwick, R.; Dyson, M.; Bannister, L. H. *Grays Anatomy*. London: Churchill Livingstone; 1989.

Wilson, Hugh R. Development of Spatiotemporal Mechanisms in Infant Vision. *Vision Research*. 1988; 28(5): 611-628.

Wong-Riley, Margaret T. T.; Hevner, Robert F.; Cutlan, Robert; Earnest, Melissa; Egan, Robert; Frost, Julie; Nguyen, Thuytien. Cytochrome Oxidase in the Human Visual Cortex: Distribution in the Developing and the Adult Brain. *Visual Neuroscience*. 1993; 10: 41-58.

Wooten, B. R. Photopic and Scotopic Contributions to the Human Visually Evoked Cortical Potential. *Vision Research*. 1972; 12: 1647-1660.

Wright, Christine E.; Drasdo, Neville; Harding, Graham F. A. Pathology of the Optic Nerve and Visual Association Areas. *Brain*. 1987; 110: 107-120.

Wysecki, G.; Stiles, W. S. *Color Science: Concepts and Methods, Quantitative Data and Formulae* 2nd Ed. New York: Wiley; 1982.

Youdelis, Christine; Hendrickson, Anita. A Qualitative and Quantitative Analysis of the Human Fovea During Development. *Vision Research*. 1986; 26(6): 847-855.

Zanker, Johannes M.; Mohn, Gesine. On the Development of Motion Perception in Human Infants. *Clinical Vision Science*. 1993; 8(1): 63-71.

Zeki, S. M. Colour Coding in Rhesus Monkey Prestriate Cortex. *Brain Research*. 1973; 53: 422-427.

Zeki, S. M. Colour Coding in the Cerebral Cortex: The Reaction of Cells in Monkey Visual Cortex to Wavelengths and Colours. *Neuroscience*, 1983; 9: 741-765.

Zeki, S. The Representation of Colours in the Cerebral Cortex. *Nature*, 1980; 284: 412-418.

Zielinski, B. S.; Hendrickson, A. E. Development of Synapses in Macaque Monkey Striate Cortex. *Visual Neuroscience*, 1992; 8: 491-504.

where: L, M and S are cone excitation values of long-, medium- and short-wavelength-sensitive cone types respectively, Z is luminance of the chromatic grating in question and x and y are CIE co-ordinates of the chromatic grating. At photometric illuminance, the value of Z is 20, for both gratings. At other colour ratios, the appropriate values were substituted for luminance of each grating.

After cone excitation values are calculated for each grating of a heterochromatic stimulus, these values are used to calculate cone contrast of that stimulus for each cone type as follows:

$$C_L = (L_1 - L_2) / L_1$$

$$C_M = (M_1 - M_2) / M_1$$

$$C_S = (S_1 - S_2) / S_1$$

where: C_L , C_M and C_S are cone contrast values and L_1 , M_1 and S_1 are cone excitation values of each of the two gratings of a heterochromatic stimulus.

APPENDIX 1

Calculation of Cone Contrast

Cone contrasts for chromatic stimuli were calculated using the Cole and Hine (1992) formulae using CIE x,y co-ordinates and luminance of each chromatic grating:

Green grating:

$$L = Z [0.15514x/y + 0.54312 - 0.03286(1-x-y)/y]$$

$$M = Z [-0.15514x/y + 0.45684 + 0.03286(1-x-y)/y]$$

$$S = Z [0.00801(1-x-y)/y]$$

where: L, M and S are cone excitation values of long-, medium- and short-wavelength-sensitive cone types respectively, Z is luminance of the chromatic grating in question and x and y are CIE co-ordinates of the chromatic grating. At photometric isoluminance, the value of Z is 20, for both gratings. At other colour ratios, the appropriate values were substituted for luminance of each grating.

After cone excitation values are calculated for each grating of a heterochromatic stimulus, these values are used to calculate cone contrast of that stimulus for each cone type as follows:

$$L = 20 [0.15514 (0.26/0.22) + 0.54312 - 0.03286(1 - 0.26 - 0.22)/0.22]$$

$$= 20 [0.15514 (1.1818) + 0.54312 - 0.07767]$$

$$C_L = (L_1 - L_2) / L_1$$

$$C_M = (M_1 - M_2) / M_1$$

$$C_S = (S_1 - S_2) / S_1$$

$$M = 20 [-0.15514 (0.26/0.22) + 0.45684 + 0.03286(1 - 0.26 - 0.22)/0.22]$$

$$= 20 [-0.15514 (1.1818) + 0.45684 + 0.07767]$$

where: C_L , C_M and C_S are cone contrast values and subscripts denote cone excitation values of each of the two gratings of a heterochromatic stimulus.

$$S = 20 [0.00801(1 - 0.26 - 0.22)/0.22]$$

$$= 20 [0.00801(2.36)]$$

$$= 0.379$$

Example calculation:

To calculate the L, M and S cone contrasts of the isoluminant Tritan stimulus at maximum contrast:

Green grating:

$$\begin{aligned}L &= 20 [0.15514 (0.36/0.45) + 0.54312 - 0.03286(1-0.36-0.45)/0.45] \\ &= 20 [0.124 + 0.54312 - 0.01387] \\ &= 13.065\end{aligned}$$

$$\begin{aligned}M &= 20 [-0.15514 (0.36/0.45) + 0.45684 + 0.03286(1-0.36-0.45)/0.45] \\ &= 20 [-0.124 + 0.45684 + 0.01387] \\ &= 6.934\end{aligned}$$

$$\begin{aligned}S &= 20 [0.00801(1-0.36-0.45)/0.45] \\ &= 20 [0.00801(0.01387)] \\ &= 0.06764\end{aligned}$$

Purple grating:

$$\begin{aligned}L &= 20 [0.15514 (0.26/0.22) + 0.54312 - 0.03286(1-0.26-0.22)/0.22] \\ &= 20 [0.183 + 0.54312 - 0.07767] \\ &= 12.969\end{aligned}$$

$$\begin{aligned}M &= 20 [-0.15514 (0.26/0.22) + 0.45684 + 0.03286(1-0.26-0.22)/0.22] \\ &= 20 [-0.183 + 0.45684 + 0.07767] \\ &= 7.03\end{aligned}$$

$$\begin{aligned}S &= 20 [0.00801(1-0.26-0.22)/0.22] \\ &= 20 [0.00801(2.36)] \\ &= 0.379\end{aligned}$$

pathways were chosen carefully to elicit responses from only one cone type. Initially, a blue-yellow heterochromatic stimulus was used. The CIE tristimulus values for this stimulus are:

$$C_L = (13.065 - 12.969) / 13.065$$

$$= 0.0073$$

to elicit responses from only one cone type.

$$= 0.73 \%$$

Initially, a blue-yellow heterochromatic stimulus was used.

blue phosphor for one green phosphor.

$$C_M = (7.03 - 6.934) / 7.03$$

$$= 0.014$$

itself composed of red and green phosphors.

$$= 1.4 \%$$

The CIE tristimulus values for this stimulus are:

$$C_S = (0.379 - 0.06764) / 0.379$$

$$= 0.82$$

$$= 82 \%$$

In order to generate trichromatic stimuli of equal luminance which selectively stimulate the S-cone system, a range of primary stimuli lying along a trichromatic cone system were chosen. This tritan stimulus, which was used in experiments reported in the main body of this thesis, is described below.

APPENDIX 2

Blue-Yellow Stimuli

Chromatic stimuli designed to selectively stimulate the colour-opponent pathways were chosen carefully to avoid luminance or brightness cues and to elicit responses from only one pathway with each chromatic stimulus. Initially, a blue-yellow heterochromatic stimulus was generated, using the blue phosphor for one grating in spatial antiphase with a yellow grating, itself composed of red and green gratings in spatial phase (see figure A2.1). The CIE co-ordinates of the blue and yellow were measured by spectroradiometry and were found to lie along a tritanopic confusion axis in CIE space. However, this stimulus was found to be impossible to render isoluminant without the two component gratings appearing unequal in brightness (see figure A2.1). When set at photometric isoluminance, or when isoluminance was determined by heterochromatic flicker photometry, the blue appeared much brighter than the yellow grating. When equalised in brightness by heterochromatic brightness matching, the two were not isoluminant, the yellow grating being of much higher luminance than the blue in this situation.

In order to generate heterochromatic stimuli of equal brightness and luminance which selectively stimulate the S-cone opponent pathway, complementary stimuli lying along a tritanopic confusion axis in CIE colour space were chosen. This tritan stimulus, which was used for all experiments reported in the main body of this thesis, is described in Chapter 5.

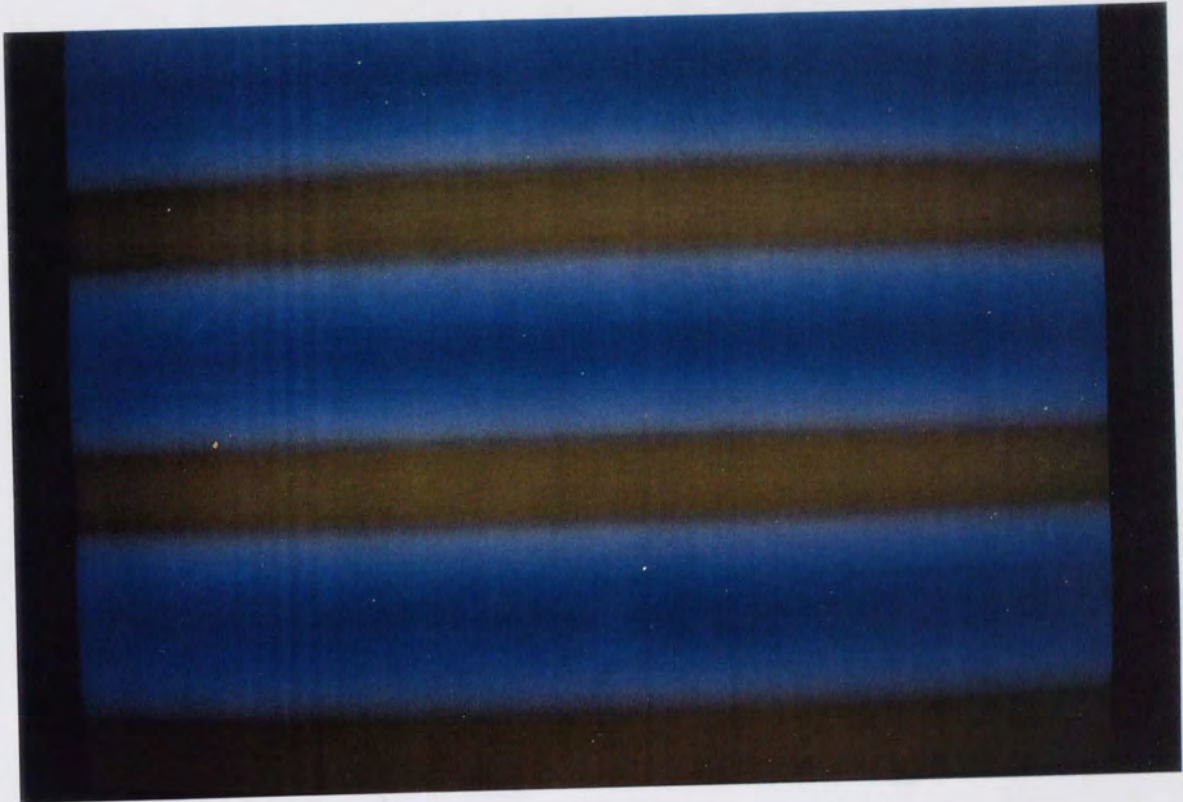


Figure A2:1
The stimulus shown here is a photometrically isoluminant blue-yellow stimulus which comprises a blue grating generated from the blue phosphors only, in spatial antiphase with a yellow grating generated using the red and green phosphors in spatial phase. This stimulus was not used for experiments reported here as the component gratings could not be equalised in luminance and brightness.

APPENDIX 3

The Chromatic Visual Evoked Response in a Colour-Defective Adult

The visual evoked response to red-green stimuli at the full range of colour luminance ratios (see Chapter 5) was recorded from a male adult, assessed as colour-defective using the Farnsworth-Munsell 100-Hue test and the Ishihara pseudoisochromatic plates, both carried out under a standard illuminant C. The red-green isoluminant point was determined in subject IP using heterochromatic flicker photometry. This test demonstrated isoluminance for this subject at a red-green colour luminance ratio of 0.55. The use of a standard illuminant C was found to be important in testing for defective colour vision after carrying out the F-M 100 Hue test under room lighting.

The results of the test under room lighting and standard illumination are shown in figures A3.1 and A3.2 for a colour-normal adult (FF). Under room lighting, the plot appears to indicate a mild defect, while under the standard illuminant the plot is normal.

The result for the colour-defective male (IP) assessed under the standard illuminant is shown in figure A3.3. The major axis of the error lies between axes indicative of protanomaly and deuteranomaly (Farnsworth, 1943; Kinnear, 1970). The Ishihara diagnostic plates indicated protanomaly.

Visual evoked responses recorded from subject IP to red-green stimuli at the full range of colour luminance ratios are shown in figure A3.4. Responses to luminance-modulated stimuli are clear, with distinct responses to stimulus offset at ratios at or close to 0.0 or 1.0. At and around photometric isoluminance, however, responses are weak, and are least distinct at a red-green colour luminance ratio of 0.6. Visual evoked responses and heterochromatic flicker photometry results indicate that the quantal catch of the long- and medium-wavelength-sensitive cones in this protanomalous subject are equalised at a colour luminance ratio away from photometric isoluminance such that the red element is of increased luminance.

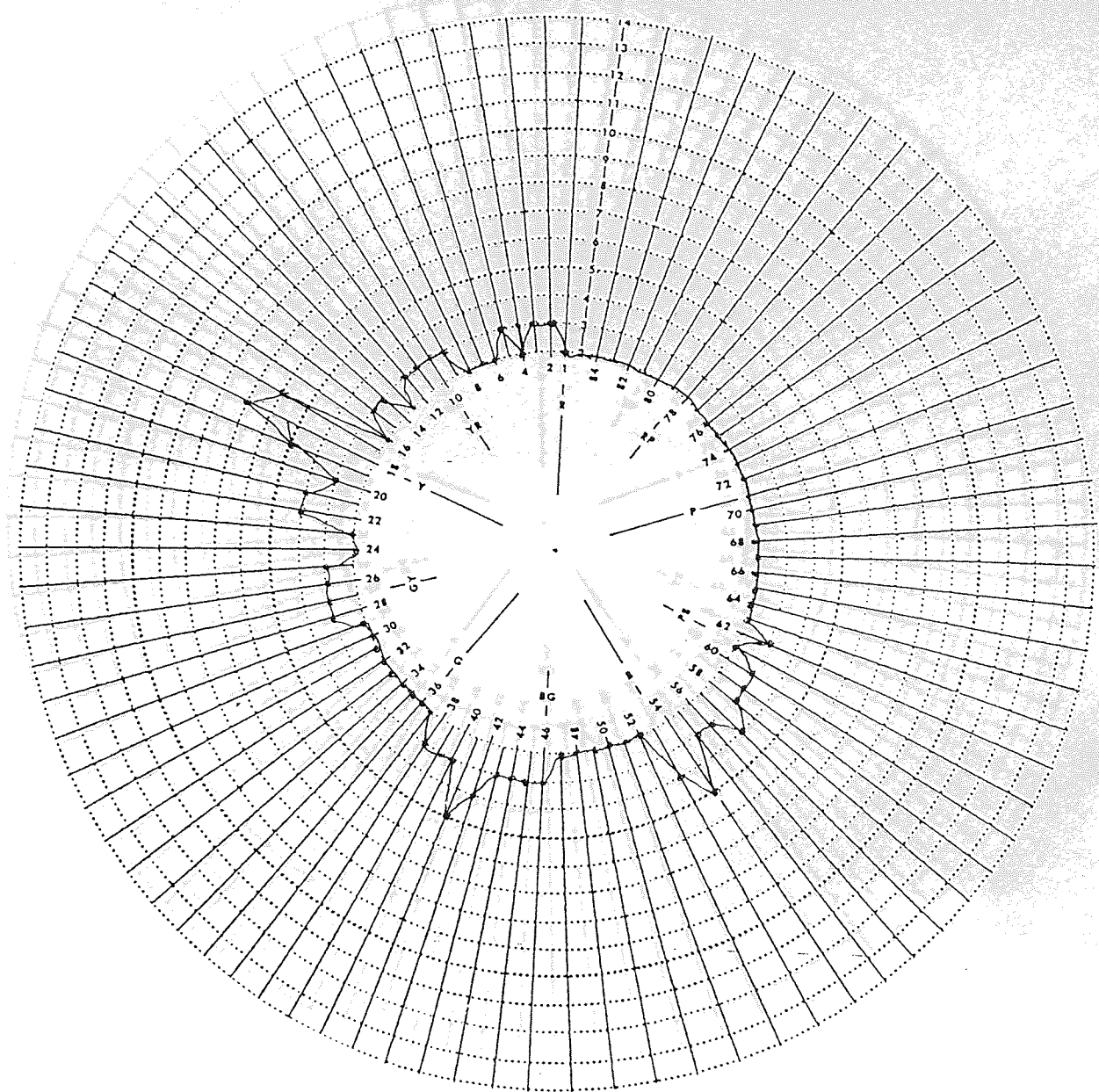


Figure A3.1
 The result of the Farnsworth-Munsell 100-Hue test for colour-normal subject FF, carried out under room lighting conditions. This plot appears to indicate a mild defect.

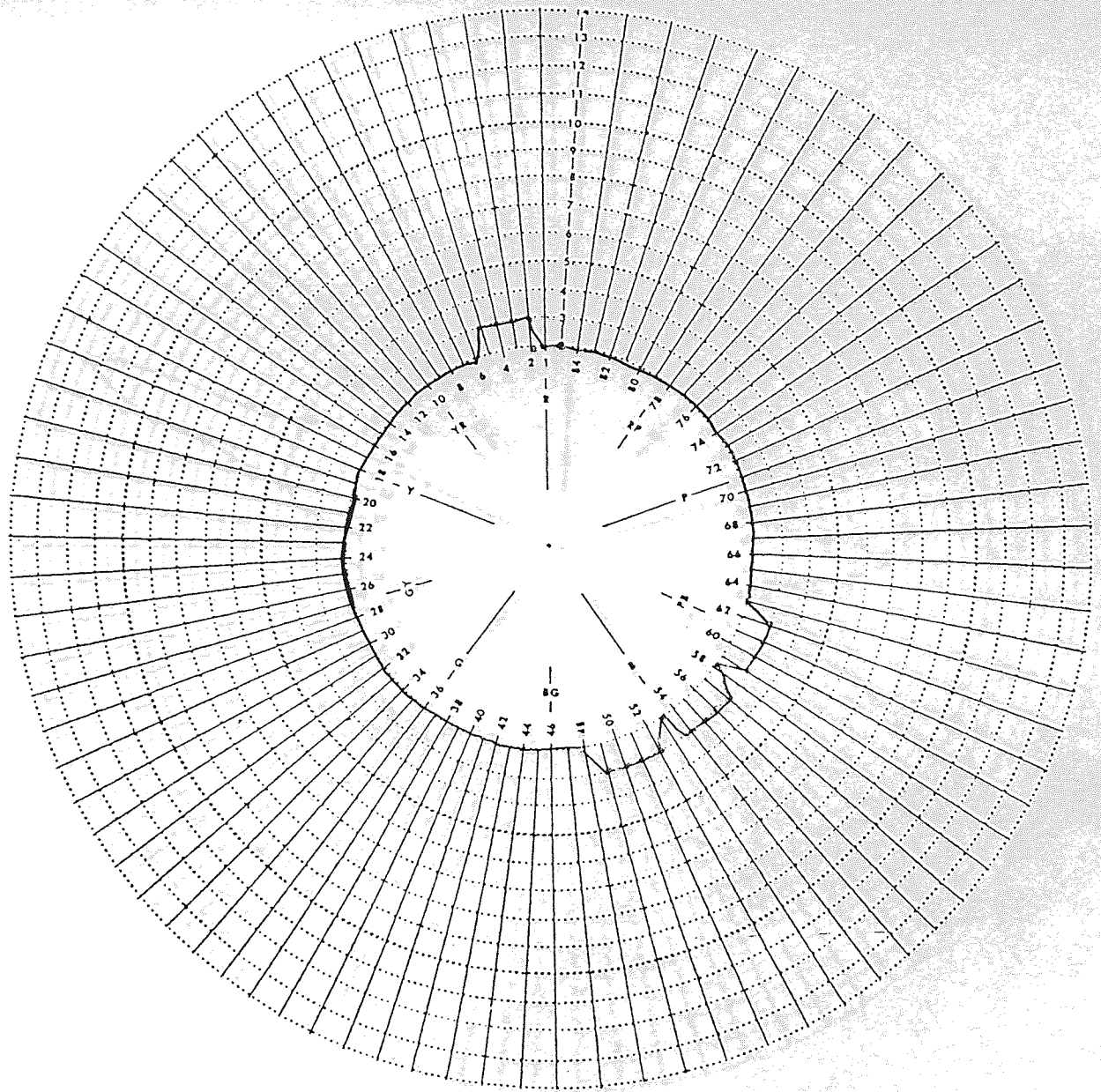


Figure A3.2
 The result of the Farnsworth-Munsell 100-Hue test for colour-normal subject FF, carried out under a standard illuminant C. This plot indicates normal colour vision.

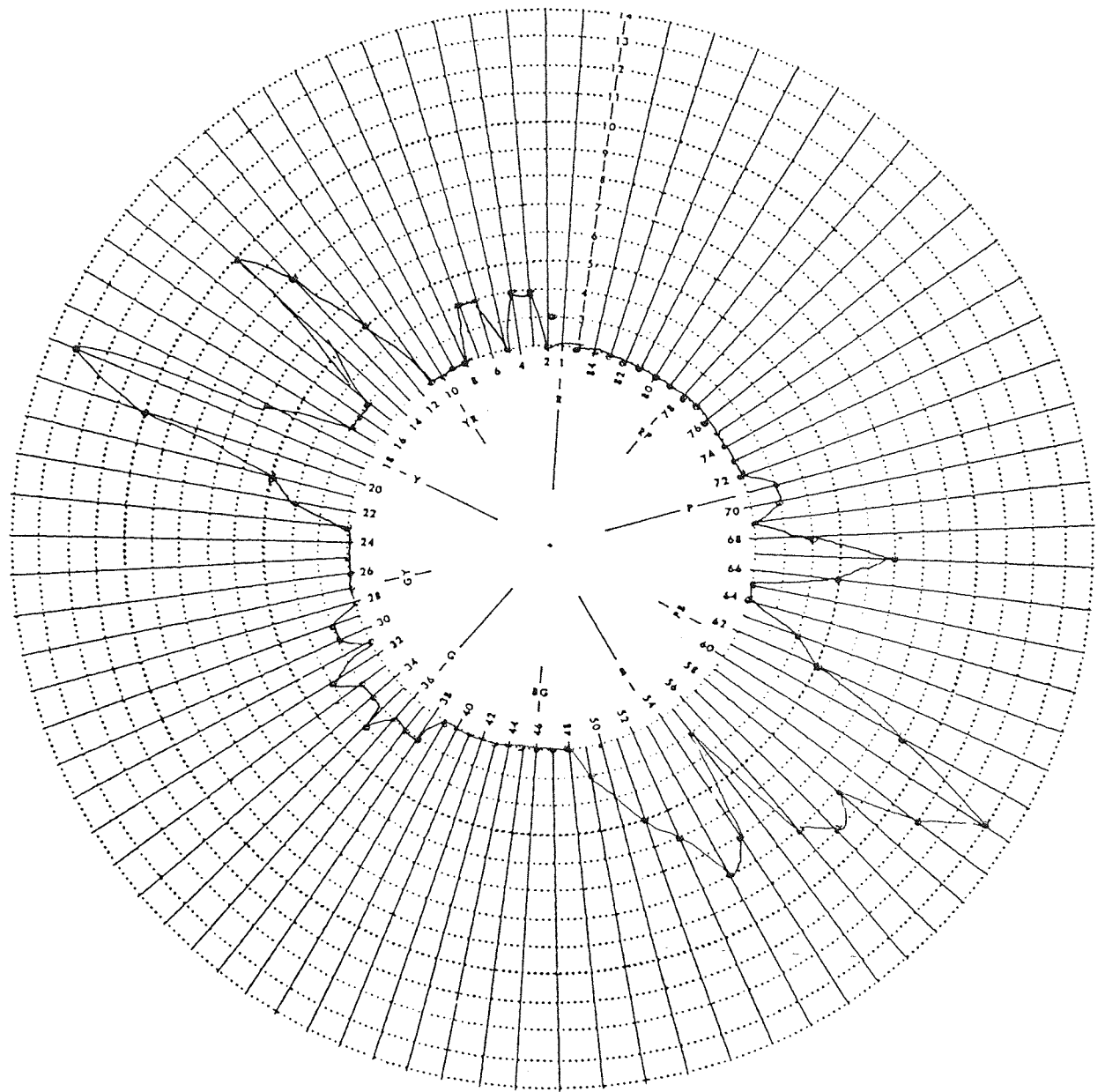


Figure A3.3

The result of the Farnsworth-Munsell 100-Hue test for colour-defective subject IP, carried out under a standard illuminant C. This plot demonstrates an axis of confusion, the angle of which is inconclusive, as it lies between deutan and protan axes.

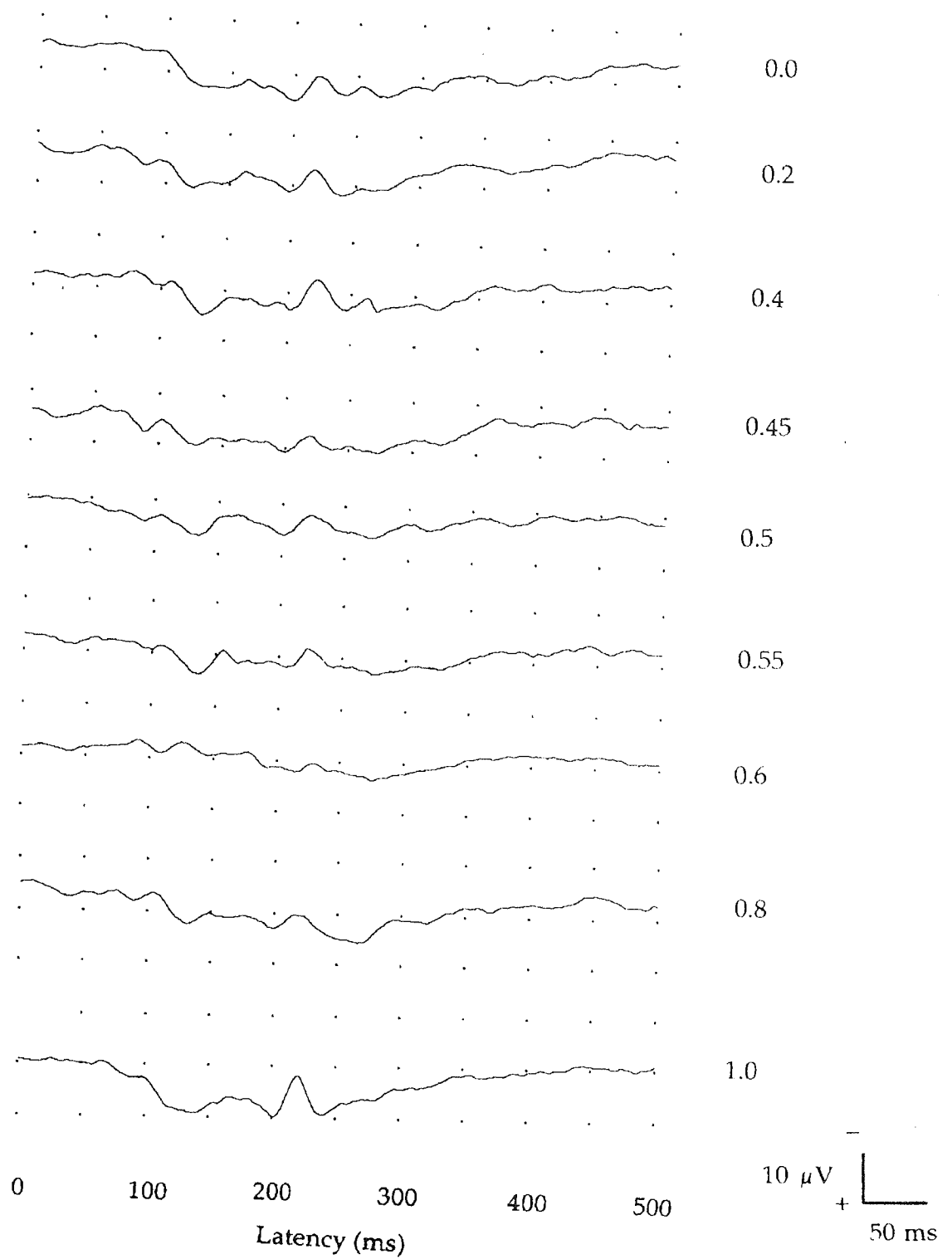


Figure A3.4
 Visual evoked responses to red-green stimuli at the full range of colour luminance ratios are shown, recorded from colour-defective adult subject IP.